ISSN: 2153-1196 Volume 12, Number 5, April 2021

Scientific Research Publishing

Journal of Modern Physics

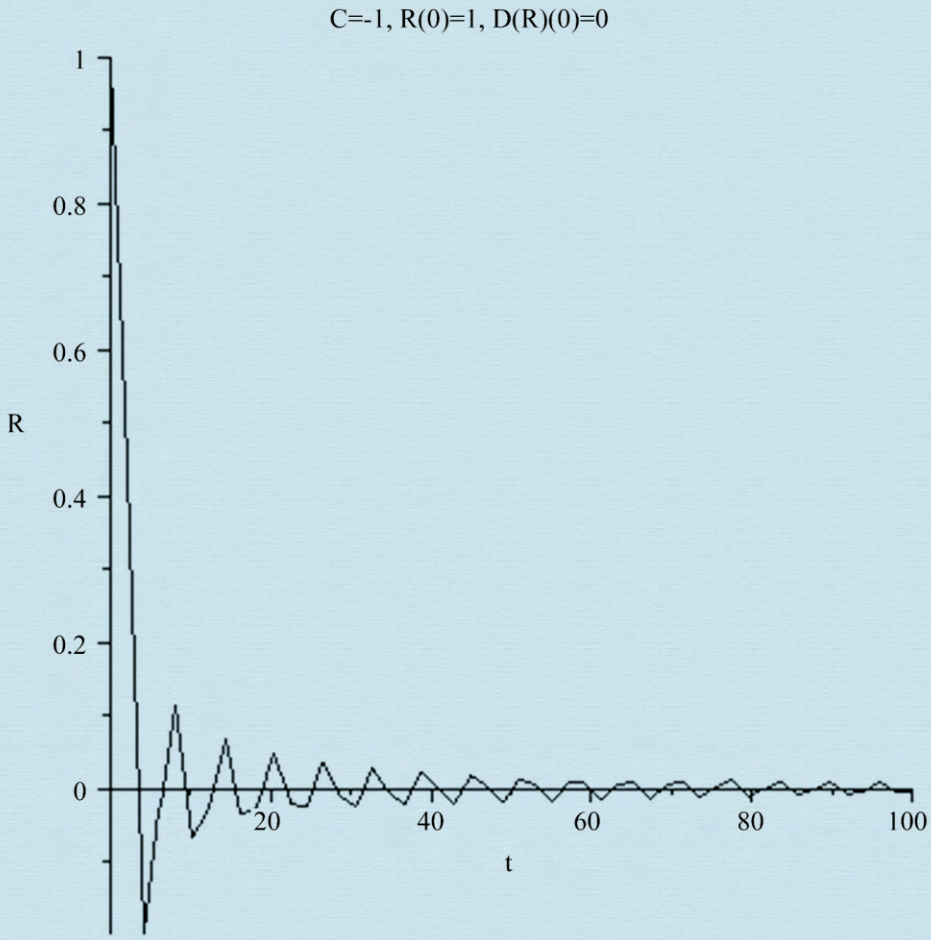

ISSN: 2153-1196
9 772153 119007 05

https://www.scirp.org/journal/jmp

Journal Editorial Board

ISSN: 2153-1196 (Print) ISSN: 2153-120X (Online)
https://www.scirp.org/journal/jmp

Editor-in-Chief

Editorial Board

Scientific Research Publishing

Journal of Modern Physics, 2021, 12, 541-729
https://www.scirp.org/journal/jmp
ISSN Online: 2153-120X
ISSN Print: 2153-1196

Table of Contents

Volume 12 Number 5 April 2021

The figure on the front cover is from the article published in Journal of Modern Physics, 2021, Vol. 12, No. 5, pp. 552-593 by Boris V. Alexeev.

Journal of Modern Physics (JMP)
Journal Information

SUBSCRIPTIONS

The *Journal of Modern Physics* (Online at Scientific Research Publishing, https://www.scirp.org/) is published monthly by Scientific Research Publishing, Inc., USA.

Subscription rates:
Print: $89 per issue.
To subscribe, please contact Journals Subscriptions Department, E-mail: sub@scirp.org

SERVICES

Advertisements
Advertisement Sales Department, E-mail: service@scirp.org

Reprints (minimum quantity 100 copies)
Reprints Co-ordinator, Scientific Research Publishing, Inc., USA.
E-mail: sub@scirp.org

COPYRIGHT

PRODUCTION INFORMATION

For manuscripts that have been accepted for publication, please contact:
E-mail: jmp@scirp.org

Journal of Modern Physics, 2021, 12, 541-551
https://www.scirp.org/journal/jmp
ISSN Online: 2153-120X
ISSN Print: 2153-1196

On the Simulation Hypothesis and Its Implications

Salah Hamieh

Nuclear Physics Laboratory, Lebanese University, Faculty of Sciences (I), Beirut, Lebanon
Email: hamiehs@yahoo.fr

How to cite this paper: Hamieh, S. (2021) On the Simulation Hypothesis and Its Implications. *Journal of Modern Physics*, **12**, 541-551.
https://doi.org/10.4236/jmp.2021.125036

Received: January 13, 2021
Accepted: April 6, 2021
Published: April 9, 2021

Abstract

This paper reports on the potential use of video games as well as gaming engines in the domain of physics and artificial intelligence. Unreal Engine 4 (UE4) [1] is used to render the history of the universe back in time to the quantum gravity era and then standard cosmology is assumed for its evolution until the appearance of life that was a simplified model of human-like evolution is rendered. The results of the simulations have a potential implication on the origin of life and matter and favorite the simulation hypothesis of the universe.

Keywords

Simulation Hypothesis, Artificial Intelligence, Quantum Gravity, Unreal Engine 4

1. Introduction

The exponential growth of game industries makes it of potential use in the domain of sciences. For instance, although the original intended use for graphics processing units (GPUs) was to compute and display computer graphics, it is now standard to use GPUs for general purpose computing including scientific computing. In addition, with the development of platforms such as OpenCL, Direct Compute or NVIDIAs Compute Unified Device Architecture (CUDA), programmable GPUs are now common place technologies for computational mathematics and artificial intelligence (AI). This naturally leads to the concept of gamification, which is a term used to describe the use of game design elements and technologies in non-game contexts [2]. In this paper, game design elements are used in the context of physics and AI. The main reason that motivates this choice is to shed some insight into the two unsolved problems in the scientific community, namely, the theory of consciousness and the theory of

quantum gravity (QG) in the hope to unify them in a single theory [3]. In fact, general relativity, like electromagnetism, is a classical field theory, so one might expect that, as with electromagnetism, the gravitational force should also have a corresponding quantum field theory. However, attempts to construct QG theory have run into difficulties. One of these difficulties is that: QG is perturbatively nonrenormalizable [4]. Furthermore, quantum gravitational effects only appear at length scales near the Planck scale, a scale only accessible with far higher energies, than those currently available in high energy particle accelerators. In another hand, the nature of consciousness, that is the mechanism by which it occurs in the brain, how it arose from matter, and its ultimate place in the universe, is unknown. Our current models of reality simply do not allow for consciousness.

In this paper, we first show how we can implement the evolution of the universe and human-like intelligence in a video game and then, based on the simulation hypothesis, we propose an approach in which we consider consciousness as absolutely fundamental to our understanding of the universe rather than being an outcome after billions of years of lifeless physical processes. The results of this simulation reveal some metaphysical, ontological, and epistemological implication pertaining life and existence.

The paper is organized as follow: in the next section, we present the results of rendering the Ekyportic model of the beginning of the universe [5]. In Section 3, we propose a simplified model for the evolution of the human-like intelligence based on the implementation of a genetic, reinforcement learning (RL) and a reasoner algorithm in different contexts. Section 4 is dedicated for the discussions about the simulation hypothesis and its physical and philosophical implications. Our conclusions are shown in Section 5.

2. Rendering a Simplified Heterotic M-Theory in UE4

The ekpyrotic scenario, which will be our model of choice for rendering the beginning of the universe, is based on simplified Heterotic M-theory with the fields whose equations of motion allow it, are set to zero [6] [7]. A numerical solution of the ekpyrotic Scenario in the moduli space approximation using vacuum solution of this theory which contains flat, parallel branes was done in [8]. The results of [8] in different scenarios of the bulk potential show no collision between the bulk brane and the visible brane in the considered cases. Therefore, in order to provoke collision and as suggested in [8] we introduced an extra kinetic energy into the initial conditions for the bulk brane.

Without going into the details about the moduli space approximation (see [8] for further details), we solved the equations of motion derived from the Lagrangian given in Equation (8) of [8], numerically from $t = 0$ to $t = 3000/M_5$ with the parameters defined in [8] have the following values $R = 1/M_5$, $\alpha = 100M_5$, $\beta = M_5$. The initial conditions are $A(0) = B(0) = 1$, $C(0) = 200$ and $A'(0) = B'(0) = C'(0) = 0$ and we used the parabolic bulk brane potential $V(Y) = M_5 Y(Y\text{-}r)$. To provoke collision, we have set the derivative of the bulk brane coordinate, to

$Y'(0)/R = 0.0001$. The results of the simulation are shown in Figure 1 where the collision between bulk brane and the universe happens at $t/M_5 \sim 1785$. To model the Bulk brane dynamics in UE4, we used a polynomial fitting of $Y(t)/R$. The result of the rendering in UE4 is shown on Figure 2 and the real time animation can be found in a simple video game which is a virtual world with one story that was constructed for this purpose [9]. Universe evolution using standard cosmology will be shown in a future investigation. This type of simulation in cosmology has already been made, e.g., in [10], "Astera", a cosmological visualization tool that renders large scale structure of the cosmic web in real time using UE4 is presented.

AI and UE4

The history of the universe can be thought of as a sequence of information processing revolutions, each of which builds on the technology of the previous ones from the big bang to human consciousness [11]. Therefore, in this section, we propose a simplified model of human-like evolution based on the following assumptions:

1) Evolution of cells and perceptions are due to a simple genetic algorithm.
2) Evolution of brain is due to RL algorithm and a reasoner algorithm.

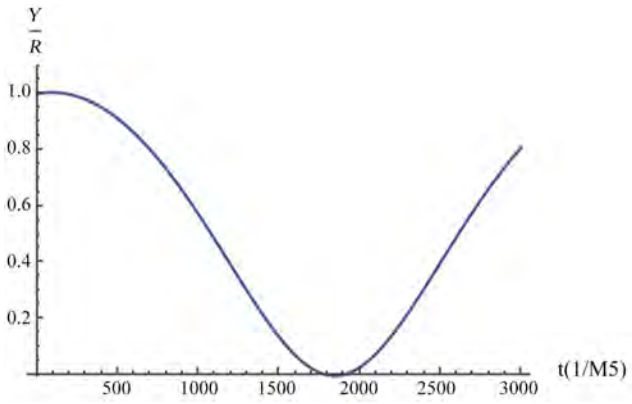

Figure 1. Collision of the bulk brane with the visible universe.

Figure 2. Rendering branes collision in UE4.

The genetic algorithm uses one chromosome and 5 genes and it is used only to gives the bots access to AI perception like sight, hearing and others functionalities. The RL algorithm is used to produce some axiom/rules from learning episodes according to only five states See Enemy, HearEnemy, TakingDamage, DealingDamage, and CriticalHealth and its 3 actions are Explore, Attack, and Flee. We did not include emotion and other states of mind in the learning episodes. The bots, uses only propositional logic for reasoning based on forward chaining inference with very simple knowledge base, namely, 5 possible facts and 3 propositions for inference. Meta-knowledge is not implemented in this simulation although this can be done in UE4 by introducing new concepts from previous one with the help of learning algorithm and a reasoner. We used UE4 in this simulation because it contains many useful tools for Machine Learning simulation. These tools include Blueprint Visual Scripting that can be converted into C++ code, simple-to-use Behavior Trees (BT) for setting up traditional AI, and more complex tools such as AIComponents and the Environment Query System (EQS) for giving an agent the ability to perceive its environment. We have implemented the genetic algorithm, the reasoner and the RL in a video game [9]. In this paper, and without loss of generality, the implementation of the RL is only shown.

We constructed a simulation environment for solo Deathmatch gameplay between a Behavior Tree Non player character (NPC) and an RL NPC. The Q-learning algorithm [12] updates what the expected reward value for each state-action. The algorithm has a function that calculates the quality of a state–action combination: Q: S × A → ℝ which is as follow:

$$Q^{\text{new}}\left(s_t, a_t\right) \leftarrow \underbrace{Q\left(s_t, a_t\right)}_{\text{old value}} + \underbrace{\alpha}_{\text{learning rate}} \cdot \left(\underbrace{r_t}_{\text{reward}} + \underbrace{\gamma}_{\text{discount factor}} \cdot \underbrace{\max_a Q\left(s_{t+1}, a\right)}_{\text{estimate of optimal future value}} - \underbrace{Q\left(s_t, a_t\right)}_{\text{old value}} \right)$$

where $Q(s_t, a_t)$ is the expected reward value for the current state-action, (st, at,) of the RL NPC at time t and $\underbrace{r_t}_{\text{reward}}$ is the rewards, α is the learning rate and γ is the discount factor.

Many simulations were made to assess the RL NPC ability to learn to defeat the BT NPC. This was accomplished by setting the learning rate $\alpha = 0.4$ and the discount factor $\gamma = 0.8$ and by rewarding the RL NPC 1 point for killing the BT NPC and 0.1 point for damaging the BT NPC. The RL NPC was given a punishment of −1 for dying from the BT NPC and a punishment of −0.1 for being damaged by the BT NPC. A screenshot of the implementation is shown in **Figure 3**. We could not find a variant of the RL NPC that could defeat the BT NPC, the best variant of the RL NPC has 63\% of the performance of the BT NPC. This is good results given that the learning episodes were very short-reaching and the state-action space was very small. Of course, this is a too simplistic approach for human evolution and human intelligence that does not include features in human behavior like planning, attentions, system behavior etc.

Figure 3. Simulation environment for RL versus AI.

Note that, this type of simulations can be used in a different context, e.g., to simulate the response of the human body immune system under viral, bacterial, fungi and other type of inflammations where communications between cells is mediated by cytokines and chemokines.

3. The Simulation Hypothesis and Its Implications

There is a long philosophical and scientific history to the underlying thesis that reality is an illusion. Perhaps, this idea was most popularized in science fiction probably in the Matrix, released in 1999. In physics, the view of the universe and its workings as the ebb and flow of information was first observed by Wheeler [13]. This shift of paradigm from understanding the universe as energy transformation to the information processing universe leads to the emergence of a new branch of science called quantum computation. Quantum evolution of a system is represented in quantum computation by a quantum circuit built from quantum gates. Consequently, two views of the world emerged, the first one, proposes that the universe is a quantum computer [11] and the other one proposes that the system performing the simulation is distinct from its simulation (the universe) [14] [15]. In this paper, we suggest another possibility which is a "hybrid" between the two propositions based on the following assumptions

1) The system performing the simulation is distinct from its simulation.

2) The rendering algorithm is based on quantum mechanical laws.

3) The universe is rendered on a pixelated screen for each observer.

4) The simulator has limited resources and always maintains a consistent world.

One may object our assumptions about the universe by claiming that classical digital devices are not very efficient to reproduce quantum dynamics. However, this is not completely true, because the computational complexity of the system could be reduced drastically if the system renders the content only when observed by an observer and if the universal wave function is known from path integral or from Schrodinger equation of quantum fields.

Under the assumption of finite computational resources, the simulation of the universe would be performed by dividing the continuum spacetime into a discrete set of points. Several observational consequences of a grid-like space-time have been proposed by Lattice QCD simulations, among them is the anisotropy

in the distribution of ultra-high-energy cosmic rays, that, if observed, would be consistent with the simulation hypothesis [16].

Many physical aspects can support the simulation hypothesis, e.g.,

- No absolute frame of reference in relativity theory.
- The measurement problem in quantum mechanics depends on observer.
- Problem of time in quantum gravity which is an extrinsic parameter and need suitable observable of the clock from outside the visible universe [17].
- The Bekenstein bound [18], which relate the curvature of the spacetime with information.
- The Holographic principle, the AdS/CFT correspondence, which relate quantum gravity and quantum information [19].
- Objective reality doesn't exist in quantum mechanics as can be seen, e.g., in the delayed choice experiment.

Many physical results can be derived from the above description of the world, e.g.

- The time dilation in special relativity can be viewed as framerate adaptation of a moving object who need more resources for rendering.
- Gravitational lensing can be interpreted as a bounded massive object need more local resources to be rendered which in turn need a compromise between the polygon counts and the model fidelity and that can be achieved by changing the structure of the spacetime around the object (less polygons).
- Extradimension and compactification are similar to a projection from 3d object to 2d screen with wireframe rendering.
- Black hole Information paradox can be understood as a memory saturation and black hole radiations as freeing that memory.
- Quantum measurement can be seen as an intelligent agent in a specific state receive and process information and then make an action from a set of possible actions which forces the system to be projected into a specific state (process similar to [20]).

Time travel paradox, antimatter, and others physical phenomenon can have their interpretation within the simulation hypothesis.

In what follows, we describe our view of the universe evolution within the simulation hypothesis framework and assuming "cosmological consciousness" [21]. Meanwhile, a very promising mechanism to generate consciousness from within the universe is proposed by R. Penrose and S. Hameroff [3], the so-called "Orchestrated objective reduction", in which consciousness can originate at the quantum level inside neurons, rather than the conventional view of neuroscience that it is a product of connections between neurons.

From the above assumptions, and inspired by the many world interpretation of quantum mechanics [20] and the subjective idealism view of reality, we hypothesize the evolution of the universe in the following fashion: a cosmological consciousness being equipped with thinking tools that include inductive, deductive, and abductive reasoning, etc., and other types of thinking [22] created/simulated the universe [8] [23] [24] and start injecting random qubits, "quantum fluctua-

tion" [25], into the baby universe where information gets processed. And by observing/measuring the results a new quantum circuits can be exited and the cycle repeat through a feedback loop in a process similar to the working of the brain where the born rule can be compared to the weights in the neural network. As the system evolves subsystems emerge each of which has its own computation abilities and functionalities. This construction is reminiscent to so called the Game of Life (GOL) which is a cellular automaton invented by Conway [26]. Although, the fundamental "physics" of this world is so simple, as the game evolve, and at different scales, new "physics", "chemistry" and "biology" emerges. In fact, by choosing an appropriate initial configuration of the game, complex system emerges and Self-replication object can appear, even more surprising, emerging laws could entail new concepts and entities which do not "apparently" exist in the original laws [27]. In a more abstract way, we can think about this construction of the universe as each cognitive subsystem is equipped with a formal language that "lives" in a metalanguage [28] and having finite set of axioms (obviously not complete [29]) that define its dynamics according to some interpretation (model dependent reality) and evolves into different forms. Furthermore, we think that, this world is decomposed into three types of entities, the inorganic matter which is small structure uses simple quantum logic gates that determine its evolution, the organic matter which acquire more computational abilities for learning and human that has ability for reasoning. Space and time and physical laws can be thought of, in a Kantian language [30], as a type of relations in a mathematical structure and matter is a realization/support of this "philosophical matter" [31]. Evolution in this structure can be imagined as a process of mind from state to another state which can be translated in the material world into a Turing machines (TM) where logical statements about proofs are translated into actions of machines. Note that, even though TM are built from a simple logic gates they are able to simulate a very sophisticated video game like World of Warcraft and Fortnite. The difference between modern computers that are built upon the Von Neumann architecture of TM and the universal computation is that TM uses deterministic computation, however, universal computation uses quantum computation to explore the whole spectrum of computation which gives the system the ability to evolve by learning and making decisions. This imagination about the universe formation is similar to Von Neumann method of creating natural numbers out of empty sets who imagined that all numbers could be bootstrapped out of the empty set by the operations of the mind. In a platonic sense, that is in the world of ideas, each partition of the world would evolve by increasing its content toward the infinity or decreasing toward the emptiness or it can be locked in a minima. Therefore, attention, play a major role in this approach which depends on the system "personalities" [32]. Furthermore, we speculate that, the driving force for a subsystem to grow, that is to increase its knowledge base, is the "force of love" [33] which, in a systemic view [34] translate into creativity and novelty (this aspect is included in the video game [9]). This construction can be compared to computa-

tional ontology, used in semantic web, which defines a set of representational primitives with which to model a domain of knowledge or discourse. The representational primitives are typically classes (or sets), attributes (or properties), and relationships (or relations among class members). Computational ontology uses description logic for reasoning and it is used to model genetic ontology, emotion ontology *etc* using language like Web Ontology Language (OWL) [35].

This view of the universe can be supported by the cutting-edge modern medicine where mind meets body, where mind meets DNA, where we can control our genes from the inside out. This development of modern medicine very much parallels to the science of meditation. In fact, at the heart of our physiology, from the surface level of organs systems to tissues cells to proteins is one molecule, the DNA molecule, which contains all of the intelligence which governs our whole physiology throughout our whole lifespan and also governs much of our behavior and even personality, and the DNA is governed by the laws of chemistry, the laws of physics, and then ultimately, at the most subtle level, the least excited state of physiology, is the unified field of all the laws of nature. Modern medicine has been progressively going through this pathway from the surface to the subtle, for the past several decades, surgery works on the more physical level the mechanical level, pharmacologic medicine works on the cellular level receptors molecules by changing those cellular components, molecular medicine works at an even deeper level attempting to manipulate on the protein level, modern genomic medicine attempts to understand the code contained within the DNA, the information that governs our life and lifespan and attempts to engineer on that level to change one's DNA to reverse disease and promote ideal health, and quantum medicine works on the most fundamental levels of the quantum mechanical laws of nature.

However, according to time magazine [36] our DNA is not our destiny but new scientific discoveries shows that our choices in lifestyle behavior what we think how we use and develop our consciousness can change our genes through epigenetic mechanisms.

In this description of reality, the view of the human body as a machine and of the mind as a separate entity is replaced by one that sees not only the brain, but also the immune system, the bodily organs, each cell, and even inorganic matter as a living, cognitive system with different degree of cognition. This view of reality can have implication on the major problems of our time: energy, environment, climate change, food security, financial security, *etc*, which state that these problems cannot be understood in isolation, they are all interconnected and interdependent [34] [37].

This type of thinking about the universe, the system thinking [34], can be supported by another argument that comes from the so called the Cosmological natural selection proposed by Smolin [38]. The hypothesis suggests that a process analogous to biological natural selection applies at the grandest of scales.

Finally, as an example of the feedback loop system that relate the central nervous system, "consciousness", with the material world, we consider the re-

nin-angiotensin-aldosterone system in human body, which is a hormone system that regulates blood pressure and fluid and electrolyte balance and which is regulated by a nucleus inside the brain called hypothalamus. From this perspective, we speculate that the brain controls the genetic code and even more can rewrite the genetic code in the same way we speculate that cosmological consciousness can reshape our universe!

We conclude our discussion with following phrase/prediction: "you are what you think", which is in the same spirit of René Descartes famous phrase "I think therefore I am" and it can be expressed by the following quote borrowed from [39].

In the end, I've come to believe in something I call "The Physics of the Quest." A force in nature governed by laws as real as the laws of gravity. The rule of Quest Physics goes something like this: If you're brave enough to leave behind everything familiar and comforting, which can be anything from your house to bitter, old resentments, and set out on a truth-seeking journey, either externally or internally, and if you are truly willing to regard everything that happens to you on that journey as a clue and if you accept everyone you meet along the way as a teacher and if you are prepared, most of all, to face and forgive some very difficult realities about yourself, then the truth will not be withheld from you.

4. Conclusion

In summary, utilizing video game technologies can be a game changer in our perception of the world. We have shown the importance of these technologies in the domain of physics and artificial intelligence. We have discussed the simulation hypothesis and proposed a model for the universe evolution. Obviously, we don't claim, up to our knowledge, that the physical universe is a simulation rather we claim that the simulation hypothesis can be very powerful tool in our understanding of the material world. At the end, we think the simulation hypothesis needs more considerations from the scientific community and all found predictions/speculations need to be tested/formulated in a formal language.

Acknowledgements

This work was performed as part of the research program of Doctorate School of Science and Technology.

Conflicts of Interest

The author declares no conflicts of interest regarding the publication of this paper.

References

[1] Unreal Engine 4 Documentation. https://docs.unrealengine.com

[2] Deterding, S., Dixon, D., Khaled, R. and Nacke, L. (2011) From Game Design Elements to Gamefulness: Defining "Gamification". *Proceedings of the* 15*th Interna-*

tional Academic MindTrek Conference: *Envisioning Future Media Environments* (*AMC*), New York, 9-15. https://doi.org/10.1145/2181037.2181040

[3] Penrose, R. and Hamero, S. (2014) *Physics of Life Reviews*, **11**, 94-100. https://doi.org/10.1016/j.plrev.2013.11.013

[4] Feynman, R.P., Morinigo, F.B. and Wagner, W.G. (1995) Feynman Lectures on Gravitation. Addison-Wesley, Reading.

[5] Khoury, J., Ovrut, B., Steinhardt, P. and Turok, N. (2001) *Physical Review D*, **64**, Article ID: 123522. https://doi.org/10.1103/PhysRevD.64.123522

[6] Lukas, A., Ovrut, B.A., Stelle, K.S. and Waldram, D. (1999) *Nuclear Physics B*, **552**, 246. https://doi.org/10.1016/S0550-3213(99)00196-0

[7] Lukas, A., Ovrut, B.A., Stelle, K.S. and Waldram, D. (1999) *Physical Review D*, **59**, Article ID: 086001. https://doi.org/10.1103/PhysRevD.59.086001

[8] Sorensen, T. (2005) *Physical Review D*, **71**, Article ID: 107302. https://doi.org/10.1103/PhysRevD.71.107302

[9] Hamieh, S. (2019) Wormhole Gate. Google Play.

[10] Marsden, C. and Shankar, F. (2020) *Universe*, **6**, 168. https://doi.org/10.3390/universe6100168

[11] Lloyd, S. (2013) The Universe as Quantum Computer. In: Zenil, H., Ed., *A Computable Universe Understanding and Exploring Nature as Computation*, World Scientific Publishing, Singapore, 567-581. https://doi.org/10.1142/9789814374309_0029

[12] Watkins, C.J. and Dayan, P. (1992) *Machine Learning*, **8**, 279-292. https://doi.org/10.1023/A:1022676722315

[13] Wheeler, J.A. (1990) Information, Physics, Quantum. In: Zurek, W.H., Ed., *Complexity*, *Entropy*, *and the Physics of Information*, Addison-Wesley, Boston, 354-368.

[14] Bostrom, N. (2003) *Philosophical Quarterly*, **53**, 243-255. https://doi.org/10.1111/1467-9213.00309

[15] Campbell, T., Owhadi, H., Sauvageau, J. and Watkinson, D. (2017) On Testing the Simulation Theory.

[16] Silas, B., Davoudi, Z. and Savage, M.J. (2012) Constraints on the Universe as a Numerical Simulation.

[17] Marletto, C. and Vedral, V. (2017) *Physical Review D*, **95**, Article ID: 043510. https://doi.org/10.1103/PhysRevD.95.043510

[18] Bekenstein, J. (1981) *Physical Review D*, **23**, 287-298. https://doi.org/10.1103/PhysRevD.23.287

[19] Ryu, J. and Takayanagi, T. (2006) *Journal of High Energy Physics*, **2006**, 45. https://doi.org/10.1088/1126-6708/2006/08/045

[20] Everett, H., Wheeler, J.A., DeWitt, B.S., Cooper, L.N., Van Vechten, D. and Graham, N. (1973) The Many-Worlds Interpretation of Quantum Mechanics. Princeton Series in Physics, Princeton University Press, Princeton.

[21] Vanchurin, V. (2020) *Entropy*, **22**, 1210. https://doi.org/10.3390/e22111210

[22] de Bono, E. (1985) Six Thinking Hats: An Essential Approach to Business Management.

[23] Hawking, S. and Hertog, T. (2018) *Journal of High Energy Physics*, **2018**, Article No. 147. https://doi.org/10.1007/JHEP04(2018)147

[24] He, D.S., Gao, D.F. and Cai, Q.-Y. (2014) *Physical Review D*, **89**, Article ID: 083510.

[25] Ade, P., *et al.* (2016) *Astronomy and Astrophysics*, **594**, 1.

[26] Gardner, M. (1970) *Scientific American*, **223**, 120-123. https://doi.org/10.1038/scientificamerican1070-120

[27] Hawking, S. (2010) The Grand Design.

[28] Tarski, A. (1944) *Philosophy and Phenomenological Research*, **4**, 341-376. https://doi.org/10.2307/2102968

[29] Godel, K. (1995) Collected Works, Vol. III. Oxford University Press, Oxford, 304-323.

[30] Kant, E. (1781) Critics of Pure Reason.

[31] Graham, B. and Ruth, G. (1991) *Physical Review Letters*, **66**, 260-263. https://doi.org/10.1103/PhysRevLett.66.260

[32] Rothmann, S. and Coetzer, E.P. (2003) *SA Journal of Industrial Psychology*, **29**, a88. https://doi.org/10.4102/sajip.v29i1.88

[33] Peirce (1893) *The Monist*, **3**, 176-200. https://doi.org/10.5840/monist18933235

[34] Capra, F. (2014) The Systems View of Life (A Unifying Vision).

[35] OWL (2012) Web Ontology Language Document Overview (Second Edition). W3C.

[36] Time Magazine, "The God Gene" Oct. 25, 2004.

[37] The Rockefeller Foundation and Global Business Network Report (2010) Scenarios for the Future of Technology and International Development.

[38] Smolin, L. (1992) *Classical and Quantum Gravity*, **9**, 173-191. https://doi.org/10.1088/0264-9381/9/1/016

[39] Robert, J. (2010) Movie "Eat Pray Love".

Journal of Modern Physics, 2021, 12, 552-593
https://www.scirp.org/journal/jmp
ISSN Online: 2153-120X
ISSN Print: 2153-1196

Nonlocal Theory of High-Temperature Superconductivity

Boris V. Alexeev

MIREA—Russian State Technological University, Moscow, Russia
Email: Boris.Vlad.Alexeev@gmail.com

How to cite this paper: Alexeev, B.V. (2021) Nonlocal Theory of High-Temperature Superconductivity. *Journal of Modern Physics*, **12**, 552-593.
https://doi.org/10.4236/jmp.2021.125037

Received: March 10, 2021
Accepted: April 10, 2021
Published: April 13, 2021

Abstract

The Boltzmann local physical kinetics forecasts the destruction of SC regime because of the heat movement of particles. Then, the most fundamental distinction between a strange metal and a conventional metal is the absence of well-defined quasi-particles. Here, we show that the mentioned "quasi-particles" are solitons, which are formed as a result of self-organization of ionized matter. Shortcomings of the Boltzmann physical kinetics consist in the local description of the transport processes on the level of infinitely small physical volumes as elements of diagnostics. The non-local physics leads to the theory superconductivity including the high temperature diapason. The generalized non-local non-stationary London's formula is derived.

Keywords

High Temperature Superconductivity, Generalized London's Formula, Nonlocal Physics, Transport Processes in Superconductors, Longitudinal Electromagnetic Waves, Solitons in Superconductors

1. Introduction: Shortcomings of Boltzmann Physical Kinetics

In 1872 L Boltzmann published his famous kinetic equation for the one-particle distribution function (DF) $f(\mathbf{r},\mathbf{v},t)$ [1] [2]. He expressed the equation in the form

$$\frac{Df}{Dt} = J^{st}(f) \tag{1.1}$$

where J^{st} is the collision ("stoß") integral, and

$$\frac{D}{Dt} = \frac{\partial}{\partial t} + \mathbf{v}\cdot\frac{\partial}{\partial \mathbf{r}} + \mathbf{F}\cdot\frac{\partial}{\partial \mathbf{v}} \tag{1.2}$$

is the substantial (particle) derivative, $\mathbf{v}$ and $\mathbf{r}$ being the velocity and ra-

dius-vector of the particle, respectively. Transport processes in open dissipative systems are considered in physical kinetics. Therefore, the kinetic description is inevitably related to the system diagnostics. Such an element of diagnostics in the case of theoretical description in physical kinetics is the concept of the physically infinitely small volume (**PhSV**). The correlation between theoretical description and system diagnostics is well-known in physics. Suffice it to recall the part played by test charge in electrostatics or by test circuit in the physics of magnetic phenomena.

Let us consider the hydrodynamic description in more detail from this point of view. Assume that we have two neighboring physically infinitely small volumes $\mathbf{PhSV_1}$ and $\mathbf{PhSV_2}$ in a non-equilibrium system. The one-particle distribution function (DF) $f_{sm,1}(\mathbf{r}_1,\mathbf{v},t)$ corresponds to the volume $\mathbf{PhSV_1}$, and the function $f_{sm,2}(\mathbf{r}_2,\mathbf{v},t)$ to the volume $\mathbf{PhSV_2}$. It is assumed in a first approximation that $f_{sm,1}(\mathbf{r}_1,\mathbf{v},t)$ does not vary within $\mathbf{PhSV_1}$, same as $f_{sm,2}(\mathbf{r}_2,\mathbf{v},t)$ does not vary within the neighboring volume $\mathbf{PhSV_2}$. This assumption of locality is implicitly contained in the Boltzmann equation (BE) [3]-[11]. However, the assumption is too crude; **PhSV** is an *open* thermodynamic system.

The Boltzmann equation (BE) fully ignores non-local effects and contains only the local collision integral J^B. But these nonlocal effects are irrelevant only in equilibrium systems, where the kinetic approach goes into methods of statistical mechanics. As a result, the difficulties of classical Boltzmann physical kinetics arise. Conclusion:

1) Kinetic theory should be non-local.

2) The effect is of the order of Knudsen number.

3) The effect is due to the reduced description and is not related to the specific division of the physical system by the **PhSV** grid.

4) Accurate derivation of the kinetic equation with respect to the one-particle DF should lead to corrections of the order of the Knudsen number before uncoupling the Bogolyubov chain.

5) This means that in the Boltzmann equation, the terms of the order of the Knudsen number are lost, significant for both large and small Knudsen numbers.

6) The Boltzmann equation does not even belong to the class of minimal models, being only a "plausible" equation.

7) Boltzmann equation in this sense is the wrong equation.

2. Generalization of the Boltzmann Kinetic Equation. Nonlocal Physical Kinetics

A rigorous approach to the derivation of the kinetic equation for the distribution function (DF) f_1 (KE_{f_1}) is based on the hierarchy of the Bogolyubov-Born-Green-Kirkwood-Yvon (BBGKY) equations [12] [13] [14] [15] [16]. The structure of the KE_f is generally as follows

$$\frac{Df}{Dt} = J^B + J^{nl}, \tag{2.1}$$

where J^{nl} is the non-local integral term incorporating in particular the time delay effect. The generalized Boltzmann physical kinetics, in essence, involves a local approximation

$$J^{nl} = \frac{D}{Dt}\left(\tau \frac{Df}{Dt}\right) \tag{2.2}$$

for the second collision integral, here τ being proportional to the mean time *between* the particle collisions. All of the known methods [3]-[11] of deriving kinetic equation relative to one-particle DF lead to approximation (2.2), including the method of many scales, the method of correlation functions, and the iteration method. We can draw here an analogy with the Bhatnagar-Gross-Krook (BGK, [17]) approximation for J^B,

$$J^B = \frac{f_0 - f}{\tau}, \tag{2.3}$$

which popularity as a means to represent the Boltzmann collision integral is due to the huge simplifications it offers.

In other words, the local Boltzmann collision integral admits approximation via the BGK algebraic expression (2.3), but more complicated non-local integral can be expressed as differential form (2.2). The ratio of the second to the first term on the right-hand side of Equation (2.1) is given to an order of magnitude as $J^{nl}/J^B \approx O\left(\mathrm{Kn}^2\right)$ and at large Knudsen numbers (defining as ratio of mean free path of particles to the character hydrodynamic length) these terms become of the same order of magnitude. It would seem that at small Knudsen numbers answering to hydrodynamic description the contribution from the second term on the right-hand side of Equation (2.1) is negligible.

This is not the case, however. When one goes over to the hydrodynamic approximation (by multiplying the kinetic equation by collision invariants and then integrating over velocities), the Boltzmann integral part vanishes, and the second term on the right-hand side of Equation (2.1) gives a single-order contribution in the generalized Navier-Stokes description. Mathematically, we cannot neglect a term with a small parameter in front of the higher derivative. Physically, the appearing additional terms are due to viscosity and they correspond to the small-scale Kolmogorov turbulence [8].

The integral term J^{nl} turns out to be important both at small and large Knudsen numbers in the theory of transport processes.

Thus, $\tau\, Df/Dt$ is the distribution function fluctuation, and we find

$$\frac{Df^a}{Dt} = J^B(f), \tag{2.4}$$

where

$$f^a = f - \tau \frac{Df}{Dt}. \tag{2.5}$$

Writing Equation (2.4) without taking into account Equation (2.5) makes the BE non-closed. From viewpoint of the fluctuation theory, Boltzmann employed

the simplest possible closure procedure $f^a = f$. Then, the additional GBE terms (as compared to the BE) are significant for any Kn, and the order of magnitude of the difference between the BE and GBE solutions is impossible to tell beforehand. For GBE the generalized H-theorem is proven [9].

Madelung's quantum hydrodynamics is equivalent to the Schrödinger equation (SE) and furnishes the description of the quantum particle evolution in the form of Euler equation and continuity equation. Madelung's interpretation of SE (connected with wave function $\psi = \alpha \exp(i\beta)$) leads to the probability density $\rho = \alpha^2$ and velocity $\mathbf{v} = \frac{\partial}{\partial \mathbf{r}}(\beta\hbar/m)$. *Schrödinger-Madelung quantum hydrodynamics does not lead to the energy equation in principle*; *then the Schrödinger-Madelung quantum mechanics cannot be used for the description of the dissipative processes*.

The dependent variable p in the energy equation of the generalized quantum hydrodynamics can be titled as the rest quantum pressure or simply quantum pressure.

Generalized Boltzmann physical kinetics brings the strict approximation of non-local effects in space and time and after transfer to the local approximation leads to parameter τ, which on the quantum level corresponds to the uncertainty principle "time-energy".

The appearance of the nonlocal τ parameter is consistent with the Heisenberg uncertainty relation. But in principle generalized nonlocal kinetic equations (and therefore GHE) needn't in using of the "time-energy" uncertainty relation for estimation of the value of the non-locality parameter τ. Moreover, the "time-energy" uncertainty relation does not produce the exact relations and from position of non-local physics is only the simplest estimation of the non-local effects. Really, let us consider two neighboring physically infinitely small volumes $\mathbf{PhSV_1}$ and $\mathbf{PhSV_2}$ in a non-equilibrium system. Obviously the time τ should tends to diminish with increasing of the velocities u of particles invading in the nearest neighboring physically infinitely small volume ($\mathbf{PhSV_1}$ or $\mathbf{PhSV_2}$):

$$\tau = H_\tau / u^n . \tag{2.6}$$

But the value τ cannot depend on the velocity direction and naturally to tie τ with the particle kinetic energy, then

$$\tau = H_\tau / mu^2 , \tag{2.7}$$

where H_τ is a coefficient of proportionality, which reflects the state of physical system. In the simplest case H_τ is equal to Plank constant $\hbar$ and relation (2.7) became compatible with the Heisenberg relation. The non-locality parameter τ plays the same role as the transport coefficients in local hydrodynamics. The different models can be introduced for the τ definition, but the corresponding results not much different like in local kinetic theory for different models of the particles interaction.

In the general case, the parameter τ is the non-locality parameter; in quan-

tum hydrodynamics, its magnitude is correlated with the Heisenberg "time-energy" uncertainty relation [18] [19] and with the Ehrenfest adiabatic theorem [20].

Now we can turn our attention to the quantum hydrodynamic description of individual particles. The abstract of the classical Madelung's paper [21] contains only one phrase: "It is shown that the Schrödinger equation for one-electron problems can be transformed into the form of hydrodynamic equations". The following conclusion of principal significance can be done from the previous consideration:

Madelung's quantum hydrodynamics is equivalent to the Schrödinger equation (SE) and leads to the description of the quantum particle evolution in the form of Euler equation and continuity equation. Generalized Boltzmann physical kinetics leads to the strict approximation of non-local effects in space and time and *in the local limit* leads to parameter τ, which on the quantum level corresponds to the uncertainty principle "time-energy". Generalized hydrodynamic equations (GHE) lead to SE as a deep particular case of the generalized Boltzmann physical kinetics and therefore of non-local hydrodynamics.

Finally of Item 2 we can state that introduction of control volume by the reduced description for ensemble of particles of finite diameters leads to fluctuations (proportional to Knudsen number) of velocity moments in the volume. This fact leads to the significant reconstruction of the theory of transport processes. The violation of Bell's inequalities [22] is found for local statistical theories, and the transition to the non-local description is inevitable.

3. Basic Quantum Nonlocal Hydrodynamic Equations. Superconducting Soliton Motion in the Two Component Physical System

In general case the strict consideration leads to the following system of the non-local quantum hydrodynamic equations written in the Generalized Hydrodynamic Form (GHE) for multi-component species (see also [4]-[11]):

Continuity equation for species α:

$$\begin{aligned}&\frac{\partial}{\partial t}\left\{\rho_\alpha-\tau_\alpha\left[\frac{\partial\rho_\alpha}{\partial t}+\frac{\partial}{\partial\mathbf{r}}\cdot\left(\rho_\alpha\mathbf{v}_0\right)\right]\right\}+\frac{\partial}{\partial\mathbf{r}}\cdot\left\{\rho_\alpha\mathbf{v}_0-\tau_\alpha\left[\frac{\partial}{\partial t}\left(\rho_\alpha\mathbf{v}_0\right)\right.\right.\\&\left.\left.+\frac{\partial}{\partial\mathbf{r}}\cdot\left(\rho_\alpha\mathbf{v}_0\mathbf{v}_0\right)+\ddot{\mathrm{I}}\cdot\frac{\partial p_\alpha}{\partial\mathbf{r}}-\rho_\alpha\mathbf{F}_\alpha^{(1)}-\frac{q_\alpha}{m_\alpha}\rho_\alpha\mathbf{v}_0\times\mathbf{B}\right]\right\}=R_\alpha.\end{aligned}\tag{3.1}$$

Continuity equation for mixture:

$$\begin{aligned}&\frac{\partial}{\partial t}\left\{\rho-\sum_\alpha\tau_\alpha\left[\frac{\partial\rho_\alpha}{\partial t}+\frac{\partial}{\partial\mathbf{r}}\cdot\left(\rho_\alpha\mathbf{v}_0\right)\right]\right\}\\&+\frac{\partial}{\partial\mathbf{r}}\cdot\left\{\rho\mathbf{v}_0-\sum_\alpha\tau_\alpha\left[\frac{\partial}{\partial t}\left(\rho_\alpha\mathbf{v}_0\right)+\frac{\partial}{\partial\mathbf{r}}\cdot\left(\rho_\alpha\mathbf{v}_0\mathbf{v}_0\right)\right.\right.\\&\left.\left.+\ddot{\mathrm{I}}\cdot\frac{\partial p_\alpha}{\partial\mathbf{r}}-\rho_\alpha\mathbf{F}_\alpha^{(1)}-\frac{q_\alpha}{m_\alpha}\rho_\alpha\mathbf{v}_0\times\mathbf{B}\right]\right\}=0.\end{aligned}\tag{3.2}$$

Momentum equation for species α:

$$\begin{aligned}
&\frac{\partial}{\partial t}\left\{\rho_\alpha \mathbf{v}_0 - \tau_\alpha\left[\frac{\partial}{\partial t}\left(\rho_\alpha \mathbf{v}_0\right) + \frac{\partial}{\partial \mathbf{r}}\cdot \rho_\alpha \mathbf{v}_0\mathbf{v}_0 + \frac{\partial p_\alpha}{\partial \mathbf{r}} - \rho_\alpha \mathbf{F}_\alpha^{(1)} - \frac{q_\alpha}{m_\alpha}\rho_\alpha \mathbf{v}_0 \times \mathbf{B}\right]\right\}\\
&-\mathbf{F}_\alpha^{(1)}\left[\rho_\alpha - \tau_\alpha\left(\frac{\partial \rho_\alpha}{\partial t} + \frac{\partial}{\partial \mathbf{r}}\left(\rho_\alpha \mathbf{v}_0\right)\right)\right] - \frac{q_\alpha}{m_\alpha}\left\{\rho_\alpha \mathbf{v}_0 - \tau_\alpha\left[\frac{\partial}{\partial t}\left(\rho_\alpha \mathbf{v}_0\right)\right.\right.\\
&\left.\left.+\frac{\partial}{\partial \mathbf{r}}\cdot \rho_\alpha \mathbf{v}_0\mathbf{v}_0 + \frac{\partial p_\alpha}{\partial \mathbf{r}} - \rho_\alpha \mathbf{F}_\alpha^{(1)} - \frac{q_\alpha}{m_\alpha}\rho_\alpha \mathbf{v}_0 \times \mathbf{B}\right]\right\}\times \mathbf{B} + \frac{\partial}{\partial \mathbf{r}}\cdot\left\{\rho_\alpha \mathbf{v}_0\mathbf{v}_0 + p_\alpha \vec{\mathrm{I}}\right.\\
&-\tau_\alpha\left[\frac{\partial}{\partial t}\left(\rho_\alpha \mathbf{v}_0\mathbf{v}_0 + p_\alpha \vec{\mathrm{I}}\right) + \frac{\partial}{\partial \mathbf{r}}\cdot \rho_\alpha\left(\mathbf{v}_0\mathbf{v}_0\right)\mathbf{v}_0 + 2\vec{\mathrm{I}}\left(\frac{\partial}{\partial \mathbf{r}}\cdot\left(p_\alpha \mathbf{v}_0\right)\right) + \frac{\partial}{\partial \mathbf{r}}\cdot\left(\vec{\mathrm{I}}p_\alpha \mathbf{v}_0\right)\right.\\
&\left.\left.-\mathbf{F}_\alpha^{(1)}\rho_\alpha \mathbf{v}_0 - \rho_\alpha \mathbf{v}_0\mathbf{F}_\alpha^{(1)} - \frac{q_\alpha}{m_\alpha}\rho_\alpha\left[\mathbf{v}_0 \times \mathbf{B}\right]\mathbf{v}_0 - \frac{q_\alpha}{m_\alpha}\rho_\alpha \mathbf{v}_0\left[\mathbf{v}_0 \times \mathbf{B}\right]\right]\right\}\\
&= \int m_\alpha \mathbf{v}_\alpha J_\alpha^{st,el}\mathrm{d}\mathbf{v}_\alpha + \int m_\alpha \mathbf{v}_\alpha J_\alpha^{st,inel}\mathrm{d}\mathbf{v}_\alpha.
\end{aligned} \tag{3.3}$$

Momentum equation for mixture

$$\begin{aligned}
&\frac{\partial}{\partial t}\left\{\rho \mathbf{v}_0 - \sum_\alpha \tau_\alpha\left[\frac{\partial}{\partial t}\left(\rho_\alpha \mathbf{v}_0\right) + \frac{\partial}{\partial \mathbf{r}}\cdot \rho_\alpha \mathbf{v}_0\mathbf{v}_0 + \frac{\partial p_\alpha}{\partial \mathbf{r}} - \rho_\alpha \mathbf{F}_\alpha^{(1)} - \frac{q_\alpha}{m_\alpha}\rho_\alpha \mathbf{v}_0 \times \mathbf{B}\right]\right\}\\
&-\sum_\alpha \mathbf{F}_\alpha^{(1)}\left[\rho_\alpha - \tau_\alpha\left(\frac{\partial \rho_\alpha}{\partial t} + \frac{\partial}{\partial \mathbf{r}}\left(\rho_\alpha \mathbf{v}_0\right)\right)\right] - \sum_\alpha \frac{q_\alpha}{m_\alpha}\left\{\rho_\alpha \mathbf{v}_0 - \tau_\alpha\left[\frac{\partial}{\partial t}\left(\rho_\alpha \mathbf{v}_0\right)\right.\right.\\
&\left.\left.+\frac{\partial}{\partial \mathbf{r}}\cdot \rho_\alpha \mathbf{v}_0\mathbf{v}_0 + \frac{\partial p_\alpha}{\partial \mathbf{r}} - \rho_\alpha \mathbf{F}_\alpha^{(1)} - \frac{q_\alpha}{m_\alpha}\rho_\alpha \mathbf{v}_0 \times \mathbf{B}\right]\right\}\times \mathbf{B}\\
&+\frac{\partial}{\partial \mathbf{r}}\cdot\left\{\rho \mathbf{v}_0\mathbf{v}_0 + p\vec{\mathrm{I}} - \sum_\alpha \tau_\alpha\left[\frac{\partial}{\partial t}\left(\rho_\alpha \mathbf{v}_0\mathbf{v}_0 + p_\alpha \vec{\mathrm{I}}\right) + \frac{\partial}{\partial \mathbf{r}}\cdot \rho_\alpha\left(\mathbf{v}_0\mathbf{v}_0\right)\mathbf{v}_0\right.\right.\\
&+2\vec{\mathrm{I}}\left(\frac{\partial}{\partial \mathbf{r}}\cdot\left(p_\alpha \mathbf{v}_0\right)\right) + \frac{\partial}{\partial \mathbf{r}}\cdot\left(\vec{\mathrm{I}}p_\alpha \mathbf{v}_0\right) - \mathbf{F}_\alpha^{(1)}\rho_\alpha \mathbf{v}_0 - \rho_\alpha \mathbf{v}_0\mathbf{F}_\alpha^{(1)}\\
&\left.\left.-\frac{q_\alpha}{m_\alpha}\rho_\alpha\left[\mathbf{v}_0 \times \mathbf{B}\right]\mathbf{v}_0 - \frac{q_\alpha}{m_\alpha}\rho_\alpha \mathbf{v}_0\left[\mathbf{v}_0 \times \mathbf{B}\right]\right]\right\} = 0
\end{aligned} \tag{3.4}$$

Energy equation for α species

$$\begin{aligned}
&\frac{\partial}{\partial t}\left\{\frac{\rho_\alpha v_0^2}{2} + \frac{3}{2}p_\alpha + \varepsilon_\alpha n_\alpha - \tau_\alpha\left[\frac{\partial}{\partial t}\left(\frac{\rho_\alpha v_0^2}{2} + \frac{3}{2}p_\alpha + \varepsilon_\alpha n_\alpha\right)\right.\right.\\
&\left.\left.+\frac{\partial}{\partial \mathbf{r}}\cdot\left(\frac{1}{2}\rho_\alpha v_0^2 \mathbf{v}_0 + \frac{5}{2}p_\alpha \mathbf{v}_0 + \varepsilon_\alpha n_\alpha \mathbf{v}_0\right) - \mathbf{F}_\alpha^{(1)}\cdot \rho_\alpha \mathbf{v}_0\right]\right\}\\
&+\frac{\partial}{\partial \mathbf{r}}\cdot\left\{\frac{1}{2}\rho_\alpha v_0^2 \mathbf{v}_0 + \frac{5}{2}p_\alpha \mathbf{v}_0 + \varepsilon_\alpha n_\alpha \mathbf{v}_0 - \tau_\alpha\left[\frac{\partial}{\partial t}\left(\frac{1}{2}\rho_\alpha v_0^2 \mathbf{v}_0\right.\right.\right.\\
&\left.+\frac{5}{2}p_\alpha \mathbf{v}_0 + \varepsilon_\alpha n_\alpha \mathbf{v}_0\right) + \frac{\partial}{\partial \mathbf{r}}\cdot\left(\frac{1}{2}\rho_\alpha v_0^2 \mathbf{v}_0\mathbf{v}_0 + \frac{7}{2}p_\alpha \mathbf{v}_0\mathbf{v}_0 + \frac{1}{2}p_\alpha v_0^2\vec{\mathrm{I}}\right.\\
&+\frac{5}{2}\frac{p_\alpha^2}{\rho_\alpha}\vec{\mathrm{I}} + \varepsilon_\alpha n_\alpha \mathbf{v}_0\mathbf{v}_0 + \varepsilon_\alpha \frac{p_\alpha}{m_\alpha}\vec{\mathrm{I}}\Big) - \rho_\alpha \mathbf{F}_\alpha^{(1)}\cdot \mathbf{v}_0\mathbf{v}_0 - p_\alpha \mathbf{F}_\alpha^{(1)}\cdot \vec{\mathrm{I}}\\
&\left.\left.-\frac{1}{2}\rho_\alpha v_0^2 \mathbf{F}_\alpha^{(1)} - \frac{3}{2}\mathbf{F}_\alpha^{(1)}p_\alpha - \frac{\rho_\alpha v_0^2}{2}\frac{q_\alpha}{m_\alpha}\left[\mathbf{v}_0 \times \mathbf{B}\right] - \frac{5}{2}p_\alpha \frac{q_\alpha}{m_\alpha}\left[\mathbf{v}_0 \times \mathbf{B}\right]\right.\right.
\end{aligned}$$

$$
\begin{aligned}
&-\varepsilon_\alpha n_\alpha \frac{q_\alpha}{m_\alpha}\left[\mathbf{v}_0\times\mathbf{B}\right]-\varepsilon_\alpha n_\alpha \mathbf{F}_\alpha^{(1)}\Bigg]\Bigg\}-\Bigg\{\mathbf{v}_0\cdot\sum_\alpha \rho_\alpha \mathbf{F}_\alpha^{(1)}\\
&+\frac{\partial}{\partial \mathbf{r}}\cdot\rho_\alpha \mathbf{v}_0\mathbf{v}_0+\frac{\partial}{\partial \mathbf{r}}\cdot p_\alpha \vec{\mathrm{I}}-\rho_\alpha \mathbf{F}_\alpha^{(1)}-q_\alpha n_\alpha\left[\mathbf{v}_0\times\mathbf{B}\right]\Bigg)\Bigg]\Bigg\}\\
&=\int\left(\frac{m_\alpha v_\alpha^2}{2}+\varepsilon_\alpha\right)J_\alpha^{st,el}\mathrm{d}\mathbf{v}_\alpha+\int\left(\frac{m_\alpha v_\alpha^2}{2}+\varepsilon_\alpha\right)J_\alpha^{st,inel}\mathrm{d}\mathbf{v}_\alpha.
\end{aligned}
\tag{3.5}
$$

Energy equation for mixture:

$$
\begin{aligned}
&\frac{\partial}{\partial t}\Bigg\{\frac{\rho v_0^2}{2}+\frac{3}{2}p+\sum_\alpha \varepsilon_\alpha n_\alpha-\sum_\alpha \tau_\alpha\Bigg[\frac{\partial}{\partial t}\left(\frac{\rho_\alpha v_0^2}{2}+\frac{3}{2}p_\alpha+\varepsilon_\alpha n_\alpha\right)\\
&+\frac{\partial}{\partial \mathbf{r}}\cdot\left(\frac{1}{2}\rho_\alpha v_0^2\mathbf{v}_0+\frac{5}{2}p_\alpha\mathbf{v}_0+\varepsilon_\alpha n_\alpha\mathbf{v}_0\right)-\mathbf{F}_\alpha^{(1)}\cdot\rho_\alpha\mathbf{v}_0\Bigg]\Bigg\}\\
&+\frac{\partial}{\partial \mathbf{r}}\cdot\Bigg\{\frac{1}{2}\rho v_0^2\mathbf{v}_0+\frac{5}{2}p\mathbf{v}_0+\mathbf{v}_0\sum_\alpha\varepsilon_\alpha n_\alpha-\sum_\alpha\tau_\alpha\Bigg[\frac{\partial}{\partial t}\left(\frac{1}{2}\rho_\alpha v_0^2\mathbf{v}_0\right.\\
&+\frac{5}{2}p_\alpha\mathbf{v}_0+\varepsilon_\alpha n_\alpha\mathbf{v}_0\Bigg)+\frac{\partial}{\partial \mathbf{r}}\cdot\left(\frac{1}{2}\rho_\alpha v_0^2\mathbf{v}_0\mathbf{v}_0+\frac{7}{2}p_\alpha\mathbf{v}_0\mathbf{v}_0+\frac{1}{2}p_\alpha v_0^2\vec{\mathrm{I}}\right.\\
&+\frac{5}{2}\frac{p_\alpha^2}{\rho_\alpha}\vec{\mathrm{I}}+\varepsilon_\alpha n_\alpha\mathbf{v}_0\mathbf{v}_0+\varepsilon_\alpha\frac{p_\alpha}{m_\alpha}\vec{\mathrm{I}}\Bigg)-\rho_\alpha\mathbf{F}_\alpha^{(1)}\cdot\mathbf{v}_0\mathbf{v}_0-p_\alpha\mathbf{F}_\alpha^{(1)}\cdot\vec{\mathrm{I}}\\
&-\frac{1}{2}\rho_\alpha v_0^2\mathbf{F}_\alpha^{(1)}-\frac{3}{2}\mathbf{F}_\alpha^{(1)}p_\alpha-\frac{\rho_\alpha v_0^2}{2}\frac{q_\alpha}{m_\alpha}\left[\mathbf{v}_0\times\mathbf{B}\right]-\frac{5}{2}p_\alpha\frac{q_\alpha}{m_\alpha}\left[\mathbf{v}_0\times\mathbf{B}\right]\\
&-\varepsilon_\alpha n_\alpha\frac{q_\alpha}{m_\alpha}\left[\mathbf{v}_0\times\mathbf{B}\right]-\varepsilon_\alpha n_\alpha\mathbf{F}_\alpha^{(1)}\Bigg]\Bigg\}-\Bigg\{\mathbf{v}_0\cdot\sum_\alpha\rho_\alpha\mathbf{F}_\alpha^{(1)}\\
&-\sum_\alpha\tau_\alpha\Bigg[\mathbf{F}_\alpha^{(1)}\cdot\left(\frac{\partial}{\partial t}\left(\rho_\alpha\mathbf{v}_0\right)+\frac{\partial}{\partial \mathbf{r}}\cdot\rho_\alpha\mathbf{v}_0\mathbf{v}_0\right.\\
&+\frac{\partial}{\partial \mathbf{r}}\cdot p_\alpha\vec{\mathrm{I}}-\rho_\alpha\mathbf{F}_\alpha^{(1)}-q_\alpha n_\alpha\left[\mathbf{v}_0\times\mathbf{B}\right]\Bigg)\Bigg]\Bigg\}=0.
\end{aligned}
\tag{3.6}
$$

Here $\mathbf{F}_\alpha^{(1)}$ are the forces (acting on the mass unit) of the non-magnetic origin, $\mathbf{B}$ —magnetic induction, $\vec{\mathrm{I}}$ —unit tensor, q_α —charge of the α -component particle, p_α —static pressure for α -component, ε_α —internal energy for the particles of α -component, $\mathbf{v}_0$ —hydrodynamic velocity for mixture, τ_α —non-local parameter.

In the following we intend to obtain the soliton's type of solution of the generalized hydrodynamic equations (GHE). The non-stationary 1D model will be used with taking into account the energy equation, external forces and non-locality parameter τ defined by the "time-energy" uncertainty relation of Heisenberg. Then GHE contain Poisson equation (reflected fluctuations of charges and flux of the charges density), two continuity equations for positive (lattice ions) and negative (electrons) species, momentum equation and two energy equations for positive and negative species. This system of six non-stationary 1D equations is written as:

(Generalized Poisson equation):

$$\frac{\partial^2\psi}{\partial x^2} = -4\pi e\left\{\left[n_i - \tau_i\left(\frac{\partial n_i}{\partial t} + \frac{\partial}{\partial x}(n_i u)\right)\right] - \left[n_e - \tau_e\left(\frac{\partial n_e}{\partial t} + \frac{\partial}{\partial x}(n_e u)\right)\right]\right\}. \quad (3.7)$$

(Continuity equation for ions):

$$\begin{aligned}&\frac{\partial}{\partial t}\left\{\rho_i - \tau_i\left[\frac{\partial \rho_i}{\partial t} + \frac{\partial}{\partial x}(\rho_i u)\right]\right\}\\ &+\frac{\partial}{\partial x}\left\{\rho_i u - \tau_i\left[\frac{\partial}{\partial t}(\rho_i u) + \frac{\partial}{\partial x}(\rho_i u^2) + \frac{\partial p_i}{\partial x} - \rho_i F_i\right]\right\} = 0\end{aligned}. \quad (3.8)$$

(Continuity equation for electrons):

$$\begin{aligned}&\frac{\partial}{\partial t}\left\{\rho_e - \tau_e\left[\frac{\partial \rho_e}{\partial t} + \frac{\partial}{\partial x}(\rho_e u)\right]\right\}\\ &+\frac{\partial}{\partial x}\left\{\rho_e u - \tau_e\left[\frac{\partial}{\partial t}(\rho_e u) + \frac{\partial}{\partial x}(\rho_e u^2) + \frac{\partial p_e}{\partial x} - \rho_e F_e\right]\right\} = 0\end{aligned}. \quad (3.9)$$

(Momentum equation):

$$\begin{aligned}&\frac{\partial}{\partial t}\left\{\rho u - \tau_i\left[\frac{\partial}{\partial t}(\rho_i u) + \frac{\partial}{\partial x}(p_i + \rho_i u^2) - \rho_i F_i\right]\right.\\ &\left.-\tau_e\left[\frac{\partial}{\partial t}(\rho_e u) + \frac{\partial}{\partial x}(p_e + \rho_e u^2) - \rho_e F_e\right]\right\}\\ &-\rho_i F_i - \rho_e F_e + F_i\tau_i\left(\frac{\partial \rho_i}{\partial t} + \frac{\partial}{\partial x}(\rho_i u)\right) + F_e\tau_e\left(\frac{\partial \rho_e}{\partial t} + \frac{\partial}{\partial x}(\rho_e u)\right)\\ &+\frac{\partial}{\partial x}\left\{\rho u^2 + p - \tau_i\left[\frac{\partial}{\partial t}(\rho_i u^2 + p_i) + \frac{\partial}{\partial x}(\rho_i u^3 + 3p_i u) - 2\rho_i u F_i\right]\right.\\ &\left.-\tau_e\left[\frac{\partial}{\partial t}(\rho_e u^2 + p_e) + \frac{\partial}{\partial x}(\rho_e u^3 + 3p_e u)\right] - 2\rho_e u F_e\right\} = 0.\end{aligned} \quad (3.10)$$

(Energy equation for ions):

$$\begin{aligned}&\frac{\partial}{\partial t}\left\{\rho_i u^2 + 3p_i - \tau_i\left[\frac{\partial}{\partial t}(\rho_i u^2 + 3p_i) + \frac{\partial}{\partial x}(\rho_i u^3 + 5p_i u) - 2\rho_i F_i u\right]\right\}\\ &+\frac{\partial}{\partial x}\left\{\rho_i u^3 + 5p_i u - \tau_i\left[\frac{\partial}{\partial t}(\rho_i u^3 + 5p_i u)\right.\right.\\ &\left.\left.+\frac{\partial}{\partial x}\left(\rho_i u^4 + 8p_i u^2 + 5\frac{p_i^2}{\rho_i}\right) - F_i(3\rho_i u^2 + 5p_i)\right]\right\}\\ &-2u\rho_i F_i + 2\tau_i F_i\left[\frac{\partial}{\partial t}(\rho_i u) + \frac{\partial}{\partial x}(\rho_i u^2 + p_i) - \rho_i F_i\right] = -\frac{p_i - p_e}{\tau_{ei}}.\end{aligned} \quad (3.11)$$

(Energy equation for electrons):

$$\begin{aligned}&\frac{\partial}{\partial t}\left\{\rho_e u^2 + 3p_e - \tau_e\left[\frac{\partial}{\partial t}(\rho_e u^2 + 3p_e) + \frac{\partial}{\partial x}(\rho_e u^3 + 5p_e u) - 2\rho_e F_e u\right]\right\}\\ &+\frac{\partial}{\partial x}\left\{\rho_e u^3 + 5p_e u - \tau_e\left[\frac{\partial}{\partial t}(\rho_e u^3 + 5p_e u)\right.\right.\\ &\left.\left.+\frac{\partial}{\partial x}\left(\rho_e u^4 + 8p_e u^2 + 5\frac{p_e^2}{\rho_e}\right) - F_e(3\rho_e u^2 + 5p_e)\right]\right\}\end{aligned} \quad (3.12)$$

$$-2u\rho_e F_e + 2\tau_e F_e\left[\frac{\partial}{\partial t}(\rho_e u)+\frac{\partial}{\partial x}\left(\rho_e u^2 + p_e\right)-\rho_e F_e\right] = -\frac{p_e - p_i}{\tau_{ei}},$$

where u is velocity of the directed motion of combined quantum object (phonon-electron), n_i and n_e—numerical density of the charged species, F_i and F_e—forces (of potential and non-potential origin), acting on the mass unit of the charged particles. The right hand sides of the energy equations are written in the relaxation forms following from BGK kinetic approximation.

For acting potential forces of the electrical origin the relations are valid

$$F_i^{(pot)} = -\frac{e}{m_i}\frac{\partial \psi}{\partial x}, \tag{3.13}$$

$$F_e^{(pot)} = \frac{e}{m_e}\frac{\partial \psi}{\partial x}, \tag{3.14}$$

where ψ—scalar potential.

Let us introduce approximations for τ_i and τ_i using (2.7)

$$\tau_i = \frac{\hbar}{m_i u^2}, \quad \tau_e = \frac{\hbar}{m_e u^2}. \tag{3.15}$$

For electron-phonon non-local parameter τ_{ei} the following relation is applicable

$$\frac{1}{\tau_{ei}} = \frac{1}{\tau_e} + \frac{1}{\tau_i}. \tag{3.16}$$

or

$$\frac{1}{\tau_{ei}} = \frac{\tau_e + \tau_i}{\tau_e \tau_i} = \frac{\dfrac{\hbar}{m_e u^2} + \dfrac{\hbar}{m_i u^2}}{\dfrac{\hbar^2}{u^4}\dfrac{1}{m_e m_i}} = \frac{u^2}{\hbar}\left(m_e + m_i\right). \tag{3.17}$$

Formula (3.17) is obvious consequence of uncertainty relation for combined particle which mass is $m_i + m_e$. Energy equation of the generalized quantum hydrodynamics contains pressures p_i, p_e, which can be named as the quantum pressure of the non-local origin. In the definite sense these pressures can be considered as analog of the Bose condensate pressure.

4. Combined Quantum Solitons in the Self-Consistent Electric Field

Let us formulate the problem in detail. The non-stationary 1D motion of the combined phonon-electron soliton is considered under influence of the self-consistent electric forces of the potential and non-potential origin. It should be shown that mentioned soliton can exists without a chemical bond formation. We introduce the coordinate system moving along the positive direction of the x axis in 1D space with the velocity $C = u_0$, which C is equal to the phase velocity of this quantum object.

$$\xi = x - Ct. \tag{4.1}$$

Taking into account de Broglie relation we should wait that the group velocity u_g is equal to $2u_0$. Really the energy of a relativistic particle is

$$E = mc^2, \tag{4.2}$$

where

$$m = m_0\left(1-\frac{v_g^2}{c^2}\right)^{-1/2} \tag{4.3}$$

and c is the light velocity, v_g is the group velocity, m_0 —the particle rest mass. Relation (4.2) can be written as

$$E = \mathrm{p}\frac{c^2}{v_g} \tag{4.4}$$

where

$$\mathrm{p} = mv_g \tag{4.5}$$

is the particle impulse. In the non-relativistic approach the relation (4.4) takes the form

$$E = \frac{1}{2}m_0 v_g^2. \tag{4.6}$$

Using the dualism principle in the de Broglie interpretation we have for the particle energy

$$E = \hbar\omega = \hbar k v_{ph}, \tag{4.7}$$

where ω is the circular frequency, $v_{ph} = \frac{\omega}{\kappa}$—the phase velocity, $\kappa = 2\pi/\lambda$ is the wave number and λ is the wave length. Correspondingly the particle impulse p is

$$\mathrm{p} = \hbar k \tag{4.8}$$

and using (4.8),

$$E = \mathrm{p}v_{ph}. \tag{4.9}$$

Then in the non-relativistic case we have

$$E = \frac{1}{2}m_0 v_g^2 = \frac{1}{2}\mathrm{p}v_g. \tag{4.10}$$

From (4.9) and (4.10) for the non-relativistic case one obtains

$$v_g = 2v_{ph}. \tag{4.11}$$

Then we should wait that the indestructible soliton has the velocity v_{ph} in the coordinate system moving with the phase velocity v_{ph}. If we pass on the moving coordinate system, all dependent hydrodynamic values will be functions of (ξ, t). But we investigate the possibility of the creation of the combined quantum object of the soliton type. For this case the explicit time dependence of solutions does not exist in mentioned coordinate system moving with the phase velocity u_0.

Write down the system of Equations (3.7)-(3.12) for the two component mixture of charged particles (without taking into account the component's internal energy) in the dimensionless form, where dimensionless symbols are marked by tildes. We introduce the scales for velocity $[u]=u_0$, for coordinate x $\frac{\hbar}{m_e u_0}=x_0$, for the potential scale $\psi_0=\frac{m_e}{e}u_0^2$ and for the density scale $\rho_0=\frac{m_e^4}{4\pi\hbar^2 e^2}u_0^4$ (e is absolute electron charge).

Generalized Poisson Equation (3.7) takes the form

$$\frac{\partial^2\tilde{\psi}}{\partial\tilde{\xi}^2}=-\left\{\frac{m_e}{m_i}\left[\tilde{\rho}_i-\frac{1}{u^2}\frac{m_e}{m_i}\left(-\frac{\partial\tilde{\rho}_i}{\partial\tilde{\xi}}+\frac{\partial}{\partial\tilde{\xi}}\left(\tilde{\rho}_i\tilde{u}\right)\right)\right]-\left[\tilde{\rho}_e-\frac{1}{\tilde{u}^2}\left(-\frac{\partial\tilde{\rho}_e}{\partial\tilde{\xi}}+\frac{\partial}{\partial\tilde{\xi}}\left(\tilde{\rho}_e\tilde{u}\right)\right)\right]\right\}. \tag{4.12}$$

Scaling forces are

$$\rho_i F_i=-\frac{u_0^2}{x_0}\rho_0\frac{m_e}{m_i}\frac{\partial\tilde{\psi}}{\partial\tilde{\xi}}\tilde{\rho}_i, \tag{4.13}$$

$$\rho_e F_e=\frac{u_0^2}{x_0}\rho_0\frac{\partial\tilde{\psi}}{\partial\tilde{\xi}}\tilde{\rho}_e. \tag{4.14}$$

Analogical transformations should be applied to other equations of the system (3.7)-(3.12). As result one obtains the six non-linear dimensionless ordinary differential equations

$$\frac{\partial^2\tilde{\psi}}{\partial\tilde{\xi}^2}=-\left\{\frac{m_e}{m_i}\left[\tilde{\rho}_i-\frac{1}{\tilde{u}^2}\frac{m_e}{m_i}\left(-\frac{\partial\tilde{\rho}_i}{\partial\tilde{\xi}}+\frac{\partial}{\partial\tilde{\xi}}\left(\tilde{\rho}_i\tilde{u}\right)\right)\right]-\left[\tilde{\rho}_e-\frac{1}{\tilde{u}^2}\left(-\frac{\partial\tilde{\rho}_e}{\partial\tilde{\xi}}+\frac{\partial}{\partial\tilde{\xi}}\left(\tilde{\rho}_e\tilde{u}\right)\right)\right]\right\}, \tag{4.15}$$

$$\frac{\partial\tilde{\rho}_i}{\partial\tilde{\xi}}-\frac{\partial\tilde{\rho}_i\tilde{u}}{\partial\tilde{\xi}}+\frac{m_e}{m_i}\frac{\partial}{\partial\tilde{\xi}}\left\{\frac{1}{\tilde{u}^2}\left[\frac{\partial}{\partial\tilde{\xi}}\left(\tilde{p}_i+\tilde{\rho}_i+\tilde{\rho}_i\tilde{u}^2-2\tilde{\rho}_i\tilde{u}_i\right)+\frac{m_e}{m_i}\tilde{\rho}_i\frac{\partial\tilde{\psi}}{\partial\tilde{\xi}}\right]\right\}=0, \tag{4.16}$$

$$\frac{\partial\tilde{\rho}_e}{\partial\tilde{\xi}}-\frac{\partial\tilde{\rho}_e\tilde{u}}{\partial\tilde{\xi}}+\frac{\partial}{\partial\tilde{\xi}}\left\{\frac{1}{\tilde{u}^2}\left[\frac{\partial}{\partial\tilde{\xi}}\left(\tilde{p}_e+\tilde{\rho}_e+\tilde{\rho}_e\tilde{u}^2-2\tilde{\rho}_e\tilde{u}_e\right)-\tilde{\rho}_e\frac{\partial\tilde{\psi}}{\partial\tilde{\xi}}\right]\right\}=0, \tag{4.17}$$

$$\begin{aligned}&\frac{\partial}{\partial\tilde{\xi}}\left\{\left(\tilde{\rho}_i+\tilde{\rho}_e\right)\tilde{u}^2+\tilde{p}_i+\tilde{p}_e-\left(\tilde{\rho}_i+\tilde{\rho}_e\right)\tilde{u}\right\}\\&+\frac{\partial}{\partial\tilde{\xi}}\left\{\frac{1}{\tilde{u}^2}\frac{m_e}{m_i}\left[\frac{\partial}{\partial\tilde{\xi}}\left(2\tilde{p}_i+2\tilde{p}_i\tilde{u}^2-\tilde{\rho}_i\tilde{u}-\tilde{\rho}_i\tilde{u}^3-3\tilde{p}_i\tilde{u}\right)+\tilde{\rho}_i\frac{m_e}{m_i}\frac{\partial\tilde{\psi}}{\partial\tilde{\xi}}\right]\right.\\&\left.+\frac{1}{\tilde{u}^2}\left[\frac{\partial}{\partial\tilde{\xi}}\left(2\tilde{p}_e+2\tilde{p}_e\tilde{u}^2-\tilde{\rho}_e\tilde{u}-\tilde{\rho}_e\tilde{u}^3-3\tilde{p}_e\tilde{u}\right)-\tilde{\rho}_e\frac{\partial\tilde{\psi}}{\partial\tilde{\xi}}\right]\right\}\\&+\tilde{\rho}_i\frac{m_e}{m_i}\frac{\partial\tilde{\psi}}{\partial\tilde{\xi}}-\tilde{\rho}_e\frac{\partial\tilde{\psi}}{\partial\tilde{\xi}}-\frac{\partial\tilde{\psi}}{\partial\tilde{\xi}}\frac{1}{\tilde{u}^2}\left(\frac{m_e}{m_i}\right)^2\left(-\frac{\partial\tilde{\rho}_i}{\partial\tilde{\xi}}+\frac{\partial}{\partial\tilde{\xi}}\left(\tilde{\rho}_i\tilde{u}\right)\right)\\&+\frac{\partial\tilde{\psi}}{\partial\tilde{\xi}}\frac{1}{\tilde{u}^2}\left(-\frac{\partial\tilde{\rho}_e}{\partial\tilde{\xi}}+\frac{\partial}{\partial\tilde{\xi}}\left(\tilde{\rho}_e\tilde{u}\right)\right)-2\frac{\partial}{\partial\tilde{\xi}}\left\{\frac{1}{\tilde{u}}\frac{\partial\tilde{\psi}}{\partial\tilde{\xi}}\left[\left(\frac{m_e}{m_i}\right)^2\tilde{\rho}_i-\tilde{\rho}_e\right]\right\}=0,\end{aligned} \tag{4.18}$$

$$\begin{aligned}&\frac{\partial}{\partial\tilde{\xi}}\left\{\tilde{\rho}_i\tilde{u}^3+5\,\tilde{p}_i\tilde{u}-\tilde{\rho}_i\tilde{u}^2-3\tilde{p}_i\right\}+\frac{\partial}{\partial\xi}\left\{\frac{1}{\tilde{u}^2}\frac{m_e}{m_i}\left[\frac{\partial}{\partial\tilde{\xi}}\left(2\tilde{\rho}_i\tilde{u}^3+10\tilde{p}_i\tilde{u}\right.\right.\right.\\&\left.\left.\left.-\tilde{\rho}_i\tilde{u}^4-8\tilde{p}_i\tilde{u}^2-5\frac{\tilde{p}_i^2}{\tilde{\rho}_i}-\tilde{\rho}_i\tilde{u}^2-3\tilde{p}_i\right)+\frac{m_e}{m_i}\frac{\partial\tilde{\psi}}{\partial\tilde{\xi}}\left(2\tilde{\rho}_i\tilde{u}-3\tilde{\rho}_i\tilde{u}^2-5\tilde{p}_i\right)\right]\right\}\\&+2\frac{m_e}{m_i}\tilde{\rho}_i\tilde{u}\frac{\partial\tilde{\psi}}{\partial\tilde{\xi}}-2\frac{\partial\tilde{\psi}}{\partial\xi}\frac{1}{\tilde{u}^2}\left(\frac{m_e}{m_i}\right)^2\left[\frac{\partial}{\partial\tilde{\xi}}\left(\tilde{\rho}_i\tilde{u}^2+\tilde{p}_i-\tilde{\rho}_i\tilde{u}\right)+\tilde{\rho}_i\frac{m_e}{m_i}\frac{\partial\tilde{\psi}}{\partial\tilde{\xi}}\right]\\&=-\left(\tilde{p}_i-\tilde{p}_e\right)\tilde{u}^2\left(1+\frac{m_i}{m_e}\right),\end{aligned}\tag{4.19}$$

$$\begin{aligned}&\frac{\partial}{\partial\tilde{\xi}}\left\{\tilde{\rho}_e\tilde{u}^3+5\,\tilde{p}_e\tilde{u}-\tilde{\rho}_e\tilde{u}^2-3\tilde{p}_e\right\}+\frac{\partial}{\partial\tilde{\xi}}\left\{\frac{1}{\tilde{u}^2}\left[\frac{\partial}{\partial\tilde{\xi}}\left(2\tilde{\rho}_e\tilde{u}^3+10\tilde{p}_e\tilde{u}\right.\right.\right.\\&\left.\left.\left.-\tilde{\rho}_e\tilde{u}^4-8\tilde{p}_e\tilde{u}^2-5\frac{\tilde{p}_e^2}{\tilde{\rho}_e}-\tilde{\rho}_e\tilde{u}^2-3\tilde{p}_e\right)+\frac{\partial\tilde{\psi}}{\partial\tilde{\xi}}\left(3\tilde{\rho}_e\tilde{u}^2+5\tilde{p}_e-2\tilde{\rho}_e\tilde{u}\right)\right]\right\}\\&-2\tilde{\rho}_e\tilde{u}\frac{\partial\tilde{\psi}}{\partial\tilde{\xi}}+2\frac{\partial\tilde{\psi}}{\partial\tilde{\xi}}\frac{1}{\tilde{u}^2}\left[\frac{\partial}{\partial\tilde{\xi}}\left(\tilde{\rho}_e\tilde{u}^2+\tilde{p}_e-\tilde{\rho}_e\tilde{u}\right)-\tilde{\rho}_e\frac{\partial\tilde{\psi}}{\partial\tilde{\xi}}\right]\\&=-\left(\tilde{p}_e-\tilde{p}_i\right)\left(1+\frac{m_i}{m_e}\right)\tilde{u}^2.\end{aligned}\tag{4.20}$$

Some comments to Equations (4.12, 4.15-4.20):

1) Equations. (4.12, 4.15-4.20) contain 6 dependent variables: $\tilde{\psi},\tilde{\rho}_e,\tilde{\rho}_i,\tilde{u},\tilde{p}_e,\tilde{p}_i$. Every equation from the system (4.12, 4.15-4.20) is of the second order and needs two conditions. The problem belongs to the class of Cauchy problems.

2) In comparison with the Schrödinger theory connected with behavior of the wave function, no special conditions are applied for dependent variables including the domain of the solution existing. This domain is defined automatically in the process of the numerical solution of the concrete variant of calculations.

3) From the introduced scales

$$u_0,\quad x_0=\frac{\hbar}{m_e}\frac{1}{u_0},\quad \psi_0=\frac{m_e}{e}u_0^2,\quad \rho_0=\frac{m_e^4}{4\pi\hbar^2e^2}u_0^4,\quad p_0=\rho_0u_0^2=\frac{m_e^4}{4\pi\hbar^2e^2}u_0^6\tag{4.21}$$

only one parameter is independent – the phase velocity u_0 of the combined quantum object. The value $\hbar/m_e=\upsilon_{qu}$ can be titled as quantum kinematic viscosity $\upsilon_{qu}=1.158\ \mathrm{cm}^2/\mathrm{s}$. From this point of view the obtained solutions which will be discussed below have the universal character defined only by Cauchy conditions.

5. Maple Program Realizing the Solution of the System of Equations (4.15)-(4.20)

The system of generalized quantum hydrodynamic Equations (4.12), (4.15)-(4.20) have the great possibilities of mathematical modeling as result of changing of twelve Cauchy conditions describing the character features of initial perturbations which lead to the soliton formation.

On this step of investigation we intend to demonstrate the influence of differ-

ence conditions on the soliton formation. The following figures reflect some results of calculations realized according to the system of Equations (4.12), (4.15)-(4.20) with the help of Maple. The following notations on figures are used: r—density $\tilde{\rho}_i$, s—density $\tilde{\rho}_e$, u—velocity $\tilde{u}$, p—pressure $\tilde{p}_i$, q—pressure $\tilde{p}_e$ and v—self consistent potential $\tilde{\psi}$. Explanations placed under all following figures, Maple program contains Maple's notations, for example the expression $D(u)(0)=0$ means in usual notations $\frac{\partial \tilde{u}}{\partial \tilde{\xi}}(0)=0$, independent variable t responds to $\tilde{\xi}$.

There is the problem of principle significance—is it possible after a perturbation (defined *by Cauchy conditions*) to obtain *the quantum object of the soliton's kind* as result of the self-organization of ionized matter? In the case of the positive answer, what is the origin of existence of this stable object?

Appendixes 1 and **2** contain the corresponding Maple programs. The programs are ready for using.

6. Super-Conductivity as Movement of Solitons without Destruction

Let us demonstrate some examples of application of non-local GHE with the help of the Maple program in the Item 5. Significant remarks:

1) We investigate the wave movement of two component ionized matter in the form of moving solitons. It is known that the Schrödinger-Madelung quantum mechanics leads to the soliton destruction.

Extremely important that the really working super-conductivity theory should lead to the soliton conservation in the frame of Cauchy problem, but not as a boundary problem. It means that we should observe the self-organization of matter.

2) The program contains the following Cauchy dimensionless parameters: $\tilde{\psi}(0)$—self-consistent potential and $\frac{\partial \tilde{\psi}}{\partial \tilde{\xi}}(0)$, $\tilde{u}(0)$—velocity and $\frac{\partial \tilde{u}}{\partial \tilde{\xi}}(0)$, $\tilde{\rho}_e(0)$ density of negative particles and $\frac{\partial \tilde{\rho}_e}{\partial \tilde{\xi}}(0)$, $\tilde{\rho}_i(0)$ density of positive particles and $\frac{\partial \tilde{\rho}_i}{\partial \tilde{\xi}}(0)$, $\tilde{p}_e(0)$ pressure of negative particles and $\frac{\partial \tilde{p}_e}{\partial \tilde{\xi}}(0)$, $\tilde{p}_i(0)$ pressure of positive particles and $\frac{\partial \tilde{p}_i}{\partial \tilde{\xi}}(0)$, and the mass ratio of hard (H) and light (L) particles. The program (**Appendix 1**) is ready for calculations.

3) Let us demonstrate some calculations changing the pressure parameters by ten orders of magnitude. We introduce the dimensionless soliton energetic temperature $\tilde{T}_{en,sol}$ using the definition

$$\tilde{T}_{en,sol}=\frac{\tilde{p}_i}{\tilde{R}_i}, \tag{6.1}$$

where

$$\tilde{R}_i = \int_{(\tilde{\xi})} \tilde{\rho}_i \mathrm{d}\tilde{\xi} \,. \tag{6.2}$$

Analogically we have

$$\tilde{S}_e = \int_{(\tilde{\xi})} \tilde{\rho}_e \mathrm{d}\tilde{\xi} \,. \tag{6.3}$$

Figures 1-6 reflect the calculations for the Cauchy conditions
v(0)=1,r(0)=1,s(0)=1/1838,u(0)=1,p(0)=1000,
q(0)=950,D(v)(0)=0,D(r)(0)=0,D(s)(0)=0,D(u)(0)=0,
D(p)(0)=0,D(q)(0)=0,R(0)=0,S(0)=0.
Figures 7-12 reflect the calculations for the Cauchy conditions
v(0)=1,r(0)=1,s(0)=1/1838,u(0)=1,p(0)=0.000001,
q(0)=.00000095,D(v)(0)=0,D(r)(0)=0,D(s)(0)=0,D(u)(0)=0,
D(p)(0)=0,D(q)(0)=0,R(0)=0,S(0)=0.
Table 1 contains the Cauchy conditions for pressure, the boundaries $\tilde{\xi}$ (designated as lim1 and lim2) of the soliton, dimensionless energetic temperature for positive particles and dimensionless concentration of the captured electrons.

From our results obtained in the frame of nonlocal physics follow:

1) Nonlocal quantum hydrodynamics leads to the following physical picture of super-conductivity. So called "quasi-particles" are in reality the solitons which cannot be discovered in Schrödinger-Madelung theory in principal.

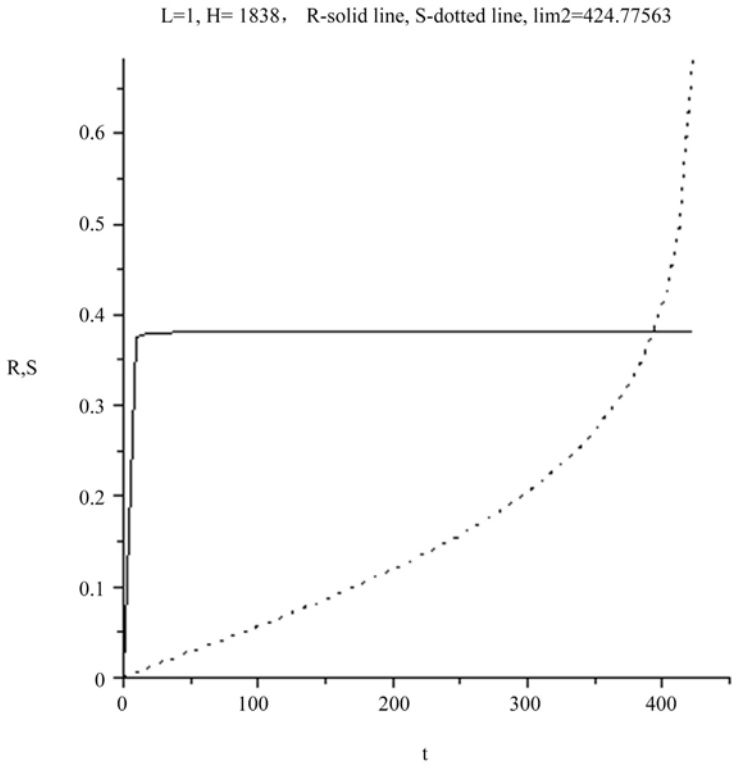

Figure 1. Dimensionless energetic temperature R for positive particles and dimensionless concentration S of the captured electrons.

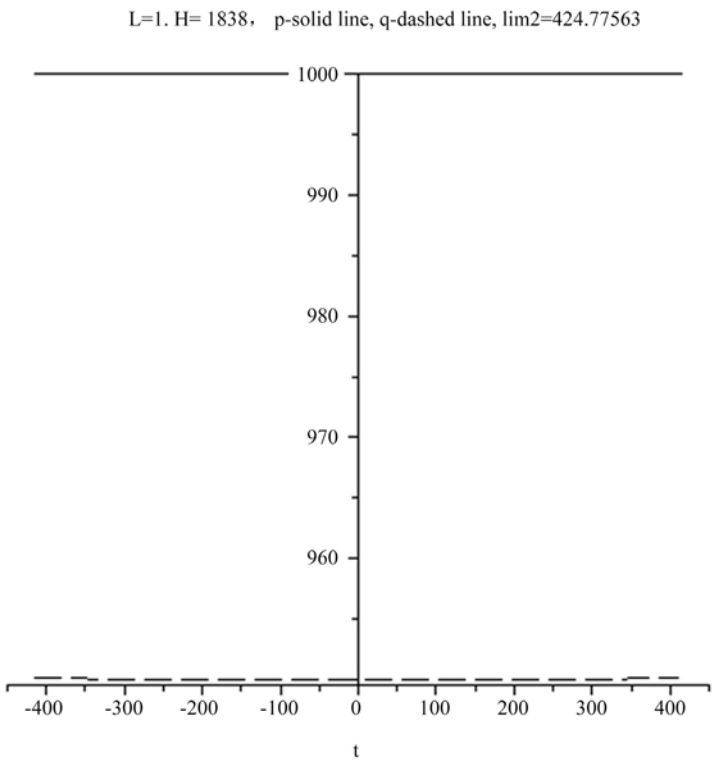

Figure 2. q— $\tilde{p}_e\left(\tilde{\xi}\right)$ pressure of negative particles, p— $\tilde{p}_i\left(\tilde{\xi}\right)$ pressure of positive particles.

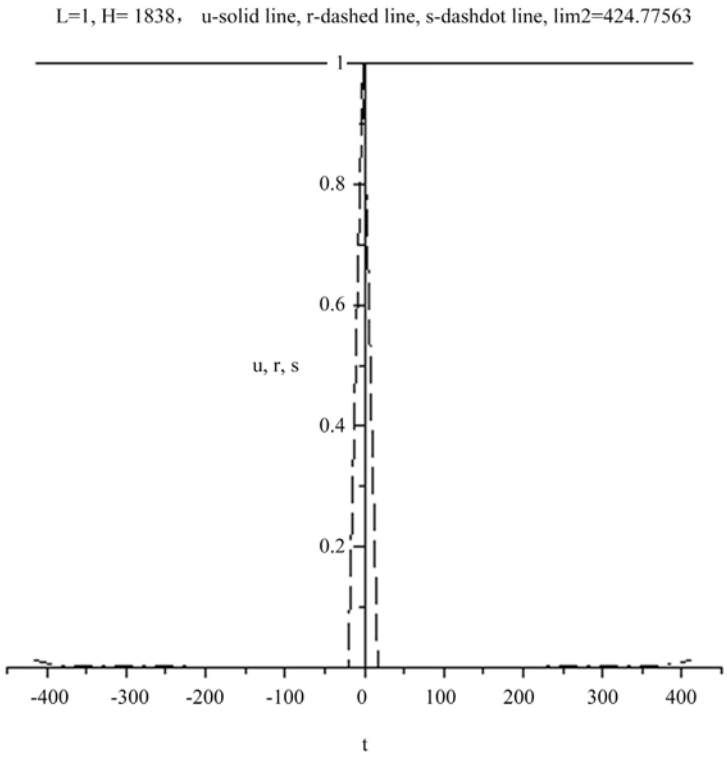

Figure 3. u—velocity $\tilde{u}\left(\tilde{\xi}\right)$, r—density $\tilde{\rho}_i\left(\tilde{\xi}\right)$.

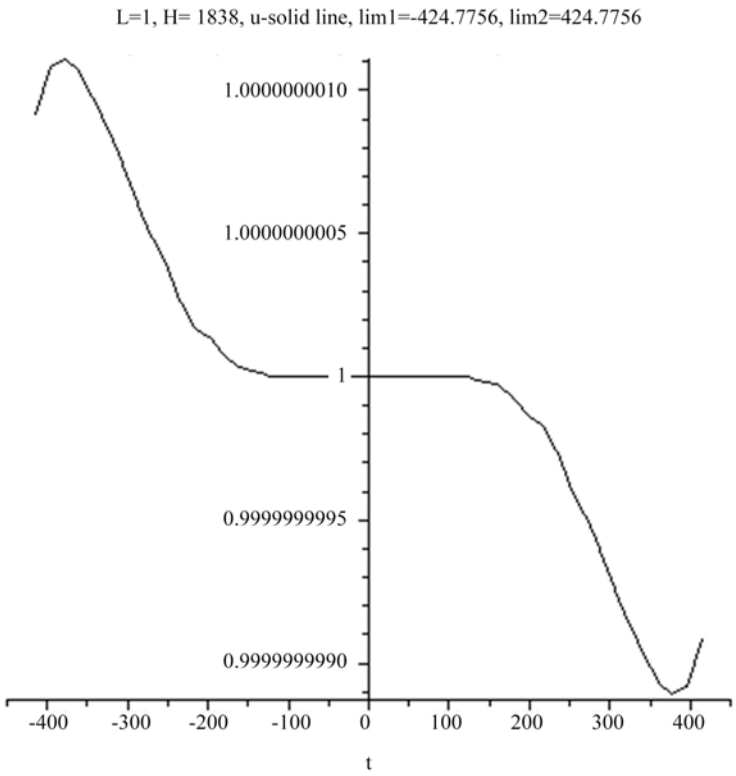

Figure 4. Velocity u— $\tilde{u}(\xi)$.

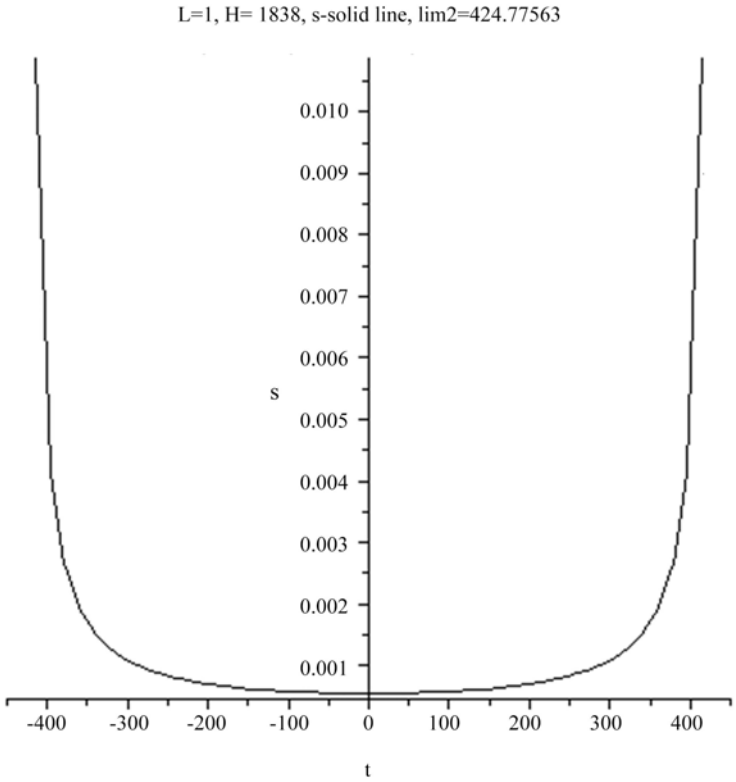

Figure 5. s—density $\tilde{\rho}_e(\tilde{\xi})$.

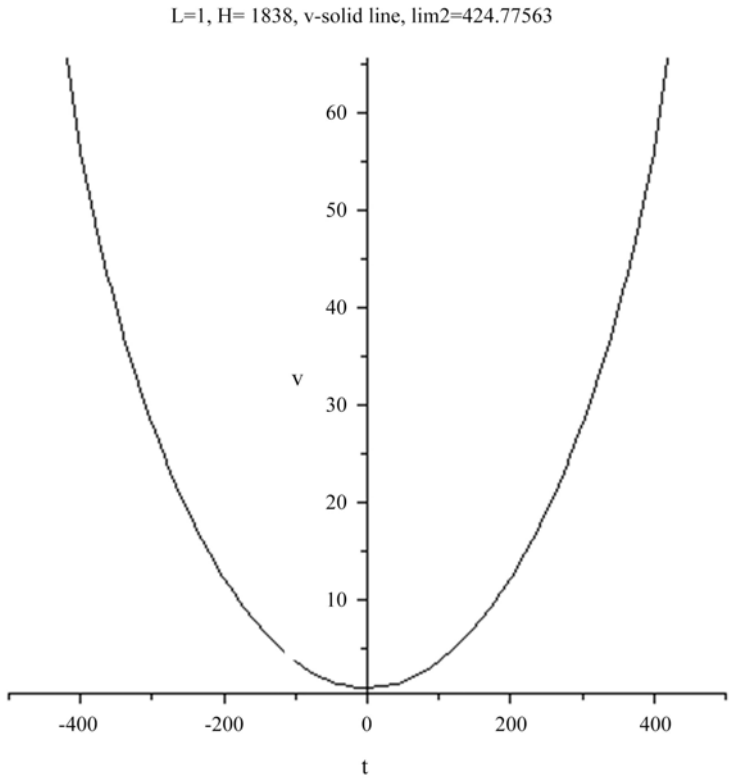

Figure 6. Self-consistent potential v— $\tilde{\psi}\left(\tilde{\xi}\right)$.

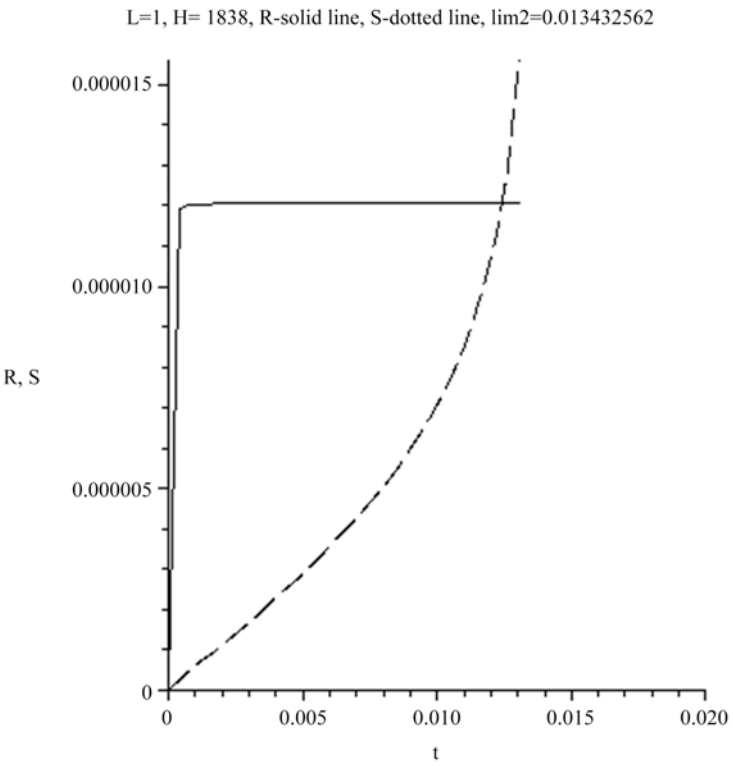

Figure 7. Dimensionless energetic temperature R for positive particles and dimensionless concentration S of the captured electrons.

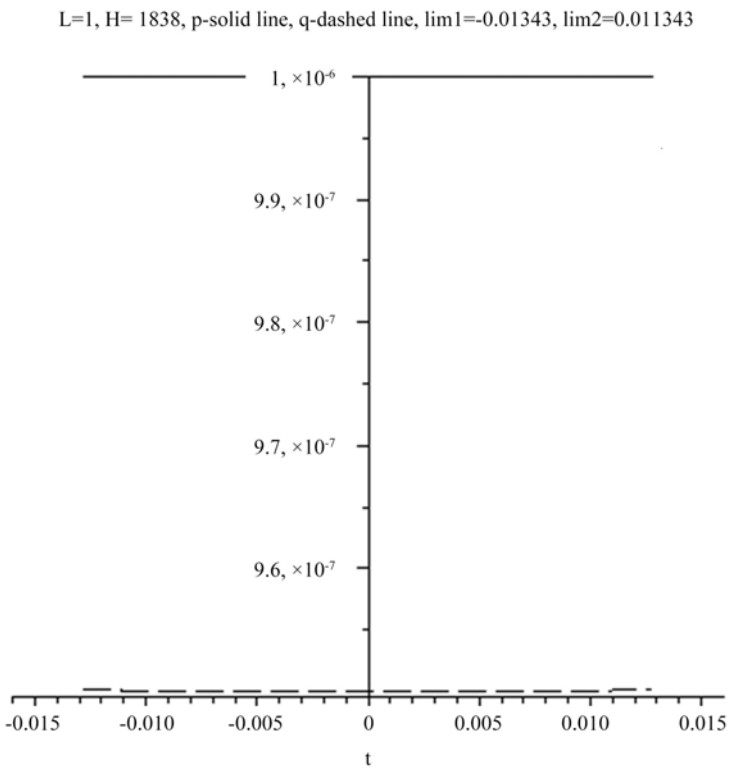

Figure 8. q— $\tilde{p}_e\left(\tilde{\xi}\right)$ pressure of negative particles, p— $\tilde{p}_i\left(\tilde{\xi}\right)$ pressure of positive particles.

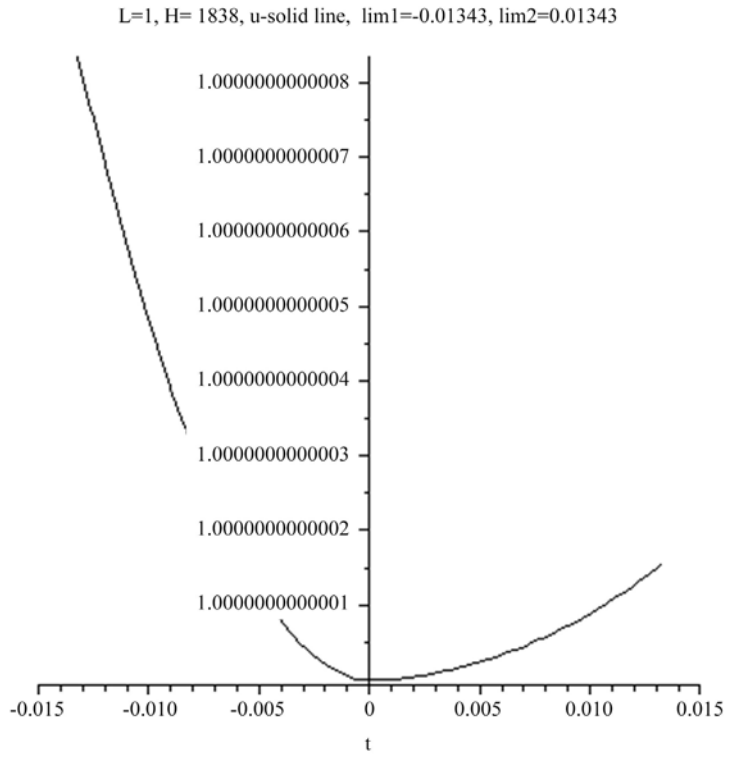

Figure 9. u—velocity $\tilde{u}\left(\tilde{\xi}\right)$.

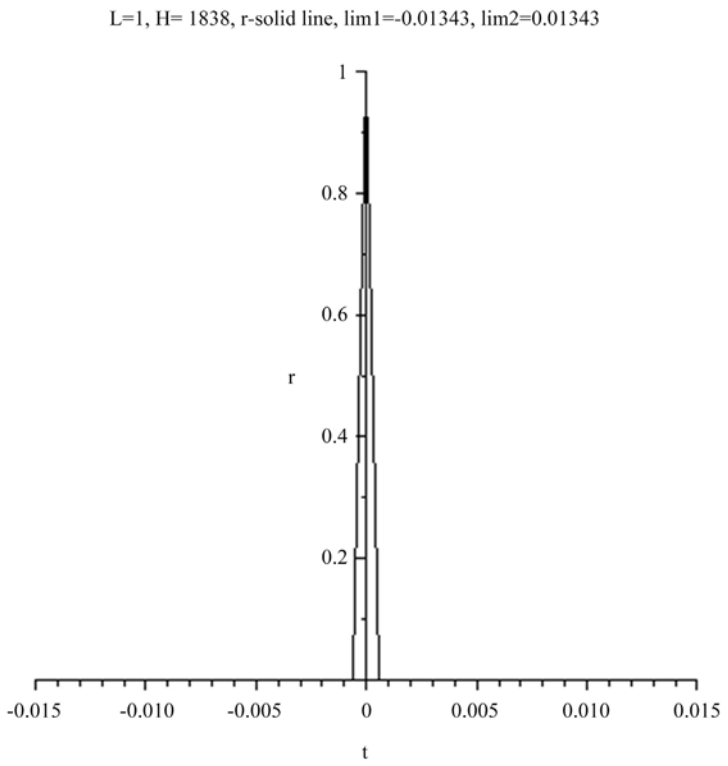

Figure 10. r—density $\tilde{\rho}_i\left(\tilde{\xi}\right)$.

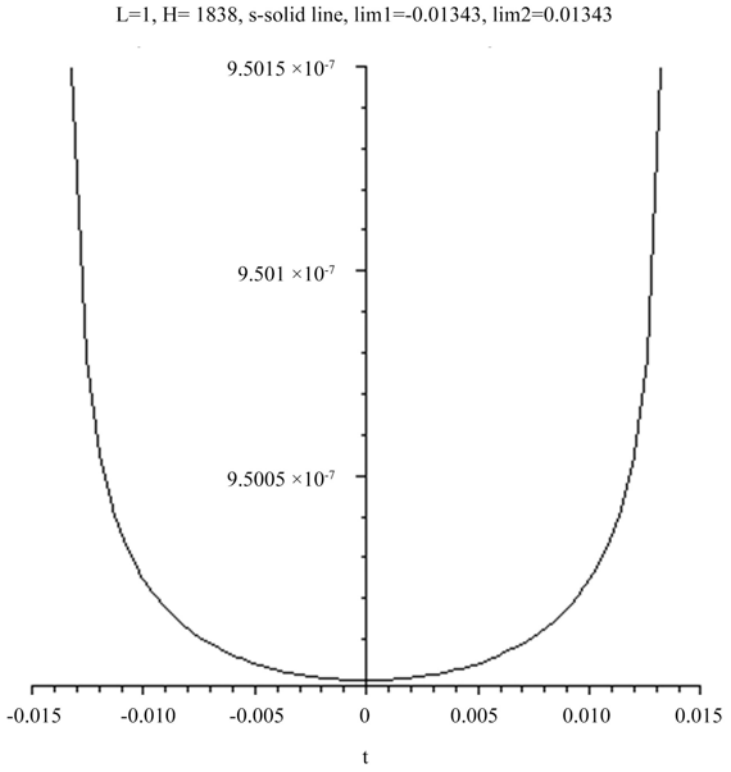

Figure 11. s—density $\tilde{\rho}_e\left(\tilde{\xi}\right)$.

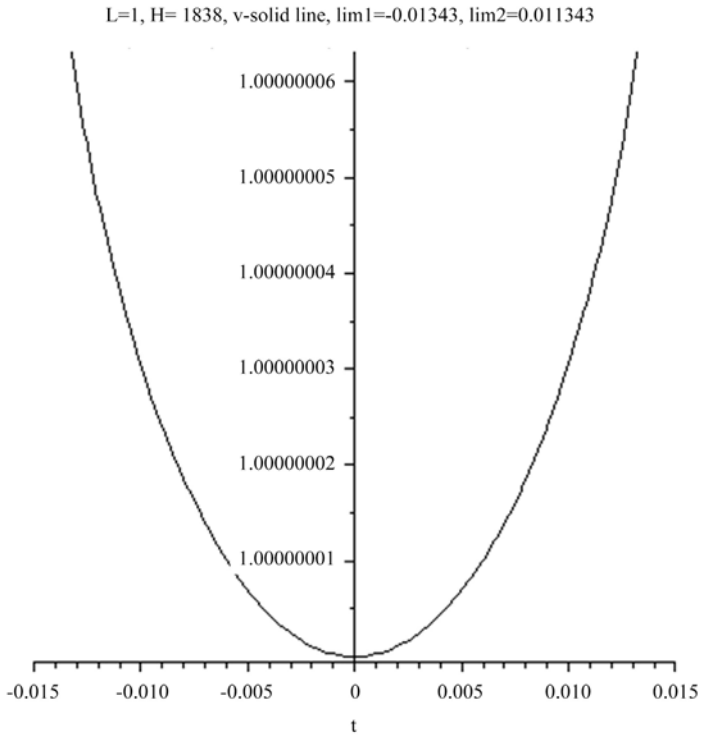

Figure 12. Self-consistent potential v— $\tilde{\psi}\left(\tilde{\xi}\right)$.

Table 1. Cauchy conditions for pressure, the boundaries $\tilde{\xi}$ (designated as lim1 and lim2) of the soliton, dimensionless energetic temperature for positive particles and dimensionless concentration of the captured electrons.

$\tilde{p}_i(0)$	$\tilde{p}_e(0)$	−lim1	lim2	$\tilde{T}_{en,sol}$	$\tilde{S}_e$
10^3	950	424.7759	424.7759	1309.9075	3.8571
10^2	95	130.8158	130.8158	436.4822	1.1636
10	9.5	42.4775	42.4775	130.9130	0.4294
1	0.95	13.4325	13.4325	41.3996	1.2591×10^{-1}
0.1	0.095	4.2477	4.2477	13.0909	4.5475×10^{-2}
0.01	0.0095	1.3432	1.3432	4.1396	1.4075×10^{-2}
10^{-3}	0.95×10^{-3}	0.4247	0.4247	1.3090	0.4019×10^{-2}
10^{-4}	0.95×10^{-4}	0.1343	0.1343	0.4139	1.2488×10^{-3}
10^{-5}	0.95×10^{-5}	0.04247	0.04247	0.1352	0.3868×10^{-3}
10^{-6}	0.95×10^{-6}	0.01343	0.01343	0.04139	1.0099×10^{-4}

2) The stability of the quantum object is result of the self organization of the ionized matter. In other words—it is self-consistent influence of electric forces and quantum pressures. Solitons defines the extremely "stiff" structure. Look at Figure 4 and Figure 9—all solitons parts are moving with the same velocity.

3) Stability can be achieved if soliton has negative "shell" and positive "nuclei" and $\tilde{p}_i(0) > \tilde{p}_e(0)$, or if soliton has positive "shell" and negative "nuclei" and

$\tilde{p}_i(0) < \tilde{p}_e(0)$. The moving plane waves remind the structure of "flat atoms" or paired electrons in BCS theory. The previous figures display the typical quantum objects placed in the bounded region of 1D space, all parts of these objects are moving with the same velocity. Namely from calculations follow that in coordinate system moving with the phase velocity, indestructible soliton has the velocity equal to the phase velocity. Moreover the attempt to impose to soliton to move with another group velocity leads to the soliton destruction.

4) Table 1 demonstrates practically the linear dependence between energetic temperature and quantity of captured electrons. All quantum fluctuations in quantum GHE (see Equations 3.1-3.6, 3.7-3.12 and relations 3.15-3.17) are proportional to the Planck constant $\hbar$.

7. The Charge Carrier's Behavior near the Critical Point

The step function for profiles in the vicinity of the critical temperature T_c can be obtained analytically from the nonlocal GHE equations. Really let us consider the generalized continuum Equations (4.16) and (4.17). Equation

$$\frac{\partial\tilde{\rho}_e}{\partial\tilde{\xi}} - \frac{\partial\tilde{\rho}_e\tilde{u}}{\partial\tilde{\xi}} + \frac{\partial}{\partial\tilde{\xi}}\left\{\frac{1}{\tilde{u}^2}\left[\frac{\partial}{\partial\tilde{\xi}}\left(\tilde{p}_e + \tilde{\rho}_e + \tilde{\rho}_e\tilde{u}^2 - 2\tilde{\rho}_e\tilde{u}_e\right) - \tilde{\rho}_e\frac{\partial\tilde{\psi}}{\partial\tilde{\xi}}\right]\right\} = 0 \tag{7.1}$$

can be immediately integrated

$$\tilde{\rho}_e(1-\tilde{u}) = -\frac{1}{\tilde{u}^2}\left[\frac{\partial}{\partial\tilde{\xi}}\left(\tilde{p}_e + \tilde{\rho}_e + \tilde{\rho}_e\tilde{u}^2 - 2\tilde{\rho}_e\tilde{u}_e\right) - \tilde{\rho}_e\frac{\partial\tilde{\psi}}{\partial\tilde{\xi}}\right]. \tag{7.2}$$

But for all parts of solitons velocity $\tilde{u} = 1$. Then

$$\frac{\partial\tilde{p}_e}{\partial\tilde{\xi}} = \tilde{\rho}_e\frac{\partial\tilde{\psi}}{\partial\tilde{\xi}}. \tag{7.3}$$

In the vicinity of T_c we have $\tilde{T}_{e,en} \sim const$ and Equation (7.3) is written as follows

$$\tilde{T}_{C,en,e}\frac{\partial\tilde{\rho}_e}{\partial\tilde{\xi}} = \tilde{\rho}_e\frac{\partial\tilde{\psi}}{\partial\tilde{\xi}} \tag{7.4}$$

or

$$\tilde{T}_{C,en,e}\frac{\partial\ln\tilde{\rho}_e}{\partial\tilde{\xi}} = \frac{\partial\tilde{\psi}}{\partial\tilde{\xi}}. \tag{7.5}$$

After (7.5) integration we have practically step function.

$$\tilde{\rho}_e = \tilde{\rho}_{e0}\mathrm{e}^{\frac{\tilde{\psi}}{\tilde{T}_{Ce,en}}}. \tag{7.6}$$

Analogically for equation

$$\frac{\partial\tilde{\rho}_i}{\partial\tilde{\xi}} - \frac{\partial\tilde{\rho}_i\tilde{u}}{\partial\tilde{\xi}} + \frac{m_e}{m_i}\frac{\partial}{\partial\tilde{\xi}}\left\{\frac{1}{\tilde{u}^2}\left[\frac{\partial}{\partial\tilde{\xi}}\left(\tilde{p}_i + \tilde{\rho}_i + \tilde{\rho}_i\tilde{u}^2 - 2\tilde{\rho}_i\tilde{u}_i\right) + \frac{m_e}{m_i}\tilde{\rho}_i\frac{\partial\tilde{\psi}}{\partial\tilde{\xi}}\right]\right\} = 0 \tag{7.7}$$

we find

$$\tilde{\rho}_i = \tilde{\rho}_{i0}\mathrm{e}^{-\frac{m_e}{m_i}\frac{\tilde{\psi}}{\tilde{T}_{C,i,en}}}. \tag{7.8}$$

Some remarks concerning the scales relations. Let us remind Homes-Zaanen relation [23] [24] [25] [26]

$$\tau\left(T_c\right) \approx \frac{\hbar}{k_B T_c} \tag{7.9}$$

or taking into account that in the soliton's boundaries

$$\tilde{u} = 1 \tag{7.10}$$

we find (see (3.15))

$$\tau_e = \frac{\hbar}{m_e u_0^2}, \tag{7.11}$$

where u_0 is the phase velocity of the soliton's movement. An attempt to impose a velocity different from the phase velocity using Cauchy conditions leads to the destruction of the soliton, and hence to the destruction of superconductivity. Then

$$m_e u_0^2 \sim k_B T_c \tag{7.12}$$

and we reach the scaling law (7.9) in the frame of nonlocal physics

$$\tau\left(T_c\right) \approx \frac{\hbar}{k_B T_c}. \tag{7.13}$$

This time is very short. By analogy with the theory of gravity, it was called the "Planck time" for dissipation. The attempt to tie the superconductivity effects with the cosmological problems seems unacceptable only from the first glance. The origin of this analogy is connected with nonlocal physical kinetics which applicable from the Planck time in the Big Bang theory to the Universe evolution, [7].

It means that we find the phase velocity

$$u_0 = \sqrt{\frac{k_B T_c}{m_e}} \tag{7.14}$$

or (the value $\hbar/m_e = \upsilon_{qu}$ can be titled as quantum kinematic viscosity $\upsilon_{qu} = 1.158\ \mathrm{cm}^2/\mathrm{s}$,

Planck constant $\hbar = 1.0545726 \times 10^{-34}\ \mathrm{J \cdot s}$, Boltzmann constant $k_B = 1.380649 \times 10^{-23}\ \mathrm{J/K}$)

$u_0 = \sqrt{\upsilon_{qu} \frac{k_B T_c}{\hbar}} = 0.389 \times 10^6 \sqrt{T_c}\ \frac{\mathrm{cm}}{\mathrm{s}}$, where T_c is the temperature measured in Kelvin.

The time scale we used

$$\tau_0 = \frac{\hbar}{m_e u_0^2} = \frac{\upsilon_{qu}}{u_0^2} = \frac{\hbar}{k_B T_c}. \tag{7.15}$$

Let us introduce and calculate the corresponding Reynolds number

$$\mathrm{Re}_{qu} = \frac{u_0 x_0}{\upsilon_{qu}} = u_0 \frac{\hbar}{m_e u_0} \frac{m_e}{\hbar} = 1. \tag{7.16}$$

In other words we consider the flow of nonlocal quantum liquid by the condition $\mathrm{Re}_{qu}=1$.

8. The Generalized Non-Local London's Theory. Longitudinal Electro-Magnetic Waves. The Basic Equations

We use generalized nonlocal Maxwell equations to prove the existence of longitudinal electromagnetic waves. To this end let's differentiate in time both parts of the Maxwell equation.

$$\frac{\partial}{\partial t}\left[\frac{\partial}{\partial \mathbf{r}}\times\mathbf{H}\right]=\frac{\partial^2\mathbf{D}}{\partial t^2}+\frac{\partial}{\partial t}\mathbf{j}^c, \tag{8.1}$$

where $\mathbf{j}^c=\mathbf{j}^a+\mathbf{j}^{fl}$, $\mathbf{j}^{fl}$ is fluctuation of the current density. We find

$$\frac{\partial}{\partial \mathbf{r}}\times\frac{\partial}{\partial t}\left(\mu\mu_0\mathbf{H}\frac{1}{\mu\mu_0}\right)=\frac{\partial^2\mathbf{D}}{\partial t^2}+\frac{\partial}{\partial t}\mathbf{j}^c \tag{8.2}$$

$$\frac{\partial}{\partial \mathbf{r}}\times\left[\frac{1}{\mu\mu_0}\frac{\partial}{\partial t}\left[\mu\mu_0\mathbf{H}\right]-\mathbf{H}\frac{\partial\ln\mu}{\partial t}\right]=\frac{\partial^2\mathbf{D}}{\partial t^2}+\frac{\partial}{\partial t}\mathbf{j}^c. \tag{8.3}$$

Obviously the second term in the square bracket can be omitted with the good accuracy, we find

$$\frac{\partial}{\partial \mathbf{r}}\times\left[\frac{1}{\mu\mu_0}\frac{\partial}{\partial t}\left[\mu\mu_0\mathbf{H}\right]\right]=\frac{\partial^2\mathbf{D}}{\partial t^2}+\frac{\partial}{\partial t}\mathbf{j}^c \tag{8.4}$$

or

$$\frac{\partial}{\partial \mathbf{r}}\times\left[\frac{1}{\mu\mu_0}\frac{\partial}{\partial \mathbf{r}}\times\mathbf{E}\right]=-\frac{\partial^2\mathbf{D}}{\partial t^2}-\frac{\partial}{\partial t}\mathbf{j}^c, \tag{8.5}$$

It is known that the double vector product is

$$\mathbf{a}\times\mathbf{b}\times\mathbf{c}=\mathbf{b}\left(\mathbf{a}\cdot\mathbf{c}\right)-\mathbf{c}\left(\mathbf{a}\cdot\mathbf{b}\right). \tag{8.6}$$

Then

$$\frac{\partial}{\partial \mathbf{r}}\times\left[\frac{1}{\mu\mu_0}\frac{\partial}{\partial \mathbf{r}}\times\mathbf{E}\right]=\frac{1}{\mu\mu_0}\frac{\partial}{\partial \mathbf{r}}\left[\frac{\partial}{\partial \mathbf{r}}\cdot\mathbf{E}\right]-\frac{1}{\mu\mu_0}\Delta\mathbf{E}. \tag{8.7}$$

Then the Equation (8.4) is written as follows

$$\frac{\partial^2\mathbf{D}}{\partial t^2}+\frac{\partial}{\partial t}\mathbf{j}^c=\frac{1}{\mu\mu_0}\Delta\mathbf{E}-\frac{1}{\mu\mu_0}\frac{\partial}{\partial \mathbf{r}}\left[\frac{\partial}{\partial \mathbf{r}}\cdot\mathbf{E}\right] \tag{8.8}$$

or if the electric permeability *does not depend on time* we have

$$\varepsilon\varepsilon_0\frac{\partial^2\mathbf{E}}{\partial t^2}+\frac{\partial}{\partial t}\mathbf{j}^c=\frac{1}{\mu\mu_0}\left\{\Delta\mathbf{E}-\frac{\partial}{\partial \mathbf{r}}\left[\frac{\partial}{\partial \mathbf{r}}\cdot\mathbf{E}\right]\right\} \tag{8.9}$$

or

$$\frac{1}{v_\phi^2}\frac{\partial^2\mathbf{E}}{\partial t^2}+\mu\mu_0\frac{\partial}{\partial t}\mathbf{j}^c=\Delta\mathbf{E}-\frac{\partial}{\partial \mathbf{r}}\left[\frac{\partial}{\partial \mathbf{r}}\cdot\mathbf{E}\right] \tag{8.10}$$

where

$$\frac{1}{v_\phi^2} = \varepsilon\varepsilon_0\mu\mu_0 . \tag{8.11}$$

We write (8.10) in the form

$$\frac{1}{v_\phi^2}\frac{\partial^2\mathbf{E}}{\partial t^2} + \mu\mu_0\frac{\partial}{\partial t}\mathbf{j}^a + \mu\mu_0\frac{\partial}{\partial t}\mathbf{j}^{fl} = \Delta\mathbf{E} - \frac{\partial}{\partial\mathbf{r}}\left[\frac{\partial}{\partial\mathbf{r}}\cdot\mathbf{E}\right], \tag{8.12}$$

where (see [4] [8])

$$\mathbf{j}^{fl} = \tau\left[\frac{\partial}{\partial t}\left(\rho\mathbf{v}_0\right) + \frac{\partial}{\partial\mathbf{r}}\cdot\left(\rho\mathbf{v}_0\mathbf{v}_0\right) + \frac{\partial p}{\partial\mathbf{r}} - \rho\mathbf{g}\right] \tag{8.13}$$

or

$$\mathbf{j}^{fl} = \tau\left[\frac{\partial}{\partial t}\left(nq\mathbf{v}_0\right) + \frac{\partial}{\partial\mathbf{r}}\cdot\left(nq\mathbf{v}_0\mathbf{v}_0\right) + \frac{q}{m}\frac{\partial p}{\partial\mathbf{r}}\left(nk_BT\right) - nq\mathbf{g}\right]. \tag{8.14}$$

Then the nonlocal Equation (8.12) takes the form

$$\begin{aligned}&\frac{1}{v_\phi^2}\frac{\partial^2\mathbf{E}}{\partial t^2} + \mu\mu_0\frac{\partial}{\partial t}\left\{\tau\frac{\partial}{\partial t}\mathbf{j}^a\right\}\\ &= \Delta\mathbf{E} - \frac{\partial}{\partial\mathbf{r}}\left[\frac{\partial}{\partial\mathbf{r}}\cdot\mathbf{E}\right] - \mu\mu_0\frac{\partial}{\partial t}\mathbf{j}^a\\ &\quad - \mu\mu_0\frac{\partial}{\partial t}\left\{\tau\left[\frac{\partial}{\partial\mathbf{r}}\cdot\left(\mathbf{j}^a\mathbf{v}_0\right) + \frac{q}{m}\frac{\partial}{\partial\mathbf{r}}\left(nk_BT\right) - nq\mathbf{g}\right]\right\}.\end{aligned} \tag{8.15}$$

Let be

$$\mathbf{j}^a = \sigma\mathbf{E}, \tag{8.16}$$

where σ is the coefficient of conductivity. In the simplest Drude model

$$\sigma = \frac{ne^2}{2m^*}\tau_r, \tag{8.17}$$

where n is numerical electron density, m^* is effective mass, τ_r is the relaxation time, the dimension of the conductivity is s^{-1}. As we see from the definition of m^*, the introduction of an "effective" mass translates the relaxation time *to the level of the fitting parameter*. If nonlocal parameter $\tau = const$ and the coefficient of conductivity $\sigma = \sigma\left(x, y, z\right)$, we have

$$\begin{aligned}&\frac{\partial^2\mathbf{E}}{\partial t^2} + \mu\mu_0 v_\phi^2\tau\frac{\partial^2\mathbf{j}^a}{\partial t^2}\\ &= v_\phi^2\left\{\Delta\mathbf{E} - \frac{\partial}{\partial\mathbf{r}}\left[\frac{\partial}{\partial\mathbf{r}}\cdot\mathbf{E}\right]\right\} - \mu\mu_0 v_\phi^2\frac{\partial}{\partial t}\mathbf{j}^a\\ &\quad - \mu\mu_0 v_\phi^2\tau\frac{\partial}{\partial t}\left[\frac{\partial}{\partial\mathbf{r}}\cdot\left(\mathbf{j}^a\mathbf{v}_0\right)\right] - \mu\mu_0 v_\phi^2\tau\frac{\partial}{\partial t}\left[\frac{q}{m}\frac{\partial}{\partial\mathbf{r}}\left(nk_BT\right) - nq\mathbf{g}\right]\end{aligned} \tag{8.18}$$

or

$$\begin{aligned}\left[1 + \frac{\tau\sigma}{\varepsilon_0\varepsilon}\right]\frac{\partial^2\mathbf{E}}{\partial t^2} &= v_\varphi^2\left\{\Delta\mathbf{E} - \frac{\partial}{\partial\mathbf{r}}\left[\frac{\partial}{\partial\mathbf{r}}\cdot\mathbf{E}\right]\right\} - \frac{\sigma}{\varepsilon_0\varepsilon}\frac{\partial\mathbf{E}}{\partial t} - \frac{\tau}{\varepsilon_0\varepsilon}\frac{\partial}{\partial t}\left[\frac{\partial}{\partial\mathbf{r}}\cdot\left(\sigma\mathbf{E}\mathbf{v}_0\right)\right]\\ &\quad - \frac{\tau}{\varepsilon_0\varepsilon}\frac{\partial}{\partial t}\left[\frac{q}{m}\frac{\partial}{\partial\mathbf{r}}\left(nk_BT\right) - nq\mathbf{g}\right]\end{aligned} \tag{8.19}$$

Equation (8.19) is the basement relation for following investigation.

9. The Nonlocal Theory of Longitudinal Electromagnetic Waves. The 1D Non-Stationary Case

Let us investigate the 1D non-stationary case. For the 1D case (x—direction), we find from (8.19)

$$\left[1+\frac{\tau\sigma}{\varepsilon_0\varepsilon}\right]\frac{\partial^2 E_x}{\partial t^2}=-\frac{\sigma}{\varepsilon_0\varepsilon}\frac{\partial E_x}{\partial t}-\frac{\tau}{\varepsilon_0\varepsilon}\frac{\partial}{\partial t}\left[\frac{\partial}{\partial x}\left(\sigma E_x v_{0x}\right)\right] -\frac{\tau}{\varepsilon_0\varepsilon}\frac{\partial}{\partial t}\left[\frac{q}{m}\frac{\partial}{\partial x}\left(nk_BT\right)-nqg_x\right]. \tag{9.1}$$

After integration we find

$$\left[1+\frac{\tau\sigma}{\varepsilon_0\varepsilon}\right]\frac{\partial E_x}{\partial t}=-\frac{\sigma}{\varepsilon_0\varepsilon}E_x-\frac{\tau}{\varepsilon_0\varepsilon}\frac{\partial}{\partial x}\left(\sigma E_x v_{0x}\right) -\frac{\tau}{\varepsilon_0\varepsilon}q\left[\frac{1}{m}\frac{\partial}{\partial x}\left(nk_BT\right)-ng_x\right]+f\left(x\right), \tag{9.2}$$

where the Boltzmann constant $k_B=1.380649\times10^{-23}\,\mathrm{J/K}$.

Let us consider the main features of the solution of Equation (9.2). With this aim we suppose that $v_{0x}=const$, $\sigma=const$ and the last term of the equation can be omitted. The penultimate term in Equation (9.2) can be omitted if the pressure gradient can compensate the influence of the gravitation force acting on the volume unit and $f\left(x\right)=0$. We have

$$\left[1+\frac{\tau\sigma}{\varepsilon_0\varepsilon}\right]\frac{\partial E_x}{\partial t}+\frac{\tau\sigma v_{0x}}{\varepsilon_0\varepsilon}\frac{\partial E_x}{\partial x}=-\frac{\sigma}{\varepsilon_0\varepsilon}E_x. \tag{9.3}$$

The solution of this equation is a damping longitudinal E-wave. Really

$$E_x=\exp\left(-\frac{1}{\tau v_{0x}}x\right)\Phi\left[\left(1+\frac{\tau\sigma}{\varepsilon_0\varepsilon}\right)x-\frac{\tau\sigma v_{0x}}{\varepsilon_0\varepsilon}t\right]. \tag{9.4}$$

Conclusions:

1) The validity of the solution (9.4) could be verified by the direct substitution of this relation (9.4) into Equation (9.3).

2) If the non-locality parameter τ is equal to zero, the electric intensity for the longitudinal waves (EMLW) also turns into zero. It means that EMLW cannot exist in the frame of the classic Maxwell electrodynamics.

Equation (9.2) can be written in the form

$$\left[1+\frac{\tau\sigma}{\varepsilon_0\varepsilon}\right]\frac{\partial E_x}{\partial t}+\frac{\tau\sigma}{\varepsilon_0\varepsilon}v_{0x}\frac{\partial E_x}{\partial x}=-\frac{\sigma}{\varepsilon_0\varepsilon}E_x-\frac{\tau}{\varepsilon_0\varepsilon}\frac{q}{m}\left[\frac{\partial}{\partial x}\left(nk_BT\right)-\rho g_x\right]. \tag{9.5}$$

The last term in square bracket takes into account the influence of the pressure gradient and the gravitation force. If nonlocal parameter $\tau=0$, then

$$\frac{\partial E_x}{\partial t}=-\frac{\sigma}{\varepsilon_0\varepsilon}E_x \tag{9.6}$$

and we have in the local electrodynamics the exponential E_x attenuation (if

$f(x)=0$ in (9.2)) without the wave creation

$$E_x = E_{x,t=0}\exp\left(-\frac{\sigma t}{\varepsilon\varepsilon_0}\right). \tag{9.7}$$

The existence of longitudinal electromagnetic waves does not contradict (nonlocal) electrodynamics if longitudinal waves are actually detected and the medium in which they are generated is known. Then in this case the problem of substantiating such waves in electrodynamics is reduced to the search for material equations characterizing the response of the medium to the influence of the field and the joint solution of these material equations and Maxwell's equations, with appropriate boundary conditions.

Let be

$$\left(1+\frac{\tau\sigma}{\varepsilon_0\varepsilon}\right)x-\frac{\tau\sigma v_0}{\varepsilon_0\varepsilon}t = const = C\,. \tag{9.8}$$

Then

$$\left(1+\frac{\tau\sigma}{\varepsilon_0\varepsilon}\right)\frac{\mathrm{d}x}{\mathrm{d}t}=\frac{\tau\sigma v_0}{\varepsilon_0\varepsilon} \tag{9.9}$$

or

$$v_{EMLW}=\frac{\mathrm{d}x}{\mathrm{d}t}=\frac{\tau\sigma v_0}{\varepsilon_0\varepsilon}\left[1+\frac{\tau\sigma}{\varepsilon_0\varepsilon}\right]^{-1}=\frac{\tau\sigma v_0}{\varepsilon_0\varepsilon}\frac{\varepsilon_0\varepsilon}{\varepsilon_0\varepsilon+\tau\sigma}=\frac{\tau\sigma}{\varepsilon_0\varepsilon+\tau\sigma}v_0=\frac{1}{1+\frac{\varepsilon_0\varepsilon}{\tau\sigma}}v_0\,. \tag{9.10}$$

Low permittivity (low epsilon) materials are now attracting wide attention due to potential novel applications in optics and radio communications. Surface plasmon polaritons (SPPs) are electromagnetic waves that travel along a metal-dielectric or metal-air interface, practically in the infrared or visible-frequency. The term "surface plasmon polariton" explains that the wave involves both charge motion in the metal ("surface plasmon") and electromagnetic waves in the air or dielectric ("polariton"). Application of SPPs enables subwavelength optics in microscopy and lithography beyond the diffraction limit. It also enables the first steady-state micro-mechanical measurement of a fundamental property of light itself: the momentum of a photon in a dielectric medium.

Longitudinal electromagnetic waves play important role in plasma, in surface plasmon polaritons in anisotropic materials, in space-charge waves in semiconductor materials. Then for so called that in Epsilon Near Zero (ENZ) materials the velocity $v_{EMLW}\cong v_0$ (the usual light velocity). For the following details of the wave process one needs the explicit form of the $\Phi(x,t)$ function and boundary and initial conditions. As we see from (9.10)

$$v_{EMLW}\to v_0 \quad \text{if} \quad \varepsilon\to 0\,. \tag{9.11}$$

Obviously to overcome this velocity limit is possible only in the systems with negative conductivity where formally

$$v_{EMLW}\to\infty \quad \text{if} \quad \sigma\to-\frac{\varepsilon_0\varepsilon}{\tau}\,. \tag{9.12}$$

The possibility of the appearance of negative conductivity in a non-equilibrium electron system, *i.e.*, a situation in which the current flows opposite to the electric field, was apparently indicated for the first time by Krömer in the late 1950s [27]. The mechanism of absolute negative conductivity (ANC) in a two-dimensional electron system placed into magnetic and ac electric fields, which is associated with two-dimensional electron scattering by impurities, accompanied by ac field photon absorption, was proposed in [28] [29]. The state with negative conductivity is unstable, the system decays into domains, and the measured macroscopic resistance becomes zero. The existence of this effect was experimentally confirmed in 2002 [30].

10. Non-Local Magnetic Field Evolution in Plasma

We consider the 3D non-stationary magnetic field evolution in plasma. With this aim let us transform Equation (8.19) written as follows

$$\left[1+\frac{\tau\sigma}{\varepsilon_0\varepsilon}\right]\frac{\partial^2\mathbf{E}}{\partial t^2}=v_\phi^2\left\{\Delta\mathbf{E}-\frac{\partial}{\partial\mathbf{r}}\left[\frac{\partial}{\partial\mathbf{r}}\cdot\mathbf{E}\right]\right\}-\frac{\sigma}{\varepsilon_0\varepsilon}\frac{\partial\mathbf{E}}{\partial t}-\frac{\tau}{\varepsilon_0\varepsilon}\frac{\partial}{\partial t}\left[\frac{\partial}{\partial\mathbf{r}}\cdot\left(\sigma\mathbf{E}\mathbf{v}_0\right)\right]$$
$$-\frac{\tau}{\varepsilon_0\varepsilon}\frac{\partial}{\partial t}\left[\frac{q}{m}\frac{\partial}{\partial\mathbf{r}}\left(nk_BT\right)-nq\mathbf{g}\right] \tag{10.1}$$

Let us apply the vector product operator to the left and right sides of (10.1)

$$\left[1+\frac{\tau\sigma}{\varepsilon_0\varepsilon}\right]\frac{\partial^2}{\partial t^2}\frac{\partial}{\partial\mathbf{r}}\times\mathbf{E}=v_\phi^2\frac{\partial}{\partial\mathbf{r}}\times\left\{\Delta\mathbf{E}-\frac{\partial}{\partial\mathbf{r}}\left[\frac{\partial}{\partial\mathbf{r}}\cdot\mathbf{E}\right]\right\}-\frac{\sigma}{\varepsilon_0\varepsilon}\frac{\partial}{\partial t}\frac{\partial}{\partial\mathbf{r}}\times\mathbf{E}$$
$$-\frac{\tau}{\varepsilon_0\varepsilon}\frac{\partial}{\partial t}\frac{\partial}{\partial\mathbf{r}}\times\left[\frac{\partial}{\partial\mathbf{r}}\cdot\left(\sigma\mathbf{E}\mathbf{v}_0\right)\right]+\frac{\tau}{\varepsilon_0\varepsilon}\frac{\partial}{\partial t}\frac{\partial}{\partial\mathbf{r}}\times\left[nq\mathbf{g}\right]. \tag{10.2}$$

Let us remind that in the coordinate notations we have

$$\left[\frac{\partial}{\partial\mathbf{r}}\cdot\left(\sigma\mathbf{E}\mathbf{v}_0\right)\right]=\frac{\partial}{\partial x}\left(\sigma E_x\mathbf{v}_0\right)+\frac{\partial}{\partial y}\left(\sigma E_y\mathbf{v}_0\right)+\frac{\partial}{\partial z}\left(\sigma E_z\mathbf{v}_0\right), \tag{10.3}$$

We use e as absolute charge of electron, $\mathbf{v}_0$ as a mean velocity of the electron motion and the operator relation

$$\frac{\partial}{\partial\mathbf{r}}\times\left[\frac{\partial p}{\partial\mathbf{r}}\right]\equiv 0 \tag{10.4}$$

The corresponding current density is

$$\mathbf{j}_0=-n_e e\mathbf{v}_0 \tag{10.5}$$

We introduce also the charge number density

$$\rho_e=en_e \tag{10.6}$$

and the character relaxation time

$$\tau_r=\frac{\varepsilon_0\varepsilon}{\sigma}. \tag{10.7}$$

We transform (10.2):

1) Keeping only the terms proportional to the first power of the non-local parameter τ,

2) Using the relations (for simplicity) $\varepsilon = const$, $\sigma = const$; the following transformation should be taken into account

$$\begin{aligned}\frac{\tau}{\varepsilon_0\varepsilon}\frac{\partial}{\partial\mathbf{r}}\times\left[\frac{\partial}{\partial\mathbf{r}}\cdot\left(\sigma\mathbf{E}\mathbf{v}_0\right)\right] &= \frac{\tau\sigma}{\varepsilon_0\varepsilon}\frac{\partial}{\partial\mathbf{r}}\times\left[\frac{\partial}{\partial x}\left(E_x\mathbf{v}_0\right)+\frac{\partial}{\partial y}\left(E_y\mathbf{v}_0\right)+\frac{\partial}{\partial z}\left(E_z\mathbf{v}_0\right)\right]\\ &= \frac{\tau\sigma}{\varepsilon_0\varepsilon}\frac{\partial}{\partial\mathbf{r}}\times\left[\mathbf{v}_0\frac{\partial}{\partial\mathbf{r}}\cdot\mathbf{E}\right]+\frac{\tau\sigma}{\varepsilon_0\varepsilon}\frac{\partial}{\partial\mathbf{r}}\times\left(\mathbf{E}\cdot\frac{\partial}{\partial\mathbf{r}}\right)\mathbf{v}_0\\ &= \frac{\tau\sigma}{\varepsilon_0\varepsilon}\frac{1}{\varepsilon_0\varepsilon}\frac{\partial}{\partial\mathbf{r}}\times\left[\mathbf{v}_0\frac{\partial}{\partial\mathbf{r}}\cdot\mathbf{D}\right]+\frac{\tau\sigma}{\varepsilon_0\varepsilon}\frac{\partial}{\partial\mathbf{r}}\times\left(\mathbf{E}\cdot\frac{\partial}{\partial\mathbf{r}}\right)\mathbf{v}_0\\ &= -\frac{\tau\sigma}{\varepsilon_0\varepsilon}\frac{\partial}{\partial\mathbf{r}}\times\mathbf{j}_{0e}+\frac{\tau\sigma}{\varepsilon_0\varepsilon}\frac{\partial}{\partial\mathbf{r}}\times\left(\mathbf{E}\cdot\frac{\partial}{\partial\mathbf{r}}\right)\mathbf{v}_{0e}.\end{aligned} \tag{10.8}$$

The last line in (10.8) corresponds the physical system in which the charge current is realized by electrons. Extremely important that the last term in (10.8) contains the hydrodynamic velocity $\mathbf{v}_{0e}$, which can be defined only as a result of the whole hydrodynamic problem.

Then if we want to separate the electro-dynamic and hydro-dynamic problems we should neglect the changes in the space of the hydrodynamic velocity fluctuations. Therefore we use the relation

$$\frac{\tau}{\varepsilon_0\varepsilon}\frac{\partial}{\partial\mathbf{r}}\times\left[\frac{\partial}{\partial\mathbf{r}}\cdot\left(\sigma\mathbf{E}\mathbf{v}_0\right)\right] = -\frac{\tau\sigma}{\varepsilon_0\varepsilon}\frac{\partial}{\partial\mathbf{r}}\times\mathbf{j}_{0e}. \tag{10.9}$$

Using also the Maxwell relation

$$\frac{\partial}{\partial\mathbf{r}}\times\mathbf{E} = -\frac{\partial\mathbf{B}}{\partial t}, \tag{10.10}$$

we write (10.2) as follows (omitting the gravitation influence)

$$-\left[1+\frac{\tau}{\tau_r}\right]\frac{\partial^2}{\partial t^2}\frac{\partial\mathbf{B}}{\partial t} = v_\phi^2\frac{\partial}{\partial\mathbf{r}}\times\left\{\Delta\mathbf{E}-\frac{\partial}{\partial\mathbf{r}}\left[\frac{\partial}{\partial\mathbf{r}}\cdot\mathbf{E}\right]\right\}+\frac{1}{\tau_r}\frac{\partial}{\partial t}\frac{\partial\mathbf{B}}{\partial t}+\frac{\tau}{\tau_r}\frac{1}{\varepsilon\varepsilon_0}\frac{\partial}{\partial t}\frac{\partial}{\partial\mathbf{r}}\times\mathbf{j}_0. \tag{10.11}$$

Keeping as before only the terms proportional to the first power of the non-local parameter τ, we can use the Maxwell relation

$$\mathbf{j}_0+\frac{\partial\mathbf{D}}{\partial t} = \frac{\partial}{\partial\mathbf{r}}\times\mathbf{H}. \tag{10.12}$$

Then

$$\begin{aligned}-\left[1+\frac{\tau\sigma}{\varepsilon_0\varepsilon}\right]\frac{\partial^2}{\partial t^2}\frac{\partial\mathbf{B}}{\partial t} &= v_\phi^2\frac{\partial}{\partial\mathbf{r}}\times\left\{\Delta\mathbf{E}-\frac{\partial}{\partial\mathbf{r}}\left[\frac{\partial}{\partial\mathbf{r}}\cdot\mathbf{E}\right]\right\}+\frac{\sigma}{\varepsilon_0\varepsilon}\frac{\partial}{\partial t}\frac{\partial\mathbf{B}}{\partial t}\\ &+\frac{\tau}{\tau_r}\frac{1}{\varepsilon\varepsilon_0}\frac{\partial}{\partial t}\frac{\partial}{\partial\mathbf{r}}\times\left\{\frac{\partial}{\partial\mathbf{r}}\times\mathbf{H}-\frac{\partial\mathbf{D}}{\partial t}\right\}\end{aligned} \tag{10.13}$$

or

$$\begin{aligned}-\left[1+\frac{\tau\sigma}{\varepsilon_0\varepsilon}\right]\frac{\partial^2}{\partial t^2}\frac{\partial\mathbf{B}}{\partial t} &= v_\phi^2\frac{\partial}{\partial\mathbf{r}}\times\left\{\Delta\mathbf{E}-\frac{\partial}{\partial\mathbf{r}}\left[\frac{\partial}{\partial\mathbf{r}}\cdot\mathbf{E}\right]\right\}+\frac{\sigma}{\varepsilon_0\varepsilon}\frac{\partial}{\partial t}\frac{\partial\mathbf{B}}{\partial t}\\ &+\frac{\tau}{\tau_r}\frac{1}{\varepsilon\varepsilon_0}\frac{\partial}{\partial t}\frac{\partial}{\partial\mathbf{r}}\times\left[\frac{\partial}{\partial\mathbf{r}}\times\mathbf{H}\right]-\frac{\tau}{\tau_r}\frac{1}{\varepsilon\varepsilon_0}\frac{\partial^2}{\partial t^2}\frac{\partial}{\partial\mathbf{r}}\times\mathbf{D}\end{aligned} \tag{10.14}$$

or

$$-\left[1+\frac{\tau\sigma}{\varepsilon_0\varepsilon}\right]\frac{\partial^2}{\partial t^2}\frac{\partial \mathbf{B}}{\partial t}=v_\phi^2\frac{\partial}{\partial \mathbf{r}}\times\left\{\Delta\mathbf{E}-\frac{\partial}{\partial \mathbf{r}}\left[\frac{\partial}{\partial \mathbf{r}}\cdot\mathbf{E}\right]\right\}+\frac{\sigma}{\varepsilon_0\varepsilon}\frac{\partial}{\partial t}\frac{\partial \mathbf{B}}{\partial t}+\frac{\tau}{\tau_r}\frac{1}{\varepsilon_0\varepsilon}\frac{\partial}{\partial t}\frac{\partial}{\partial \mathbf{r}}\times\left[\frac{\partial}{\partial \mathbf{r}}\times\mathbf{H}\right]+\frac{\tau}{\tau_r}\frac{\partial}{\partial t}\frac{\partial^2 \mathbf{B}}{\partial t^2} \tag{10.15}$$

Let us use the identity

$$\frac{\partial}{\partial \mathbf{r}}\times\left(\frac{\partial}{\partial \mathbf{r}}\times\mathbf{B}\right)\equiv\frac{\partial}{\partial \mathbf{r}}\left(\frac{\partial}{\partial \mathbf{r}}\cdot\mathbf{B}\right)-\Delta\mathbf{B} \tag{10.16}$$

and the Maxwell relation

$$\frac{\partial}{\partial \mathbf{r}}\cdot\mathbf{B}=0, \tag{10.17}$$

we have

$$-\left[1+\frac{\tau\sigma}{\varepsilon_0\varepsilon}\right]\frac{\partial^2}{\partial t^2}\frac{\partial \mathbf{B}}{\partial t}=v_\phi^2\frac{\partial}{\partial \mathbf{r}}\times\left\{\Delta\mathbf{E}-\frac{\partial}{\partial \mathbf{r}}\left[\frac{\partial}{\partial \mathbf{r}}\cdot\mathbf{E}\right]\right\}+\frac{\sigma}{\varepsilon_0\varepsilon}\frac{\partial}{\partial t}\frac{\partial \mathbf{B}}{\partial t}-\frac{\tau}{\tau_r}\frac{1}{\mu_0\mu}\frac{1}{\varepsilon_0\varepsilon}\frac{\partial}{\partial t}\Delta\mathbf{B}+\frac{\tau}{\tau_r}\frac{\partial}{\partial t}\frac{\partial^2 \mathbf{B}}{\partial t^2} \tag{10.18}$$

or, if the reverse relaxation time is

$$\frac{1}{\tau_r}=\frac{\sigma}{\varepsilon_0\varepsilon}, \tag{10.19}$$

we have

$$\left[1+2\frac{\tau}{\tau_r}\right]\frac{\partial^2}{\partial t^2}\frac{\partial \mathbf{B}}{\partial t}+\frac{1}{\tau_r}\frac{\partial}{\partial t}\frac{\partial \mathbf{B}}{\partial t}=\frac{\tau}{\tau_r}v_\phi^2\frac{\partial}{\partial t}\Delta\mathbf{B}-v_\phi^2\frac{\partial}{\partial \mathbf{r}}\times\left\{\Delta\mathbf{E}-\frac{\partial}{\partial \mathbf{r}}\left[\frac{\partial}{\partial \mathbf{r}}\cdot\mathbf{E}\right]\right\}. \tag{10.20}$$

Then

$$\left[1+2\frac{\tau}{\tau_r}\right]\frac{\partial^2}{\partial t^2}\frac{\partial \mathbf{B}}{\partial t}+\frac{1}{\tau_r}\frac{\partial}{\partial t}\frac{\partial \mathbf{B}}{\partial t}=\frac{\tau}{\tau_r}v_\phi^2\frac{\partial}{\partial t}\Delta\mathbf{B}+v_\phi^2\frac{\partial}{\partial \mathbf{r}}\times\left\{\frac{\partial}{\partial \mathbf{r}}\times\left(\frac{\partial}{\partial \mathbf{r}}\times\mathbf{E}\right)\right\} \tag{10.21}$$

or

$$\left[1+2\frac{\tau}{\tau_r}\right]\frac{\partial^2}{\partial t^2}\frac{\partial \mathbf{B}}{\partial t}+\frac{1}{\tau_r}\frac{\partial}{\partial t}\frac{\partial \mathbf{B}}{\partial t}=\frac{\tau}{\tau_r}v_\phi^2\frac{\partial}{\partial t}\Delta\mathbf{B}-v_\phi^2\frac{\partial}{\partial t}\left\{\frac{\partial}{\partial \mathbf{r}}\times\left[\frac{\partial}{\partial \mathbf{r}}\times\mathbf{B}\right]\right\} \tag{10.22}$$

or after integration on time we reach

$$\left[1+2\frac{\tau}{\tau_r}\right]\frac{\partial^2 \mathbf{B}}{\partial t^2}+\frac{1}{\tau_r}\frac{\partial \mathbf{B}}{\partial t}=\frac{\tau}{\tau_r}v_\phi^2\Delta\mathbf{B}-v_\phi^2\left\{\frac{\partial}{\partial \mathbf{r}}\times\left[\frac{\partial}{\partial \mathbf{r}}\times\mathbf{B}\right]\right\}+f(x,y,z). \tag{10.23}$$

11. Quantization in the Theory of the Magnetic Field Penetration. Comparison of the Non-Local and London's Theories

Let us consider the 1D non-stationary electron evolution in plasma. We suppose that

$$\tau\ll\tau_r. \tag{11.1}$$

After using (11.1) we have from (10.23)

$$\frac{\partial^2 B}{\partial t^2}+\frac{1}{\mathrm{T}_r}\frac{\partial B}{\partial t}=v_\phi^2\frac{\partial^2 B}{\partial x^2}+f\left(x\right). \tag{11.2}$$

In the following T_r and L_r are character time and length relaxation. Let us remind the London's equation written here as

$$\Delta\mathbf{B}=\mu\mu_0\frac{n_e e^2}{m_e}\mathbf{B} \tag{11.3}$$

or

$$\Delta\mathbf{B}=\frac{1}{\ell^2}\mathbf{B}, \tag{11.4}$$

where ℓ is the London penetration depth.

$$\ell=e\sqrt{\mu\mu_0\frac{n_e}{m_e}}. \tag{11.5}$$

This London equation predicts that the magnetic field in a superconductor decays exponentially decays from whatever value it possesses at the surface.

We choose the function $f\left(x\right)$ in the form

$$f\left(x\right)\to-\frac{v_\phi^2}{\mathrm{L}_r^2}B, \tag{11.6}$$

or

$$f\left(x\right)\to-\frac{1}{\mathrm{T}_r^2}B. \tag{11.7}$$

Relation

$$\frac{\partial^2 B}{\partial t^2}+\frac{1}{\mathrm{T}_r}\frac{\partial B}{\partial t}=v_\phi^2\frac{\partial^2 B}{\partial x^2}-\frac{1}{\mathrm{T}_r^2}B_0\left(x\right) \tag{11.8}$$

is telegraph equation which contains now $\tau_r=\mathrm{T}_r=const$ and $v_\phi=const$ as calculations parameters.

Solution of Equation (11.8) can be written in the form

$$B\left(x,t\right)=\mathrm{e}^{-\frac{t}{2\mathrm{T}_r}}\sum_{n=1}^{\infty}B_n\sin\left(\lambda_n t\right)\cos\frac{\pi nx}{\mathrm{L}_r}+B\left(0,0\right)\mathrm{e}^{-\frac{x}{\mathrm{L}_r}}, \tag{11.9}$$

where L_r is the character scale of the relaxation length.

Solution (11.9) responds to natural initial and boundary conditions, namely

$$B\left(0,t\right)=\mathrm{e}^{-\frac{1}{2}\frac{t}{\mathrm{T}_r}}\sum_{n=1}^{\infty}B_n\sin\left(\lambda_n t\right)+B\left(0,0\right), \tag{11.10}$$

$$B\left(0,0\right)=const, \tag{11.11}$$

$$B\left(x,t\to\infty\right)=B\left(0,0\right)\mathrm{e}^{-\frac{x}{\mathrm{L}_r}}, \tag{11.12}$$

$$B\left(x\to\infty,t\right)=\mathrm{e}^{-\frac{1}{2}\frac{t}{\mathrm{T}_r}}\sum_{n=1}^{\infty}B_n\sin\left(\lambda_n t\right)\cos\frac{\pi nx}{\mathrm{L}_r}. \tag{11.13}$$

Solution (11.9) can satisfy the Equation (11.8) if a condition should be satisfied. This condition can be found after the direct substitution of (11.9) in (11.8). We have

$$\mathrm{e}^{-\frac{t}{2\mathrm{T}_r}}\sum_{n=1}^{\infty}B_n\left\{\left[\frac{1}{2\mathrm{T}_r}\right]^2-\lambda_n^2-\frac{1}{2\mathrm{T}_r}\frac{1}{\mathrm{T}_r}+v_\phi^2\left[\frac{\pi n}{\mathrm{L}_r}\right]^2\right\}\sin\left(\lambda_n t\right)\cos\frac{\pi n x}{\mathrm{L}_r}=0\,. \quad (11.14)$$

The relation (11.14) is fulfilled if the expression in the curly bracket is equal to zero.

$$\left[\frac{1}{2\mathrm{T}_r}\right]^2-\lambda_n^2-\frac{1}{2\mathrm{T}_r}\frac{1}{\mathrm{T}_r}+v_\phi^2\left[\frac{\pi n}{\mathrm{L}_r}\right]^2=0\,, \quad (11.15)$$

or

$$\lambda_n^2\mathrm{T}_r^2=\left(\pi n\right)^2-\frac{1}{4} \quad (11.16)$$

or

$$\lambda_n=\frac{1}{\mathrm{T}_r}\sqrt{\left(\pi n\right)^2-\frac{1}{4}}\,. \quad (11.17)$$

As we see in the stationary case we have known equation

$$v_\phi^2\frac{\partial^2 B_0}{\partial x^2}=\frac{1}{\mathrm{T}_r^2}B_0\,, \quad (11.18)$$

or

$$\mathrm{L}_r^2\frac{\partial^2 B_0}{\partial x^2}=B_0\,, \quad (11.12)$$

which has a solution

$$B_0=B\left(0,0\right)\mathrm{e}^{-\frac{x}{\mathrm{L}_r}}\,. \quad (11.13)$$

Finally, we have non-stationary solution as a wave with the time attenuation.

$$B\left(x,t\right)=\mathrm{e}^{-\frac{t}{2\mathrm{T}_r}}\sum_{n=1}^{\infty}B_n\sin\left(\lambda_n t\right)\cos\frac{\pi n x}{\mathrm{L}_r}+B\left(0,0\right)\mathrm{e}^{-\frac{x}{\mathrm{L}_r}}\,, \quad (11.14)$$

$$\lambda_n=\frac{1}{\mathrm{T}_r}\sqrt{\left(\pi n\right)^2-\frac{1}{4}}\sim\frac{1}{\mathrm{T}_r}\pi n,\ \ n=1,2,\cdots \quad (11.15)$$

and approximately we reach

$$B\left(x,t\right)=\mathrm{e}^{-\frac{t}{2\mathrm{T}_r}}\sum_{n=1}^{\infty}B_n\sin\frac{\pi n t}{\mathrm{T}_r}\left(\lambda_n t\right)\cos\frac{\pi n x}{\mathrm{L}_r}+B\left(0,0\right)\mathrm{e}^{-\frac{x}{\mathrm{L}_r}}\,. \quad (11.16)$$

Some conclusions:

1) Relation (11.16) defines penetration of the longitudinal magnetic field in space.

2) This non-stationary attenuation has the character of wave damping.

3) The stationary case corresponds to the London's regime.

4) It is interesting to notice that the regime of the non-stationary wave attenu-

ation exists for the evolution of the spherical object without fields (see **Appendix 3**).

12. Nonlocal Pointing-Umov Theorem

Let us obtain now the generalized nonlocal formulation of the Pointing-Umov theorem. In other words we intend to obtain the law of the energy conservation for electro-magnetic processes in the frame of non-local physics. We use the Equation (8.19) for following transformations.

$$\left[1+\frac{\tau\sigma}{\varepsilon_0\varepsilon}\right]\frac{\partial^2\mathbf{E}}{\partial t^2}=v_\phi^2\left\{\Delta\mathbf{E}-\frac{\partial}{\partial\mathbf{r}}\left[\frac{\partial}{\partial\mathbf{r}}\cdot\mathbf{E}\right]\right\}-\frac{\sigma}{\varepsilon_0\varepsilon}\frac{\partial\mathbf{E}}{\partial t}-\frac{\tau}{\varepsilon_0\varepsilon}\frac{\partial}{\partial t}\left[\frac{\partial}{\partial\mathbf{r}}\cdot\left(\sigma\mathbf{E}\mathbf{v}_0\right)\right]$$
$$-\frac{\tau}{\varepsilon_0\varepsilon}\frac{\partial}{\partial t}\left[\frac{q}{m}\frac{\partial}{\partial\mathbf{r}}\left(nk_BT\right)-nq\mathbf{g}\right] \tag{12.1}$$

We use the vector identity

$$\frac{\partial}{\partial\mathbf{r}}\times\left(\frac{\partial}{\partial\mathbf{r}}\times\mathbf{E}\right)\equiv\frac{\partial}{\partial\mathbf{r}}\left(\frac{\partial}{\partial\mathbf{r}}\cdot\mathbf{E}\right)-\Delta\mathbf{E}, \tag{12.2}$$

then

$$\left[1+\frac{\tau\sigma}{\varepsilon_0\varepsilon}\right]\frac{\partial^2\mathbf{E}}{\partial t^2}=-v_\phi^2\left\{\frac{\partial}{\partial\mathbf{r}}\times\left(\frac{\partial}{\partial\mathbf{r}}\times\mathbf{E}\right)\right\}-\frac{\sigma}{\varepsilon_0\varepsilon}\frac{\partial\mathbf{E}}{\partial t}-\frac{\tau}{\varepsilon_0\varepsilon}\frac{\partial}{\partial t}\left[\frac{\partial}{\partial\mathbf{r}}\cdot\left(\sigma\mathbf{E}\mathbf{v}_0\right)\right]$$
$$-\frac{\tau}{\varepsilon_0\varepsilon}\frac{\partial}{\partial t}\left[\frac{q}{m}\frac{\partial}{\partial\mathbf{r}}\left(nk_BT\right)-nq\mathbf{g}\right]. \tag{12.3}$$

Let us transform now the first term of the right-hand-side of (12.3)

$$\left[1+\frac{\tau\sigma}{\varepsilon_0\varepsilon}\right]\frac{\partial^2\mathbf{E}}{\partial t^2}=v_\phi^2\frac{\partial}{\partial t}\left\{\frac{\partial}{\partial\mathbf{r}}\times\mathbf{B}\right\}-\frac{\sigma}{\varepsilon_0\varepsilon}\frac{\partial\mathbf{E}}{\partial t}-\frac{\tau}{\varepsilon_0\varepsilon}\frac{\partial}{\partial t}\left[\frac{\partial}{\partial\mathbf{r}}\cdot\left(\sigma\mathbf{E}\mathbf{v}_0\right)\right]$$
$$-\frac{\tau}{\varepsilon_0\varepsilon}\frac{\partial}{\partial t}\left[\frac{q}{m}\frac{\partial}{\partial\mathbf{r}}\left(nk_BT\right)-nq\mathbf{g}\right]. \tag{12.4}$$

After integration on time, we reach

$$\left[1+\frac{\tau\sigma}{\varepsilon_0\varepsilon}\right]\frac{\partial\mathbf{E}}{\partial t}=v_\phi^2\left\{\frac{\partial}{\partial\mathbf{r}}\times\mathbf{B}\right\}-\frac{\sigma}{\varepsilon_0\varepsilon}\mathbf{E}-\frac{\tau}{\varepsilon_0\varepsilon}\left[\frac{\partial}{\partial\mathbf{r}}\cdot\left(\sigma\mathbf{E}\mathbf{v}_0\right)\right]$$
$$-\frac{\tau}{\varepsilon_0\varepsilon}\left[\frac{q}{m}\frac{\partial}{\partial\mathbf{r}}\left(nk_BT\right)-nq\mathbf{g}\right]+\mathbf{F}\left(x,y,z\right), \tag{12.5}$$

where a function $\mathbf{F}\left(x,y,z\right)$ is defined by the initial and boundary conditions. Scalar multiplication by $\mathbf{E}$ of the both parts of Equation (12.5) gives the relation

$$\left[1+\frac{\tau\sigma}{\varepsilon_0\varepsilon}\right]\mathbf{E}\cdot\frac{\partial\mathbf{E}}{\partial t}=v_\phi^2\mathbf{E}\cdot\left\{\frac{\partial}{\partial\mathbf{r}}\times\mathbf{B}\right\}-\frac{\sigma}{\varepsilon_0\varepsilon}E^2-\frac{\tau}{\varepsilon_0\varepsilon}\mathbf{E}\cdot\left[\frac{\partial}{\partial\mathbf{r}}\cdot\left(\sigma\mathbf{E}\mathbf{v}_0\right)\right]$$
$$-\frac{\tau}{\varepsilon_0\varepsilon}\mathbf{E}\cdot\left[\frac{q}{m}\frac{\partial}{\partial\mathbf{r}}\left(nk_BT\right)-nq\mathbf{g}\right]+\mathbf{E}\cdot\mathbf{F}\left(x,y,z\right). \tag{12.6}$$

Let us use the vector identity

$$\mathbf{E}\cdot\left\{\frac{\partial}{\partial\mathbf{r}}\times\mathbf{B}\right\}\equiv\mu_0\mu\mathbf{H}\cdot\left\{\frac{\partial}{\partial\mathbf{r}}\times\mathbf{E}\right\}-\mu_0\mu\frac{\partial}{\partial\mathbf{r}}\cdot\left[\mathbf{E}\times\mathbf{H}\right]. \tag{12.7}$$

We find

$$\frac{1}{2}\left[1+\frac{\tau\sigma}{\varepsilon_0\varepsilon}\right]\frac{\partial E^2}{\partial t}=v_\phi^2\left\{\mu_0\mu\mathbf{H}\cdot\left\{\frac{\partial}{\partial\mathbf{r}}\times\mathbf{E}\right\}-\mu_0\mu\frac{\partial}{\partial\mathbf{r}}\cdot\left[\mathbf{E}\times\mathbf{H}\right]\right\}$$
$$-\frac{\sigma}{\varepsilon_0\varepsilon}E^2-\frac{\tau}{\varepsilon_0\varepsilon}\mathbf{E}\cdot\left[\frac{\partial}{\partial\mathbf{r}}\cdot\left(\sigma\mathbf{E}\mathbf{v}_0\right)\right] \tag{12.8}$$
$$-\frac{\tau}{\varepsilon_0\varepsilon}\mathbf{E}\cdot\left[\frac{q}{m}\frac{\partial}{\partial\mathbf{r}}\left(nk_BT\right)-nq\mathbf{g}\right]+\mathbf{E}\cdot\mathbf{F}\left(x,y,z\right)$$

or (for simplicity $\sigma=const$, $\varepsilon=const$ and $\mu=const$)

$$\left[1+\frac{\tau\sigma}{\varepsilon_0\varepsilon}\right]\frac{\partial}{\partial t}\frac{\varepsilon_0\varepsilon E^2}{2}=\mathbf{H}\cdot\left\{\frac{\partial}{\partial\mathbf{r}}\times\mathbf{E}\right\}-\frac{\partial}{\partial\mathbf{r}}\cdot\left[\mathbf{E}\times\mathbf{H}\right]-\sigma E^2-\tau\mathbf{E}\cdot\left[\frac{\partial}{\partial\mathbf{r}}\cdot\left(\sigma\mathbf{E}\mathbf{v}_0\right)\right] \tag{12.9}$$
$$-\tau\mathbf{E}\cdot\left[\frac{q}{m}\frac{\partial}{\partial\mathbf{r}}\left(nk_BT\right)-nq\mathbf{g}\right]+\varepsilon_0\varepsilon\mathbf{E}\cdot\mathbf{F}\left(x,y,z\right)$$

or

$$\left[1+\frac{\tau\sigma}{\varepsilon_0\varepsilon}\right]\frac{\partial}{\partial t}\frac{\varepsilon_0\varepsilon E^2}{2}=-\mathbf{H}\cdot\frac{\partial\mathbf{B}}{\partial t}-\frac{\partial}{\partial\mathbf{r}}\cdot\left[\mathbf{E}\times\mathbf{H}\right]-\sigma E^2$$
$$-\tau\mathbf{E}\cdot\left[\frac{\partial}{\partial\mathbf{r}}\cdot\left(\sigma\mathbf{E}\mathbf{v}_0\right)+\frac{q}{m}\frac{\partial p}{\partial\mathbf{r}}-nq\mathbf{g}\right]+\varepsilon_0\varepsilon\mathbf{E}\cdot\mathbf{F}\left(x,y,z\right) \tag{12.10}$$

or

$$\frac{\partial}{\partial t}\frac{\varepsilon_0\varepsilon E^2+\mu_0\mu H^2}{2}+\frac{\tau\sigma}{\varepsilon_0\varepsilon}\frac{\partial}{\partial t}\frac{\varepsilon_0\varepsilon E^2}{2}$$
$$=-\frac{\partial}{\partial\mathbf{r}}\cdot\left[\mathbf{E}\times\mathbf{H}\right]-\sigma E^2-\tau\mathbf{E}\cdot\left[\frac{\partial}{\partial\mathbf{r}}\cdot\left(\sigma\mathbf{E}\mathbf{v}_0\right)+\frac{q}{m}\frac{\partial}{\partial\mathbf{r}}\left(nk_BT\right)-nq\mathbf{g}\right] \tag{12.11}$$
$$+\varepsilon_0\varepsilon\mathbf{E}\cdot\mathbf{F}\left(x,y,z\right).$$

It is the nonlocal formulation of the Umov-Pointing theorem which takes into account transport processes in physical system. In the local case we find

$$\frac{\partial}{\partial t}\frac{\varepsilon_0\varepsilon E^2+\mu_0\mu H^2}{2}=-\frac{\partial}{\partial\mathbf{r}}\cdot\left[\mathbf{E}\times\mathbf{H}\right]-\sigma E^2+\varepsilon_0\varepsilon\mathbf{E}\cdot\mathbf{F}\left(x,y,z\right). \tag{12.12}$$

As usual a function $\mathbf{F}\left(x,y,z\right)$ is originated by integration on time and can be taken as zero; we obtain the classical formulation of the Umov-Pointing theorem.

$$\sigma E^2=-\frac{\partial}{\partial t}\left[\frac{\varepsilon_0\varepsilon E^2+\mu_0\mu H^2}{2}\right]-\mathrm{div}\left[\mathbf{E},\mathbf{H}\right]. \tag{12.13}$$

This equation is well known local energy equation, where the left hand side of this equation corresponds to the Joule heating.

13. The Soliton Movement in One Species Physical System about the Heat Transfer in Graphene

Particular attention of researchers has been recently attracted to a new carbon material, *i.e.*, graphene, consisting of a single layer of carbon atoms and having a

planar hexagonal structure. Electromagnetic waves propagating in carbon structures become highly nonlinear even at relatively weak fields, which results in possible propagation of electromagnetic solitary waves (which are soliton analogs, or even solitons) in carbon nanotubes and graphene (see review in [31] [32] [33]). The discussed properties of carbon structures have generated both increased theoretical interest and attempts at application in nonlinear optical devices.

The fundamental result also consists in discovering of the extremely high thermal conductivity in two-dimensional crystals including graphene. This effect (which takes place even in room-temperature) can be explained as a result of soliton movements without destruction. This effect was forecasted by me many years ago. Really, the transport processes in graphene as the effect of the soliton movement are investigated by me many years ago. The fundamental monograph [5] contains Chapter 6 (Quantum Solitons in Solid Matter), Item 6.2 (Application of non-local quantum hydrodynamics to the description of the charge density waves in the graphene crystal lattice) with the fundamental conclusion (p. 178): **"*Important conclusion*: high temperature superconductors demonstrate new type of electronic order and modulation of atomic positions. The above mentioned graphene properties can be explained only in the frame of the self-consistent non-local quantum theory which leads to the appearance of the soliton waves moving in graphene."**

Then it is impossible to talk about individual particles as heating transfer carriers. In the definite sense the high temperature super conductivity and super heat conductivity have the same origin—the appearance of moving solitons without destruction.

Let us demonstrate the example of the electron soliton movement in 1D physical system.

We transform nonlocal Maxwell equation

$$\frac{\partial}{\partial x}E = 4\pi\left[\rho_e - \tau\left(\frac{\partial \rho_e}{\partial t} - \frac{\partial}{\partial x}\left(\rho_e u\right)\right)\right], \tag{13.1}$$

where ρ_e is the electron charge density, or

$$-\frac{\partial^2}{\partial x^2}U_e = 4\pi\left[n_e - \tau\left(\frac{\partial n_e}{\partial t} - \frac{\partial}{\partial x}\left(n_e u\right)\right)\right]e, \tag{13.2}$$

where U_e is electrical potential and n_e is the electron number density. Equation (13.2) can be written in terms of wave parameters ($\xi = x - Ct$). Namely

$$-\frac{\partial^2}{\partial \xi^2}U_e = 4\pi\frac{e}{m_e}\left[\rho - \tau\left(-C\frac{\partial \rho}{\partial \xi} - \frac{\partial}{\partial \xi}\left(\rho u\right)\right)\right], \tag{13.3}$$

where ρ is the mass density, or introducing the absolute electron charge and potential $U = U_e/m_e$ we find

$$\frac{\partial^2}{\partial \xi^2}U = 4\pi\frac{|e|}{m_e^2}\left[\rho + \tau\left(C\frac{\partial \rho}{\partial \xi} + \frac{\partial}{\partial \xi}\left(\rho u\right)\right)\right]. \tag{13.4}$$

We use the following system of scales:

$$C_0 = x_0 \frac{1}{\tau_0},\ \tilde{C} = 1,\ \rho_0 = \frac{m_e}{4\pi x_0^3},\ U_0 = \frac{|e|}{m_e x_0},\ u_0 = \sqrt{\frac{\hbar}{4m_e}} = \frac{1}{2}\sqrt{\frac{\hbar}{m_e}}, \quad (13.5)$$

$$\tau = \tau^{(qu)} = t_0 \frac{1}{\tilde{u}^2} = t_0 \frac{u_0^2}{u^2} = \frac{\hbar}{4m_e}\frac{1}{u^2}\tau_0,\ \tau_0 = \frac{x_0}{u_0} = 2x_0\sqrt{\frac{m_e}{\hbar}},$$

$$C_0 = 2\sqrt{\frac{\hbar}{m_e}} = 2.1519\frac{\text{cm}}{\text{s}}. \quad (13.6)$$

The single independent scale is x_0.

Taking into account $\hbar = 1.054572\times 10^{-27}\,\text{erg}\cdot\text{s}$, $m_e = 0.9109383\times 10^{-27}\,\text{g}$, we have

$$\sqrt{\frac{\hbar}{m_e}} = 1.0759538\frac{\text{cm}}{\text{s}},\ \sqrt{\frac{m_e}{\hbar}} = 0.964058\frac{\text{s}}{\text{cm}},\ \tilde{\tau} = \frac{1}{\tilde{u}^2}. \quad (13.7)$$

The considered physical system works in Meissner regime, and then we needn't to use the influence of magnetic field. We reach the system of dimensionless equations

$$\frac{\partial^2}{\partial\tilde{\xi}^2}\tilde{U} = \tilde{\rho} + \frac{1}{\tilde{u}^2}\frac{\partial}{\partial\tilde{\xi}}\left[\tilde{\rho}\left(1+\tilde{u}\right)\right] \quad (13.8)$$

$$\frac{\partial\tilde{\rho}}{\partial\tilde{\xi}} - \frac{\partial\tilde{\rho}\tilde{u}}{\partial\tilde{\xi}} + \frac{\partial}{\partial\tilde{\xi}}\left\{\frac{1}{\tilde{u}^2}\left[\frac{\partial}{\partial\tilde{\xi}}\left(\tilde{p}+\tilde{\rho}+\tilde{\rho}\tilde{u}^2 - 2\tilde{\rho}\tilde{u}\right) + \tilde{\rho}\frac{\partial\tilde{U}}{\partial\tilde{\xi}}\right]\right\} = 0, \quad (13.9)$$

$$\frac{\partial}{\partial\tilde{\xi}}\left(\tilde{\rho}\tilde{u}^2 + \tilde{p} - \tilde{\rho}\tilde{u}\right) + \frac{\partial}{\partial\tilde{\xi}}\left\{\frac{1}{\tilde{u}^2}\left[\frac{\partial}{\partial\tilde{\xi}}\left(2\tilde{\rho}\tilde{u}^2 - \tilde{\rho}\tilde{u} + 2\tilde{p} - \tilde{\rho}\tilde{u}^3 - 3\tilde{p}\tilde{u}\right) + \tilde{\rho}\frac{\partial\tilde{U}}{\partial\tilde{\xi}}\right]\right\}$$
$$+\frac{\partial\tilde{U}}{\partial\tilde{\xi}}\left\{\tilde{\rho} - \frac{1}{\tilde{u}^2}\left[-\frac{\partial\tilde{\rho}}{\partial\tilde{\xi}} + \frac{\partial}{\partial\tilde{\xi}}\left(\tilde{\rho}\tilde{u}\right)\right]\right\} - 2\frac{\partial}{\partial\tilde{\xi}}\left\{\frac{\tilde{\rho}}{\tilde{u}}\frac{\partial\tilde{U}}{\partial\tilde{\xi}}\right\} = 0, \quad (13.10)$$

$$\frac{\partial}{\partial\tilde{\xi}}\left(\tilde{\rho}\tilde{u}^2 + 3\tilde{p} - \tilde{\rho}\tilde{u}^3 - 5\tilde{p}\tilde{u}\right)$$
$$-\frac{\partial}{\partial\tilde{\xi}}\left\{\frac{1}{\tilde{u}^2}\frac{\partial}{\partial\tilde{\xi}}\left(2\tilde{\rho}\tilde{u}^3 + 10\tilde{p}\tilde{u} - \tilde{\rho}\tilde{u}^2 - 3\tilde{p} - \tilde{\rho}\tilde{u}^4 - 8\tilde{p}\tilde{u}^2 - 5\frac{\tilde{p}^2}{\tilde{\rho}}\right)\right\}$$
$$+\frac{\partial}{\partial\tilde{\xi}}\left\{\frac{1}{\tilde{u}^2}\left(3\tilde{\rho}\tilde{u}^2 + 5\tilde{p}\right)\frac{\partial\tilde{U}}{\partial\tilde{\xi}}\right\} - 2\tilde{\rho}\tilde{u}\frac{\partial\tilde{U}}{\partial\tilde{\xi}} - 2\frac{\partial}{\partial\tilde{\xi}}\left\{\frac{\tilde{\rho}}{\tilde{u}}\frac{\partial\tilde{U}}{\partial\tilde{\xi}}\right\} \quad (13.11)$$
$$+\frac{2}{\tilde{u}^2}\frac{\partial\tilde{U}}{\partial\tilde{\xi}}\left[-\frac{\partial}{\partial\tilde{\xi}}\left(\tilde{\rho}\tilde{u}\right) + \frac{\partial}{\partial\tilde{\xi}}\left(\tilde{\rho}\tilde{u}^2 + \tilde{p}\right) + \tilde{\rho}\frac{\partial\tilde{U}}{\partial\tilde{\xi}}\right] = 0,$$

Appendix 2 contains the corresponding Maple program.

The following **Figure 13** reflects the result of calculations for the Cauchy conditions:

u(0)=1,p(0)=2,r(0)=1,D(u)(0)=0,D(p)(0)=0,D(r)(0)=0, D(v)(0)=0,v(0)=1.

As we see from **Figure 13**: the pressure distribution (leading to the heat transport) and the density distribution (leading to the charge transport) have the character of moving solitons.

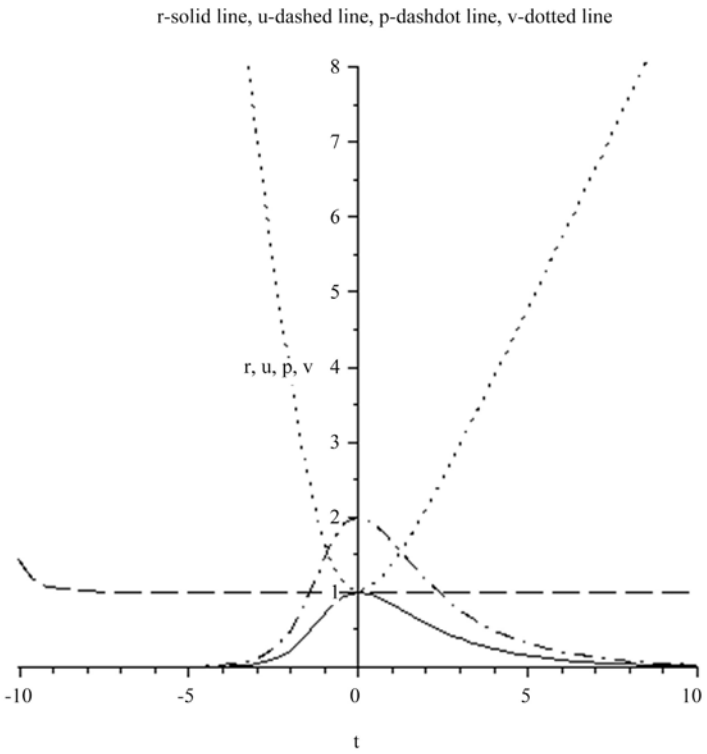

Figure 13. Density r ($\tilde{\rho}$)—solid line, velocity u ($\tilde{u}$)—dashed line, pressure p ($\tilde{p}$)—dash-dot line, self-consistent potential v ($\tilde{U}$)—dotted line.

14. Discussion, Principal Derivations, Conclusion and Proposals

Research of superconductors is curried out very actively. But in spite of obvious success, the following conclusion could be established:

1) Contemporary theories of superconductivity based on the Schrödinger equation, practically exhaust their arguments and have no possibility to explain effects of the high temperature superconductivity.

2) Contemporary theories of superconductivity (including BCS) based on the Schrödinger equation, can't propose the principles of search and creation of superconducting materials.

The most impressive demonstration of these difficulties consists in the fundamental distinction between a strange metal and a conventional metal; in other words in the absence of well-defined quasi-particles in the frame of local physics. This is manifested in transport properties which defy conventional theory, the most famous of which is a T-linear resistivity that persists from nearly 0 K to high temperatures above the proposed Mott-Ioe-Regel (MIR) limit, beyond which Boltzmann theory ceases to be valid.

Without exception, all existing before proposals fail this test. Most of these theories depart from the assumption that the electrical currents are carried by one or the other system of quasi-particles. This is fundamental: it is impossible to identify the simplicity principle dealing with particle physics. The transport is

assumed to be due to thermally excited quasi-particles behaving like classical balls being scattered in various ways, dumping eventually their momentum in the lattice. However, it is a matter of principle that the physics of such quasi-particles in real solids is never simple. These interact with phonons which are very efficient sources of momentum dissipation which should be strongly temperature dependent for elementary reasons.

The conclusion is that quasi-particles are quantum solitons which are moving without destruction.

From position of the quantum non-local hydrodynamics, the problem of search and creation of superconductive materials come to the search of materials which lattices ensure the soliton movement without destruction. In my opinion, *the mentioned materials can be created artificially using the technology of the special introduction of quantum dots in matrices on the basement of proposed quantum hydrodynamics*. It is known that technology of material creation with special quantum dots exists now in other applications.

Conflicts of Interest

The author declares no conflicts of interest regarding the publication of this paper.

References

[1] Boltzmann, L. (1872) Weitere Studien über das Wärmegleichgewicht unter Gasmolekulen. Sitz. Ber. Kaiserl. Akad. Wiss. 66(2) s.275.

[2] Boltzmann, L. (1912) Vorlesungen über Gastheorie. Leipzig: Verlag von Johann Barth. Zweiter unveränderten Abdruck. 2 Teile.

[3] Alekseev, B.V. (1982) Matematicheskaya Kinetika Reagiruyushchikh Gazov (Mathematical Theory of Reacting Gases). Nauka, Moscow.

[4] Alexeev, B.V. (2004) Generalized Boltzmann Physical Kinetics. Elsevier, Amsterdam, 368 p. https://doi.org/10.1016/B978-044451582-7/50027-8

[5] Alexeev, B.V. (2015) Unified Non-Local Theory of Transport Processes. Elsevier, Amsterdam, 644 p.

[6] Alexeev, B.V. (2016) Unified Non-Local Relativistic Theory of Transport Processes. Elsevier, Amsterdam, 455 p.

[7] Alexeev, B.V. (2017) Nonlocal Astrophysics. Dark Matter, Dark Energy, Physical Vacuum. Elsevier, Amsterdam, 454 p.

[8] Alexeev, B.V. (1994) *Philosophical Transactions of the Royal Society of London*, **349**, 417-443. https://doi.org/10.1098/rsta.1994.0140

[9] Alexeev, B.V. (1995) *Physica A*, **216**, 459-468. https://doi.org/10.1016/0378-4371(95)00044-8

[10] Alekseev, B.V. (2000) *Physics-Uspekhi*, **170**, 601-629. https://doi.org/10.1070/PU2000v043n06ABEH000694

[11] Alekseev, B.V. (2003) *Physics-Uspekhi*, **173**, 139-167. https://doi.org/10.1070/PU2003v046n02ABEH001221

[12] Bogolyubov, N.N. (1946) Problemy Dinamicheskoi Teorii v Statisticheskoi Fizike (Dynamic Theory Problems in Statistical Physics). Gostekhizdat, Moscow Lenin-

grad. [Translated into English The Dynamical Theory in Statistical Physics (Hindustan Publ. Corp., Delhi, 1965)]

[13] Born, M. and Green, H.S. (1946) *Proceedings of the Royal Society*, **188**, 10. https://doi.org/10.1098/rspa.1946.0093

[14] Green, H.S. (1952) The Molecular Theory of Fluids. North-Holland Publishing Company, Amsterdam.

[15] Kirkwood, J.G. (1947) *The Journal of Chemical Physics*, **15**, 72. https://doi.org/10.1063/1.1746292

[16] Yvon, J. (1935) La Theorie Statistique des Fluide et l'Equation d'etat. Hermann & Cie, Paris.

[17] Bhatnagar, P.L., Gross, E.P. and Krook, M.A. (1954) *Physical Review*, **94**, 511-525. https://doi.org/10.1103/PhysRev.94.511

[18] Alexeev, B.V. (2008) *Journal of Nanoelectronics and Optoelectronics*, **3**, 143-158. https://doi.org/10.1166/jno.2008.207

[19] Alexeev, B.V. (2008) *Journal of Nanoelectronics and Optoelectronics*, **3**, 316-328. https://doi.org/10.1166/jno.2008.311

[20] Ehrenfest, P. (1979) Collected Scientific Papers. North-Holland Publ. Co., Amsterdam.

[21] Madelung, E. (1927) *Zeitschrift für Physik*, **40**, 322-326. https://doi.org/10.1007/BF01400372

[22] Bell, J.S. (1964) *Physics*, **1**, 195-290. https://doi.org/10.1103/PhysicsPhysiqueFizika.1.195

[23] Homes, C.C., *et al.* (2004) *Nature*, **430**, 539-541. https://doi.org/10.1038/nature02673

[24] Hartnoll, S.A. (2014) *Nature Physics*, **11**, 54. https://doi.org/10.1038/nphys3174

[25] Zaanen, J. (2004) *Nature*, **430**, 512-513. https://doi.org/10.1038/430512a

[26] Zaanen, J. (2018) *SciPost Physics*, **6**, 61. https://doi.org/10.21468/SciPostPhys.6.5.061

[27] Krömer, H. (1958) *Physical Review*, **109**, 1856. https://doi.org/10.1103/PhysRev.109.1856

[28] Ryzhii, V.I. (1969) *Soviet Physics*, *Solid State*, **11**, 1995.

[29] Ryzhii, V.I. (2005) *Uspekhi Fizicheskikh Nauk*, **175**, 205. https://doi.org/10.1070/PU2005v048n02ABEH002104

[30] Monstein, C. and Wesley, J.P. (2002) *Europhysics Letters*, **59**, 514-520. https://doi.org/10.1209/epl/i2002-00136-9

[31] Novoselov, K.S., Geim, A.K., Morozov, S.V., Jiang, D., Zhang, Y., Dubonos, S.V., Grigorieva, I.V. and Firsov, A.A. (2004) *Science*, **306**, 666. https://doi.org/10.1126/science.1102896

[32] Novoselov, K.S., Geim, A.K., Morozov, S.V., Jiang, D., Katsnelson, M.I., Grigorieva, I.V., Dubonos, S.V. and Firsov, A.A. (2005) *Nature*, **438**, 197. https://doi.org/10.1038/nature04233

[33] Geim, A.K. and Novoselov, K.S. (2007) *Nature Materials*, **6**, 183. https://doi.org/10.1038/nmat1849

Appendix 1

Maple program for modeling of soliton motion in two species physical system.

(the program is ready for application)

The ratio L/H is ratio of masses of the light and heavy particles; for example $L = 1$, $H = 1838$.

```
dsolve[interactive]({
diff(v(t),t$2)=-r(t)*(L/H)+(L/H)^2*diff(r(t)*u(t)-r(t),t)/u(t)^2+
s(t)-diff(s(t)*u(t)-s(t),t)/u(t)^2,
diff(r(t)*(1-u(t)),t)+(L/H)*diff(diff(p(t)+r(t)+r(t)*u(t)^2-
2*r(t)*u(t),t)/u(t)^2,t)+(L/H)^2*diff(r(t)*diff(v(t),t)/u(t)^2,t)=0,
diff(s(t)*(1-u(t)),t)+diff((diff(q(t)+s(t)+s(t)*u(t)^2-2*s(t)*u(t),t))/u(t)^2,
t)-diff(s(t)*diff(v(t),t)/u(t)^2,t)=0,
diff((r(t)+s(t))*u(t)^2+p(t)+q(t)-(r(t)+s(t))*u(t),t)+
diff(diff(2*r(t)*u(t)^2+2*p(t)-r(t)*u(t)-r(t)*u(t)^3-
3*p(t)*u(t),t)/(u(t)^2*(H/L)),t)+
diff(diff(2*s(t)*u(t)^2+2*q(t)-s(t)*u(t)-s(t)*u(t)^3-
3*q(t)*u(t),t)/u(t)^2,t)+
diff(r(t)*diff(v(t),t)*(L/H)^2/u(t)^2,t)-
diff(s(t)*diff(v(t),t)/u(t)^2,t)+
r(t)*diff(v(t),t)*(L/H)-s(t)*diff(v(t),t)-
(L/H)^2*diff(v(t),t)*diff(r(t)*(u(t)-1),t)/u(t)^2+
diff(v(t),t)*diff(s(t)*(u(t)-1),t)/u(t)^2-
2*diff(((L/H)^2*r(t)-s(t))*diff(v(t),t)/u(t),t)=0,
diff(r(t)*u(t)^3+5*p(t)*u(t)-r(t)*u(t)^2-3*p(t),t)+
(L/H)*diff(diff(2*r(t)*u(t)^3+10*p(t)*u(t)-r(t)*u(t)^4-8*p(t)*u(t)^2-5*p(
t)^2/r(t)-r(t)*u(t)^2-3*p(t),t)/u(t)^2,t)+
(L/H)^2*diff((2*r(t)*u(t)-3*r(t)*u(t)^2-5*p(t))*diff(v(t),t)/u(t)^2,t)+
2*(L/H)*r(t)*diff(v(t),t)*u(t)-
2*(L/H)^2*diff(v(t),t)*diff(r(t)*u(t)^2+p(t)-r(t)*u(t),t)/u(t)^2-
2*(L/H)^3*r(t)*diff(v(t),t)^2/u(t)^2=-(p(t)-q(t))*u(t)^2*((L+H)/L),
diff(s(t)*u(t)^3+5*q(t)*u(t)-s(t)*u(t)^2-3*q(t),t)+
diff(diff(2*s(t)*u(t)^3+10*q(t)*u(t)-s(t)*u(t)^4-8*q(t)*u(t)^2-5*q(t)^2/s(
t)-s(t)*u(t)^2-3*q(t),t)/u(t)^2,t)+
diff(diff(v(t),t)*(3*s(t)*u(t)^2+5*q(t)-2*s(t)*u(t))/u(t)^2,t)-
2*s(t)*diff(v(t),t)*u(t)+
2*diff(v(t),t)*diff(s(t)*u(t)^2+q(t)-s(t)*u(t),t)/u(t)^2-2*s(t)*diff(v(t),t)^2
/u(t)^2=-(q(t)-p(t))*u(t)^2*((L+H)/L),
diff(R(t),t)=r(t),diff(S(t),t)=s(t),
v(0)=1,r(0)=1,s(0)=1/1838,u(0)=1,p(0)=1000,q(0)=950,R(0)=0, S(0)=0,
D(v)(0)=0,D(r)(0)=0,D(s)(0)=0,D(u)(0)=0,D(p)(0)=0,D(q)(0)=0
});
```

Appendix 2

Maple program for modeling of soliton motion in one species physical system.

(the program is ready for application)

```
dsolve[interactive]({
diff(r(t)*(1-u(t)),t)+diff((diff(p(t)+r(t)+r(t)*u(t)^2-2*r(t)*u(t),t))/u(t)^2,
t)+diff(r(t)*diff(v(t),t)/u(t)^2,t)=0,
diff(r(t)*u(t)^2+p(t)-r(t)*u(t),t)+diff(diff(2*r(t)*u(t)^2+2*p(t)-r(t)*u(t)-
r(t)*u(t)^3-3*p(t)*u(t),t)/u(t)^2,t)+diff(diff(v(t),t)*r(t)/u(t)^2,t)+r(t)*diff(
v(t),t)-diff(v(t),t)*diff(r(t)*(u(t)-1),t)/u(t)^2-
2*diff(diff(v(t),t)*r(t)/u(t),t)=0,
diff(r(t)*u(t)^2+3*p(t)-r(t)*u(t)^3-5*p(t)*u(t),t)-diff(diff(2*r(t)*u(t)^3+
10*p(t)*u(t)-r(t)*u(t)^2-3*p(t)-r(t)*u(t)^4-8*p(t)*u(t)^2-5*p(t)^2/r(t),t)/u
(t)^2,t)+diff(diff(v(t),t)*(3*r(t)*u(t)^2+5*p(t))/u(t)^2,t)-2*r(t)*diff(v(t),t)*
u(t)-2*diff(r(t)*diff(v(t),t)/u(t),t)+2*diff(v(t),t)*(r(t)*diff(v(t),t)+diff(p(t)+r
(t)*u(t)^2-r(t)*u(t),t))/u(t)^2=0,
diff(v(t),t$2)=r(t)+(1/u(t)^2)*diff(r(t)*(1+u(t)),t),
u(0)=1,p(0)=2,r(0)=1,D(u)(0)=0,D(p)(0)=0,D(r)(0)=0,D(v)(0)=0,v(0)=1}
);
```

Appendix 3

The non-stationary wave attenuation of the spherical object without fields.

Let us consider the nonlocal space—time evolution of the spherical object. We suppose:

1) The nonlocal parameter $\tau = const$.

2) Radial velocity of the object $v_{0r} = const$.

3) The thermal velocity $v_T = const$, then

$$p = \rho v_T^2 . \tag{A3.1}$$

The nonlocal system of hydrodynamic equation has the following form—the continuity equation is [5]

$$\frac{\partial^2 \rho}{\partial t^2} + \frac{\partial^2 p}{\partial r^2} + \frac{2}{r}\frac{\partial p}{\partial r} = \frac{1}{\tau}\frac{\partial \rho}{\partial t} \tag{A3.2}$$

and

$$\frac{\partial^2 p}{\partial t^2} + \frac{5}{3}\frac{\partial^2}{\partial r^2}\left(\frac{p^2}{\rho}\right) + \frac{10}{3r}\frac{\partial}{\partial r}\left(\frac{p^2}{\rho}\right) = \frac{1}{\tau}\frac{\partial p}{\partial t}. \tag{A3.3}$$

The system consists of the continuity equation and the energy equation (ρ—density, p—quantum pressure). The equation of motion in a spherical coordinate system is absent if the radial component of the velocity is absent in the case of radial symmetry. Using (A3.1) we find in the dimensionless form; continuity equation

$$\frac{\partial^2 \tilde{\rho}}{\partial \tilde{t}^2}+\frac{\partial^2 \tilde{\rho}}{\partial \tilde{r}^2}+\frac{2}{\tilde{r}}\frac{\partial \tilde{\rho}}{\partial \tilde{r}}=\frac{\partial \tilde{\rho}}{\partial \tilde{t}} \tag{A3.4}$$

and

$$\frac{\partial^2 \tilde{p}}{\partial \tilde{t}^2}+\frac{\partial^2 \tilde{p}}{\partial \tilde{r}^2}+\frac{2}{\tilde{r}}\frac{\partial \tilde{p}}{\partial \tilde{r}}=\frac{3}{5}\frac{\partial \tilde{p}}{\partial \tilde{t}}. \tag{A3.5}$$

The following scales are used: $t \leftrightarrow \tau$, $r \leftrightarrow v_T \tau$. Nonlinear parabolic Equations (A3.4), (A3.5) can be solved by Fourier method. Really, for (A3.4) we separate the unknown variables using

$$\tilde{\rho}=R(\tilde{r})T(\tilde{t}). \tag{A3.6}$$

We find

$$R(\tilde{r})\frac{\partial T(\tilde{t})}{\partial \tilde{t}}=R(\tilde{r})\frac{\partial^2 T(\tilde{t})}{\partial \tilde{t}^2}+T(\tilde{t})\frac{\partial^2 R(\tilde{r})}{\partial \tilde{r}^2}+2\frac{T(\tilde{t})}{\tilde{r}}\frac{\partial R(\tilde{r})}{\partial \tilde{r}} \tag{A3.7}$$

or

$$\frac{1}{T(\tilde{t})}\frac{\partial T(\tilde{t})}{\partial \tilde{t}}-\frac{1}{T(\tilde{t})}\frac{\partial^2 T(\tilde{t})}{\partial \tilde{t}^2}=\frac{1}{R(\tilde{r})}\frac{\partial^2 R(\tilde{r})}{\partial \tilde{r}^2}+2\frac{1}{\tilde{r}R(\tilde{r})}\frac{\partial R(\tilde{r})}{\partial \tilde{r}}. \tag{A3.8}$$

Relations (A3.7) and (A3.8) lead to two ordinary differential equations

$$\frac{\partial^2 T(\tilde{t})}{\partial \tilde{t}^2}-\frac{\partial T(\tilde{t})}{\partial \tilde{t}}+CT(\tilde{t})=0 \tag{A3.9}$$

and

$$\frac{\partial^2 R(\tilde{r})}{\partial \tilde{r}^2}+\frac{2}{\tilde{r}}\frac{\partial R(\tilde{r})}{\partial \tilde{r}}-CR(\tilde{r})=0. \tag{A3.10}$$

If $C<0$

$$T=\exp\left(\frac{1-\sqrt{1-4C}}{2}\tilde{t}\right),\quad C<0. \tag{A3.11}$$

Equation (A3.10) can be solved by numerical methods. For example

$$\tilde{r}\frac{\partial^2 R(\tilde{r})}{\partial \tilde{r}^2}+2\frac{\partial R(\tilde{r})}{\partial \tilde{r}}-C\tilde{r}R(\tilde{r})=0. \tag{A3.12}$$

The solution for the quantum pressure can be found by the analogical way. It should be noticed that the solution of the homogeneous Equations (A3.4) and (A3.5) for unknown variables p and ρ can be found up to an additive arbitrary constant (**Figure 14**).

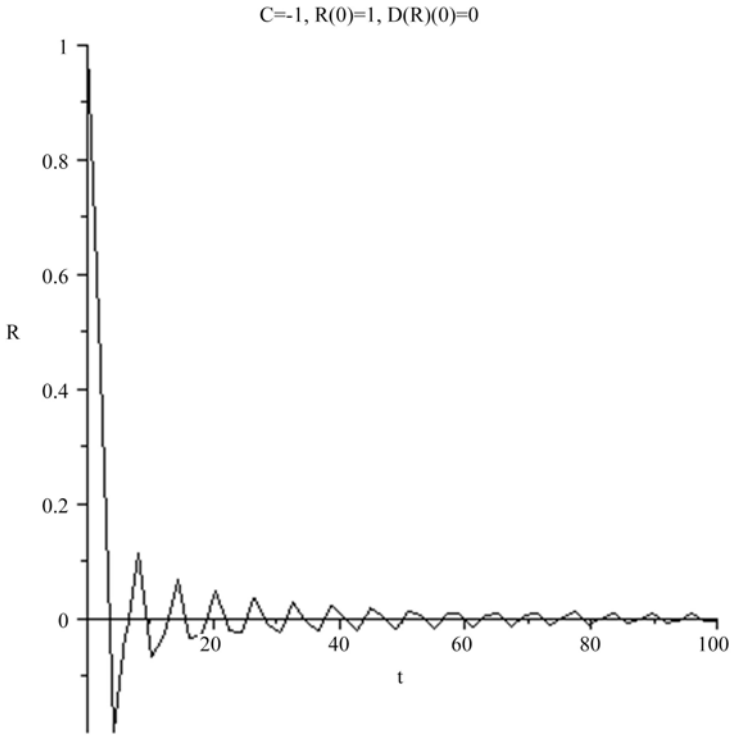

Figure 14. Radial density damping.

Journal of Modern Physics, 2021, 12, 594-604
https://www.scirp.org/journal/jmp
ISSN Online: 2153-120X
ISSN Print: 2153-1196

A Possible Explanation for the Acceleration of the Universe's Expansion without Dark Energy

Dongbiao Kang

School of Physics and Electrical Engineering, Anyang Normal University, Anyang, China
Email: dbkang@aynu.edu.cn

How to cite this paper: Kang, D.B. (2021) A Possible Explanation for the Acceleration of the Universe's Expansion without Dark Energy. *Journal of Modern Physics*, **12**, 594-604.
https://doi.org/10.4236/jmp.2021.125038

Received: March 9, 2021
Accepted: April 13, 2021
Published: April 16, 2021

Abstract

The acceleration of the expansion of the universe has been observed. To explain this phenomenon, physicists usually introduce the dark energy (DE) whose pressure is negative, or they need to modify the gravity to produce a term equivalent to the dark energy. Are there other possibilities? Combining our previous works about statistical mechanics of self-gravitating system with the derivation of van der waals equation, we propose a different matter's equation of state (EoS) in this paper. Then, we find that if the matter's density is low enough, its pressure can always be negative, which means that it is the matter that drives the expansion's acceleration. So here we will not need to add the DE to the universe. Our results also predict that the universe finally will tend to be dominated by an approximately constant energy density whose value can be smaller than DE. The data of Supernova cannot differentiate our model from the standard model, but they may possibly indicate some deviations from ΛCDM.

Keywords

Cosmology, Statistical Mechanics, Dark Energy, Dark Matter

1. Introduction

Under the assumption of isotropy and homogeneity of our Universe at large scale structure, people make a successful explanation to the cosmology accelerating expansion [1] by introducing a new component called DE, which constitutes of about 70% energy of the universe. Up to now, the most successful view about the DE is the ΛCDM model in which the energy density of DE is constant. Although ΛCDM model is very consistent with all observational data, it faces the fine tuning problem [2] and coincidence problem. Alternatively, plenty of other DE models have also been proposed ([3] [4] [5] [6], also see some reviews, such

as [7] [8]), but almost all of them solves the acceleration problem either by introducing new degree of freedom or by modifying gravity, which challenges both cosmology and nuclear physics.

However, do we really need the DE? Or do we need so much DE? We notice that commonly the matter's EoS comes from the classical thermodynamics without consideration of the gravity, has it been confirmed to be reasonable at the cosmological scale? We think that the answer may be not sure, and [9] has ever considered the dark matter as van der waals gas to explain the acceleration of the universe's expansion. Besides, our latest studies also provide different understandings of the long-range statistical mechanics as simply shown in the following: if we apply the Boltzmann entropy

$$S = -\int f \ln f \mathrm{d}\tau \tag{1}$$

into the Newtonian self-gravitating system, with the principle of maximum entropy we will always obtain the isothermal solution with infinite mass and energy [10], which is a serious problem; [11] preliminarily studies the entropy form taken by [12] and proposes that a self-gravitating system's entropy may be a saddle point and not a maximum; [13] completes the variation process of entropy and confirms that we can obtain an EoS which is different from the isothermal solution and can give finite mass; [14] shows the different thermodynamics of self-gravitating system.

In this paper, we will further discuss that the general relativity may also have similar effects on the matter's EoS at the cosmological scale. In the next section, we will show our findings and propose a reason for the universe's accelerating expansion without DE. In section 3, we will use the data of supernova to shorten the range of the values of the parameters in our model. Some discussions and conclusions will be made in the final section. In this paper, we set $c=1$ and use "0" to denote quantity's current value except Ω_{x0} below.

2. Explanation for the Acceleration

According to the cosmological principle, the universe is homogeneous and isotropic. The homogeneity and isotropy of the universe requires the energy-momentum tensor of the matter to be written as

$$T^{\mu\nu} = (\rho + p)U^{\mu}U^{\nu} + pg^{\mu\nu}. \tag{2}$$

where ρ is the energy density, p is the pressure, and U^{μ} is the velocity four-vector. After we substitute (2) into the Einstein's equation, we can get the Friedmann equation:

$$\ddot{a} = -4\pi G\left(\frac{\rho}{3} + p\right)a, \dot{a}^2 + \kappa = \frac{8\pi G}{3}\rho a^2, \tag{3}$$

where a is the scale factor. The energy-momentum conservation law is

$$\dot{\rho} = -\frac{3\dot{a}}{a}(\rho + p), \tag{4}$$

which also can be obtained from Equation (3). Combining the EoS $p = p(\rho)$ with Equation (3), we can get the solution of a, p and ρ. After the inflation, the universe is assumed to be a gas whose pressure is [15]

$$p = \frac{v^2}{3}\rho, \tag{5}$$

where v^2 is the mean-square velocity, m is the mass of particle, and T is the defined temperature. We usually use $p = 0$ and $p = \rho/3$ to denote the matter ($v^2 = \frac{3kT}{m} \ll 1$) and radiation's ($v = 1$) EoSs respectively, but by Equation (5) we cannot understand the nature of the DE whose pressure is negative, even commonly we understand DE by that it does negative work to the universe.

Notice that Equation (5) can be derived by two ways [16]: we can use the related formulas of the classical statistical mechanics to calculate the matter and radiation's EoSs, both of which satisfy Equation (5); it also can be obtained by the kinetics alone, which needs to consider the bombardment by the particles (rigid body) on the walls of the container to calculate the kinetic pressure. However, the classical statistical mechanics does not consider the effects of gravity; besides, the wall of the container does not exist in the universe, and in fact we can treat the wall to be a potential well with minus infinity at the boundary for the particles, while the gas in the universe is in the gravitational potential well which is different from the wall. If we treat the universe as a thermodynamical system whose particles interact by gravity, will these two ways mentioned above still be available under the cosmic background where the effect of general relativity cannot be neglected? We think that the answer is yes for the radiation, because the effect of gravity can be neglected compared with the electromagnetic force; but for the matter whose main component is the dark matter for which the gravity plays the most important role, the answer may be not sure. In [13] by the method of statistical mechanics we have obtained an EoS which is used to describe the thermodynamical equilibrium state of a virialized Newtonian self-gravitating system:

$$\rho = \beta p + \alpha p^{4/5}, \tag{6}$$

where β and α are positive and determined by the energy and mass respectively. β has been identified to m/kT in [14]. Notice that the power index of the second term of Equation (6)'s right ride is less than 5/6, which ensures that the mass and energy are finite galdyn08. From Equation (6) we can obtain $p = p(\rho)$, which can be approximately written as [14]

$$p = \frac{kT\rho}{m} - \alpha\left(\frac{kT}{m}\right)^{\frac{9}{5}}\rho^{\frac{4}{5}}. \tag{7}$$

Of course, Equation (7) is different from Equation (5) even we let $v^2 = 3kT/m$. Next we will compare Equation (6) with the van der waals to further explain the possible reasonability of Equation (6). The van der waals equation is:

$$\left(p+\frac{n^2a}{V^2}\right)(V-nb)=NkT, \tag{8}$$

where a and b is used to describe the attractive and repulsive interactions among the molecules of gas respectively, and they are determined by the potential of the molecules' two-body interactions and can be calculated by the method of cluster expansion in the canonical ensemble (see some books of statistical mechanics such as [16]). If the potential of the molecules' two-body interactions has other forms, a and b will still appear in Equation (8) but their values will be changed. When we neglect the repulsive interactions and set $b=0, V=Nm/\rho$, Equation (8) becomes

$$p=\frac{kT}{m}\rho-a\left(\frac{n}{Nm}\right)^2\rho^2, \tag{9}$$

which is very analogous to Equation (7), even we can speculate that existence of α in Equation (7) should be a requirement of possible statistical mechanics dealing with Newtonian gravitating systems. This speculation is also supported by the following: the two-body interaction is the main interaction in van der waals gas and a and b in Equation (8) are related to the two-body interaction; while the force on the single particle of gravitating system is mainly determined by the gravitational field generated by all the particles [10], and coincidentally α in Equation (7) is determined by the total mass. The change of index from 2 to 4/5 may be caused by the change from two-body interactions among molecules to long-range Newtonian gravity. If this speculation is correct, can general relativity cause similar effect on the EoS of the matter? We do not know the answer, but if such theory exists we may do some guess of its results as the following: based on above analysis, we find that β is related to the temperature, α is necessary to denote the effect of the long-range statistical mechanics, and neither of them will disappear if the gravity changes from the Newtonian to the general relativity; but the index 4/5 in Equation (7) may be changed in the general relativity. So we assume that at the cosmological scale the EoS of the matter may be written as

$$p_m=\frac{v^2}{3}\rho_m-\Omega_{x0}\rho_0^{1-t}\rho_m^t, t<1, \Omega_{x0}>0, \tag{10}$$

where $\rho_0=\frac{3H_0^2}{8\pi G}$, t is a constant, and v and Ω_{x0} are about constants or very slowly changing functions of the time at the matter dominated era. Here we temporally do not assume that v^2 is as small as its value in ΛCDM. Notice that the form of Equation (10) can be directly borrowed from the van der waals equation, and only $t<1$ is speculated from our previous works. Notice that [9] even considers the dark matter as the van der waals gas with an EoS $p=\gamma\rho/(1-\beta)-\alpha\rho^2$ to explain the acceleration problem, which is very similar to this paper. Besides, [17] treats the dark matter interaction as an alternative of dark energy; [18] [19] also introduce the fluids with $p=-\rho-A\rho^\alpha$, which is to

describe the dark energy. These works are similar but different from this paper.

Now we will analyze the effect of Equation (10) on the universe's evolution. Our model only modifies the pressure of matter, so the cosmic history before the matter-dominated era is almost not effected and we only consider the later time. From observations we know that the universe is always expanding, so ρ_m is decreasing with time. When ρ_m is large enough, p_m is positive but is smaller than Equation (5). After some time, there will be an era described by $p_m \sim 0$, just like CDM. But it is evident that the pressure in Equation (10) can be negative if

$$\left(\frac{\rho_m}{\rho_0}\right)^{1-t} < \frac{\Omega_{x0}}{v^2}, \tag{11}$$

which tells us that when the matter reaches the thermodynamical equilibrium, its pressure will be negative if its density is low enough. This really is a surprising thing but may be natural in our model. Here we will also mention the work of [20] which proves that the N-particle system's thermodynamic pressure cannot be negative if the force between two particles is short range, while coincidentally the gravity is long-range, which means that the pressure of N-particle gravitating system has not been ensured to be not negative. Because the matter's density is always decreasing, it will satisfy Equation (11) at some time, then can this negative pressure accelerate the universe's expansion? This requires $p < -\rho/3$, *i.e.*

$$\left(\frac{\rho_m}{\rho_0}\right)^{1-t} < \frac{3\Omega_{x0}}{3v^2+1}. \tag{12}$$

Of course this equation also can be satisfied because of the expansion of the universe, so we find that if the long-range statistical mechanics is really different from the classical one and can produce an EoS like Equation (10), it will be the matter that drives the universe's accelerated expansion! The next question is how the universe will evolve in the future, which requires some detailed calculations. We substitute Equation (10) into the Equation (4), then the matter's density will evolve as

$$\frac{\rho_m}{\rho_0} = \left[\frac{C\left(\frac{a_0}{a}\right)^{3B(1-t)} + \Omega_{x0}}{B}\right]^{\frac{1}{1-t}} = \left[\left(\frac{C}{B}\right)^{1-t}\left(\frac{a_0}{a}\right)^{3B} + \cdots + \left(\frac{\Omega_{x0}}{B}\right)^{\frac{1}{1-t}}\right] \tag{13}$$

where

$$B = 1 + \frac{v^2}{3}, C = B\left(1-\Omega_{r0}\right)^{1-t} - \Omega_{x0}, \tag{14}$$

and Ω_r is the current radiation's density parameter. Notice that $1 < B < 4/3$. From observations we know $\kappa \sim 0$ and $\Omega_{r0} \sim 0.04$, if we define

$$\Omega_m = \frac{\rho_m}{\rho_0}, \tag{15}$$

its current value $\Omega_{m0}=1-\Omega_{r0}$ will be much closer to 1, which is a major difference of our model from ΛCDM. When $\Omega_{x0}=0$ (or a is small enough so that Ω_{x0} can be neglected) and B tends to be 1, Equation (13) will become $\rho\propto a^{-3}$. If $B=1$ and $t=0$, the form of Equation (13) will be the same as a direct addition of the matter and DE, and our model gives the same results as ΛCDM, but even at this case our results still provide a different understanding of the universe, and any deviations from $B=1$ or $t=0$ will indicate the preferences of our model. Because of the universe's expansion, from Equation (13) we can easily find that the density will finally approximately become a constant

$$\rho_x=\rho_0\left(\frac{\Omega_{x0}}{B}\right)^{\frac{1}{1-t}}, \tag{16}$$

If we neglect the variations of v and Ω_{x0} with time. So our model predicts almost the same destiny of the universe as ΛCDM: the standard model says that the energy consists of the radiation, the matter and the DE, with the expansion of the universe the DE will dominate and the expansion will accelerate; while our result states that because there is some unknown physics such as long-range statistical mechanics, even the universe always expands there is a no-zero minimum of the energy density of the matter, which also accelerates the expansion of the universe. However, this minimized density can be smaller than DE because: from Equation (3) we know that $\ddot{a}>0$ requires that ρ decreases slower than a^{-2}, so from Equation (13) we know that not only the constant term but also other terms whose power indexes are larger than −2 makes the expansion accelerate. So the value of Equation (16) should be smaller than DE if $t>0$. If in the future the universe's density becomes a constant, according to Equation (3) our results may give a smaller value of the Hubble parameter than the standard model, which also differentiates our results from the standard model.

3. Compared with the Data of SNIa

3.1. Data Analysis

Next we will analyze the data of SNIa. First we need to calculate the Hubble parameter. It can be expressed by four parameters $\left(t,\Omega_{x0},B,h_0\right)$ in our model,

$$\frac{H(z)}{H_0}=\left(\frac{C(1+z)^{-3B(1-t)}+\Omega_{x0}}{B}\right)^{\frac{1}{1-t}}+\Omega_{r0}(1+z)^4. \tag{17}$$

where h_0 is the present value of the Hubble parameter H_0 in unit 100 km/s/Mpc and z is the redshift.

To check our proposals made in Sec. II and to constrain the model parameters, we take use of the Union2 dataset [21] and the Hubble evolution data. The Union2 dataset contains 557 type Ia SN data and covers the redshift range $z=[0.015,1.4]$, including samples from other surveys, such as CfA3 [22], SDSS-II Supernova Search [23] and high-z Hubble Space Telescope.

We fit the SNIa data by minimizing the χ^2 value of the distance modulus.

χ^2_{sn} for SNIa is obtained by comparing theoretical distance modulus $\mu_{th}(z)=5\log_{10}\left[(1+z)\int_0^z \mathrm{d}x/E(x)\right]+\mu_0$ ($\mu_0=42.384-5\log_{10}h_0, E(z)=H(z)/H_z$) with observed μ_{ob} of supernova:

$$\chi^2_{sn}=\sum_i^{557}\frac{\left[\mu_{th}(z_i)-\mu_{ob}(z_i)\right]^2}{\sigma^2(z_i)}.$$

To reduce the effect of μ_0, we expand χ^2_{sn} with respect to μ_0 [24]:

$$\chi^2_{sn}=F+2G\mu_0+H\mu_0^2 \tag{18}$$

where

$$F=\sum_i\frac{\left[\mu_{th}(z_i;\mu_0=0)-\mu_{ob}(z_i)\right]^2}{\sigma^2(z_i)},$$

$$G=\sum_i\frac{\mu_{th}(z_i;\mu_0=0)-\mu_{ob}(z_i)}{\sigma^2(z_i)},$$

$$H=\sum_i\frac{1}{\sigma^2(z_i)}$$

(18) has a minimum as

$$\tilde{\chi}^2_{sn}=\chi^2_{sn,\min}=F-G^2/H$$

which is independent of μ_0. In fact, it is equivalent to perform an uniform marginalization over μ_0, and the difference between $\tilde{\chi}^2_{sn}$ and the marginalized χ^2_{sn} is just a constant [17]. We will adopt $\tilde{\chi}^2_{sn}$ as the goodness of fit between theoretical model and SNIa data.

We also use the 12 Hubble evolution data from [25] and [26], its χ^2_H is defined as

$$\chi^2_H=\sum_{i=1}^{12}\frac{\left[H(z_i)-H_{ob}(z_i)\right]^2}{\sigma_i^2}.$$

Note that the redshift of these data falls in the region $z\in(0,1.75)$.

In summary,

$$\chi^2_{tot}=\tilde{\chi}^2_{sn}\chi^2_H$$

and we assume uniform priors on all the parameters. We also prior assume that the age of our universe T_0 satisfies $10\ \mathrm{Gyr}<T_0<20\ \mathrm{Gyr}$.

3.2. Results and Discussions

The analysis is performed by using the Monte Carlo Markov Chain in the multi-dimensional parameter space to derive the likelihood. Naturally, we employ some physically obvious limitations to make the estimation of parameters more robust, for example, we set $t<1, 1\le B<4/3$ in our analysis. We first investigate the constraint on the model parameters, and the best-fit values and errors of parameters are summary in **Table 1**. We also plot the 1D marginalized distribution probability of each parameter, shown in **Figure 1**. The likelihood distribution

shows a remarkable deviation from the Gaussian distribution, which result in a discrepancy between the best-fit values and the expected values of the parameters, as consistent with the result in Table 1.

Further, we focus on parameters (t, B), which play a more important role in our model. The 2D contour plot is shown in Figure 2, which shows that the results of standard ΛCDM model are contained in our model. The 2σ errors mean that the case with $t > 0.80$ is excluded at 95.4% confidence level, which is very consistent with our speculation. But constraint on B cannot be obtained.

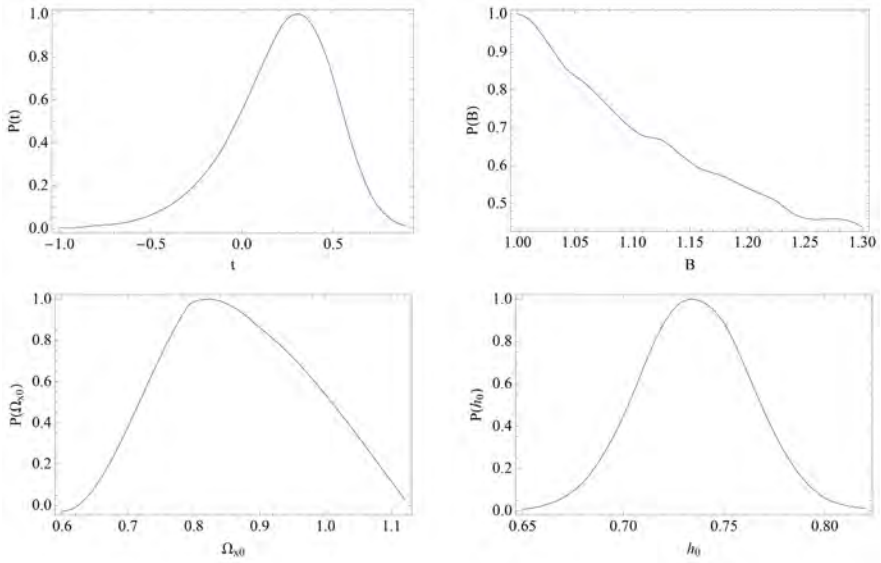

Figure 1. 1D marginalized distribution probability of t, Ω_{x0}, B, h_0.

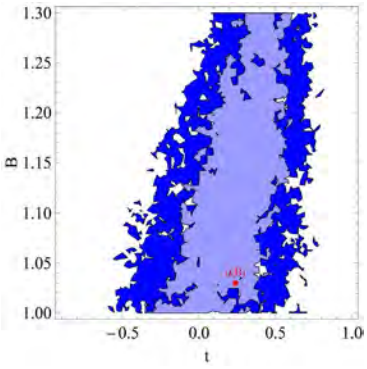

Figure 2. 68% and 95% contour plot in t-B plane. Red dot in the center is the expected value.

Table 1. Expected values, $1-\sigma$ and $2-\sigma$ error of t, Ω_{x0}, B, h_0 in this model. The second line is in form of $\text{Expectation}^{-1\sigma,-2\sigma}_{+1\sigma,+2\sigma}$. And the best-fit values are also shown in the last line, which are different from the expected values.

t	Ω_{x0}	B	h_0
$0.237^{-0.347,-1.237}_{+0.346,+0.562}$	$0.824^{-0.107,-0.161}_{+0.200,+0.271}$	1.030	$0.724^{-0.025,-0.052}_{+0.050,+0.074}$
0.051	0.734	1.008	0.738

From above results, we find that the data of SNIa cannot differentiate our model from ΛCDM. We need to consider the perturbation theory to further test our model, which will be another work. But from Table 1 and Figure 1 we can see that the data seem to indicate some deviations from $B=1$ and $t=0$, *i.e.* ΛCDM. Notice that according to current criteria, the dark matter is called to be cold if $v<0.1$[1], which means that $B<1.0033$, so there is only a very short range of B for the cold matter. However, both the best-fit and expected value of B are larger than 1.0033, which suggests that the matter may be not so cold as ΛCDM predicts. This conclusion also agrees with some works [27] [28] which aim to use the warm dark matter to solve the contradictions between observations and numerical simulations of ΛCDM at the galaxy scale.

4. Conclusions

Our previous works have proved that the thermodynamics of gravitating systems at the galaxy scale may be different from the classical one, and we obtain an EoS like Equation (7), which is in analogy with the van der waals equation. We speculate that it is the long-range statistical mechanics that produces the Equation (7). Based on possible effect of the general relativity on the matter's EoS, we propose that at the cosmological scale, the form of the matter's EoS may be like the Equation (10). Then, we find that with the universe's expansion the matter's density will decrease with time to be a no-zero minimized constant, and it is the matter that drives the expansion's acceleration. Our work is similar to [9], but with different form of EoS and different motivation. So our model may provide a new kind of explanation for the expansion's acceleration, and there are three major different results of our model from ΛCDM:

1). our new defined $\Omega_m=1-\Omega_r$ is close to 1 and is much larger than its value in ΛCDM;

2). B and t may be not exactly to 1 and 0 respectively;

3). if the universe's density becomes a constant in the future, its value can be smaller than DE.

It is easier to compare our model with ΛCDM by the second point, so we use the data of SNIa to constrain the value of B and t. After analyzing the data's, we cannot differentiate our model from ΛCDM, but there seems to be some indications of deviations from ΛCDM. To further test our model, we need to consider the density's perturbation in the future.

Acknowledgements

DBK is very grateful for Zhong-Liang Tuo's many helps of dealing with the data of supernova. This work is supported by the National Natural Science Foundation of China, No. 11947098.

Conflicts of Interest

The author declares no conflicts of interest regarding the publication of this paper.

[1]http://en.wikipedia.org/wiki/Dark_matter.

References

[1] Perlmutter, S., *et al.*, Supernova Cosmology Project Collaboration (1999) *The Astrophysical Journal*, **517**, 565. arXiv:astro-ph/9812133

[2] Copeland, E.J., Sami, M. and Tsujikawa, S. (2006) *International Journal of Modern Physics D*, **15**, 1753.

[3] Copeland, E.J., Sami, M. and Tsujikawa, S. (2006) *International Journal of Modern Physics D*, **15**, 1753. https://doi.org/10.1142/S021827180600942X

[4] Caldwell, R.R. and Steinhardt, P.J. (1998) *Physical Review D*, **57**, 6057. https://doi.org/10.1103/PhysRevD.57.6057

[5] Steinhardt, P.J., Wang, L.M. and Zlatev, I. (1999) *Physical Review D*, **59**, Article ID: 123504. https://doi.org/10.1103/PhysRevD.59.123504

[6] Capozziello, S., Cardone, V.F., Carloni, S. and Troisi, A. (2003) *International Journal of Modern Physics D*, **12**, 1969.

[7] Nojiri, S.I. and Odintsov, S.D. (2011) *Physics Reports*, **505**, 59. https://doi.org/10.1016/j.physrep.2011.04.001

[8] Cai, Y.-F., Saridakis, E.N., Setare, M.R. and Xia, J.-Q. (2010) *Physics Reports*, **493**, 1. https://doi.org/10.1016/j.physrep.2010.04.001

[9] Capozziello, S., Cardone, V.F., Carloni, S., De Martino, S., Falanga, M., Troisi, A. and Bruni, M. (2005) *JCAP*, **0504**, 005. https://doi.org/10.1088/1475-7516/2005/04/005

[10] Binney, J. and Tremaine, S. (2008) Galactic Dynamics. 2nd Edition, Princeton University Press, Princeton. https://doi.org/10.1515/9781400828722

[11] He, P. and Kang, D.B. (2010) *MNRAS*, **406**, 2678. https://doi.org/10.1111/j.1365-2966.2010.16869.x

[12] White, S.D.M. and Narayan, R. (1987) *MNRAS*, **229**, 103. https://doi.org/10.1093/mnras/229.1.103

[13] Kang, D.B. and He, P. (2011) *MNRAS*, **416**, 32. https://doi.org/10.1016/j.destud.2011.05.002

[14] Kang, D.B. (2011) Different Thermodynamics of Self-Gravitating Systems and Discussions for Some Observations and Simulations.

[15] Liddle & Lyth (2000) Cosmological Inflation and Large-Scale Structure. Cambridge University Press, Cambridge. https://doi.org/10.1017/CBO9781139175180

[16] Pathria, R.K. (1996) Statistical Mechanics. 2nd Edition, Butterworth-Heinemann, Oxford.

[17] Basilakos, S. and Plionis, M. (2009) *A&A*, **507**, 47B. https://doi.org/10.1051/0004-6361/200912661

[18] Stefancic, H. (2005) *Physical Review D*, **71**, Article ID: 084024. https://doi.org/10.1103/PhysRevD.71.124036

[19] Nojiri, S.I. and Odintsov, S.D. (2005) *Physical Review D*, **72**, Article ID: 023003. https://doi.org/10.1103/PhysRevD.72.023003

[20] van Hove, L. (1949) *Physica*, **15**, 11. https://doi.org/10.1016/0031-8914(49)90059-2

[21] Amanullah, R., *et al.* (2010) *The Astrophysical Journal*, **716**, 712.

[22] Hicken, M., *et al.* (2009) *The Astrophysical Journal*, **700**, 1097.

[23] Holtzman, J.A., *et al.* (2008) *The Astrophysical Journal*, **136**, 2306.

[24] Nesseris, S. and Perivolaropoulos, L. (2005) *Physical Review D*, **72**, Article ID:

123519. https://doi.org/10.1103/PhysRevD.72.123519

[25] Simon, J., Verde, L. and Jimenez, R. (2005) *Physical Review D*, **71**, Article ID: 123001. https://doi.org/10.1103/PhysRevD.71.123001

[26] Gaztanaga, E., Cabre, A. and Hui, L. (2008) Clustering of Luminous Red Galaxies IV: Baryon Acoustic Peak in the Line-of-Sight Direction and a Direct Measurement of H(z).

[27] Colin, P., Avila-Reese, V. and Valenzuela, O. (2000) *The Astrophysical Journal*, **542**, 622. https://doi.org/10.1086/317057

[28] Bode, P., Ostriker, J.P. and Turok, N. (2001) *The Astrophysical Journal*, **556**, 93. https://doi.org/10.1086/321541

Journal of Modern Physics, 2021, 12, 605-622
https://www.scirp.org/journal/jmp
ISSN Online: 2153-120X
ISSN Print: 2153-1196

General Operational Protocol for Coherence. Central Limit Theorem as Approximation

Maria K. Koleva

Institute of Catalysis, Bulgarian Academy of Sciences, Sofia, Bulgaria
Email: mkoleva_1113@yahoo.com

How to cite this paper: Koleva, M.K. (2021) General Operational Protocol for Coherence. Central Limit Theorem as Approximation. *Journal of Modern Physics*, **12**, 605-622.
https://doi.org/10.4236/jmp.2021.125039

Received: March 8, 2021
Accepted: April 13, 2021
Published: April 16, 2021

Abstract

A general operational protocol which provides permanent macroscopic coherence of the response of any stable complex system put in an ever-changing environment is proposed. It turns out that the coherent response consists of two parts: 1) a specific discrete pattern, called by the author homeostatic one, whose characteristics are robust to the statistics of the environment; 2) the rest part of the response forms a stationary homogeneous process whose coarse-grained structure obeys universal distribution which turns out to be scale-invariant. It is demonstrated that, for relatively short time series, a measurement, viewed as a solitary operation of coarse-graining, superimposed on the universal distribution results in a rich variety of behaviors ranging from periodic-like to stochastic-like, to a sequences of irregular fractal-like objects and sequences of random-like events. The relevance of the Central Limit theorem applies to the latter case. Yet, its application is still an approximation which holds for relatively short time series and for specific low resolution of the measurement equipment. It is proven that the asymptotic behavior in each and every of the above cases is provided by the recently proven decomposition theorem.

Keywords

Decomposition Theorem, Central Limit Theorem, Notion of a General Operational Protocol, Notion of a Law, Coarse-Graining, Scale Invariance

1. Introduction

So far, the generally accepted view on the notion of coherence assumes that isolated systems synchronize the behavior of their constituents by means of establishing a steady interference pattern throughout the whole system by means of evening the frequencies, wave numbers and sustaining a constant phase shift of

the waves emitted by the constituents. The quantum mechanical dualism wave-particle renders this mechanism to be proclaimed ubiquitous since atoms and molecules that constitute each and every object in the Universe are quantum objects.

However, a closer look on this consideration displays some fundamental flaws:

1) An interference pattern stays steady if only the environment is kept permanently the same. This precludes the application of the above idea to any system put in ever-changing environment which, however, is the vast amount of real systems. Thus, all living things, although constituted by atoms and molecules, exchange matter and energy with the environment (we eat, sweat etc.) which is ever-changing (day-night shift, seasonal changes etc.);

2) Interference patterns are unstable: they are vulnerable to tiniest local perturbations of the major characteristics which provide the interference: frequency, wave number and phase shift;

3) The interference pattern is static. The latter implies that once established, a pattern stays the same forever. Thus, the idea about coherence through interference becomes inapplicable to living organisms and open systems which change their current status in the process of exchanging matter/energy with a an ever-changing environment in a dynamical way;

4) The interference is an addition of waves and thus cannot launch chemical transformations.

The above considerations are persuasive enough to call for a new general idea about coherence which would be available for all complex systems put in an ever-changing environment.

To remind, the complex system is a new field of science that aims to provide answers to the questions: how parts of a system give rise to a variety of its collective behaviors, and how the system interacts with its environment. It is easy to enumerate examples of complex systems. These are, for example, the social systems whose constructive elements are the people; the brain as a biological system is composed out of neurons; molecules are formed out of atoms; the weather is formed out of air flaws. This new field of study of complex systems cuts across all traditional disciplines of science, as well as engineering, management, and medicine.

The intensive empirical examination that was going on in the last decades displays the remarkable enigma of their behavior: the highly specific for each complex system properties persistently coexist with certain universal, shared by each of them ones. Thus on the one hand, they all share the same characteristics, such as power law distribution and sensitivity to environmental variations, for example; one the other hand, each system has its unique "face", *i.e.* one can distinguish between an earthquake and heartbeat of a mammal. What makes the study of this coexistence so important is the enormous diversity of systems where it has been established. In order to get an idea about this vast ubiquity, let us present a brief list of such phenomena: earthquakes, traffic noise, heartbeat of

mammals, public opinion, currency exchange rate, electrical current, chemical reactions, weather, ant colonies, DNA sequences, telecommunications, etc.

It is obvious that the coexistence of universal characteristics along with specific, even unique ones, suggests that its successful explanation must be insensitive both to the dynamical details of each and every system and to the statistics of the environmental impacts. Thus, the mathematical frame of any such explanation is rather closer to a general protocol then to a law in its traditional meaning. To remind, the notion of a law constitutes specific recursive relations between specific variables characterizing any given phenomenon which remain invariant on repetition. What is tacitly presupposed is that, on repetition, the environment must re-occur the same.

A general operational protocol which successfully explains the enigmatic coexistence of specific and universal properties shared by all stable complex systems has been put forward by the author in her book [1]. It consists of idea that this bizarre coexistence can be explained in the setting of a general operational protocol, called by the author boundedness, which asserts that a system stays stable if and only if the rates and amplitudes of both local and global exchange of matter/energy are permanently sustained not to exceed specific margins. It is obvious that this idea brings about a coherence of the response which comes from different parts of a system: indeed, the boundedness of rates and amplitudes implies establishing of long-range spatio-temporal correlations among distant parts of a system. In turn, a macroscopic coherence of any response of any complex system is established. The major advantage of the concept of boundedness consists of its central result which proves that the coherent response of any stable complex system comprises both a specific and a universal part: the specific one consists of a steady specific to a system pattern whose characteristics are robust to the details of the environmental impact and to the specific dynamics of the corresponding system, and the rest part which obeys universal distribution on a coarse-grained scale which is also insensitive to the details of the environmental impact and to the specific dynamics of the corresponding system.

Yet, 4 questions arise:

1) Which are the major characteristics of the macroscopic coherence? do they provide coexistence of universal and specific properties? Is the macroscopic coherence stable in a long run?;

2) Since this coherence is spontaneous, what is the general physical protocol which provides it so that to be universally available on the one hand, and robust to the details of any concrete dynamics on the other hand;

3) How the spontaneous development of internal fluctuations affects the macroscopic coherence? The importance of this matter lies in claim of the fluctuation-dissipation theorem which states that any response of any system exactly matches the behavior of an appropriate fluctuation. Then, why giant internal fluctuations do not destroy the permanent macroscopic coherence of the response;

4) How the coherence interferes with the measurement.

In the setting of boundedness the answers above 4 questions turn intertwined. The general physical protocol governing the dynamics of the spontaneously executed physico-chemical processes has been put forward in [1] and consists in the following: local exceeds of energy are dissipated as emission of local acoustic phonons at a given spatio-temporal point and their absorption at another spatio-temporal point; local exceeds of matter are dissipated by means of targeted transportation of a specific constituents from a specific initial spatio-temporal point to a specific distant spatio-temporal point. Thus, the travel of matter waves between specific distant points serves as a general protocol for launching specific chemical reactions so that the input reagents and the output products are produced at distant points leaving at the same time the chemical reactions to be local events. Then, the global coherence appears as sequences of local emissions and absorptions of acoustic phonons and mater waves. The ubiquity of that mechanism is grounded on the ubiquitous presence of acoustic phonons and on the recently proved ubiquity of the matter wave emission [1] [2] in any system regardless to its nature and its physico-chemical characteristics.

The sequences of local acoustic phonon and /or matter wave emissions and absorptions are described mathematically through the properties of specially introduced for this purpose mathematical objects called by the author bounded irregular sequences (BIS) so that each term of any BIS consists of a unique piece of wave (local acoustic phonon and/or local matter wave). A systematic study of their behavior is provided in Chapter 1 and Chapter 2 of [1] where it is proven that they exhibit certain exclusive properties which are not shared by their unbounded and/or periodic counterparts. Some of these excusive properties come next.

The greatest importance of the proposed physical protocol is best pronounced through the proof that the power spectrum of any long-running BIS comprises additively two parts: a specific discrete pattern, called a homeostatic one, and a continuous band of universal shape $1/f^{\alpha(f)}$ so that both the homeostatic pattern and the shape of the continuous band are robust to the details of the statistics of the succession of the members in any BIS. This result constitutes the notion of the called by the author decomposition theorem. Thus, the decomposition theorem proves that the response of any stable complex system is permanently macroscopic coherent and it consists of a specific steady pattern (the current homeostatic pattern) and the deviations from it which are also macroscopically coherent. Further, it is proven that the deviations from a homeostatic pattern obey a universal distribution whenever the continuous band in the power spectrum is a smooth one and does not signals out any special component. Thus, the central result of the decomposition theorem proves in most general terms the ubiquity of the coexistence of specific and universal properties for each and every complex system put in an ever-changing environment.

Next in the line of questions comes the following one: Under what conditions

a homeostatic pattern remains stable and intact in a long-run? The proof of the decomposition theorem states that formally this is a condition about a uniform distribution of the zeroes of a BIS. Yet, the greatest advantage of the decomposition theorem is that the same condition provides not only a stable in a long-run existence of a specific coherent pattern (that is a homeostatic pattern) but a long-term stable functioning of the entire system by means of providing a BIS to form a stationary homogeneous process. In turn, the obtained robustness of the structure of a homeostatic pattern to the statistical and dynamical details of the interaction of the corresponding system with an ever-changing environment allows unambiguous separation of an object from its environment. Indeed, the notion of an object consists of its homeostatic pattern because the characteristics of a homeostatic pattern remain intact in an ever-changing environment. Moreover, one can define them regardless to the details of that environment.

Next in the present paper special attention to the role of the condition about uniform distribution of the zeroes for establishing a scale-invariant coarse-grained general distribution of any stationary BIS regardless to the details of the member succession in the original BIS, is paid. The importance of this attention lies in the considered in the section 3 highly non-trivial relation between the scale-invariance of the coarse-graining which produces a universal distribution of stationary BIS and the specific resolution of any measurement. Indeed, it is demonstrated that, although the notions of coarse-graining and resolution imply the same, namely non-discernibility of certain fine details, the superimposing of the resolution of any measurement, viewed as solitary operation of coarse-graining, onto scale-invariant universal distribution, results in a rich variety of behaviors. Some of those cases are considered in section 3. It turns out that the relevance of the Central Limit Theorem appears as an approximation appropriate for specific relations between the characteristics of a given measurement and the characteristics of the corresponding universal behavior. Yet, the major result is that the asymptotic behavior of each and every stable complex system is governed by the decomposition theorem.

Outlining, the rich variety of behaviors is a highly non-trivial result of the impact of a measurement which, though being a specific form of coarse-graining, is not scale-invariant. It is worth noting once again that the universal behavior of a coarse-grained stationary BIS is scale-invariant unlike a measurement which is a solitary non-scale-invariant operation superimposed on the scale-invariant universal behavior.

The central for the present paper assertion states that the Central Limit Theorem (CLT) appears as a specific outcome of the role of measurement and turns out to be a good approximation to the decomposition theorem for relatively short time series. That is why, now I present the major clues and consequences of the decomposition theorem so that to reveal in the clearest way why and how CLT appears as an approximation to the decomposition theorem.

The high non-triviality of the above matter is best illustrated by the following

consideration: the additive decomposition of a power spectrum to a homeostatic pattern and a continuous band does not involve any information about the details of the statistics and dynamics of the variations in any time series. To compare, the shape of the power spectrum of any unbounded time series explicitly depends on concrete statistics of the time series. The robustness of any homeostatic pattern and the robustness of the shape of the corresponding continuous band render the resultant decomposition generic property of each and every stable complex system. Thus, the decomposition theorem appears as the widest grounds for the concept of boundedness and thus it serves for the widest grounds for the description of the behavior of all stable complex systems.

It is worth noting that the decomposition theorem is fundamentally different from the Central Limit Theorem which serves as the widest grounds for the traditional theory of probabilities. Indeed, while the Central Limit Theorem holds for independent random variables (yet unbounded), the decomposition theorem holds for arbitrary variables provided the latter are bounded (yet not independent). Thus, the subjects of both theorems have no common background. So, it is to be expected that such fundamental difference would have far going consequences one of which is subject of the present paper.

2. Decomposition Theorem Revisited

The major goal of the present section is to elucidate that the conditions which provide stable long-run functioning of a complex system ensure also a permanent robustness of a specific macroscopic coherent pattern (that is a homeostatic pattern) to the details of the interaction of the corresponding system with a non-specified ever-changing environment. It should be stressed that the persistent presence of accompanied continuous band in the power spectrum implies that not only the homeostatic pattern is coherent but the entire current response to any environment (non-homogeneous environment included) is permanently coherent. Thus, although the physical interactions are short-ranged, the boundedness of rates and amplitudes of exchanging matter/energy/information viewed as a general operational protocol, are sufficient to substantiate coherence of the response throughout the entire system.

The conditions which provide permanent long-term stable functioning of any complex system are: 1) permanent avoidance of resonances viewed as a general condition for permanent maintenance of the boundedness; 2) scale invariance of the uniform distribution of the zeroes of a BIS viewed as a condition for permanent maintenance of the smoothness of the shape of a continuous band. In turn the latter sustains the avoidance of resonances on each and every scale. It is proven also that at the same time, the scale invariant uniform distribution of zeroes provides universality of the distribution of a coarse-grained BIS.

The smoothness of the shape of the continuous band is considered in the first sub-section while the universality of the distribution is considered in the second subsection.

Next the role of the condition about avoidance of resonances for permanent maintenance of the boundedness of amplitude is considered.

The proof of the decomposition theorem is rather lengthy and is a result of a highly non-trivial interplay of the above assumptions. Details are presented in the Appendix to Chapter 1, Chapter 2 and Chapter 10 of the [1]. Now I present the major clues which yield that theorem. The foremost clue is that the separation of the power spectrum to a specific pattern and a continuous band must stay steady regardless to the details of the succession of terms in the corresponding BIS. The latter implies that both the intensity of each and every component along with the structure of the discrete pattern must stay intact. The condition for keeping the intensity of those lines intact is permanent avoidance of resonances among their members. The sources for a resonance are two: 1) resonances which come from the interference between the discrete and the continuous band; 2) non-smoothness of the shape of the continuous band. Thus, in order to avoid the resonances among the lines which belong to a discrete pattern and those ones which belong to the corresponding continuous band, it is sufficient to impose additivity of their coexistence in a power spectrum. In Chapter 2 of [1] it is proven that the additivity is an exclusive property of the concept of boundedness. As a consequence of that additivity, the additive separation of the zeroes of BIS'es to those which belong to a discrete band and those which belong to the corresponding continuous band commences.

In the sub-section 2.1 the condition about scale-invariance of the uniform distribution of zeroes for providing the smoothness of the continuous part is considered. In the sub-section 2.2 the same condition is considered with regards to its role for providing a universal distribution of the coarse-grained structure of a BIS.

It should be stressed that each and every stationary BIS is a complex interplay between two types of stationary BIS: one that commences from the discrete pattern in a power spectrum and one that commences from the continuous band. Their properties are additively separated in the corresponding power spectrum but in the time series they are intertwined. A self-consistent procedure for their separation in a time series itself will be presented in the next section. Now the assumption that such separation is available is taken for granted. Next in this section only properties of BIS that come from the continuous part of a power spectrum are discussed. For the sake of brevity, next in this section I call a stationary BIS any BIS which comes from a continuous band.

2.1. Universality of the Shape of the Continuous Band in a Power Spectrum

Next the highly non-trivial role of the condition about the uniform distribution of zeroes of a stationary BIS for providing the universality and smoothness of the shape of the continuous band in a power spectrum is considered. In consequence, the latter occurs to be sufficient condition for substantiation of permanent additive separation of the homeostatic pattern and the continuous band in

a power spectrum. Recalling that the latter additivity along with the considered next robustness of the shape of continuous band to the statistics of the corresponding time series are the key factors providing stationarity of the corresponding BIS, the condition about uniform distribution of the zeroes on each and every scale alone turns necessary and sufficient for providing stationarity and homogeneity of the corresponding process. And vice versa: at the end of the sub-section 2.2. it is demonstrated that the boundedness renders an exclusive property of thus formed stationary and homogeneous process to be a permanent sustaining of the uniform distribution of zeroes.

Let us now consider the non-trivial role of the condition about uniform distribution of zeroes at each and every scale for providing the smoothness of the shape of the continuous band in a power spectrum of a stationary BIS of length T. Given the condition $zT \to const$ to hold at every point of a BIS where z is the corresponding zero in the window of length T. If a BIS has this property, its Fourier transform is given by:

$$g(Tf) = \lim_{\substack{T\to\infty \\ zT\to const}} \frac{1}{\sqrt{T}} \int_0^T \exp(ifx) f(x) \mathrm{d}x \tag{1}$$

where f is the frequency and x is the current variable, e.g. the time.

The goal is to find $g(Tf)$. It is majorized by:

$$G(Tf) = \lim_{\substack{T\to\infty \\ zT\to const}} \frac{1}{\sqrt{T}} \int_{1/T}^T \exp(ifx) \mathrm{d}x = \lim_{\substack{T\to\infty \\ zT\to const}} = \frac{const}{f^{\frac{\alpha(f,T)}{2}}} \tag{2}$$

Here the term $\frac{1}{f^{\frac{\alpha(f,T)}{2}}}$ is derived by the condition of continuation: indeed for any frequency different from $1/T$, the corresponding component in the power spectrum fits the shape $\frac{1}{f^{\frac{\alpha(f,T)}{2}}}$ where $\alpha(f,T) > 1$. Then, the continuity imposes the same shape to hold for the frequency $1/T$. It is worth noting that the condition of continuation is a mathematical expression of the condition that all components in a continuous band participate equally in it and thus the continuous band does not signal out any special component. The question is whether the boundedness alone is sufficient for a unique determination of $\alpha(f,T)$.

It should be stressed that the condition about continuity of the power spectrum is verifiable only analytically since the shape $1/T$ holds only at a point but in any of its infinitesimally small neighborhood the shape is $\frac{1}{f^{\frac{\alpha(f,T)}{2}}}$; on the other hand the computations of all sorts operate only with finite intervals and thus "smear out" the special role of a single point although not eliminating its special role.

Thus, the condition about continuity indeed turns necessary and sufficient to provide uniform contribution of all frequencies in the power spectrum. It is worth noting on the condition about the continuity is an immediate conse-

quence of the condition about the uniform distribution of zeroes. Indeed, if otherwise, a special point would appear immediately.

It is worth noting also on inappropriateness of all types of "cut-off" technics for elimination of the considered here divergences because, although they succeed in elimination, neither of them is able to provide uniform contribution of all points. That is why the relevance of those technics is limited the field of critical phenomena only where the existence of a special point is an experimental fact, e.g. at phase transitions. On the contrary, the behavior of complex systems exhibit stable in a long-run behavioral pattern which does not signal out any special spatio-temporal point and thus the leading property of the corresponding behavioral pattern is its time-translational invariance.

It is worth noting that, if the condition for boundedness of amplitudes and rates does not exist, the Fourier spectrum would be white noise. Further, if the function is bounded but the condition about uniform distribution of zeroes is not imposed, $G(f) \sim \frac{1}{f}$.

In order to reveal better the highly non-trivial role of persistence of the condition $zT \to const$ over taking the limit $\to \propto$, the following paradox is presented. Given a BIS but the limit $T \to \propto$ is taken first. Then, taking into account the above result about the shape of $G(f) \sim \frac{1}{f}$, a logarithmic divergence of the variance is yielded. Indeed, according to its definition the variance can be presented as an integral over the entire power spectrum:

$$Var \propto \int_{1/T}^{\infty} \frac{\mathrm{d}f}{f} \propto \ln \frac{1}{T} \tag{3}$$

Thus, whenever the condition $zT \to const$ does not persist prior to the limit $T \to \propto$, the variance in Equation (3) diverges logarithmically on increasing the length of the time window T. It is worth noting that in this case the divergence holds regardless to what the value of the variance calculated by traditional means is. To remind the variance of any BIS, according to the traditional definition of variance, yields always a well-defined finite value and thus never diverges.

Moreover, the paradox escalates further through the following considerations. Taking into account that the variance of the fluctuations is a measure how probable the largest fluctuations are, the logarithmic divergence implies that on increasing the length of the time window, the largest fluctuations become more and more probable. In turn, this implies that the corresponding system is not stable, and its current state explicitly depends on the beginning and the end of the time window. Thus each system would appear as unstable and plastic so that any measurement induces changes in it regardless to how mild it could be. Further the paradox becomes even greater since these changes should appear in a universal way. The latter is a set by the robustness of shape of the continuous band to the nature of the system, to its dynamics and to the statistics of the corresponding time series. Alongside, it turns out that the moment of development

of those fluctuations is not well-defined because it depends explicitly on the length of the time window and changes with it. In a nutshell the above paradox constitutes the conflict of $1/f$ shape with time translational invariance. To remind, time translational invariance implies that a given phenomenon is reproducible if and only if there exists measurement such that the corresponding system neither selects nor signals out any special time or space point. Thus, the shape $1/f$ is in conflict with time translational invariance.

Let us now consider the impact of the imposing the condition about the uniform distribution of the zeroes. The grounding fact is that in the frame of boundedness the variance of fluctuations in each and every time series is bounded and independent from the length of the time series. Thus, it is not divergent. But then how to overcome the difficulty with the logarithmic divergence which appears when the variance is presented through the integrated power spectrum? In order to overcome this difficulty I assume that the shape of the power spectrum follows the shape of $\alpha(f,T)$ established in Equation (2):

$$1/f \quad \text{but} \quad 1/f^{\alpha(f,T)} \tag{4}$$

where $\alpha(f,T)=1$ at $f=\frac{1}{T}$ and $\alpha(f,T)$ is a continuous monotonically increasing function of the frequency. The idea about the replacement of the shape $1/f$ with $1/f^{\alpha(f,T)}$ is an immediate outcome of the persistent priority of the condition $zT \sim const$ over the limit $T \to \infty$ presented in Equation (2).

The proof how the logarithmic divergence is eliminated is rather lengthy and highly non-trivial. I strongly recommend its careful study. It can be found in the Appendix to Chapter 1 and in Chapter 2 in the [1].

In order to get the idea how boundedness takes part in the proof let me present the following brief sketch:

Given a bounded time series and it is assumed that its power spectrum fits the shape $1/f^{\alpha(f,T)}$. The question is whether the function $\alpha(f,T)$ can be determined by the boundedness alone. This question is highly non-trivial since it is well known that the shape of the power spectrum of any unbounded time series explicitly depends on its statistics.

The answer is positive and comes as follow: the boundedness implies that the amplitude of the fluctuations in any time series is independent from the length of the window where the measurement is made. That is:

$$I_{\max} \propto T^0 \tag{5}$$

On the other hand, the inverse Fourier transform gives the following estimation of the amplitude of members of a BIS:

$$I_{\max} \propto \sqrt{T}\int_{1/T}^{\infty}\frac{1}{f^{\frac{\alpha(f,T)}{2}}}\mathrm{d}f = \sqrt{T}\left(\frac{1}{T}\right)^{1-\frac{\alpha\left(\frac{1}{T},T\right)}{2}} \tag{6}$$

Equality of $I_{\max}$ from both presentations in Equations (5)-(6) sets the value

of $\alpha\left(\frac{1}{T},1\right)=1$ and requires $\alpha(f,T)$ to be monotonically increasing function.

Further, it turns out that the time translational invariance sets $\alpha(f,T)$ to be a linear function. Indeed, the time-translational invariance requires uniform contribution of all frequencies. Then neither of them signals out any special line. Simple calculations show that this is possible if and only if $\alpha(f,T)$ is a linear function:

$$\alpha(f,T)=1+k\left(f-\frac{1}{T}\right) \tag{7}$$

where k is a specific to a system parameter related to the properties of the U-turns.

If for example $\alpha(f,T)$ is a quadratic function, for every time window there is a frequency where the second derivative of the power spectrum shape changes its sign.

It should be stressed that the determination of the properties of the function $\alpha(f,T)$ does not involve any reference to nature of a system and to the statistics of the corresponding time series! Thus, the conclusion is that the shape $1/f^{\alpha(f,T)}$ is independent from the statistics of the time series, from the nature of the system and from the length of the time window where the measurement is made. At the same time the linearity of the function $\alpha(f,T)$ ensures its time-translational invariance.

It should be stressed on the self-consistency of the above proof. Indeed, it starts with imposing the requirement about smoothness and continuity of the continuous band viewed as a necessary condition for avoidance of resonances. In turn, the boundedness alone turns sufficient to provide not only the smoothness of that shape and its universality, but the time translational invariance and long-term stability of the entire behavior of a complex system. A special attention must paid on the necessity that the condition about the uniform distribution of zeroes must hold on each and every scale so that to provide the smoothness of the shape of a continuous band and thus to all other derived from it properties. It is worth noting that this sequence of conclusions is an exclusive property of the concept of boundedness because the shape of the power spectrum of any unbounded sequence explicitly depends on the statistics of the corresponding time series.

Another far-going consequence of the condition about uniform distribution of zeroes is that it provides Euclideanity of the functional metrics by means of maintaining the countability of the number of zeroes and their uniformity.

At this point a question arises: the maintenance of permanent Euclideanity of the functional metrics implies that the local deviations from it must be sustained bounded and short-lived. However, this contradicts the fluctuation-dissipation theorem, according to which any response of any system exactly matches the development of an appropriate fluctuation. However, the latter implies that since the response is macroscopic, fluctuations also develop to macroscopic size. The

way out is again highly non-trivial and passes through the utilization of a novel notion of chemical potential. The latter is necessary since simple considerations presented in [1] [2] [3] prove that the traditional notion of chemical potential is inherently contradictive. In turn, the novel notion of the chemical potential put forward by the author yields that all local fluctuations have bounded size and bounded lifetime [1] [2] [3]. In turn, the latter ensures that all internal fluctuations remain local and dissipate in microscopic time. In turn, their impact on macroscopic coherence turns out to be minor. Alongside, the latter ensures stability and robustness to the local details of the general physical protocol for self-sustaining the Euclideanity of the local functional metrics along with the execution of smooth U-turns on reaching the thresholds of stability. It should be stressed that the latter properties of the general physical protocol are exclusive for stationary homogeneous processes presented through stationary BIS only.

It is worth noting on the fundamental difference with the periodic functions utilized in the traditional approach for substantiation of the process of synchronization. Unlike the periodic functions which impose specific prerequisite structure on the entire space-time, i.e. an infinite set of nodes, stationary BIS, coarse-grained included, being irregular functions, impose coherence on bounded region of space-time only, that is the corresponding homeostatic pattern. At the same time the continuous band of a stationary BIS does not signals out any special component thus providing time-translational invariance of the functional relations encapsulated in the corresponding homeostatic pattern.

2.2. Universal Coarse-Grained Distribution of a Stationary BIS

Before focusing on the properties of the universal coarse-grained distribution of a stationary BIS let us consider the procedure for taking away that part of a BIS which belongs to its homeostatic pattern. To remind, while the power spectrum is additively decomposable, the homeostasis and the deviations from it are intertwined in the original BIS. Then, by means of making inverse Fourier transform of the discrete pattern, a periodic function which represents the homeostatic pattern alone is produced. By means of its extraction from the original BIS, a BIS which commences from the continuous part of the power spectrum is obtained. My assertion is that this part of a stationary BIS is subject to universal coarse-grained distribution.

Let us suggest that a coarse-grained structure exists. Since the boundedness of rates introduces a long-range persistence of the succession of jumps in the finer structure, the latter could be excellently approximated by fractal Brownian walks superimposed onto the coarse-grained structure. The major suggestion is that the universal coarse-grained structure consists of a train of excursions which forms a homogeneous stationary process and which acquire some exclusive properties set by the boundedness. Recalling that an excursion consists of a trajectory of walk originating at a given point at moment t and returning to it for the first time at the moment $t + \Delta$. The characteristics of each excursion amplitude A, duration Δ and embedding interval T are illustrated at **Figure 1**.

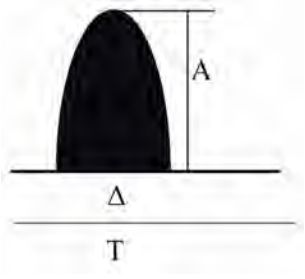

Figure 1. Characteristics of an excursion.

The embedding is a property which explicitly commences from the permanent smoothness of the shape of the continuous band of a stationary BIS. In a nutshell, the universality and the scale invariance of the coarse-grained distribution are derived on the exclusive grounds of the smoothness of the shape of the continuous band in the power spectrum which provides an exclusive shape of the autocorrelation function of a stationary BIS; details of its derivation can be found in Chapter 5 of [1]. Thus, the universality and the scale-invariance of a coarse-grained stationary BIS are immediately related to the condition about the uniform distribution of zeroes on each and every scale viewed as a condition for providing a long-term stable running of a complex system.

The notion of embedding implies that each excursion is embedded in a larger interval whose duration is interrelated with the duration of the excursion itself. The major role of the embedding is that it does not allow overlapping of the successive excursions and thus prevents growing of the excursion amplitude to arbitrary size. In turn, it results in permanent preservation of both boundedness of amplitude and boundedness of rates. Alongside, the disposition of an excursion onto its embedding interval is almost equi-probable along the entire interval. In turn, this prevents any periodicity in the sequences of excursions and thus provides scale invariance of BIS by means of making a coarse-grained BIS to be again a BIS.

It is worth noting that embedding is an exclusive property of a stationary BIS and has no analog for the unbounded sequences.

Then, the notion of an excursion along with the above consideration renders the size, the duration and the length of embedding interval of an excursion to be related by a power dependence of the following type:

$$A \sim \Delta^{\alpha(\Delta)} \tag{8}$$

The non-constant power $\alpha(\Delta)$ is set by the corresponding specific dynamics. Now the difference between a law and a general operational protocol becomes apparent. Indeed, a law viewed as quantified recursive relation among specific variables characterizing a given phenomenon put in a steady environment is expressed through the concrete values of the non-constant power $\alpha(\Delta)$ which thus quantifies the concrete relations between the size, the duration and the size of the embedding interval for any given excursion at current environment. Note that in an ever-changing environment the details of the

non-constant power $\alpha(\Delta)$ could vary from one realization of the environment to another. On the other hand, the very existence of a universal scale-invariant coarse-grained structure of a stationary BIS, viewed as a part of the response of any stable complex system to an un-specified ever-changing environment is robust to the details of any concrete dynamics and the details of any concrete interaction with the environment. Thus, the above considerations confirm the difference between a law and an operational protocol with respect to their holding in a steady or in an ever-changing environment.

The idea that the coarse-grained structure of each and every BIS consists of embedded excursions which form a stationary homogeneous process implies that the frequency of occurrence of an excursion of size A is time-independent and reads:

$$P(A) = cA^{\alpha(A)} \frac{\exp\left(-A^2/\sigma^2\right)}{\sigma} \tag{9}$$

The required probability $P(A)$ is given as a product of the term $A^{\alpha(A)}$ which is the statistical weight of an excursion of amplitude A and its embedding interval, and the probability for appearance of excursion of that size (normal distribution); σ is the variance of the BIS; $c = 1/\sigma^{\alpha(\sigma)}$ is the normalizing term. The homogeneity of the excursion succession ensures the time-independence of $P(A)$. It is worth noting that the Gaussian-like term $\frac{\exp\left(-A^2/\sigma^2\right)}{\sigma}$ in Equation (9) commences from the scale invariance of the coarse-grained structure of any BIS: a coarse-grained BIS is again BIS and this happens on each and every scale. Then, taking into account that the process is a stationary homogeneous one and fact that, according to the Lindeberg theorem [4] it has well-defined mean and variance, it turns out to be a subject to the normal distribution. It is worth noting that the latter does not imply that the succession of excursions consists of random independent events. On the contrary, the succession of excursions on any scale has residual memory which is dictated by the formation of larger excursions on the next scale. The residual memory is best pronounced through the appearance of some trend of the average on the development of an excursion. Yet, on elimination of a trend, excursions appear as random, independent events.

The universal distribution $P(A)$ from Equation (9) is presented in **Figure 2**. The dotted line represents the excellent approximation of the fat tail with power dependence. Yet, it is worth noting one of the greatest advantages of the universal distribution $P(A)$ from Equation (9) is that it is time-translational invariant unlike a power dependence which is in a conflict with it. More about this matter can be found in Chapter 5 of [1].

Let us now pay special attention to the self-consistency between obtained universal distribution of a stationary BIS and condition about the uniform distribution of the zeroes of a stationary BIS. Indeed, the universality of the coarse-grained distribution is derived on the exclusive grounds of the smoothness of the shape

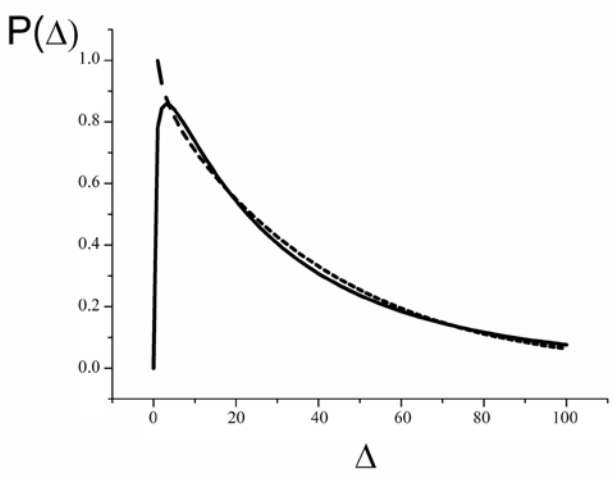

Figure 2. The shape of the universal distribution of a stationary BIS (continuous line) and approximation of its fat tail with a power dependence (dotted line).

of the continuous band in the power spectrum. Taking into account that the latter smoothness is an immediate consequence of imposing the condition about the uniform distribution of zeroes on each and every scale, the universal coarse-grained distribution is an immediate consequence of that condition. Vice versa: the constraint over the size and correspondingly duration of the largest excursions by the margins of stability and by the embedding render the number of zeroes in any window of recording of the corresponding BIS countable and independent from the length of that window which holds at each and every scale. Consequently, the latter provides a scale invariance of the uniform distribution of the zeroes of a BIS. In turn, the latter scale invariance results in the scale invariance of the universal distribution.

3. Role of the Resolution of Measurements. Central Limit Theorem as Approximation

At first glance the title of the present section sounds bizarre since the coarse-graining and the resolution of a measurement involve the same operations which consist of the notion that certain fine details become non-discernable. Yet, although that is correct, there is a fundamental difference between them: unlike the resolution which a solitary operation and thus not scale-invariant, the coarse-graining which yields the universal structure of a BIS is a scale-invariant operation. Next it is demonstrated that the superimposing of both operations results in mimicking the widest variety of behavior: from stochastic-like to periodic-like, to sequence of irregular fractals and to series of random independent events.

Thus, the stochastic-like behavior appears at very high resolution and relatively short time series. Then the role of the fine-structure becomes predominant. The distribution of the variations can be any one. Yet, most probably it is noisy and not well-defined.

The behavior which mimics best a sequence of irregular fractals appears for intermediate resolutions both of the amplitude and time so that the shape and the durations of excursions to be recorded. Again, most probably the distribution of the excursions is not well-defined for relatively short time series.

A periodic-like behavior appears as a limit case of the fractal-like behavior. This happens at low resolution of the amplitudes of excursions so that almost only largest size excursions are discerned. Then, as a special occasion, the record could match an almost periodic train of impulses. The shape of the power spectrum is defined mainly by the shape of the corresponding impulse function.

Next in the line comes the case when the duration of the most of excursions is not discerned. Then, their appearance matches best random-like events so that a specific for each of them probability could be assigned. Yet, since the randomness is still approximation (remember the ubiquitous trend of local average), this probabilities could effectively vary in the course of recording. Thus, in the frame of the traditional theory of probability, such behavior would match rather a non-stationary process. However, the latter conclusion is in sharp contradiction with the reality since the underlying process is a stationary and homogeneous one. It is worth noting that a true non-stationary process is characterized by the appearance of an extra-line in a power spectrum [5]. Yet, the question whether it brings about adaptation or destruction is mathematically undecidable [5] and so it needs additional experiments for an irrefutable resolution.

This conflict is fundamental since it concerns the grounds of both the decomposition theorem and the Central Limit Theorem viewed as counterparts each of which establishes an asymptotic behavior for different and non-overlapping subjects. To remind, while the Central Limit Theorem holds for independent random variables (yet unbounded), the decomposition theorem holds for arbitrary variables provided the latter are bounded (yet not independent). The major clue for resolution of that conflict lies in the colocation "asymptotic behavior". Keeping in mind that the original times series is represented by a stationary BIS, the asymptotic behavior of the real process gradually approaches the asymptotic characteristics of a BIS, those are additively decomposed power spectrum and universal distribution of the members of the corresponding coarse-grained BIS. Practically, the later conclusion is verifiable by means of recording long enough time series. The guess is that when the length of a time series is much longer than the duration of the largest excursion, the asymptotic behavior of a BIS starts to reveal best. So, in this case the Central Limit Theorem appears as an approximation for relatively short time series while the asymptotic behavior is governed by the decomposition theorem for each and every of the above cases.

Outlining, the considerations in the present section are an excellent methodological example for the role of taking into account the grounds of any approach for the conclusions drawn from an experiment. Moreover, in order to make decisive conclusions, additional experiments are always necessary because the reading of any experiment strongly depends on the explanatory setting where it is put in and so it is not immunized from incorrect conclusions.

4. Conclusions

A general operational protocol which provides permanent macroscopic coherence of the response of any stable complex system to an ever-changing environment is proposed. It turns out that the coherent response consists of two parts: 1) a specific discrete pattern, called by the author homeostatic one, whose characteristics are robust to the statistics of the environment; 2) the rest part of the response forms a stationary homogeneous process whose coarse-grained structure obeys universal distribution where the coarse-graining has the property to be scale-invariant.

The general physical protocol governing the dynamics of the spontaneously executed physico-chemical processes has been put forward by the author and consists in the following: local exceeds of energy are dissipated as emission of local acoustic phonons at a given spatio-temporal point and their absorption at another spatio-temporal point; local exceeds of matter are dissipated by means of targeted transportation of a specific constituents from a specific initial spatio-temporal point to a specific distant spatio-temporal point. Thus, the travel of matter waves between specific distant points serves as a general protocol for launching specific chemical reactions so that the input reagents and the output products are produced at distant points leaving at the same time the chemical reactions to be local events. Then, the global coherence appears as sequences of local emissions and absorptions of acoustic phonons and mater waves. The ubiquity of that mechanism is grounded on the ubiquity of the presence of the acoustic phonons and on the recently proved ubiquity of the matter wave emission in any system regardless to its nature and its physico-chemical characteristics.

Mathematically, the ubiquity of that protocol is established by the highly non-trivial properties of the new mathematical objects called stationary BIS (bounded irregular sequences) introduced for its description. The major of those properties consists of the fact that the coarse-grained structure of a stationary BIS is scale invariant and robust to the nature of system, its dynamics and the details of the environmental impact. The latter implies that the fine structure of a stationary BIS has minor effect on the coarse-grained one. In turn, the latter substantiates the ubiquitous availability of the proposed general protocol of coherence to systems of different nature, different dynamics etc. It is worth noting that this property of BIS is exclusive for them and it is not shared by periodic functions. Moreover, the BIS remain stable under local perturbations unlike their periodic counterparts where even tiniest local perturbations of the characteristics of a periodic function affect the entire function. The latter implies that local perturbations have global impact on any periodic function on the contrary to the stationary BIS where a local perturbation remains local and have minor effect on the coarse-grained structure.

Moreover, the universality of the coarse-grained structure provides uniform asymptotic behavior for systems of different nature and dynamics which is go-

verned by the recently proven by the author decomposition theorem.

The high non-triviality of that mater consists of the consideration that for relatively short time series, a measurement, viewed as a solitary operation of coarse-graining, superimposed on the universal distribution results in a rich variety of behaviors ranging from a periodic-like to a stochastic-like, to sequences of irregular fractal-like objects and sequences of random-like events. The relevance of Central Limit theorem applies to the latter case. This, to certain extent unexpected, rich variety of behaviors is a direct consequence of the superimposing of the resolution, viewed as a solitary scale-non-invariant operation of coarse-graining, and the scale-invariance of coarse-graining which yields the universal distribution. Then, the application of the Central Limit Theorem is relevant only as an approximation which holds for relatively short time series and specific low resolution of the measurement equipment while the asymptotic behavior in each and every of the above cases is governed by the decomposition theorem.

Outlining, the present paper appears as an excellent methodological example for the role of taking into account the grounds of any approach for the conclusions drawn from an experiment. Moreover, in order to make decisive conclusions, additional experiments are always necessary because the reading of any experiment strongly depends on the explanatory setting where it is put in and so it is not immunized from misleading conclusions.

Conflicts of Interest

The author declares no conflicts of interest regarding the publication of this paper.

References

[1] Koleva, M.K. (2012) Boundedeness and Self-Organized Semantics: Theory and Applications, IGI-Global, Hershey, PA. https://doi.org/10.4018/978-1-4666-2202-9

[2] Koleva, M.K. (2021) *Journal of Modern Physics*, **12**, 167-178. https://doi.org/10.4236/jmp.2021.123015

[3] Koleva, M.K. (2005) Fluctuations and Long Term Stability: From Coherence to Chaos. https://arxiv.org/abs/physics/0512078v1

[4] Feller, W. (1970) An Introduction to Probability Theory and Its Applications. John Willey & Sons, New-York.

[5] Koleva, M.K. (2020) *Journal of Modern Physics*, **11**, 767-778. https://doi.org/10.4236/jmp.2020.116049

Journal of Modern Physics, 2021, 12, 623-634
https://www.scirp.org/journal/jmp
ISSN Online: 2153-120X
ISSN Print: 2153-1196

Various Empirical Equations for the Electromagnetic Force in Terms of the Cosmic Microwave Background Temperature

Tomofumi Miyashita

Miyashita Clinic, Osaka, Japan
Email: tom_miya@plala.or.jp

How to cite this paper: Miyashita, T. (2021) Various Empirical Equations for the Electromagnetic Force in Terms of the Cosmic Microwave Background Temperature. *Journal of Modern Physics*, **12**, 623-634.
https://doi.org/10.4236/jmp.2021.125040

Received: February 13, 2021
Accepted: April 18, 2021
Published: April 21, 2021

Abstract

Previously, we proposed an empirical equation describing the relationship between the gravitational force and the temperature of the cosmic microwave background (CMB). After evaluating our equation, we discovered many empirical equations describing the electromagnetic force in terms of the CMB, including equations for the Rydberg constant, the Bohr radius, the Compton wavelength, the classical electron radius, the Hartree energy, the Coulomb's law with distance, and the ratio between the gravitational force and electric force. The background theory is not yet complete. However, we can justify why the discovered empirical equations should not be coincidence.

Keywords

Temperature of the Cosmic Microwave Background

1. Introduction

Previously, we reported the following equation [1] [2]:

$$\frac{Gm_p}{\frac{\lambda_p}{2}} \times 1\,\text{kg} = \frac{9}{2} kT_c \tag{1}$$

where G, m_p, λ_p, k, T_c and 1 kg are the gravitational constant, the rest mass of a proton, the Compton wavelength, the Boltzmann constant, the temperature of the cosmic microwave background (CMB) and the standard unit of mass, respectively. Then,

$$\frac{Gm_p}{\frac{\lambda_p}{2}} \times 1\,\text{kg} = \frac{6.6743\times10^{-11}\times1.6726\times10^{-27}}{\frac{1.3241\times10^{-15}}{2}} = 1.6897\times10^{-22}\,(\text{J}) \tag{2}$$

$$\frac{9}{2}kT_c = \frac{9}{2}\times 1.3807\times 10^{-23}\times 2.7255 = 1.6933\times 10^{-22}\,(\mathrm{J}) \tag{3}$$

$$\text{Error} = \frac{1.6897\times 10^{-22}}{1.6933\times 10^{-22}} - 1 = -0.00217 \tag{4}$$

The temperature (T_c) calculated from Equation (1) is 2.71957 K, and the measured CMB is 2.72548 K. Accordingly, using Jarzynski's equality [3] and Ted Jacobson's theory [4], we attempted to explain Equation (1).

According to Jarzynski, Jarzynski's equality may be useful for quantum mechanics [3]. We searched for empirical equations for the electromagnetic force in terms of the temperature of the cosmic microwave background using Excel sheets. This search method relied almost entirely on chance, requiring much time and perseverance. In this way, we discovered several empirical equations. Unfortunately, the background theory still could not be sufficiently completed. Therefore, we abandoned the attempt to provide a theoretical explanation in this report. However, we can justify why the discovered empirical equations should not be coincidence.

The rest of the paper is organized as follows. In Section 2, we present the symbol list and the calculation results for frequently used values. In Section 3, we present our empirical equations. In Section 4, we explain the relationships among our empirical equations.

2. Symbol List and Frequently Used Values

2.1. Symbol List

These values were obtained from Wikipedia.

G: gravitational constant: 6.6743×10^{-11} ($m^3 \cdot kg^{-1} \cdot s^{-2}$)

T_c: temperature of the cosmic microwave background: 2.72548 (K)

k: Boltzmann constant: 1.380649×10^{-23} ($J \cdot K^{-1}$)

c: speed of light: 299792458 (m/s)

h: Planck constant: $6.62607015 \times 10^{-34}$ (Js)

$\hbar$: Dirac constant (reduced Planck constant): $1.054\ 571\ 817 \times 10^{-34}$ (Js)

ε_0: electric constant: $8.8541878128 \times 10^{-12}$ ($N \cdot m^2 \cdot C^{-2}$)

μ_0: magnetic constant: $1.25663706212 \times 10^{-6}$ ($N\ A^{-2}$)

e: electric charge of one electron: $-1.602176634 \times 10^{-19}$ (C)

q_m: magnetic charge of one magnetic monopole: $4.13566770 \times 10^{-15}$ (Wb)
(this value is only a theoretical value, $q_m = h/e$)

m_p: rest mass of a proton: $1.672621923 \times 10^{-27}$ (kg)

m_e: rest mass of an electron: $9.1093837 \times 10^{-31}$ (kg)

λ_p: Compton wavelength for a proton: 1.32141×10^{-15} (m)

λ_e: Compton wavelength for an electron: $2.4263102367 \times 10^{-12}$ (m)

r_e: classical electron radius: $2.8179403227 \times 10^{-15}$ (m)

a_0: Bohr radius: $0.529177210 \times 10^{-10}$ (m)

R_∞: Rydberg constant: 10973731.568 (m^{-1})

E_h: Hartree energy: 27.211386245988 (eV)
R_k: von Klitzing constant: 25812.80745 (Ω)
Z_0: wave impedance in free space: 376.730313668 (Ω)
α: fine-structure constant: 1/137.0359991

2.2. Calculation Results for Frequently Used Values

The calculation results for several frequently used values are presented in this section. The number of significant figures used is 5.

$$\frac{e^2}{4\pi\varepsilon_0}=\frac{\left(1.6022\times10^{-19}\right)^2}{4\pi\times8.8542\times10^{-12}}=2.3071\times10^{-28}\left(\mathrm{J\cdot m}\right) \tag{5}$$

$$\frac{e}{4\pi\varepsilon_0}=\frac{1.6022\times10^{-19}}{4\pi\times8.8542\times10^{-12}}=1.4400\times10^{-9}\left(\mathrm{J\cdot m/C}\right) \tag{6}$$

$$\frac{e^2}{4\pi\varepsilon_0}\frac{e}{4\pi\varepsilon_0}=2.3071\times10^{-28}\times1.4400\times10^{-9}=3.3221\times10^{-37}\left(\mathrm{J^2\cdot m^2\cdot C^{-1}}\right) \tag{7}$$

$$kT_c=1.3807\times10^{-23}\times2.7255=3.7629\times10^{-23}\left(\mathrm{J}\right) \tag{8}$$

3. Our Empirical Equations

We present our empirical equations and their verification and errors in detail.

3.1. Four Special Lengths

First, we present the empirical equations for four special lengths.

3.1.1. Classical Electron Radius

$$\frac{1}{\frac{2r_e\pi}{2}}\times\frac{e^2}{4\pi\varepsilon_0}\times\frac{e}{4\pi\varepsilon_0}\times\left(1\frac{\mathrm{C}}{\mathrm{J\cdot m}}\right)=kT_c \tag{9}$$

where 1 C/J/m is the standard electrostatic quantity, which is explained in a later section.

$$\frac{1}{\frac{2r_e\pi}{2}}\frac{e^2}{4\pi\varepsilon_0}\frac{e}{4\pi\varepsilon_0}\times\left(1\frac{\mathrm{C}}{\mathrm{J\cdot m}}\right)=\frac{3.3221\times10^{-37}}{\pi\times2.8179\times10^{-15}}=3.7526\times10^{-23}\left(\mathrm{J}\right) \tag{10}$$

$$\mathrm{Error}=\frac{3.7526\times10^{-23}}{3.7629\times10^{-23}}-1=-0.00274 \tag{11}$$

3.1.2. Compton Wavelength for an Electron

$$\frac{1}{\frac{\lambda_e}{2}}\times\frac{1}{\alpha}\times\frac{e^2}{4\pi\varepsilon_0}\times\frac{e}{4\pi\varepsilon_0}\times\left(1\frac{\mathrm{C}}{\mathrm{J\cdot m}}\right)=kT_c \tag{12}$$

$$\frac{1}{\frac{\lambda_e}{2}}\frac{1}{\alpha}\frac{e^2}{4\pi\varepsilon_0}\frac{e}{4\pi\varepsilon_0}\times\left(1\frac{\mathrm{C}}{\mathrm{J\cdot m}}\right)=\frac{3.3221\times10^{-37}\times137.036}{2.4263\times10^{-12}}=3.7526\times10^{-23}\left(\mathrm{J}\right) \tag{13}$$

$$\text{Error} = \frac{3.7526\times10^{-23}}{3.7629\times10^{-23}} - 1 = -0.00274 \tag{14}$$

3.1.3. Bohr Radius

$$\frac{1}{\frac{2\pi a_0}{2}} \times \frac{1}{\alpha^2} \times \frac{e^2}{4\pi\varepsilon_0} \times \frac{e}{4\pi\varepsilon_0} \times \left(1\frac{\text{C}}{\text{J}\cdot\text{m}}\right) = kT_c \tag{15}$$

$$\begin{aligned} &\frac{1}{\pi a_0}\frac{1}{\alpha^2}\frac{e^2}{4\pi\varepsilon_0}\frac{e}{4\pi\varepsilon_0} \times \left(1\frac{\text{C}}{\text{J}\cdot\text{m}}\right) \\ &= \frac{3.3221\times10^{-37}\times(137.036)^2}{\pi\times5.2918\times10^{-11}} = 3.7526\times10^{-23}\,(\text{J}) \end{aligned} \tag{16}$$

$$\text{Error} = \frac{3.7526\times10^{-23}}{3.7629\times10^{-23}} - 1 = -0.00274 \tag{17}$$

3.1.4. Rydberg Constant

$$\frac{1}{\frac{1}{4R_\infty}} \times \frac{1}{\alpha^3} \times \frac{e^2}{4\pi\varepsilon_0} \times \frac{e}{4\pi\varepsilon_0} \times \left(1\frac{\text{C}}{\text{J}\cdot\text{m}}\right) = kT_c \tag{18}$$

$$\begin{aligned} &\frac{1}{\frac{1}{4R_\infty}}\frac{1}{\alpha^3}\frac{e^2}{4\pi\varepsilon_0}\frac{e}{4\pi\varepsilon_0} \times \left(1\frac{\text{C}}{\text{J}\cdot\text{m}}\right) \\ &= \frac{3.3221\times10^{-37}\times(137.036)^3}{\frac{1}{4\times1.0973\times10^7}} = 3.7526\times10^{-23}\,(\text{J}) \end{aligned} \tag{19}$$

$$\text{Error} = \frac{3.7526\times10^{-23}}{3.7629\times10^{-23}} - 1 = -0.00274 \tag{20}$$

3.2. Two Special Energies

We next present the empirical equations for two special energies.

3.2.1. Rest Mass of an Electron

$$\frac{m_e c^2}{e\pi} \times \frac{e^2}{4\pi\varepsilon_0} \times \left(1\frac{\text{C}}{\text{J}\cdot\text{m}}\right) = kT_c \tag{21}$$

$$m_e c^2 = 9.1094\times10^{-31}\times\left(2.9979\times10^8\right)^2 = 8.1871\times10^{-14}\,(\text{J}) \tag{22}$$

$$\frac{m_e c^2}{e\pi}\frac{e^2}{4\pi\varepsilon_0} \times \left(1\frac{\text{C}}{\text{J}\cdot\text{m}}\right) = \frac{8.1871\times10^{-14}\times2.3071\times10^{-28}}{\pi\times1.6021\times10^{-19}} = 3.7526\times10^{-23}\,(\text{J}) \tag{23}$$

$$\text{Error} = \frac{3.7526\times10^{-23}}{3.7629\times10^{-23}} - 1 = -0.00274 \tag{24}$$

3.2.2. Hartree Energy

$$E_h \times \frac{1}{\alpha^2} \times \frac{1}{e\pi} \times \frac{e^2}{4\pi\varepsilon_0} \times \left(1\frac{\text{C}}{\text{J}\cdot\text{m}}\right) = kT_c \tag{25}$$

$$\frac{E_h}{e\pi}\frac{e^2}{4\pi\varepsilon_0}\times\left(1\frac{\mathrm{C}}{\mathrm{J\cdot m}}\right)$$
$$=\frac{4.3597\times10^{-18}\times2.3071\times10^{-28}\times\left(137.036\right)^2}{\pi\times1.6021\times10^{-19}}=3.7526\times10^{-23}\left(\mathrm{J}\right) \tag{26}$$

$$\mathrm{Error}=\frac{3.7526\times10^{-23}}{3.7629\times10^{-23}}-1=-0.00274 \tag{27}$$

3.3. Ratio between the Gravitational Force and Electric Force

Below, we present the empirical equation for the ratio between the gravitational force and electric force:

$$\frac{Gm_p^2}{\frac{e^2}{4\pi\varepsilon_0}}=4.5\times\frac{m_e}{e}\times\hbar c\times\left(1\frac{\mathrm{C}}{\mathrm{J\cdot m}}\times\frac{1}{1\,\mathrm{kg}}\right) \tag{28}$$

where 1 kg is the standard unit of mass, as previously explained [1].

$$\frac{Gm_p^2}{\frac{e^2}{4\pi\varepsilon_0}}=\frac{6.6743\times10^{-11}\times\left(1.6726\times10^{-27}\right)^2}{2.3071\times10^{-28}}=8.0936\times10^{-37} \tag{29}$$

$$\hbar c=1.0546\times10^{-34}\times2.9979\times10^{8}=3.1615\times10^{-26}\left(\mathrm{J\cdot m}\right) \tag{30}$$

$$4.5\frac{m_e}{e}\hbar c=\frac{4.5\times9.1094\times10^{-31}\times3.1615\times10^{-26}}{1.6021\times10^{-19}}=8.0889\times10^{-37} \tag{31}$$

$$\mathrm{Error}=\frac{8.0936\times10^{-37}}{8.0889\times10^{-37}}-1=0.000578 \tag{32}$$

It is important to note that this error is small compared to the errors of the other empirical equations. The very large ratio between the gravitational force and electric force has long been a mystery in science. Such a simple empirical equation with high numerical accuracy has not been previously reported. Therefore, these values are emphasized here.

4. Discussion

4.1. Relationships among Various Equations

The relationships among several sets of equations are obvious. In this section, we explain these obvious relationships.

4.1.1. Relationship among the Equations for the Four Special Lengths

Equations (9), (12), (15) and (18) indicate that

$$r_e 2\pi=\alpha\lambda_e=\alpha^2 a_0 2\pi=\alpha^3\frac{1}{2R_\infty} \tag{33}$$

Equation (33) is already known. From Equation (9),

$$\frac{e^3}{r_e\pi\left(4\pi\varepsilon_0\right)^2}\times\left(1\frac{\mathrm{C}}{\mathrm{J\cdot m}}\right)=kT_c \tag{34}$$

r_e can be defined as follows:

$$m_e c^2 = \frac{e^2}{4\pi\varepsilon_0 r_e} \tag{35}$$

Then, the Coulomb's law with distance can be expressed in terms of the CMB as

$$\frac{e^2}{4\pi\varepsilon_0 r^2} = \frac{1}{r^2}\frac{e\pi}{m_e c^2} kT_c \times \left(1\frac{\mathrm{J\cdot m}}{\mathrm{C}}\right) \tag{36}$$

where r is the distance between two electrons and 1 Jm/C is the standard electrostatic quantity, which is explained in a later section.

4.1.2. Relationship among Equations (21), (25) and (36)

From Equations (36),

$$\frac{m_e c^2}{e\pi} \times \frac{e^2}{4\pi\varepsilon_0} = kT_c \times \left(1\frac{\mathrm{J\cdot m}}{\mathrm{C}}\right) \tag{37}$$

Equation (37) is equal to Equation (21). Next, the following equation is well known:

$$E_h = \alpha^2 m_e c^2 \tag{38}$$

Using Equations (37) and (38), we obtain

$$E_h \times \frac{1}{\alpha^2} \times \frac{1}{e\pi} \times \frac{e^2}{4\pi\varepsilon_0} \times \left(1\frac{\mathrm{C}}{\mathrm{J\cdot m}}\right) = kT_c \tag{39}$$

Equation (39) is equal to Equation 25.

4.2. Explanation of the Standard Electrostatic Quantity (1 C/J/m)

As shown above, we can calculate the Coulomb potential energy with distance in terms of the CMB. Equation (34) is not complex. The difficulty in Equation (34) lies in the dimensional mismatch. Thus, we apply the majority of our efforts to resolving this dimensional mismatch.

$$\frac{e^2}{4\pi\varepsilon_0} = 2.3071\times10^{-28}\left(\mathrm{J\cdot m}\right) \tag{40}$$

$$n = \frac{1\,\mathrm{C}}{e} = 6.2415\times10^{18} \tag{41}$$

where n is the number of electrons.

$$\frac{e^2}{4\pi\varepsilon_0} \times n = \frac{e}{4\pi\varepsilon_0} \times 1\,\mathrm{C} = 1.4400\times10^{-9}\left(\mathrm{J\cdot m}\right) \tag{42}$$

Therefore,

$$\frac{e}{4\pi\varepsilon_0} = 1.4400\times10^{-9}\left(\frac{\mathrm{J\cdot m}}{\mathrm{C}}\right) \tag{43}$$

From Equation (5),

$$\frac{e^2}{r_e \pi 4\pi\varepsilon_0} \times \frac{e}{4\pi\varepsilon_0} \times \left(1\frac{\mathrm{C}}{\mathrm{J\cdot m}}\right) = kT_c \tag{44}$$

From Equations (43) and (44),

$$\frac{e^2}{4\pi\varepsilon_0 r_e \pi}\times 1.4400\times 10^{-9} = kT_c \tag{45}$$

In Equation (45), the standard electrostatic quantity (1 C/J/m) is absent, and 1.4400×10^{-9} is a dimensionless constant. We have multiplied and divided by the number of electrons.

In Equation (42), n is meaningful. However, in Equation (45), n has disappeared. The right-hand side of Equation (44) is defined for only one electron. However, when 1 C was defined as the standard charge, the relation to the number of electrons was unknown. If 10 C were to be defined as the standard charge, then the number of electrons on the left-hand side would become ten times larger. In this case, the dimensionless constant (1.4400×10^{-9}) should be changed to 1.4400×10^{-10} because of the division by the number of electrons. However, Equation (44) cannot be changed.

4.3. Four Empirical Equations for Important Lengths without Using α

From Equation (33), it is unclear that λ_e, r_e, a_0, and $1/2R_\infty$ are special lengths. In Equations (9), (12), (15) and (18), we have used α. The definitions of α are as follows:

$$\frac{e^2}{4\pi\varepsilon_0\hbar c} = \alpha = \frac{1}{137.036} \tag{46}$$

$$\frac{q_m^2}{\mu_0\pi\hbar c} = \frac{1}{\alpha} = 137.036 \tag{47}$$

Thus,

$$\frac{1}{\alpha} = \left(\frac{e^2}{4\pi\varepsilon_0\hbar c}\right)^{-\frac{1}{2}}\left(\frac{q_m^2}{\mu_0\pi\hbar c}\right)^{\frac{1}{2}} = \left(\frac{e^2}{4\pi\varepsilon_0}\right)^{-\frac{1}{2}}\left(\frac{q_m^2}{\mu_0\pi}\right)^{\frac{1}{2}} \tag{48}$$

Using Equation (48), α can be eliminated from Equations (9), (12), (15) and (18). The error does not change.

$$\frac{1}{e\times\dfrac{2r_e\pi}{2}}\times\left(\frac{e^2}{4\pi\varepsilon_0}\right)^2\times\left(1\frac{\mathrm{C}}{\mathrm{J\cdot m}}\right) = kT_c \tag{49}$$

$$\frac{1}{e\times\dfrac{\lambda_e}{2}}\times\left(\frac{e^2}{4\pi\varepsilon_0}\right)^{\frac{3}{2}}\times\left(\frac{q_m^2}{\mu_0\pi}\right)^{\frac{1}{2}}\times\left(1\frac{\mathrm{C}}{\mathrm{J\cdot m}}\right) = kT_c \tag{50}$$

$$\frac{1}{e\times\dfrac{2\pi a_0}{2}}\times\left(\frac{e^2}{4\pi\varepsilon_0}\right)^{1}\times\left(\frac{q_m^2}{\mu_0\pi}\right)^{1}\times\left(1\frac{\mathrm{C}}{\mathrm{J\cdot m}}\right) = kT_c \tag{51}$$

$$\frac{1}{e\times\dfrac{1}{4R_\infty}}\times\left(\frac{e^2}{4\pi\varepsilon_0}\right)^{\frac{1}{2}}\times\left(\frac{q_m^2}{\mu_0\pi}\right)^{\frac{3}{2}}\times\left(1\frac{\mathrm{C}}{\mathrm{J\cdot m}}\right) = kT_c \tag{52}$$

Equations (49), (50), (51) and (52) clearly show that λ_e, r_e, a_0, and $1/2R_\infty$ are special lengths. We predict that 0.9937 μm (=$a_0 \times 137.036 \times 137.036$) is the fundamental special length. At this length, there should be an influence from the force between magnets near electrons. These special lengths have long been a mystery in science. Such simple empirical equations with high numerical accuracy have not been previously reported. Therefore, these values are emphasized here.

4.4. Our Empirical Equations Are Not Coincidence

We have presented many empirical equations. There are obvious relationships among several of these empirical equations, which clearly are not independent. However, the following three equations do seem to be independent.

Based on Equation (1), the gravitational force can be explained. For convenience, Equation (1) is rewritten below:

$$\frac{Gm_p}{\frac{\lambda_p}{2}} \times 1\,\text{kg} = \frac{9}{2}kT_c \tag{53}$$

Based on Equation (28), the ratio between the gravitational force and electric force can be explained. For convenience, Equation (28) is rewritten below:

$$\frac{Gm_p^2}{\frac{e^2}{4\pi\varepsilon_0}} = 4.5 \times \frac{m_e}{e} \times \hbar c \times \left(1\frac{\text{C}}{\text{J}\cdot\text{m}} \times \frac{1}{1\,\text{kg}}\right) \tag{54}$$

Based on Equation (36), the Coulomb's law with distance in terms of the CMB can be explained. For convenience, Equation (36) is rewritten below:

$$\frac{e^2}{4\pi\varepsilon_0 r^2} = \frac{1}{r^2}\frac{e\pi}{m_e c^2}kT_c \times \left(1\frac{\text{J}\cdot\text{m}}{\text{C}}\right) \tag{55}$$

The roles of these three empirical equations are clearly different.

We discovered Equation (53) first. Next, we discovered Equations (54) and (55). After the discovery of Equations (54) and (55), we noted that Equation (55) can be deduced from Equations (53) and (54). The mathematical proof is shown in Appendix A. We strongly believe that the mathematical connection among these three equations provides evidence that they are not coincidence.

4.5. Comparison of Equation (1) and Equation (21)

We will attempt to explain the various quantities considered dimensions and also to point out the major results in a more transparent way in this section.

The factor of 9/2 in Equation (1) can be explained as follows [2]. The proton consists of three quarks. Therefore, we must consider $9/2kT$ and not $3kT$. Accordingly, the number of degrees of freedom inside the proton may be 9. From Equation (21),

$$m_e c^2 \times \frac{e}{4\pi\varepsilon_0} \times \left(1\frac{\text{C}}{\text{J}\cdot\text{m}}\right) = \pi kT_c \tag{56}$$

Based on our consideration to resolve the dimension mismatch problem in section 4.2, from Equation (56), the number of degrees of freedom inside the electron seems to be 2π. Much previous work has been done to unify different theories within a single equation/result. In particular, the recent work by Angrick *et al.* has done this for electronic structure calculations in quantum mechanics [5]. These authors showed that the spin of electrons cannot be ignored thermodynamically. Then, considering the spin, the number of degrees of freedom inside an electron may be different from 3. Furthermore, Aquino *et al.* discovered new methods using vector analysis [6]. Perhaps it can be inferred that there is an unknown relationship in the present electromagnetic vector analysis.

5. Conclusions

Previously, we discovered an empirical equation (Equation (1)) relating the gravitational force and the CMB. However, according to Jarzynski, Jarzynski's equality can be used to determine the electromagnetic force in quantum physics [3]. Therefore, we searched for further empirical equations. Thus, equations for the Coulomb's law with distance in terms of the CMB (Equation (36)) and the ratio between the gravitational force and electric force (Equation (28)) were discovered. Empirical equations for the Rydberg constant, Bohr radius, Compton wavelength and classical electron radius in terms of the CMB have also been presented here, along with their verification and errors. These lengths can be understood as special lengths related to the force between magnets. We predict that 0.9937 μm should be the fundamental special length. These special lengths have long been a mystery in science. Such simple empirical equations with high numerical accuracy have not been previously reported. Regarding the ratio between the gravitational force and electric force, the very large ratio between these forces also has long been a mystery in science, and such a simple empirical equation with high numerical accuracy has not been previously reported. Unfortunately, the background theory still is not sufficiently complete. Therefore, we have abandoned the attempt to present any theoretical explanation in this report. We expect to publish such theoretical explanations in a future report.

Furthermore, we can show a clear connection among three different empirical equations. Thus, we conclude that our empirical equations are not coincidence.

Conflicts of Interest

The author declares no conflicts of interest regarding the publication of this paper.

References

[1] Miyashita, T. (2020) *Journal of Modern Physics*, **11**, 1180-1192. https://doi.org/10.4236/jmp.2020.118074

[2] Miyashita, T. (2020) *Journal of Modern Physics*, **11**, 1559-1560. https://doi.org/10.4236/jmp.2020.1110096

[3] Jarzynski, C. (2017) *Physical Review X*, **7**, Article ID: 011008. https://doi.org/10.1103/PhysRevX.7.011008

[4] Jacobson, T. (1995) *Physical Review Letters*, **75**, 1260-1263. https://doi.org/10.1103/PhysRevLett.75.1260

[5] Angrick, C., Braun, J., Ebert, H. and Donath, M. (2021) *Journal of Physics*: *Condensed Matter*, **33**, Article ID: 115501. https://doi.org/10.1088/1361-648X/abd338

[6] Aquino, F.W. and Wong, B.M. (2018) *Journal of Physical Chemistry Letters*, **9**, 6456-6462. https://doi.org/10.1021/acs.jpclett.8b02786

Appendix A

The mathematical connection of the three equations is shown in this appendix.

$$\frac{e^2}{4\pi\varepsilon_0\hbar c}=\alpha=\frac{1}{137.036} \tag{A1}$$

$$\frac{q_m^2}{\mu_0\pi\hbar c}=\frac{1}{\alpha}=137.036 \tag{A2}$$

So,

$$\hbar c=\left(\frac{e^2}{4\pi\varepsilon_0}\right)^{\frac{1}{2}}\left(\frac{q_m^2}{\mu_0\pi}\right)^{\frac{1}{2}} \tag{A3}$$

For convenience, Equation (53) is rewritten as (A4).

$$\frac{Gm_p}{\frac{\lambda_p}{2}}=\frac{9}{2}kT_c \tag{A4}$$

Here,

$$\lambda_p=\frac{h}{m_pc} \tag{A5}$$

From Equations (A4) and (A5),

$$\frac{Gm_pm_pc^2}{hc}=\frac{9}{4}kT_c \tag{A6}$$

From Equations (A3) and (A6),

$$Gm_p^2=\frac{4.5\pi}{c^2}\left(\frac{e^2}{4\pi\varepsilon_0}\right)^{\frac{1}{2}}\left(\frac{q_m^2}{\mu_0\pi}\right)^{\frac{1}{2}}kT_c \tag{A7}$$

For convenience, Equation (54) is rewritten as (A8).

$$\frac{Gm_p^2}{\frac{e^2}{4\pi\varepsilon_0}}=4.5\times\frac{m_e}{e}\times\hbar c \tag{A8}$$

From Equations (A3) and (A8),

$$Gm_p^2=4.5\times\frac{m_e}{e}\times\left(\frac{e^2}{4\pi\varepsilon_0}\right)^{\frac{3}{2}}\left(\frac{q_m^2}{\mu_0\pi}\right)^{\frac{1}{2}} \tag{A9}$$

For convenience, Equation (55) is rewritten as Equation (A10).

$$\frac{m_ec^2}{e\pi}\times\frac{e^2}{4\pi\varepsilon_0}=kT_c \tag{A10}$$

From Equations (A7) and (A9),

$$\frac{4.5\pi}{c^2}\left(\frac{e^2}{4\pi\varepsilon_0}\right)^{\frac{1}{2}}\left(\frac{q_m^2}{\mu_0\pi}\right)^{\frac{1}{2}}kT_c=4.5\frac{m_e}{e}\left(\frac{e^2}{4\pi\varepsilon_0}\right)^{\frac{3}{2}}\left(\frac{q_m^2}{\mu_0\pi}\right)^{\frac{1}{2}} \tag{A11}$$

So,

$$\frac{\pi}{c^2}kT_c = \frac{m_e}{e} \times \frac{e^2}{4\pi\varepsilon_0} \tag{A12}$$

So,

$$\frac{m_e c^2}{e\pi} \times \frac{e^2}{4\pi\varepsilon_0} = kT_c \tag{A13}$$

Equation (A13) is the same as Equation (A10).

Consequently, Equation (55) can be deduced from Equations (53) and (54).

Journal of Modern Physics, 2021, 12, 635-645
https://www.scirp.org/journal/jmp
ISSN Online: 2153-120X
ISSN Print: 2153-1196

A Junction Electric Field Determination of a Bifacial Silicon Solar Cell under a Constant Magnetic Field Effect by Using the Photoconductivity Method

Amadou Diao[1], Bada Thiaw[2], Mountaga Boiro[1], Senghane Mbodji[2], Gregoire Sissoko[1]

[1]Semiconductors and Solar Energy Laboratory, Cheikh Anta Diop University, Dakar, Senegal
[2]Research Team in Renewable Energies, Materials and Laser, Alioune Diop University, Bambey, Senegal
Email: ama_diao@yahoo.fr, amadou.diao@ucad.edu.sn

How to cite this paper: Diao, A., Thiaw, B., Boiro, M., Mbodji, S. and Sissoko, G. (2021) A Junction Electric Field Determination of a Bifacial Silicon Solar Cell under a Constant Magnetic Field Effect by Using the Photoconductivity Method. *Journal of Modern Physics*, **12**, 635-645.
https://doi.org/10.4236/jmp.2021.125041

Received: March 17, 2021
Accepted: April 23, 2021
Published: April 26, 2021

Abstract

In this work, a theory based on the steady photoconductivity method, of a bifacial silicon solar cell under polychromatic illumination and a magnetic field effect, is presented. The resolution of the continuity equation in the base of the solar cell, allowed us to establish the expression of the minority carriers' density from which the photoconductivity, the photocurrent density, the photovoltage and the solar output power as function of the junction recombination velocity and the applied magnetic field, were deduced. From I-V and P-V characteristics of the solar cell, optimal photovoltage and optimal photocurrent obtained at the maximum power point corresponding to a given operating point which is correlated to an optimal junction recombination velocity, were determined according to the magnetic field. By means of the relation between the photocurrent density and the photoconductivity, the junction electric field has been determined at a given optimal junction recombination velocity.

Keywords

Bifacial Solar Cell, Photoconductivity, Junction Recombination Velocity, Magnetic Field, Electric Field

1. Introduction

The photoconductivity is due to the absorption of incident photons that create free charge carriers in the conduction band and/or in the valence band of a conducting material. The photoconductivity is one of the important quantities of

solar cells or semiconductors [1] [2] [3]. It is a useful tool to study the properties of semiconductors like the recombination centers and the distribution of the deep levels states in the forbidden band. Many studies on the photoconductivity, have been utilized for determining a few intrinsic parameters of semiconductors in different regimes, as: in transient one [4] [5], where a relationship between the photoconductivity, the average lifetime and the generation rate of the photogenerated minority carriers has led to determine the density of states as function of the temperature; in steady-state [6]-[12], without an applied magnetic field, the effective lifetime of the minority carriers is determined and then the photoconductivity according to the temperature, the generation rate and the incident light intensity, what permits to determine the recombination density of states. While, with an applied magnetic field, the photoconductivity is, on one hand, as function of the magnetic field and the junction recombination velocity [13] and on the other hand, as function of the wavelength, the magnetic field and the incident power [14] [15]. By the use of the Fermi-Dirac distribution, it is demonstrated that the electrical conductivity of a silicon material decreased with the electric field [16]. Many researches have been carried out on the determination of the junction electric field by considering any more a magnetic field effect at a corresponding functioning point of a solar cell. That permits us to study, in this work, the photoconductivity of a bifacial silicon solar cell according to the magnetic field and the junction recombination velocity in order to determine the optimal operating point and the corresponding junction electric field.

2. Theory

2.1. Mathematical Equations

In **Figure 1**, an n+-p-p+ type of a bifacial silicon solar cell [17] [18], in 1D, is represented:

With d and H respectively the emitter thickness and the solar cell base thickness

We consider a constant magnetic field vector $\vec{B}$ [19] [20] [21], that is applied following the y-axis perpendicularily to the solar cell plane.

So, the expression of the photoconductivity is given by [22]:

$$\sigma_{ph} = \frac{q\mu_o\delta_n}{1+\mu_o^2 B^2} \tag{1}$$

where q is the elementary charge of electron and μ_o the quasi-static mobility of the minority carriers without magnetic field.

One can see, in Equation (1) that the expression of the photoconductivity depends on the minority carriers' density δ_n and magnetic field. Thus, in steady-state, the minority carriers' density can be determined by resolving the following continuity equation:

$$D_n \frac{\partial^2 \delta_n}{\partial x^2} - \frac{\delta_n}{\tau} = -G \tag{2}$$

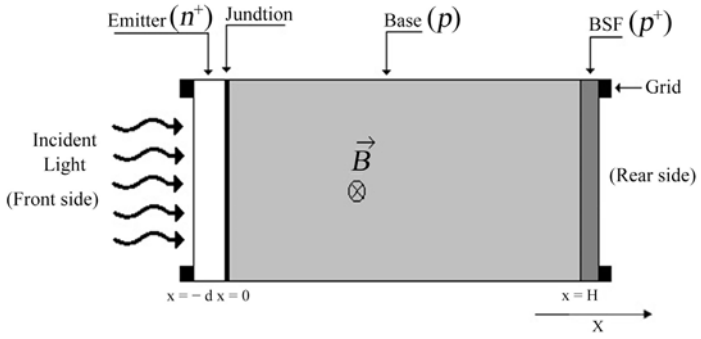

Figure 1. Schematic structure of a bifacial silicon solar cell under an applied magnetic field.

where τ is the average lifetime of the minority carriers in the base; D_n is the minority carriers' diffusion coefficient which expression is given by:

$$D_n = \frac{D_o}{1+\mu_o^2 B^2} \tag{3}$$

With D_o being the minority carriers diffusion coefficient without applied magnetic field; G the minority carriers generation rate [23] at the position x.

The expression of the minority carriers' generation rate, can be given as:

$$G = \eta \sum_{i=1}^{3} a_i \mathrm{e}^{-b_i x} \tag{4}$$

with η being the solar number, a_i and b_i are coefficients deduced from modelling of the generation rate considered over all solar radiation spectrum under AM 1.5.

The solution of Equation (2) can be written as:

$$\delta_n = A\mathrm{e}^{-\frac{x}{L_n}} + C\mathrm{e}^{\frac{x}{L_n}} - \sum_{i=1}^{3} \frac{a_i L_n^2 \mathrm{e}^{-b_i x}}{D_n\left(b_i^2 L_n^2 - 1\right)} \tag{5}$$

with:

$$L_n = \sqrt{D_n \tau} \tag{6}$$

and:

$$\left(b_i^2 L_n^2 - 1\right) \neq 0 \tag{7}$$

where L_n is the minority carriers diffusion length in the base.

The coefficients A and C are determinated by the following boundary conditions [24] [25]:

- at the junction ($x = 0$)

$$D_n \cdot \left.\frac{\partial \delta_n}{\partial x}\right|_{x=0} = Sf \cdot \delta_n\big|_{x=0} \tag{8}$$

- at the rear side ($x = H$)

$$D_n \cdot \left.\frac{\partial \delta_n}{\partial x}\right|_{x=H} = -Sb \cdot \delta_n\big|_{x=H} \tag{9}$$

where *Sf* and *Sb* are respectively the junction recombination velocity that defines the solar cell operating point and the back surface recombination velocity.

2.2. The Photocurrent Density, Photovoltage and Solar Cell Output Power

- The photocurrent density is related to the gradient of the photogenerated minority carriers at the junction and is given by:

$$J_{ph} = qD_n \left.\frac{\partial \delta_n}{\partial x}\right|_{x=0} \tag{10}$$

- The storage of the photogenerated minority carriers to the vicinity of the junction creates a photovoltage whose expression is given by the following Boltzmann equation:

$$V_{ph} = V_T \ln\left(1 + \frac{N_B}{n_i^2}\delta_n(0)\right) \tag{11}$$

With:

$$V_T = KT/q \tag{12}$$

where V_T is the thermal voltage at temperature $T = 300\ K$; N_B is the doping acceptor atoms in the base; n_i is the intrinsic concentration of the minority carriers at temperature T and K is the Boltzmann constant.

- The solar cell output power is the energy supplied, at a time t, by the solar cell. Its expression is given by:

$$P_{ph} = J_{ph} \cdot V_{ph} \tag{13}$$

3. Results and Discussions

We present, in first, the photoconductivity profile, the *I-V* and *P-V* characteristics and then in the second time, the determination method of the optimal operating point and junction electric field.

3.1. Profile of the Photoconductivity According to the Junction Recombination Velocity

In Figure 2, the photoconductivity versus the junction recombination velocity, is represented for different values of the magnetic field:

In Figure 2, we obtain the same behavior for the four curves of the photoconductivity versus junction recombination velocity. Considering curve 1, without an applied magnetic field, in the interval of the junction recombination velocity [0 $cm{\cdot}s^{-1}$; 2×10^2 $cm{\cdot}s^{-1}$] where the solar cell operates in an open circuit situation, we note a high value of the photoconductivity that stays constant. This is related to a great photogeneration of the minority carriers around the junction where they cannot cross since they have not enough kinetic energy. However, in the interval [2×10^2 $cm{\cdot}s^{-1}$; 5×10^5 $cm{\cdot}s^{-1}$] that corresponds to a variable operating point of the solar cell, the photoconductivity decreases because the minor-

ity carriers gradually gain a kinetic energy to across the junction. When the solar cell operates in a short-circuit situation, for a junction recombination velocity $Sf \geq 5\times10^{5}\,\mathrm{cm}\cdot\mathrm{s}^{-1}$, the photoconductivity is lesser than of in open circuit one. In this situation, the minority carriers have enough kinetic energy to across the junction and there is no more new photogenerated carriers.

3.2. I-V Characteristics

The *I-V* characteristics, for different values of the magnetic field, are given in Figure 3:

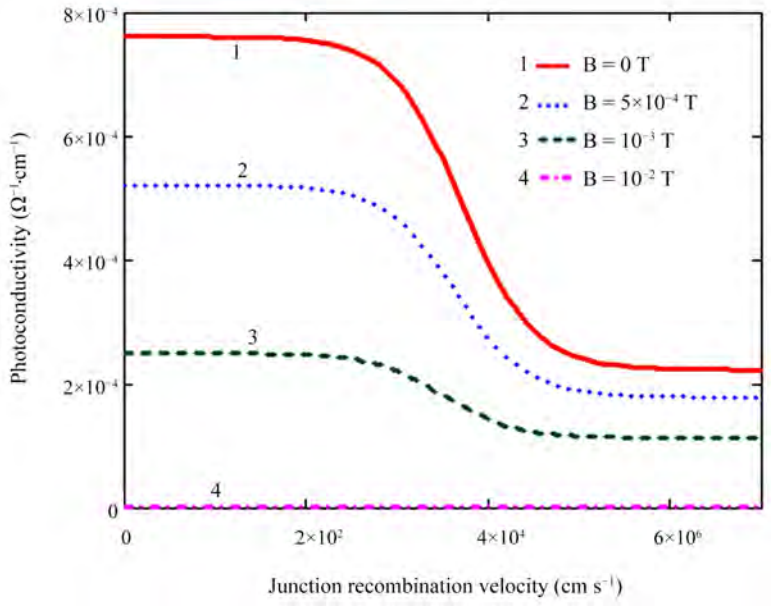

Figure 2. Photoconductivity versus junction recombination velocity for different magnetic field values.

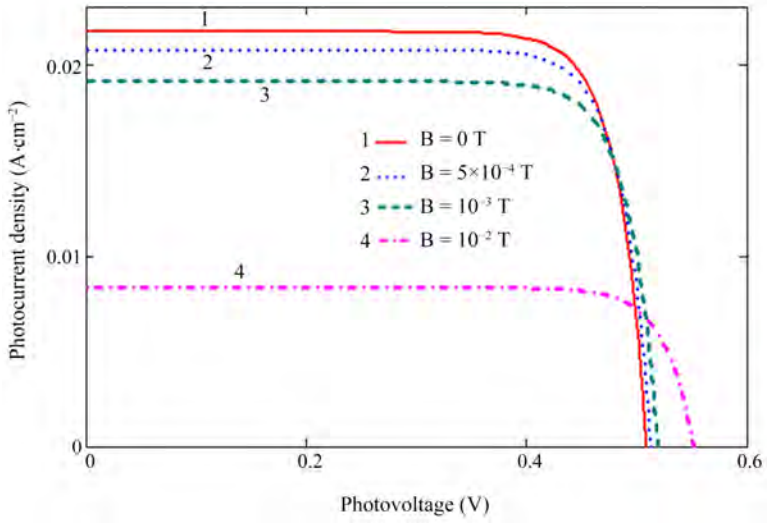

Figure 3. Photocurrent density versus photovoltage for different magnetic field values.

The four curves in Figure 3, exhibit the same behaviour. For a low photovoltage, the photocurrent is maximum and corresponds to the short-circuit photocurrent: there is no significant storage of the photogenerated minority carriers in the vicinity of the junction since the majority of these carriers have acrossed the junction. This situation occurs when the junction recombination velocity is very high while the load is low. However, in the open circuit situation of the solar cell, there is a significant storage of the minority carriers in the vicinity of the junction; this implies a high photovoltage which corresponds to the open circuit photovoltage and where the photocurrent is closed to zero. With a magnetic field, the amplitude of the photocurrent decreases while the photovoltage increases. We note that the magnetic field slows down the photogenerated minority carriers in the vicinity of the junction or deviates them from their initial direction. We note that the operating point of the solar cell depends on the load and the magnetic field. That is why this operating point will impact on the output power delivered by the solar cell.

3.3. P-V Characteristics

In Figure 4, the output power versus the photovoltage, for different values of the magnetic field, is represented:

The curves of the *P-V* characteristics, in Figure 4, show similar profiles. For a given curve and its corresponding value of magnetic field, we note three zones:

1) a first zone which corresponds to the short-circuit situation of the solar cell and where the power increases linearly with the photovoltage. The fit of the curve give positive slope that corresponds to a short-circuit photocurrent;

2) a second zone corresponding to the open circuit situation of the solar cell where the power decreases with the photovoltage: it is like a solar cell that loses an energy and cannot work correctly since the load is high;

3) a third zone which is curvated and located between the two zones mentioned above, where the solar cell operates around the optimal power point.

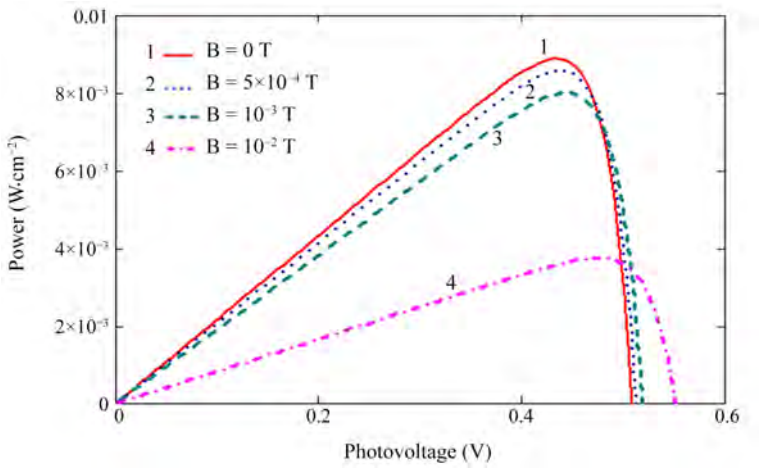

Figure 4. Power versus photovoltage for different magnetic field values.

The increase of the magnetic field decreases the power delivered by the solar cell on the load.

From *I-V* and *P-V* characteristics, we propose a method for determining the optimal power operating point and the corresponding junction electric field.

3.4. Determination Method of the Optimal Operating Point and Junction Electric Field

We give, at first, a relationship between the photocurrent density and the electric field, as followed:

$$J_{ph} = \sigma_{ph} \cdot E \tag{14}$$

where E is the electric field.

In **Figure 5**, a graphical determination method of the optimal operating point, is presented [26].

The *I-V* and *P-V* characteristics, in **Figure 5**, are given without an applied magnetic field and for an operating point that varies from the open circuit situation to the short-circuit one. The operating point is as function of the junction recombination velocity which is linked to the load. A high load corresponds to a low junction recombination velocity while a feeble load corresponds to a high junction recombination velocity. Therefore, there is a load that is linked to an operating point in which the solar cell delivers a maximum power P_{max}. This operating point of the solar cell, which corresponds to the maximum power, is called the optimal operating point and is showed in **Figure 5** by the point P. The P point projection on the photovoltage axis, gives us the optimal photovoltage V_{phop}. Its extension on the I-V characteristic, gives a point whose projection on the photocurrent axis allows us to obtain the optimal photocurrent J_{phop}. With the obtained values of V_{phop} and J_{phop}, we deduce the optimal junction recombination velocity Sf_{op} which corresponds to the optimal operating point of the solar cell.

In **Figure 6**, the optimal junction recombination velocity Sf_{op} and the optimal photoconductivity σ_{phop}, are determined:

The photoconductivity and the photocurrent density are represented on both sides, in **Figure 6**, according to the junction recombination velocity which defines the operating point of the solar cell. From the curve of the photocurrent density versus the junction recombination velocity, the optimal photocurrent J_{phop} gives a point whose projection on the junction recombination velocity axis, allows us to obtain the value of Sf_{op}. With the curve of the photoconductivity versus the junction recombination velocity, we determine the optimal photoconductivity σ_{phop}. From the values of J_{phop} and σ_{phop} that are obtained, we deduce the value of the junction electric field E for a given optimal operating point of the solar cell.

These steps of determining all of the optimal values corresponding to an optimal operating point, are considered for different magnetic field values. What permits us to give **Table 1** below:

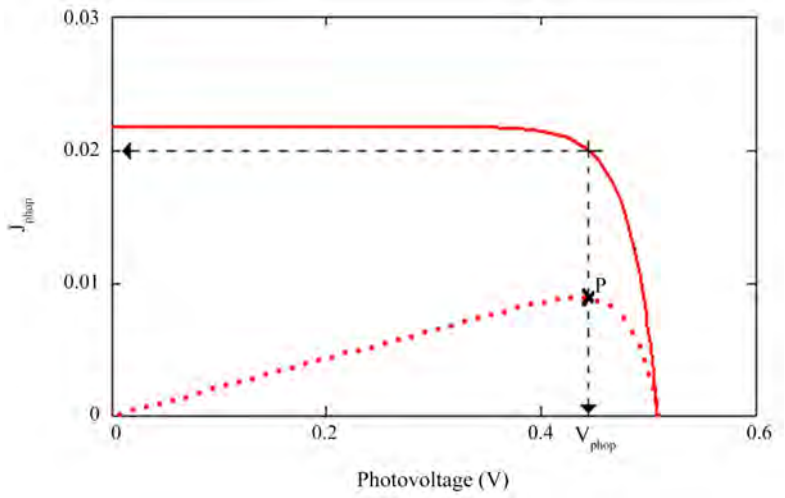

Figure 5. Determination of the maximum power and the optimal photocurrent for a given magnetic field $B = 0$ T.

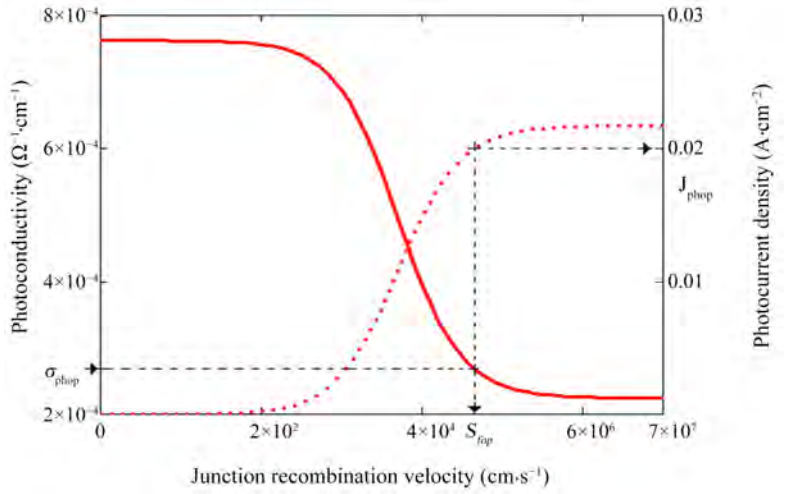

Figure 6. Determination of the optima of junction recombination velocity and photoconductivity for a given magnetic field $B = 0$ T.

Table 1. A few values of V_{phop}, J_{phop}, P_{max}, Sf_{op}, σ_{phop} and E.

B(T)	0	5×10^{-4}	10^{-3}	10^{-2}
V_{phop} (mV)	438	442	445	480
J_{phop} (A·cm^{-2})	0.02	0.019	0.018	0.0078
P_{max} (mW·cm^{-2})	8.76	8.39	8.01	3.74
Sf_{op} (cm·s^{-1})	3×10^5	2×10^5	1.8×10^5	2×10^4
σ_{phop} (Ω^{-1}·cm^{-1})	2.59×10^{-4}	2.02×10^{-4}	1.22×10^{-4}	1.78×10^{-6}
E (V·cm^{-1})	77	94	147	4382

Both the optimal photovoltage and the junction electric field increase with the magnetic field because the magnetic field slows down and stores the photocreated minority carriers in the vicinity of the junction. The optimal photocur-

rent density, the maximum power, the optimal junction recombination velocity and the optimal photoconductivity decrease with the magnetic field. Therefore, we note that, a high photoconductivity corresponds to an ohmic solar cell in which the electric field is weak since the recombination of the minority carriers in the bulk of the solar cell becomes weak. However, a low photoconductivity corresponds to a nonohmic solar cell in which the electric field and the minority carriers' recombination in bulk are high. From these results we note a degradation of the intrinsic parameters of the solar cell when a magnetic field is applied.

4. Conclusions

A theoretical study has been done on a bifacial silicon solar cell. The photoconductivity, the photocurrent density and the photovoltage are determined according to the junction recombination velocity and the magnetic field. From the I-V and P-V characteristics, the maximum power operating point of the solar cell, the optimal photocurrent and the optimal photovoltage were determined for different magnetic field values. The optimal junction recombination velocity, the optimal photoconductivity and the electric field were deduced. The photovoltage and the electric field increase with the increase of magnetic field while the maximum power and the photoconductivity decrease. These obtained results were satisfactory and matched to other works in the research field. A simple method is utilized to determine the optimal operating point and it can be used for photovoltaic panels in order to optimize the load.

The flux of the incident photons and the temperature of the solar cell were assumed to be constant. The degenerated density of states and the change of the energy gap with the magnetic field were not taken into account in this work. In the future, we will consider these new elements in order to improve the analysis of our results. We intend to propose an algorithm to determine the maximum power and the corresponding electric field at the optimal operating point of the solar cell.

Acknowledgements

We acknowledge the Semiconductors and Solar Energy Laboratory and the Research team in renewable energies, materials and laser for supporting this work.

Conflicts of Interest

The authors declare no conflicts of interest regarding the publication of this paper.

References

[1] Bube, R.H. (1960) Photoconductivity of Solids. Wiley, New York.

[2] Joshi, N.V. (1990) Photoconductivity: Art, Science and Technology. Marcel Dekker, New York.

[3] Orton, J. (2004) The Story of Semiconductors. Oxford University Press, Oxford.

[4] Adriaenssens, G.J., Baranovskii, S.D., Fuhs, W., Jansen, J. and Öktü, Ö. (1995) *Physical Review B*, **51**, 9661-9667. https://doi.org/10.1103/PhysRevB.51.9661

[5] Belgacem, H. and Merazga, A. (2008) *Solid-State Electronics*, **52**, 73-77. https://doi.org/10.1016/j.sse.2007.07.023

[6] Sinton, R.A. and Cuevas, A. (1996) *Applied Physics Letters*, **69**, 2510-2512. https://doi.org/10.1063/1.117723

[7] Qiu, F., Xiang, J.Z., Kong, J.C., Yu, L.J., Kong, L.D., Wang, G.H., Li, X.J., Yang, L.L., Li, C. and Ji, R.B. (2011) *Journal of Semiconductors*, **32**, 26-30. https://doi.org/10.1088/1674-4926/32/3/033004

[8] Qamhieh, N. and Adriaenssens, G.J. (2001) *Journal of Non-Crystalline Solids*, **292**, 80-87. https://doi.org/10.1016/S0022-3093(01)00855-9

[9] Pal, R.K., Krishna, J., Agnihotri, A.K., Singh, C.P., Yadav, S. and Kumar, A. (2009) *Chalcogenide Letters*, **6**, 29-34.

[10] Reis, F.T. and Chambouleyron, I. (2002) *Journal of Non-Crystalline Solids*, **299-303**, 179-184. https://doi.org/10.1016/S0022-3093(01)01159-0

[11] Sharmin, M., Choudhury, S., Akhtar, N. and Begum, T. (2012) *Journal of Bangladesh Academy of Sciences*, **36**, 97-107. https://doi.org/10.3329/jbas.v36i1.10926

[12] Schmidt, J.A., Longeaud, C. and Kleider, J.P. (2005) *Thin Solid Films*, **493**, 319-324. https://doi.org/10.1016/j.tsf.2005.08.060

[13] Diao, A., Wade, M., Thiame, M. and Sissoko, G. (2017) *Journal of Modern Physics*, **8**, 2200-2208. https://doi.org/10.4236/jmp.2017.814135

[14] Omar, M.S. and Abbas, T.A. (2010) *Iranian Journal of Physics Research*, **9**, 99-102.

[15] Heisel, W., Bohm, W. and Prettl, W. (1981) *International Journal of Infrared and Millimeter Waves*, **2**, 829-837. https://doi.org/10.1007/BF01007279

[16] Getinet, T. (2010) *Indian Journal of Pure & Applied Physics*, **48**, 192-195.

[17] Meier, D.L., Hwang, J.-M. and Campbell, R.B. (1998) *IEEE Transactions on Electron Devices*, **ED-35**, 70-78. https://doi.org/10.1109/16.2417

[18] Hüber, A., Aberle, A.G. and Hezel, R. (2001) 20% Efficient Bifacial Silicon Solar Cells. 14*th European Photovoltaic Solar Energy Conference*, Munich, 22-26 October 2001, 1796-1798.

[19] Madougou, S., Made, F., Boukary, M.S. and Sissoko, G. (2007) *Advanced Materials Research*, **18-19**, 303-312. https://doi.org/10.4028/www.scientific.net/AMR.18-19.303

[20] Thiam, N., Diao, A., Ndiaye, M., Dieng, A., Thiam, A., Sarr, M., Maiga, A.S. and Sissoko, G. (2012) *Research Journal of Applied Sciences, Engineering and Technology*, **4**, 4646-4655.

[21] Madougou, S., Made, F., Boukary, M.S. and Sissoko, G. (2007) *Advanced Materials Research*, **18-19**, 313-324. https://doi.org/10.4028/www.scientific.net/AMR.18-19.313

[22] Kittel, C. (1972) Introduction à la Physique de l'étatsolide. Université, Dunod, 284-286.

[23] Mohammad, S.N. (1987) *Journal of Applied Physics*, **61**, 767-772. https://doi.org/10.1063/1.338230

[24] Sissoko, G., Sivoththanam, S., Rodot, M. and Mialhe, P. (1992) Constant Illumination-Induced Open Circuit Voltage Decay (CIOCVD) Method, as Applied to High Efficiency Si Solar Cells for Bulk and Back Surface Characterization. 11*th European Photovoltaic Solar Energy Conference and Exhibition*, *Poster* 1*B*, Montreux, 12-16

October 1992, 352-354.

[25] Sissoko, G., Nanéma, E., Corréa, A., Biteye, P.M., Adj, M. and N'Diaye, A.L. (1998) Silicon Solar Cell Recombination Parameters Determination Using the Illuminated I-V Characteristic. *World Renewable Energy Congress*, Florence, 20-25 September 1998, 1847-1851.

[26] Lipinski, M. (1996) *Opto-Electronics Review*, **4**, 129-133.

Journal of Modern Physics, 2021, 12, 646-660
https://www.scirp.org/journal/jmp
ISSN Online: 2153-120X
ISSN Print: 2153-1196

Antimatter, Anti-Space, Anti-Time

Alexander Alexandrovich Antonov

Independent Researcher, Kiev, Ukraine
Email: telan@bk.ru

How to cite this paper: Antonov, A.A. (2021) Antimatter, Anti-Space, Anti-Time. *Journal of Modern Physics*, **12**, 646-660.
https://doi.org/10.4236/jmp.2021.125042

Received: March 29, 2021
Accepted: April 25, 2021
Published: April 28, 2021

Abstract

The article shows that the special theory of relativity (STR) created in the last century was based on postulates due to the lack of the required experimental information and turned out to be incorrect, as its principle of light speed non-exceedance was refuted by studies of special processes in linear electric circuits in the 21st century. And thus, it made obsolete the unsuccessful OPERA and ICARUS experiments carried out at the Large Hadron Collider. Therefore, an alternative version of the STR has been proposed. Its relativistic formulas imply the existence of numerous mutually invisible parallel universes and antiverses. It is explained how they can be seen. There is anti-matter, as well as anti-space and anti-time in antiverses in the same quantities as matter, space and time in universes.

Keywords

Imaginary Numbers, Special Theory of Relativity, Invisible Universes, Multiverse, Hyperverse, Antimatter, Anti-Space, Anti-Time

1. Introduction

In 1826, when Georg Simon Ohm (1789-1854) discovered the law named after him, the science of physics did not yet exist. There was a natural philosophy. Alexander Grigorievich Stoletov (1839-1896) wrote in this regard: "… physics especially tempted natural philosophers. What a favorable theme were electrical phenomena for the most riotous imaginations … Attractive and vague deductions were in the foreground: hard work of experimenter and exact mathematical analysis were not honored; they seemed superfluous and harmful in the study of nature …" And in 1828, Ohm was fired by personal order of Minister of Education for publishing his physics discoveries. The senior official believed that the use of mathematics in physics was unacceptable.

In 1897, Charles Proteus Steinmetz (1865-1923) proposed his interpretation of Ohm's law in respect to linear AC circuits ref. [1]. Now, it is daily used by mil-

lions of engineers in their practice. Moreover, in addition to its direct purpose of calculating electrical circuits, it also proved physical reality of imaginary numbers in the simplest and most convincing way, and thereby refuted generally accepted version of the special theory of relativity (STR).

However, the STR had to be first created and then refuted. And such a version of the STR was created by efforts of Joseph Larmor (1857-1942) [2], Nobel laureate Hendrik Antoon Lorentz (1853-1928) [3], Jules Henri Poincaré (1854-1912) [4] and Nobel laureate Albert Einstein (1859-1955) [5] in the 20th century. Due to the lack of experimental data required for its creation, that were obtained only in the 21st century, it was created using the postulates, *i.e.* assumptions from which the principle of light speed non-exceedance turned out to be incorrect.

But that's not a big deal. Ultimately, all scientific theories are created as a result of identifying and correcting the errors of previously created theories. And then, sooner or later, they are inevitably refuted by subsequent newer theories. Otherwise, science would not have developed. Therefore, this article further proposes a corrected version of the STR.

2. Refutation of the Principle of Light Speed Non-Exceedance

Since the principle of light speed non-exceedance in the generally accepted version of the STR, set forth in all university and school textbooks of physics, has still been believed to be true, it will be necessary to explain why this is not so and why this principle, which is just a postulate, since it has never been proven by anyone, turned out to be in demand.

That is because the relativistic formulas obtained in the generally accepted version of the STR couldn't be explained by its creators. For example, the relativistic mass m, apparently, takes imaginary values at hyper-light speeds, when $v > c$, in the Lorentz-Einstein formula

$$m = \frac{m_0}{\sqrt{1-\left(\frac{v}{c}\right)^2}} \tag{1}$$

where m_0 is the rest mass of a moving physical body (e.g. elementary particle);

m is the relativistic mass of a moving physical body;

v is the velocity of a physical body;

c is the speed of light.

However, the authors of the STR did not know how to explain such a result. As well as no one could explain physical meaning of imaginary numbers 400 years before them. Admittedly, today no one can do it so far. Indeed, everyone knows what 2 kg is, but, no one knows what $2i$ kg is, where $i = \sqrt{-1}$.

Even if the relativistic mass m at hyper-light speeds, when $v > c$, in function (1) corresponded to real numbers, then its graph would still be inexplicable in this velocity range (see **Figure 1a**), since it corresponds to a physically unstable process that cannot exist in nature. Consequently, formula (1) is incorrect and that is why it could not be explained.

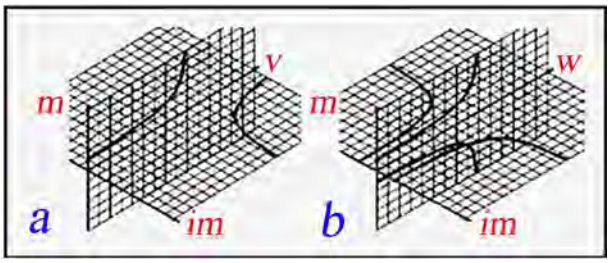

Figure 1. (Color online) Graphs of functions (1) and (2).

After all, physical reality of imaginary numbers has been proven and explained in publications [6]-[21]. In order not to repeat these proofs, we only note that it follows from them that if the principle of light speed non-exceedance were true,

- no shock oscillations such as tsunami, Indian summer, noise of bells, piano music could exist in nature, and even a kid's swing couldn't swing after being pushed by parents;
- there could be no resonance in electric circuits, as well as no electric filters could exist; and thus, there would be neither television, nor telecommunication, nor radiolocation, nor many other things without which modern life would be unthinkable;
- even Ohm's law in Steinmetz's interpretation would not exist.

Since, in accordance with Ohm's law in Steinmetz's interpretation, inductive and capacitive reactances the values of which are imaginary numbers, are measured by the devices available in each radio engineering laboratory, this unambiguously proves their physical reality. After all, it is exactly the ability to register with devices X-ray, radioactive, ultraviolet and infrared radiation, infra and ultrasound, magnetic field, atoms and subatomic particles, as well as many other physical entities that are not registered by the human senses, proves their physical reality. Why, then, a simple and cheap experiment using an ordinary tester in physics is less convincing in solving the problem of proving physical reality of imaginary numbers than the unique expensive OPERA and ICARUS experiments at the Large Hadron Collider?

In fact, since mathematics is the unique universal language of all exact sciences, the correct mathematical interpretation of, let's say, radio engineering and any other experiment is indisputably convincing for all other exact sciences. After all, the Nature is unique, and only people, solely because of their barrenness of intellect, invented many sciences to describe it.

Due to experimental proof of the principle of physical reality of imaginary numbers in the STR, the principle of light speed non-exceedance is no longer required and there is a need for corrected relativistic formulas that allow explaining STR at speeds $v > c$.

3. Relativistic Formulas of the Corrected Version of the STR

How can corrected relativistic formulas be obtained? Different approaches can,

actually, be proposed to solve this issue. And one can reason as follows [22]. The graph of the corrected Lorentz-Einstein function in the range of velocities, must in some respect be similar to the graph of this function in the range of velocities. For example, as in **Figure 1b**. A simple and understandable analytical description can be offered for such a graph

$$m = \frac{m_0 (i)^q}{\sqrt{1-\left(\frac{v}{c}-q\right)^2}} = \frac{m_0 (i)^q}{\sqrt{1-\left(\frac{w}{c}\right)^2}} \tag{2}$$

where $q = \left\lfloor \frac{v}{c} \right\rfloor$ is the "floor" function of argument $\frac{v}{c}$ in discreet mathematics (see **Figure 2a**);

$w = v - qc$ is the local velocity (see **Figure 2a**), the meaning of which will be explained below.

Other relativistic formulas can be corrected in a similar manner.

4. Explanation of Relativistic Formulas of the Corrected Version of the STR

A simple explanation can be proposed for the simple formula (2). The quantity $q = 0$ obviously corresponds to our visible universe, which is assumed to be the one and the only in the existing version of the STR. However, this version turned out to be incorrect, as its principle of light speed non-exceedance had been refuted.

Therefore, the quantity $q = 1$ corresponds to another really existing universe, for which $v = w + c$ follows from $w = v - 1c$, *i.e.* we get $c \le v < 2c$ for $0 \le w < c$. In other words, another adjacent universe is beyond the event horizon and therefore is invisible to us. Therefore, let it for definiteness be called a tachyon universe, like subatomic particles possessing superluminal speed. Herewith, we get $m = m_0 i$ for a tachyon universe from the formula (2).

By a similar argument let our visible universe be called a tardyon universe. For our tardyon universe $m = m_0$.

Subsequently, the quantity $q = 2$ corresponds to one more really existing universe, for which $v = w + 2c$ follows from $w = v - 2c$, *i.e.* we get $2c \le v < 3c$ for $0 \le w < c$. Consequently, this one more universe is also beyond the event horizon and therefore is also invisible to us. It is also invisible to the adjacent universe that is closer to us. Herewith, we get $m = -m_0$ for this universe from the formula (2). That is, this universe can be called an antiverse in relation to our universe.

The quantity $q = 3$ corresponds to one more really existing universe, for which $v = w + 3c$ follows from $w = v - 3c$, *i.e.* we get $3c \le v < 4c$ for $0 \le w < c$. Consequently, this universe is also beyond the event horizon and therefore is also invisible to us and to other universes. We get $m = -im_0$ for this universe from the formula (2). And therefore let it be called a tachyon antiverse, etc.

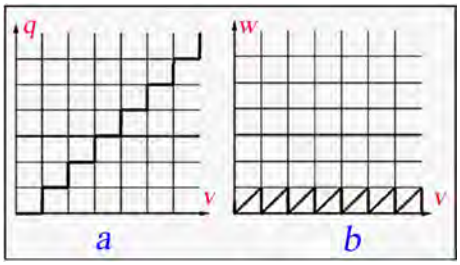

Figure 2. (Color online)Graphs of functions $q(v)$ and $w(v)$.

Hence, it turns out that we live in the Multiverse containing a plenty of mutually invisible universes, rather than in a unique visible universe as asserted in the generally accepted version of the STR. Let this Multiverse be called a hidden Multiverse [23] [24] [25] [26] [27].

5. Dark Matter, Dark Energy, Dark Space

Many interesting hypotheses of the Multiverse have been proposed by now [28]-[35]. However, they all are unverifiable, *i.e.* their truth or falsity can be proven experimentally neither now nor in the distant future. Therefore, they are of limited interest. Another drawback is the fact that they do not anyhow explain extremely incomprehensible phenomena of dark matter and dark energy [36]-[48].

Such extreme incomprehensibility refers also to the hypothesis of the visible Monoverse in the generally accepted version of the STR, about which Albert Einstein spoke very clearly: "Insanity: doing the same thing over and over again and expecting different results"

However, the phenomena of dark matter and dark energy can be quite explicable within the framework of the hypothesis of the hidden Multiverse. Besides the phenomenon of dark space can also be discovered and explained:

- invisibility of dark matter and dark energy is explained by the fact that they are actually neither matter, nor energy, nor any other material physical substance, but only images (though not optical and still less electromagnetic, but gravitational), a sort of a shadow;
- impossibility of detecting any of the chemical elements known to us in the composition of dark matter and dark energy is also explained by the absence of any material content in them, since they are just images;
- at the same time the phenomenon of dark matter is evoked by invisible parallel universes of the hidden Multiverse adjacent to our visible universe;
- the phenomenon of dark energy is evoked by other universes except for our visible universe and invisible parallel universes of the hidden Multiverse adjacent to it;
- in addition, the phenomenon of dark space is similarly evoked by invisible universes outside the hidden Multiverse;
- universes located in and beyond the hidden Multiverse together form the Hyperverse.

6. Analysis of WMAP and Planck Spacecraft Data

Albert Einstein did not exclude such correction of the STR in future. He wrote: "There is no single idea, which I would be sure that it will stand the test of time". And he was absolutely right. After all, if this were not so, then the development of science would be impossible.

An example of the structure of such a hypothetical hidden Multiverse is shown in Figure 3. As can be seen, the universes drifting in the extra spatial dimension are interconnected through portals [49] [50] indicated by single two-sided arrows. The portals arise due to shallow mutual local penetration of the universes into each other. Moreover, the end universes in such a helical structure, evoking the phenomena of dark matter and dark energy, are connected with the universes of dark space.

In order not to repeat the mistake of Albert Einstein due to erroneous assumptions, it is useful to check these results for compliance with the data obtained in the 21st century by the WMAP [51] and Planck [52] spacecraft. According to the WMAP data, the entire universe (in fact, the entire hidden Multiverse, as suggested in the article) is 4.6% of baryonic matter, 22.4% of dark matter and 73.0% of dark energy. According to more recent Planck data, the entire universe (in fact, the entire hidden Multiverse) is 4.9% of baryonic matter, 26.8% of dark matter and 68.3% of dark energy.

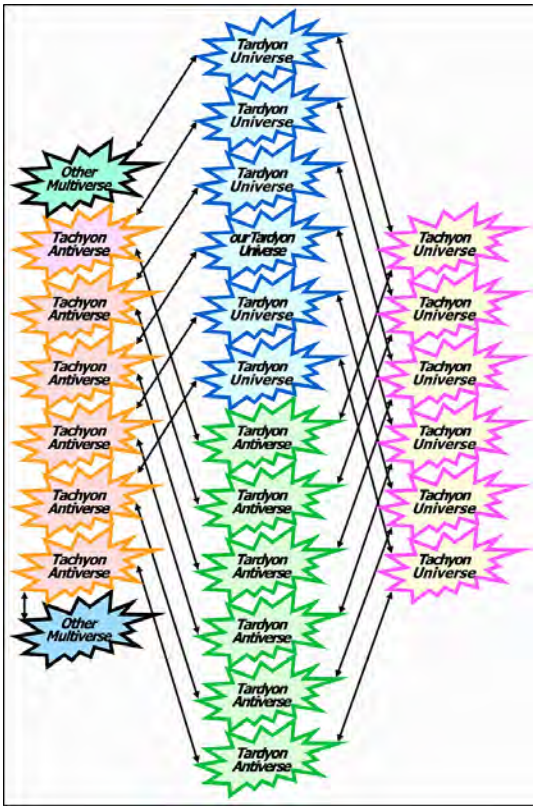

Figure 3. (Color online) The screw structure of the hidden Multiverse corresponding to the formula (2), which illustrates the existence of other Multiverse beyond its borders.

Based on these data, it is conceivable that mass-energy of parallel universes of the hidden Multiverse has largely averaged over billions of years of existence as a result of the mutual exchange of their micro- and mini-content through the portals (even if for some reason their mass-energy in different universes turned out to be different immediately after the Big Bang) and it is equal to the mass-energy of our visible universe, with precise accuracy.

Thus:

- according to Planck data, the hidden Multiverse contains 100%/4.9% = 20.4 parallel universes (according to WMAP data 100%/4.6% = 21.8 parallel universes), *i.e.* probably 20 … 22 parallel universes;
- according to Planck data, the hidden Multiverse contains 26.8%/4.9 = 5.5 parallel universes (according to WMAP data 22.4%/4.6% = 4.9 parallel universes), evoking the phenomenon of dark space, *i.e.* probably 5 … 6 parallel universes;
- according to Planck data, the hidden Multiverse includes 68.3%/4.9 = 13.9 parallel universes (according to WMAP data 73.0%/4.6% = 15.9 parallel universes), evoking the phenomenon of dark energy, *i.e.* e. probably14 … 16 parallel universes.

However, these results do not correspond to the structure of the hidden Multiverse shown in **Figure 3**, since our visible universe should have not two, but 5 … 6 adjacent invisible universes.

Admittedly, each tardyon universe in **Figure 3** is adjacent to one tachyon universe and one tachyon antiverse. And according to the above mathematical analysis of the data obtained by the WMAP and Planck spacecraft, each tardyon universe should have three tachyon universes and antiverses. Therefore, the assumption that the structure of the hidden Multiverse is described by complex numbers and has one extra spatial dimension turned out to be incorrect. In fact, the hidden Multiverse has three extra dimensions and is described by hyper-complex numbers $f_{q,r,s}(x,y,z)+i_1q+i_2r+i_3s$ [53], where the function $f_{q,r,s}(x,y,z)$ describes distribution of material content of the corresponding parallel universe with coordinates in coordinates x,y,z, and the imaginary units i_1,i_2,i_3 are connected by the following relations

$$i_1^2=i_2^2=i_3^2=1 \tag{3}$$

$$i_1i_2i_3=i_2i_3i_1=i_3i_1i_2=-1 \tag{4}$$

$$i_1i_3i_2=i_2i_1i_3=i_3i_2i_1=1 \tag{5}$$

Lisa Randall wrote in this regard: "We can be living in a three-dimensional space sinkhole in a higher-dimensional universe". And she was right.

7. Correction of Relativistic Formulas of the Corrected Version of the STR

Repeatedly corrected relativistic Lorentz-Einstein formula will be written as follows

$$m = \frac{m_0 (i_1)^q (i_2)^r (i_3)^s}{\sqrt{1-\left[\frac{v}{c}-(q+r+s)\right]^2}} = \frac{m_0 (i_1)^q (i_2)^r (i_3)^s}{\sqrt{1-\left(\frac{w}{c}\right)^2}} \tag{6}$$

where $w = v-(q+r+s)c$ is the local velocity for the corresponding universe, which can take values only in the range $0 \le w \le c$.

Other relativistic formulas can be corrected in a similar manner [54] [55] [56] [57]

$$\begin{aligned} \Delta t &= \Delta t_0 (i_1)^q (i_2)^r (i_3)^s \sqrt{1-\left[\frac{v}{c}-(q+r+s)\right]^2} \\ &= \Delta t_0 (i_1)^q (i_2)^r (i_3)^s \sqrt{1-\left(\frac{w}{c}\right)^2} \end{aligned} \tag{7}$$

$$\begin{aligned} l &= l_0 (i_1)^q (i_2)^r (i_3)^s \sqrt{1-\left[\frac{v}{c}-(q+r+s)\right]^2} \\ &= l_0 (i_1)^q (i_2)^r (i_3)^s \sqrt{1-\left(\frac{w}{c}\right)^2} \end{aligned} \tag{8}$$

The structure of the hidden Multiverse corresponding to the formulas (6), (7), and (8) can be as shown in **Figure 4**. As can be seen, its quaternionics [58] [59] structure differ from the one shown in **Figure 3** in that it contains three tachyon universes i_1, i_2, i_3 and three tachyon antiverses i_1, i_2, i_3, which provides three required extra dimensions. Thus, the six-dimensional space of the hidden Multiverse (see **Figure 5**) has three extra dimensions q, r, s, where parallel universes are located, and three dimensions x, y, z, where material content of each of these universes is located. Moreover, the structure of the hidden Multiverse corresponding to the formulas (6), (7) and (8) differs from the one shown in **Figure 3** by the fact that it contains unidirectional portals corresponding to the formulas (4) and (5) in addition to bidirectional portals corresponding to the formula (3).

8. Antimatter, Anti-Space, Anti-Time

The 20th century turned out to be rich in outstanding physical discoveries, such as special and general theory of relativity, quantum mechanics, radio electronics, radioactivity, X-ray, dark matter, dark energy, etc. And if radioactivity and X-ray were almost immediately explained and used, dark matter and dark energy have remained unexplained to this day.

Antimatter [42] [60] [61] is another no less incomprehensible astrophysical object than dark matter and dark energy. It is now generally accepted that the Big Bang produced not only matter, but also antimatter. Moreover, they were generated in equal quantities. However, no antimatter has been found in any noticeable quantities in our visible universe. It was obtained only in the form of subatomic antiparticles and some antiatoms, and also was found in some natural phenomena in negligible quantity for a very short time. Synthesis of such anti-

matter was extremely expensive. Thus, one gram of anti-hydrogen would cost $662.5 trillion.

So, where can antimatter in the form of antiverses be found? And does it at all exist anywhere in this form? It cannot apparently be in our visible universe, since otherwise it would annihilate with matter and the universe would be destroyed. By the way, this fact is another refutation of the generally accepted version of the STR. Hence, it can be found only in another universe. And the hidden Multiverse, unlike other hypothetical Multiverse, is quite suitable for this role, since it has antiverses. Moreover, tardyon and tachyon universes and antiverses alternate in the hidden Multiverse in such a way that they assuredly prevent their mutual annihilation. Thus, the hypothesis of the hidden Multiverse completely solves the problem of the existence of antimatter.

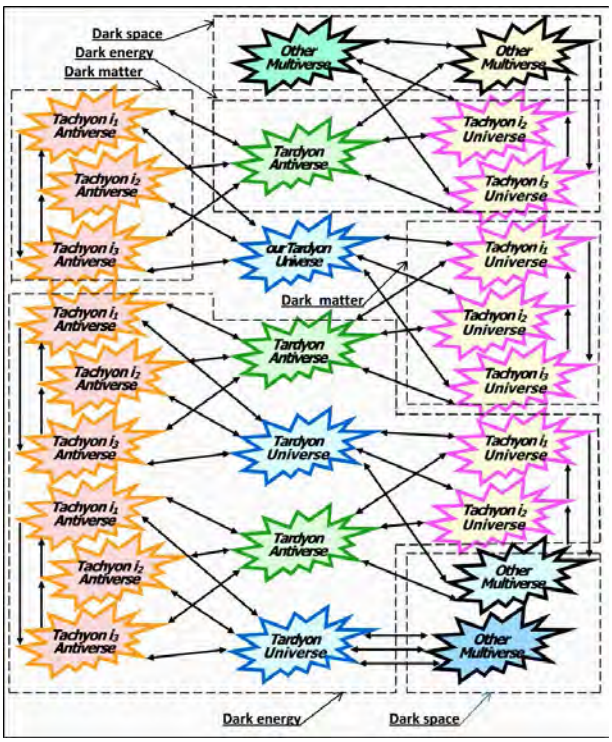

Figure 4. (Color online) The structure of the hidden Multiverse corresponding to the formulas (6), (7) and (8).

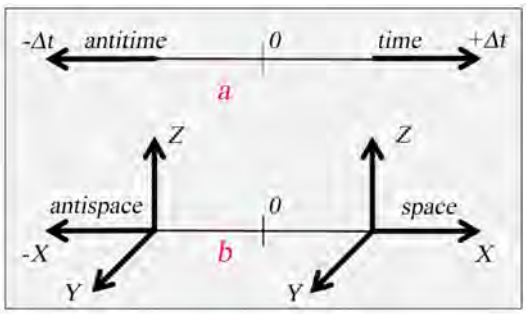

Figure 5. (Color online) Geometric interpretation of the concepts "anti-time" and "anti-space".

The most interesting thing is that existence of antimatter in antiverses follows from the formula (6), just as existence of anti-space and anti-time in antiverses naturally follows from the formulas (7) and (8). Moreover, people would find nothing unusual in these antiverses, if they got there, since there operate the same physical, chemical and other laws of nature as in our visible universe.

Figure 5 shows a fairly obvious geometric interpretation of these new concepts. As can be seen, time and anti-time differ by the sign of the value appearing in formula (7), and space and anti-space differ by the sign of the value appearing in formula (8). Time and anti-time, in addition, can differ in their different distance on the time axis from the common origin, which depends on the time of occurrence of the corresponding universes and antiverse. Figure 5, for example, depicts a situation in which the universe and the antiverse arose simultaneously.

9. How to See Invisible Universes

Thus, the hidden Multiverse is quite unusual in many respects. This arouses some mistrust. Does it exist at all? Nature can give an unequivocal and convincing answer to this question only if its invisible universes are seen. And they can be seen as follows [62] [63].

Since the sky maps of invisible parallel universes are supposedly extremely different, their constellations can be confidently distinguished from those observed in the starry sky by observatories on Earth. Moving along the Earth portals between our visible universe and adjacent invisible universes, one can observe as the star map of one universe is gradually replaced by the star map of the adjacent universe. Therefore, all it takes to make sure of existence of invisible universes is to register differences between the constellations in the starry sky in the portals from the constellations observed in the starry sky outside the portals.

What needs to be done to carry out such an experiment is to find a portal and perform the astronomical observation therein. And although it is clear that entrances to portals are located, at least, in some anomalous zones, which are quite numerous on Earth, no one has yet been engaged in the study of portals directly in portals, since no one has needed it. And besides, it is unsafe, since portals are a sort of invisible labyrinths. Therefore, one can get lost there without an appropriate portal orientation device (similar to marine compass). Such a danger can be minimized, if such observations are carried out at the very entrance to the portal, in the anomalous zone. It is conceivable that some astronomical observatories are already in the anomalous zones, without knowing it. As, for example, the Main Astronomical Observatory of the National Academy of Sciences of Ukraine, which is located in the Holosiivskyi forest, just 12 km from Kyiv, the capital of Ukraine (see Figure 6).

Therefore, an experiment in detecting invisible universes turns out to be very simple and inexpensive in this case. It consists in comparing computer images of the same area of the starry sky provided by several observatories located close to each other, at least one of which being located in the anomalous zone (see Figure 7);

Figure 6. (Color online) Main astronomical observatory of the national academy of science of ukraine.

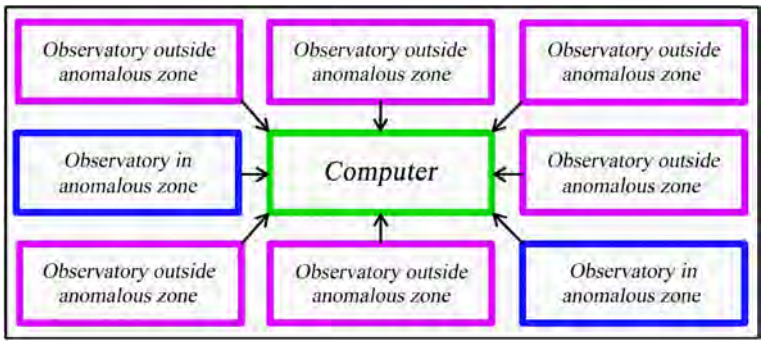

Figure 7. (Color online) Scheme of an experiment to detect invisible universes by identifying differences as a result of comparing the constellations of the starry sky in anomalous zones and outside anomalous zones.

and in revealing differences in the relative position of the stars depicted in these images. If such an experiment is successful, its significance for human civilization will significantly exceed the significance of the discovery of America by Columbus.

10. Conclusions

The answer given in the article to one of the questions from the list of unsolved issues of modern physics "where is antimatter?" turned out to be simple and quite logical: it is in the antiverses. At the same time, it has been explained that there are many pairs of universes-antiverses in nature. And therefore, there are many antimatters. Moreover, it has been explained that, in addition to antimatter, there is anti-time and anti-space in the antiverses.

However, the answer to this question has first required the answer to another question from the same list "do invisible parallel universes exist at all?" And the article not only makes it clear that they exist in the Multiverse, which we have

called hidden, but also why they are parallel and invisible. It also clarifies how and where on Earth invisible universes can be seen.

Notably, the answer to the second question was obtained in the process of answering two more questions from the list of unsolved issues of modern physics "are there extra dimensions?" and "what is dark matter and dark energy?" Due to mathematical analysis of the data obtained by the WMAP and Planck spacecraft, it has been concluded that our hidden Multiverse has a quaternion structure in six-dimensional space. And the phenomenon of dark matter and dark space is explained by the existence in our visible universe of a gravitational wave background generated by the rest of the invisible universes of the hidden Multiverse.

All these answers to the questions from the list of unsolved issues of modern physics became possible after receiving an answer to one more question, although from the list of unsolved issues of modern mathematics, "can imaginary numbers be physically real?" An affirmative answer has been obtained as a result of theoretical and experimental studies of special processes in linear electric circuits, which made it possible to prove the general scientific principle of physical reality of imaginary numbers that, in its turn, refuted the principle of light speed non-exceedance in the STR. And this enabled us to assert that the relativistic formulas obtained in the generally accepted version of the STR are incorrect; they have been incorrectly explained and entailed wrong conclusions. Therefore, attempts to solve the above-mentioned and other physical issues within the framework of this theory were certainly destined for failure.

Thus, it is logical to conclude that the version of the STR presented in textbooks is outdated, since it does not correspond to the experimental data obtained in the 21st century, and therefore it hinders the development of modern physics.

Acknowledgements

Many famous scientists, such as Albert Einstein, Max Planck, Ernest Rutherford and others, argued that an author does not completely understand his own scientific theory if he is not able to explain it to his wife, mother-in-law and other non-specialists. Therefore, the author of this article, who set himself a goal of presenting the above-presented unconventional approach to solving some issues of astrophysics as clearly as possible, even for non-specialists, used the help of his wife for achieving it. The author expresses appreciation to Olga Ilyinichna Antonova for the help. Being an academic economist, she, nevertheless, took part in discussion of the foregoing alternative version of the STR. Her critical remarks and valuable advice contributed to its more understandable presentation to a general reader.

Conflicts of Interest

The author declares no conflicts of interest regarding the publication of this paper.

References

[1] Steinmetz, C.P. (2010) Theory and Calculation of Electric Circuit. Nabu Press, Charleston.

[2] Larmor, J.J. (1897) *Philosophical Transactions of the Royal Society A*: *Mathematical, Physical and Engineering Sciences*, **190**, 205-300. https://doi.org/10.1098/rsta.1897.0020

[3] Lorentz, H.A. (1899) *Proceedings of the Royal Netherlands Academy of Arts and Sciences*, **1**, 427-442.

[4] Poincaré, H. (1905) *Comptes Rendus*, **140**, 1504-1508.

[5] Einstein, A. (1905) *Annalen der Physik*, **17**, 891-921. https://doi.org/10.1002/andp.19053221004

[6] Antonov, A.A. (2008) *European Journal of Scientific Research*, **21**, 627-641.

[7] Antonov, A.A. (2009) *European Journal of Scientific Research*, **28**, 193-204.

[8] Antonov, A.A. (2010) *General Mathematics Notes*, **1**, 11-16. https://doi.org/10.17686/sced_rusnauka_2010-887

[9] Antonov, A.A. (2010) *International Journal of Pure and Applied Sciences and Technology*, **1**, 1-12.

[10] Antonov, A.A. (2010) *American Journal of Scientific and Industrial Research*, **1**, 342-349. https://doi.org/10.5251/ajsir.2010.1.2.342.349

[11] Antonov, A.A. (2013) *International Journal of Management, IT and Engineering*, **3**, 219-230. https://doi.org/10.17686/sced_rusnauka_2013-898

[12] Antonov, A.A. (2015) *General Mathematics Notes*, **31**, 34-53. http://www.emis.de/journals/GMN/yahoo_site_admin/assets/docs/4_GMN-9212-V31N2.1293701.pdf

[13] Antonov, A.A. (2015) *Journal of Russian Physical and Chemical Society*, **87**, 328-355. (In Russian)

[14] Antonov, A.A. (2015) *American Journal of Electrical and Electronics Engineering*, **3**, 124-129.

[15] Antonov, A.A. (2015) *Global Journal of Physics*, **2**, 145-149.

[16] Antonov, A.A. (2016) *Ponte Academic Journal*, **72**, 131-142. https://doi.org/10.21506/j.ponte.2016.7.9

[17] Antonov, A.A. (2016) *Journal of Modern Physics*, **7**, 2299-2313. https://doi.org/10.4236/jmp.2016.716198

[18] Antonov, A.A. (2016) *General Mathematics Notes*, **35**, 40-63.

[19] Antonov, A.A. (2016) *International Review of Physics*, **10**, 31-35.

[20] Antonov, A.A. (2017) *Norwegian Journal of Development of the International Science*, **6**, 50-63.

[21] Antonov, A.A. (2018) *Natural Science*, **10**, 11-30. https://doi.org/10.4236/ns.2018.101002

[22] Antonov, A.A. (2014) *American Journal of Scientific and Industrial Research*, **5**, 40-52.

[23] Antonov, A.A. (2011) *British Journal of Science*, **2**, 51-60. https://doi.org/10.17686/sced_rusnauka_2011-892

[24] Antonov, A.A. (2012) *International Journal of Pure and Applied Sciences and Technology*, **12**, 43-56. https://doi.org/10.17686/sced_rusnauka_2012-896

[25] Antonov, A.A. (2012) *Encyclopedia of Russian Thought*: *Reports to Russian Physical Society*, **16**, 3-20. (In Russian)

[26] Antonov, A.A. (2015) *International Journal of Advanced Research in Physical Science*, **2**, 25-32.

[27] Antonov, A.A. (2017) *Natural Science*, **9**, 43-62. https://doi.org/10.4236/ns.2017.93005

[28] Deutch, D. (1998) The Fabric of Reality: The Science of Parallel Universes and Its Implications. Penguin Books, London.

[29] Green, B. (2000) The Elegant Universe: Superstrings, Hidden Dimensions, and the Quest for the Ultimate Theory. Random House Inc., New York. https://doi.org/10.1119/1.19379

[30] Vilenkin, A. (2006) Many Worlds in One: The Search for Other Universes. Hill and Wong, New York.

[31] Steinhardt, P.J. and Turok, N. (2007) Endless Universe: Beyond the Big Bang. Doubleday, New York.

[32] Carr, B. (2009) Universe or Multiverse? Cambridge Univ. Press, Cambridge.

[33] Greene, B. (2011) The Hidden Reality: Parallel Universes and the Deep Laws of the Cosmos. Random House Inc., New York.

[34] Deutsch, D. (2012) The Beginning of Infinity: Explanations That Transform the World. Penguin Books, New York.

[35] Tegmark, M. (2015) Our Mathematical Universe: My Quest for the Ultimate Nature of Reality. Vintage, New York.

[36] Antonov, A.A. (2015) *International Journal of Physics*, **3**, 84-87.

[37] Antonov, A.A. (2015) *Global Journal of Science Frontier Research*: *A Physics and Space Science*, **15**, 33-38.

[38] Antonov, A.A. (2015) *Cosmology*, **19**, 40-61.

[39] Antonov, A.A. (2015) *American Journal of Modern Physics*, **4**, 1-9. https://doi.org/10.11648/j.ajmp.20150401.11

[40] Antonov, A.A. (2015) *American Journal of Modern Physics*, **4**, 180-188. https://doi.org/10.11648/j.ajmp.20150404.14

[41] Antonov, A.A. (2015) *Optics*, **4**, 43-47.

[42] Antonov, A.A. (2016) *Ponte*, **72**, 288-300. https://doi.org/10.21506/j.ponte.2016.9.22

[43] Antonov, A.A. (2016) *Frontiers of Astronomy, Astrophysics and Cosmology*, **2**, 1-9.

[44] Antonov, A.A. (2016) *Journal of Modern Physics*, **7**, 1228-1246. https://doi.org/10.4236/jmp.2016.710111

[45] Antonov, A.A. (2017) *Applied Physics Research*, **9**, 30-41. https://doi.org/10.5539/apr.v9n2p30

[46] Antonov, A.A. (2017) *Journal of Modern Physics*, **8**, 567-582. https://doi.org/10.4236/jmp.2017.84038

[47] Antonov, A.A. (2018) *Journal of Modern Physics*, **9**, 14-34. https://doi.org/10.4236/jmp.2018.91002

[48] Antonov, A.A. (2019) *Journal of Modern Physics*, **10**, 1006-1028. https://doi.org/10.4236/jmp.2019.108067

[49] Antonov, A.A. (2012) *American Journal of Scientific and Industrial Research*, **3**, 464-473. https://doi.org/10.5251/ajsir.2012.3.6.464.473

[50] Antonov, A.A. (2016) *Philosophy and Cosmology*, **6**, 11-27. (In Russian)

http://ispcjournal.org/journals/2016-16/Antonov_16.pdf

[51] Hinshaw, G., Larson, D., Komatsu, E., *et al.* (2013) Nine Year Wilkinson Anisotropy Probe (WMAP) Observations: Cosmological Parameter Results.

[52] Adam, R., Ade, P.A.R., Aghanim, N., *et al.* (2015) Plank 2015 Results. 1. Overview of Products and Scientific Results.

[53] Kantor, I.L. and Solodovnikov, A.S. (1989) Hypercomplex Numbers. Springer Verlag, Berlin. https://doi.org/10.1007/978-1-4612-3650-4

[54] Antonov, A.A. (2020) *Journal of Russian Physicochemical Society*, **91**, 57-94. (In Russian)

[55] Antonov, A.A. (2020) *Journal of Modern Physics*, **11**, 324-342. https://doi.org/10.4236/jmp.2020.112020

[56] Antonov, A.A. (2020) *Journal of Russian Physicochemical Society*, **92**, 39-72. (In Russian)

[57] Antonov, A.A. (2021) *German International Journal of Modern Science*, **4**, 38-47.

[58] Antonov, A.A. (2015) *Global Journal of Science Frontier Research*: *A Physics and Space Science*, **15**, 8-15.

[59] Antonov, A.A. (2020) *Österreichisches Multiscience Journal* (*Innsbruck*, *Austria*), **35**, 61-72. http://osterr-science.com

[60] Alfvén, H. (1966) Worlds-Antiworlds: Antimatter in Cosmology. W. H. Freeman & Co., San Francisco.

[61] Frazer, G. (2004) Antimatter: The Ultimate Mirror. Cambridge University Press, Cambridge.

[62] Antonov, A.A. (2020) *Journal of Modern Physics*, **11**, 593-607. https://doi.org/10.4236/jmp.2020.115039

[63] Antonov, A.A. (2020) *Natural Science*, **12**, 569-587. https://doi.org/10.4236/ns.2020.128044

Journal of Modern Physics, 2021, 12, 661-670
https://www.scirp.org/journal/jmp
ISSN Online: 2153-120X
ISSN Print: 2153-1196

Time Intervals of the Energy Emission in Quantum Systems Obtained from the Conservation Rule of the Electron Momentum

Stanisław Olszewski

Institute of Physical Chemistry, Polish Academy of Sciences, Warsaw, Poland
Email: olsz@ichf.edu.pl

How to cite this paper: Olszewski, S. (2021) Time Intervals of the Energy Emission in Quantum Systems Obtained from the Conservation Rule of the Electron Momentum. *Journal of Modern Physics*, **12**, 661-670.
https://doi.org/10.4236/jmp.2021.125043

Received: March 12, 2021
Accepted: April 26, 2021
Published: April 29, 2021

Abstract

The paper presents a non-probabilistic approach to the time interval associated with the energy emission produced by the electron transition in a quantum system. The calculations were performed for the hydrogen atom and the electron particle in a one-dimensional potential box. In both cases, the rule of conservation of the electron momentum has been applied. The results, limited to the time intervals of transitions between two neighbouring quantum energy levels, occur to be much similar to those obtained earlier with the aid of the Joule-Lenz energy emission theory.

Keywords

Non-Probabilistic Approach to the Electron Transition Time, Conservation Rule of the Electron Momentum, Joule-Lenz Energy Emission Theory

1. Introduction

In principle, we assume that some interval of time should accompany any quantum process in which a change of a quantum physical system does occur. In the previous approach to such processes, a probabilistic analysis accompanied any electron transition phenomenon (see e.g. [1] [2] [3] [4]), leaving unknown the corresponding interval, or intervals, of time. In general, such situation did not change in the modern quantum theory [5] [6].

A different, viz. non-probabilistic situation, took place when the classical Joule-Lenz theorem for the energy emission (see e.g. [7]) has been adapted in calculating the transition time of an electron between two quantum energy levels [8]-[14]. In this case, a very simple rule coupling the distance between two quantum energy levels with the size of the time interval for the electron transi-

tion could be found. Nevertheless, the limitations of that rule became rather evident. In consequence, an alternative approach to the time interval of the electron transition seemed to be of use. Such approach is outlined in the next Sections of the present paper.

2. Electron Momentum, Its Change and a Use of the Postulate Concerning Conservation of the Momentum. The Case of the Hydrogen Atom Taken as an Example

In principle any change of the electron energy, say obtained in effect of the electron transition between two quantum levels, can be associated with a corresponding change of the electron momentum. By taking into account the bound electron states of the hydrogen atom, the state n of the energy is given by [15] [16]

$$E_n = -E_{\text{kin}}^{(n)} = -\frac{m}{2}v_n^2, \tag{1}$$

where the first equation in (1) is due to the virial theorem

$$2E_{\text{kin}}^{(n)} + E_{\text{pot}}^{(n)} = 0 \tag{2}$$

in result of which the total electron energy of the atom equal to a sum of the kinetic and potential parts becomes

$$E_{\text{tot}}^{(n)} = E_{\text{kin}}^{(n)} + E_{\text{pot}}^{(n)} = E_n. \tag{3}$$

The electron velocity entering (1) is [17]

$$v_n = \frac{e^2}{n\hbar} \tag{4}$$

and the electron momentum in state n becomes

$$p^n = mv_n. \tag{5}$$

Another approach to p^n can be obtained from the quanta of the electron angular momentum

$$L_n = mv_n r_n = \frac{me^2}{n\hbar}\frac{n^2\hbar^2}{me^2} = n\hbar. \tag{6}$$

which holds because

$$r_n = \frac{n^2\hbar^2}{me^2} \tag{7}$$

is the radius of the electron circular orbit in the hydrogen atom [17].

A final result for the quanta of energy in (1) is

$$E_n = -\frac{m}{2}\frac{e^4}{n^2\hbar^2} \tag{8}$$

and the energy change

$$\Delta E = E_{n+1} - E_n \tag{9}$$

due to the change of the quantum state is equal to

$$\Delta E = \frac{m}{2}\frac{e^4}{\hbar^2}\left[\frac{1}{n^2} - \frac{1}{(n+1)^2}\right] = \frac{m}{2}\frac{e^4}{\hbar^2}\frac{(n+1)^2 - n^2}{n^2(n+1)^2} = \frac{me^4}{\hbar^2}\frac{n+1/2}{n^2(n+1)^2} \cong \frac{me^4}{\hbar^2}\frac{1}{n^3}. \quad (10)$$

The last step in (10) is valid on condition n is a large number.

Respectively to (9) we have the momentum change

$$\Delta p^n = p^{n+1} - p^n = \frac{me^2}{\hbar}\left(\frac{1}{n+1} - \frac{1}{n}\right) = -\frac{me^2}{\hbar}\frac{1}{(n+1)n} \approx -\frac{me^2}{\hbar n^2} \quad (11)$$

which provides us evidently with a smaller electron momentum in state $n+1$ than in state n.

If the momentum in states $n+1$ and n should be conserved, the negative difference in (11) has to be compensated by the momentum supplement resulting from the orbit change, viz.

$$\Delta r_n = r_{n+1} - r_n, \quad (12)$$

in effect of which we obtain the momentum change

$$m\frac{\Delta r_n}{\Delta t} = m\frac{r_{n+1} - r_n}{\Delta t} = \frac{m}{\Delta t}\left[\frac{(n+1)^2\hbar^2}{me^2} - \frac{n^2\hbar^2}{me^2}\right] = \frac{(2n+1)\hbar^2}{\Delta t e^2} \approx \frac{2n\hbar^2}{\Delta t e^2}. \quad (13)$$

We postulate that the sum of (11) and (13) has to be zero, so

$$\Delta p_n + m\frac{\Delta r_n}{\Delta t} = 0 \quad (14)$$

or

$$-\frac{me^2}{\hbar n^2} + \frac{2n\hbar^2}{\Delta t e^2} = 0. \quad (15)$$

It should be noted that the momenta balance postulated in (15) concerns solely the momenta values and not directions of the vectors. The requirement in (15) gives

$$\frac{me^2}{\hbar n^2} = \frac{2n\hbar^2}{\Delta t e^2} \quad (16)$$

from which

$$\Delta t = \frac{2n^3\hbar^3}{me^4}. \quad (17)$$

This Δt is a time interval necessary to provide us with a conservation of momentum represented by the formula (14).

3. Comparison with the Joule-Lenz Law [8]-[14]

According to that law the time interval

$$\Delta t^{(JL)} \quad (18)$$

should approximately satisfy the formula

$$\Delta E\,\Delta t^{(JL)} = \frac{me^4}{\hbar n^3}\Delta t^{(JL)} = h, \quad (19)$$

where the interval ΔE is taken from (10). In virtue of (19) we have

$$\Delta t^{(JL)} = \frac{2\pi\hbar^3 n^3}{me^4}. \tag{20}$$

In result we find that the Joule-Lenz emission time (20) differs from the time interval obtained in (17) solely by the factor of π.

4. Time Interval Connected with the Absorption of Energy Compared with the Time of the Emission Process

Both the absorption and emission processes are of a semiclassical nature. Therefore if in case of absorption we have a change of quantum indices

$$n \to n+1 \tag{21}$$

the result for the time interval Δt becomes equal to that for the case of emission between the levels

$$n+1 \to n \tag{22}$$

A different situation can be obtained when the emission change of states

$$n \to n-1 \tag{23}$$

is compared with the absorption change which is for example

$$n \to n+1. \tag{24}$$

In the case of (23) we have the momentum balance given by the condition

$$\begin{aligned} p^{n-1} - p^n + m\frac{r_{n-1} - r_n}{\Delta t} &= \frac{me^2}{\hbar}\left(\frac{1}{n-1} - \frac{1}{n}\right) + m\frac{(n-1)^2 - n^2}{\Delta t}\frac{\hbar^2}{me^2} \\ &= \frac{me^2}{\hbar}\frac{1}{(n-1)n} + \frac{m}{\Delta t}(-2n+1)\frac{\hbar^2}{me^2} = 0 \end{aligned} \tag{25}$$

from which we obtain the equation

$$\frac{me^2}{\hbar}\frac{1}{(n-1)n} = \frac{m}{\Delta t}(2n-1)\frac{\hbar^2}{me^2} \tag{26}$$

or

$$\Delta t = \Delta t_{em} = \frac{\hbar^3}{me^4}(2n-1)(n-1)n \cong \frac{\hbar^3}{me^4}2n^3 \tag{27}$$

where the last step holds for the large n.

On the other hand, for the absorption process in (24), we have the balance

$$\begin{aligned} &p^{n+1} - p^n + \frac{m}{\Delta t}\left[(n+1)^2 - n^2\right]\frac{\hbar^2}{me^2} \\ &= \frac{me^2}{\hbar}\left(\frac{1}{n+1} - \frac{1}{n}\right) + \frac{m}{\Delta t}(2n+1)\frac{\hbar^2}{me^2} = 0 \end{aligned} \tag{28}$$

from which

$$\frac{me^2}{\hbar}\frac{-1}{(n+1)n} = -\frac{m}{\Delta t}(2n+1)\frac{\hbar^2}{me^2} \tag{29}$$

or

$$\Delta t = \Delta t_{abs} = \frac{\hbar^3}{me^4}(2n+1)(n+1)n \approx \frac{\hbar^3}{me^4}2n^3, \tag{30}$$

where the last step holds for the large n.

Evidently

$$\Delta t_{abs} - \Delta t_{em} = \frac{\hbar^3 n}{me^4}\left[(2n+1)(n+1)-(2n-1)(n-1)\right] = \frac{\hbar^3}{me^4}6n^2. \tag{31}$$

For large n the difference (31) becomes only a small fraction of Δt in (27) or (30).

5. Electron Particle Moving in a One-Dimensional Potential Box and Its Transition Process

A reasoning similar to that developed for the electron in the hydrogen atom can be applied also in case of the electron particle moving in a one-dimensional potential box.

Let the box has the length L. The electron quantum states for the energy are [18]

$$E_n = \frac{n^2h^2}{8mL^2} = \frac{m}{2}v_n^2 \tag{32}$$

or

$$E_n = \frac{p_n^2}{2m} \tag{32a}$$

where v_n are the electron velocities:

$$v_n = \frac{nh}{2mL} \tag{33}$$

and p_n are the electron momenta

$$p_n = \frac{nh}{2L}. \tag{33a}$$

The electron can have the momenta in both motion directions along the box, so p_n in (33a) can have both positive and negative values. Let the energy emission produces the difference of momenta equal to that in the states n and $n-1$. This difference becomes:

$$\Delta p_n = p_n - p_{n-1} = \frac{h}{2L}. \tag{34}$$

Due to the momentum conservation the difference (34) should be cancelled by the momentum

$$m\frac{2L}{\Delta t} \tag{35}$$

where Δt is the time interval of the electron motion along the box length, first from zero to L, next from L to zero. This implies

$$\frac{2L}{\Delta t} = v_n \tag{36}$$

which is the velocity of the particle. This velocity has been obtained from the electron energy in the formula (33).

The momentum balance provides us with the equation

$$-\Delta p_n + m\frac{2L}{\Delta t} = 0 \tag{37}$$

which gives

$$\Delta p_n = \frac{h}{2L} = m\frac{2L}{\Delta t} = mv_n \tag{38}$$

where the last step is due to (36).

From (38) we obtain the relation for Δt:

$$\Delta t = \frac{2L}{v_n} = 2L\frac{2mL}{nh} = \frac{4mL^2}{nh} \tag{39}$$

identical to that calculated from [19]:

$$\Delta t = \frac{\Delta q}{\partial E_n/\partial p_n} = \frac{2L}{p_n/m} = \frac{2L}{v_n} \tag{39a}$$

because the distance $\Delta q = 2L$. This result can be compared with the formula represented by the Joule-Lenz law, viz.

$$\Delta E \Delta t = h. \tag{40}$$

Since ΔE in (40) becomes for a free particle

$$\Delta E = E_n - E_{n-1} = \frac{n^2 - (n-1)^2}{8mL^2}h^2 \approx \frac{2nh^2}{8mL^2} = \frac{nh^2}{4mL^2} \tag{41}$$

we obtain from (41) the time interval

$$\Delta t = \frac{h}{\Delta E} = h\frac{4mL^2}{nh^2} = \frac{4mL^2}{nh}. \tag{42}$$

This is a result identical to Δt in (39) and (39a).

6. Size Limits of Mechanical Parameters Entering Simple Quantum Systems

Conservation of momentum suggests to calculate the limits of mechanical parameters like energy, velocity, distance and time entering the examined simple quantum systems. These limits can be obtained in an equally simple way.

Beginning with the hydrogen atom, the relativistic limit of the electron velocity leads to requirement

$$v_n\big|_{n=1} = v_1 = \frac{e^2}{\hbar} < c \tag{43}$$

which gives

$$1 < \frac{\hbar c}{e^2} \cong 137. \tag{44}$$

A limit for the absolute value of the electron energy is represented by the formula

$$E_1 = E_{\text{kin}}^{(n=1)} = \frac{mv_1^2}{2} = \frac{me^4}{2\hbar^2} < mc^2 \tag{45}$$

which gives the relation

$$\frac{e^4}{2\hbar^2} < c^2. \tag{46}$$

This relation is equivalent to the formula

$$1 < \frac{2\hbar^2 c^2}{e^4} \cong 2 \cdot 137^2. \tag{47}$$

The result in (47) is an extension of that presented in (44).

The properties connected with the radius limit of the electron orbit which for the quantum number $n = 1$ is equal to

$$r_n = r_1 = \frac{\hbar^2}{me^2} \tag{48}$$

can be deduced from the virial theorem

$$2E_{\text{kin}} + E_{\text{pot}} = 0. \tag{49}$$

This gives the largest negative size of the electron potential energy equal to

$$E_{\text{pot}}^{(n=1)} = -\frac{e^2}{r_1} = -2E_{\text{kin}}^{(n=1)} \tag{50}$$

coupled with the largest kinetic electron energy value. From (50) we have the relation

$$\frac{e^2}{r_1} = 2E_{\text{kin}}^{(n=1)} = mv_1^2. \tag{51}$$

Since $v_1 < c$ we obtain

$$\frac{e^2}{r_1} < mc^2 \tag{52}$$

or

$$r_1 > \frac{e^2}{mc^2}. \tag{52a}$$

By taking into account (48), we obtain from (52a):

$$\frac{\hbar^2}{me^2} > \frac{e^2}{mc^2} \tag{53}$$

according to which

$$1 > \frac{e^4}{\hbar^2 c^2} \cong \frac{1}{137^2}. \tag{54}$$

There remains still the condition satisfied by the time interval Δt of the electron transition. We have the formula

$$\Delta r_n = r_{n+1} - r_n = \frac{(n+1)^2 - n^2}{me^2}\hbar^2 = \frac{2n+1}{me^2}\hbar^2 \tag{55}$$

which gives the change of the radius of the electron orbit. For two neighbouring quantum numbers, n and $n+1$, we have

$$\frac{\Delta r_n}{\Delta t} = \Delta v_n, \tag{56}$$

where the velocity change satisfies the condition:

$$\left|\Delta v_n\right| = \left|\frac{e^2}{(n+1)\hbar} - \frac{e^2}{n\hbar}\right| = \frac{n+1-n}{(n+1)n}\frac{e^2}{\hbar} \approx \frac{1}{n^2}\frac{e^2}{\hbar} < \frac{e^2}{\hbar} < c \tag{57}$$

where the last steps hold for any large n. An alternative formula for the last step in (57) is:

$$\frac{\hbar}{e^2} > \frac{1}{c}. \tag{58}$$

We obtain

$$\Delta t = \frac{\Delta r_n}{\left|\Delta v_n\right|} = \frac{2n+1}{me^2}\hbar^2\frac{n^2\hbar}{e^2} \approx \frac{2n^3\hbar^3}{me^4}. \tag{59}$$

For very low n, say $n=1$, relation (59) for Δt becomes

$$\Delta t = \frac{3\hbar^3}{me^4} > \frac{3\hbar}{mc^2} \tag{60}$$

on condition (58) does hold.

A similar reasoning can be performed for the electron particle moving in a one-dimensional potential box. In the first step, from the requirement that the kinetic energy on the quantum level $n=1$ is smaller than the rest energy of the electron particle, we obtain the formula:

$$E_{n=1} = \frac{h^2 1^2}{8mL^2} = \frac{mv_1^2}{2} < mc^2 \tag{61}$$

which gives the requirement

$$v_1 < 2^{1/2}c. \tag{62}$$

Therefore, with the aid of the first equation given in (61), we obtain:

$$v_1 = \frac{h}{2mL} < 2^{1/2}c. \tag{63}$$

In effect it should be

$$\frac{h}{2^{3/2}mc} < L. \tag{64}$$

The limits obtained for L and v_1 can provide us with the size of the interval Δt according to the formula

$$\Delta t v_1 \cong 2L, \tag{65}$$

so a maximal size of the interval Δt for the electron oscillation in the box be-

comes:

$$\Delta t \cong \frac{2L}{v_1} = \frac{2L \cdot 2mL}{h} = \frac{4mL^2}{h}. \tag{66}$$

Another approach applies L calculated in (64) and v_1 in (63):

$$\Delta t \cong \frac{2L}{v_1} \cong \frac{h}{2^{1/2}mc} \cdot \frac{1}{2^{1/2}c} = \frac{h}{2mc^2}. \tag{67}$$

7. Summary

In the paper, the transition time between the nearest quantum energy levels is examined for the case of the Bohr hydrogen atom and the electron particle enclosed in a one-dimensional potential box. In both cases, the calculations are based on the assumption that the electron momentum in course of the electron transition is conserved.

It is found that the time intervals of the electron transitions obtained in this way are much similar to those calculated on the basis of the Joule-Lenz law for the energy emission: in the case of hydrogen, a difference between the results of both kinds is represented by a constant factor π; for the electron particle moving in a one-dimensional potential box there exists an identity of the results for Δt calculated in both ways. The limiting sizes of the mechanical parameters characterizing the quantum states in the systems considered in the paper have been also calculated.

It should be noted that the electron transition time Δt considered in the paper does not correspond, in general, to the reciprocal time of the frequency $\nu_{n+q,n}$ joining the energy difference of two quantum states E_{n+q} and E_n by the formula

$$E_{n+q} - E_n = h\nu_{n+q,n} = \frac{h}{T_{n+q,n}}. \tag{68}$$

Only for the case of

$$q = 1 \tag{69}$$

we have proved the formula

$$T_{n+1,n} = \Delta t; \tag{70}$$

see [8] [9] [10] [11].

Conflicts of Interest

The author declares no conflicts of interest regarding the publication of this paper.

References

[1] Einstein, A. (1917) *Physikalische Zeitschrift*, **18**, 121. https://doi.org/10.1007/BF01809624

[2] Planck, M. (1923) Vorlesungen über Theorie der Wärmestrahlung. Johann Ambro-

sius Barth, Leipzig.

[3] Planck, M. (1932) Theorie der Wärme. S. Hirzel, Leipzig.

[4] Van der Waerden, B.L. (1967) Sources of Quantum Mechanics. Dover, New York.

[5] Schiff, L.I. (1968) Quantum Mechanics. 3rd Edition, McGraw-Hill, New York.

[6] Slater, J.C. (1960) Quantum Theory of the Atomic Structure. McGraw-Hill, New York.

[7] Lass, H. (1950) Vector and Tensor Analysis. McGraw-Hill, New York. https://doi.org/10.1119/1.1932684

[8] Olszewski, S. (2015) *Journal of Modern Physics*, **6**, 1277-1288. https://doi.org/10.4236/jmp.2015.69133

[9] Olszewski, S. (2016) *Journal of Modern Physics*, **7**, 162-174. https://doi.org/10.4236/jmp.2016.71018

[10] Olszewski, S. (2016) *Journal of Modern Physics*, **7**, 827-851. https://doi.org/10.4236/jmp.2016.78076

[11] Olszewski, S. (2016) *Journal of Modern Physics*, **7**, 1004-1020. https://doi.org/10.4236/jmp.2016.79091

[12] Olszewski, S. (2016) *Reviews in Theoretical Science*, **4**, 336-352. https://doi.org/10.1166/rits.2016.1066

[13] Olszewski, S. (2019) *Journal of Modern Physics*, **10**, 1522-1531. https://doi.org/10.4236/jmp.2019.1013101

[14] Olszewski, S. (2020) *Journal of Quantum Information Science*, **10**, 1-9. https://doi.org/10.4236/jqis.2020.101001

[15] Bohr, N. (1922) The Theory of Spectra and the Atomic Constitution. Cambridge University Press, Cambridge.

[16] Olszewski, S. (2017) *Journal of Computational and Theoretical Nanoscience*, **14**, 3662-3664. https://doi.org/10.1166/jctn.2017.7006

[17] Sommerfeld, A. (1931) Atombau und Spektrallinien. Vol. 1, 5th Edition, Vieweg, Braunschweig.

[18] Eyring, H., Walter, J. and Kimball, G.E. (1957) Quantum Chemistry. Wiley, New York.

[19] Landau, L.D. and Lifshitz, E.M. (1948) The Field Theory. 2nd Edition, OGIZ, Moscow. (In Russian)

Journal of Modern Physics, 2021, 12, 671-699
https://www.scirp.org/journal/jmp
ISSN Online: 2153-120X
ISSN Print: 2153-1196

Cosmic Ether, Possessing Electric-Tension and Magnetic-Resistance, Is the Unified Field for Physics

Chandrasekhar Roychoudhuri

Physics Department, University of Connecticut, Storrs, USA
Email: Chandra.Roychoudhuri@uconn.edu

How to cite this paper: Roychoudhuri, C. (2021) Cosmic Ether, Possessing Electric-Tension and Magnetic-Resistance, Is the Unified Field for Physics. *Journal of Modern Physics*, **12**, 671-699.
https://doi.org/10.4236/jmp.2021.125044

Received: March 12, 2021
Accepted: April 26, 2021
Published: April 29, 2021

Abstract

The paper presents the case that physics is already and effectively unified by the energetic tension field, ether. We identify this integrating power of ether first, by re-defining the action generating parameters of this energetic tension field as the electric-tension, ε_0^{-1}, and the magnetic-resistance, μ_0, while re-deriving the Maxwell's wave equation in analogy with the mechanically stretched string, where the $c_0^2 = \varepsilon_0^{-1}/\mu_0$. Then, replacing c_0^2 by ε_0^{-1}/μ_0 and m_0 by $E/c_0^2 = E\left(\mu_0/\varepsilon_0^{-1}\right)$, one can find that almost all working physics theories are being energized by ε_0^{-1} and μ_0. To complete the unification, we can now postulate that the particles are also freely propagating EM waves, but they are spatially localized as in-phase, close-looped (IP-CL) vortex-like propagation modes of ether. Because of their IP-CL mode structure, they have space-finite spatial structures and remain spatially stationary in the absence of any spatially influencing potential gradients (forces) in their vicinity. Particles' *harmonic phase* driven interactions between quantum particles give birth to the *appearance* of wave-particle duality. There is no need for the confusing and unnecessary de Broglie's Pilot Wave. The inertia to spatial motion of IP-CL modes automatically accommodates Newton's laws of motion. The cosmic universality of Maxwellian wave velocity, and particles as IP-CL modes, jointly accommodate the two key postulates of special relativity without the need for unphysical four-dimensionality. The observable universe is represented only by its diverse oscillatory excited states. The stable and stationary Cosmic Ether keeps holding 100% of its energy all the time. We have proposed a one-way light pulse propagation experiment to directly validate the existence of ether, rather than approaching Michelson's way of measuring the ether drag. We have identified a good number of examples of working theoretical expressions in terms of ε_0^{-1} and μ_0 and presented our critical

views in physics thinking, belonging to Classical, Relativity, Quantum and Cosmology Physics.

Keywords

Cosmic Ether, Ether as the Unifying Field, Ether Energetic Tension Field, $(1/\varepsilon_0)$-Electric Tension of Ether, μ_0-Magnetic Resistance of Ether, Particles as Localized EM Oscillating Modes of Ether

1. Introduction

1.1. Preamble

Since ancient times, ether has been recognized as the physical medium for the transportation of light all across the cosmic space [1] [2] [3]. In a previous paper in this journal [4], we have presented the rationale that this ether is a physically real, energetic tension field, holding 100% of the energy of the universe. Our key message in the current paper is that we have already been using the ether tension field as the unified field for physics, but is remaining buried under our current mathematical representation habits. Ether allows for the emergence of EM waves as freely *propagating undulations* of all possible frequencies and the emergence of particles as localized EM *oscillators* with quantized energies, $E = hf_{icl}$, with built-in inertia to spatial translation. We suggest that we should re-name the old ether as Cosmic Ether, to incorporate this new property of allowing the emergence and also sustaining the elementary particles as oscillations of its tension field. Schrodinger's equation works, because the particles are oscillators with intrinsic harmonic phase variations, which is critical for the emergence of Superposition Principle (SP). The emergence of SP is not because the particles are "plane waves". Plane waves do not exist in nature as they violate the conservation of energy. Accordingly, we also do not need separate de Broglie's "Pilot Waves" to guide the localized particles. Inertial particles are always constrained to move only with the help of some physical potential gradients of the ether, which we included into the traditional Hamiltonian. The key purpose of this paper is to provide extensive examples and rationale to overcome the currently prevailing resistance to accept the reality of Cosmic Ether.

1.2. The Methodology of Physics-Thinking that Guides the Paper

We believe that the key tool is to think like a system engineer—visualize the invisible *physical interaction processes* that nature is utilizing to maintain the ongoing perpetual and causally ordered evolution in the universe. Evidence based science, or experimentally validated theory, has been stagnant for some time [5] [6] [7] [8] [9], because of our excessive reliance on elegant mathematical theories and rationalization of the observations. Let us mention the thinking of some major contributors in physics that we would try to emulate. Newton, as a *hands-on engineer* and as a creative mathematician, underscored the necessity of a physi-

cal medium intervening the Sun and all the planets to establish the gravitational potential gradient that keeps holding the planets. Newton's contemporary, Huygens, gave the description of the *physical processes* behind the perpetual diffractive propagation of light waves as due to the persistent generation of secondary spherical wavelets out of every point on all the wave fronts [10] in an energetic tension medium, the ether. Huygens' postulate was formalized into a Huygens-Fresnel diffraction integral [11], which has been guiding, later strengthened by Maxwell's equations, the sustained and continued growth of the fields of optical science and engineering. Planck triggered the concept of quantumness in our world by mathematically showing that the measured Blackbody radiation curve can be matched analytically only if the surface molecules inside the blackbody cavity surface emits and absorbs light as individual discrete quantum hv. However, Planck gave us a very valuable lesson—identify the *primary physical parameter* that plays the key operational (engineering process) role in triggering a particular phenomenon to generate a measurable physical transformation. Avoid using any secondary parameter as the key guiding parameter to develop the main formalism. The author is making this paraphrase from Planck's book [12] where Planck underscored that he succeeded in deriving his desired expression only after he switched to using the frequency v, instead of using wavelength λ, where $\lambda = c/\nu$. Twenty five years later, QM formalism proved him right. The primary action parameter for atomic and molecular energy exchange is driven by the dipolar interaction frequencies of the involved radiations, not the wavelength. The wavelength varies from medium to medium, but not the frequency. Accordingly, we will stay focused on the parameters that are primary action drivers in nature. We will find that the primary action parameters for ether are ε_0^{-1} & μ_0 and not ε_0 & μ_0.

1.3. Flow of the Paper

All perpetual wave propagation requires a parent tension field, like air-pressure-tension field for sound waves. Maxwell's wave equation and his differential calculus based derivation of the velocity of light, $c_0^2 = (1/\varepsilon_0\mu_0)$, does not identify what represents the built-in tension of the ether field and what provides the reactional resistance against the generation of the electric vector. In Section 2, we re-derive EM wave equation using Newton's first two laws, the inertia of rest and the inertia of motion, to identify that ε_0^{-1} & μ_0 physically represent the electric tension and the magnetic resistance, respectively, to generate the perpetually moving EM waves in ether.

In section 3, we use the physics of light propagation to analyze why Michelson's null experiment failed to validate either the ether-drag, or the very existence of ether. We then use this knowledge to develop and propose a one-way light pulse propagation experiment that can directly validate the existence of ether.

Section 4 details the core of this paper. It explores the unifying roles of ε_0^{-1} & μ_0 throughout major physics theories. We have proposed that the elementary particles arise as perpetually moving EM waves, but with a complex, and loca-

lized doughnut-like wave motion. The wave motion is *in-phase*, *closed-looped* (IP-CL), somewhat like a stable ring laser with perpetually recycling EM wave. We have discussed how the IP-CL model accommodates most of the quantum mechanical behaviors of particles and atoms and resolves wave-particle duality. We have also discussed that the measurable superposition effect, always registered by a finite size detector, must be a causal and local phenomenon. We cite examples to justify the emergence of gravity out of electromagnetism. Our cosmic ether model naturally accommodates the two key postulates of the special theory of relativity without the need for a four dimensional universe.

The section 5 has two subsections—first conclusion and then discussions, presenting further justification of our physics-thinking.

2. Excavating the Operational Meaning for ε_0 & μ_0 Hidden behind the Perpetual Velocity of Light

2.1. Integrating Concepts from Newton, Maxwell and Einstein to Define Cosmic Ether

Maxwell derived his wave equation by first reconstructing the integral forms of the already existing empirical laws from the integral calculus forms to the differential calculus forms of the 1) Ampere's law, 2) Faraday's law, 3) Coulomb's law, and 4) the absence of magnetic monopole. His derivation gave the velocity of light as $c_0^2 = 1/\varepsilon_0\mu_0$. These parameters ε_0 & μ_0 were already defined by his predecessors as electric permittivity and magnetic permeability of the *free space*, respectively. These descriptions do not clarify the operational origin, or the engineering lever used by nature to generate the observed *perpetual velocity of EM waves* in the "free space". Inspection of the wave equation for an ideal classical mechanical tension field, like that for a long stretched string, does imply the emergence of a perpetually propagating wave, once the string is externally perturbed, provided there are no energy dissipating mechanism associated with the string. Accordingly, we will derive the EM wave equation emulating the procedure used for a mechanically stretched string. In other words, we will unite Newtonian particle mechanics (2^{nd} law) with Maxwellian wave mechanics. We also justify the emergence of Newtonian inertia of "mass" out of the electromagnetic properties of the free space, or ether, using Einstein's mass-energy equivalence relation:

$$m_0 = E_0 / c_0^2 = E_0 \varepsilon_0 \mu_0 \tag{1}$$

The first part of this equation is very well validated in the fields of chemistry and physics. The second part is an identity relation from Maxwell's wave equation. Accordingly, we feel confident that ε_0 & μ_0, associated with a lump of energy E_0 must play critical roles in the emergence of inertia of a material particle of mass m_0.

2.2. Deriving EM Wave Equation with Mechanical Analogy to Define Operational Meaning for ε_0 & μ_0

We are now re-defining ε_0^{-1} as the "electric tension" in analogy with the me-

chanical tension "T" on a stretched string and μ_0 as "magnetic resistance" in analogy with the "inertia (or mass) per unit length" σ [13] (the choice will be apparent later). Our objective is to derive $c_0^2 = \varepsilon_0^{-1}/\mu_0$, just like for mechanical string, $v^2 = T/\sigma$, mechanical tension divided by the inertia of mass per unit length. Let us consider a one-dimensional segment of the 3D ether where a moving electric dipole has just triggered the emergence of electric fields E_1 & E_2 at the spatial locations x_1 & x_2 due to the local live electric tension ε_0^{-1}. Let us chose a small elemental spatial segment Δx of the electric tension field ε_0^{-1} in **Figure 1** triggered by a dipole with the emergent electric fields E_1 and E_2 at locations x_1 & x_2. Then the component of the unbalanced force in the vertical direction would be $\varepsilon_0^{-1}(\sin\theta_2 - \sin\theta_1)$. The angles being very small, $\sin\theta_{2,1}$'s can be replaced by $\tan\theta_{2,1}$'s, and hence by $(\partial E_{2,1}/\partial x)$. Then the vertical unbalanced force, or the rate of change of the E-field along the x-direction can be expressed as $\varepsilon_0^{-1}(\partial E_2/\partial x - \partial E_1/\partial x)$. The horizontal unbalanced force would be $\varepsilon_0^{-1}(\cos\theta_2 - \cos\theta_1) \approx 0$, for small angle approximation. Then the final resultant unbalanced force is only the vertical force $\varepsilon_0^{-1}(\partial E_2/\partial x - \partial E_1/\partial x)$. This emerging spatially varying E-field (current) generates $\mu_0 \Delta x$ quantity of temporally changing magnetic field for the element Δx. Then, by Newton's second law, the unbalanced force can be equated with the magnetic *inertial resistance* of this segment $\mu_0 \Delta x$ multiplied by the temporal acceleration $\partial^2 E/\partial t^2$ experienced by this segment of electric tension filled space:

$$\varepsilon_0^{-1}(\partial E_2/\partial x - \partial E_1/\partial x) = (\mu_0 \Delta x)(\partial^2 E/\partial t^2) \tag{2}$$

By rearranging the parameters and by taking the limit $\Delta x \to 0$, we get the Maxwell's wave equation:

$$\varepsilon_0^{-1} \lim_{\Delta x \to 0} \frac{1}{\Delta x}\left[\frac{\partial E_2}{\partial x} - \frac{\partial E_1}{\partial x}\right] = \mu_0 \frac{\partial^2 E}{\partial t^2} \quad \Rightarrow \quad \frac{\partial^2 E}{\partial t^2} = \frac{\varepsilon_0^{-1}}{\mu_0}\frac{\partial^2 E}{\partial x^2} \equiv c_0^2 \frac{\partial^2 E}{\partial x^2} \tag{3}$$

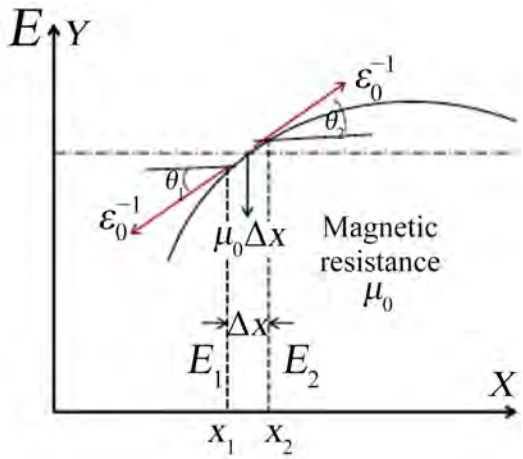

Figure. 1. Unifying classical electromagnetism with Newtonian mechanics by re-deriving Maxwell's wave equation using Newton's second law of motion. We have re-defined ε_0^{-1} as the electric tension and μ_0 as the magnetic resistance to increasing local electric current.

Thus, by re-deriving Maxwell's wave Equation (3) in analogy with a classical stretched string, we have found the operational (functional) meaning behind the emergence of perpetual velocity of an EM wave in its parent tension field, the Cosmic Ether. In general, an *energetic tension field tends to stay in its energetic quiescent state*. If a disturbance is introduced at a point by some external energy, the tension field at that point immediately pushes it away to all possible spherically accessible neighboring points so that it can come back to its original quiescent (equilibrium) state. Then all the forward points execute the same actions to come back to their respective quiescent states. As if, the tension field is forever searching out for energy sinks to eliminate it, since the system cannot assimilate the external energy which triggered the original deformation on the quiescent tension field. In the absence of any frequency resonant energy sink, the process continues perpetually. Hence, a disturbance introduced on an energetic tension field, will always generate a perpetually moving wave. This engineering process (action) taking place behind wave propagation, was first presented by Huygens in his book of 1690 while describing the propagation of EM waves in free space [10], although the mathematical wave equation was developed almost a century later by Maxwell. This natural action-picture is true for all tension fields: 1) mechanically stretched tension on a string, 2) surface tension on a water surface, 3) pressure tension in air, etc.

By integrating Newtonian mechanics into classical electromagnetism, we have now established the *physical reality* of the electromagnetic tension properties of free space as ε_0^{-1} & μ_0, with modified physical definition as "electric tension" and "magnetic resistance", which give us the operational meaning behind the generation of perpetually moving EM wave when triggered by the movement of an electric dipole within it.

3. How to Experimentally Validate the Existence of Cosmic Ether

The cultural demise of electromagnetic ether in physics was triggered by the "null" results obtained by a series of Michelson-Morley experiments (MMX), starting from 1887 [14], while attempting to measure the drag of cosmic ether by the earth. Michelson strongly believed that the all-pervading electromagnetic ether is real and exists. Since ancient times, *the belief has been that materials exist separate from ether*. Then there must be an ether drag against material bodies.

Then the 1905 paper by Einstein on Special Relativity (SR) [15] eliminated the need for ether, which was further supported by a second paper on "photoelectric effect" [16], where Einstein described EM waves as independent elementary particle-like, or "indivisible light quanta", without requiring a supporting tension field for perpetual propagation. These two papers triggered the steady evolution of a decisive physics culture that the ancient concept of ether is not correct, even though Einstein later corrected himself while defining gravity as a "curvature of space" through his theory of General Relativity. Space needs to have some phys-

ical properties, which can be "curved". However, the physics culture has been persisting that the cosmic space is a vacuum, filled with photons, elementary particles and vacuum fluctuations ([17], and references there), besides observable macro galaxies with stars, built out of elementary particles. However, this picture does not explain how the photons always experience perpetual, and the highest possible velocity without the support from their emitters. These obvious contradictions, along with the re-definition of ε_0^{-1} & μ_0 in the last section as the operational cause behind the perpetual motion of EM waves packets, there is an urgent need to carry out new experiments for the direct validation of the existence of cosmic ether as an energetic physical tension field.

3.1. Why MMX Experiments Cannot Discern Either the Ether-Drag or the Absence of Ether?

To appreciate the limitations of MMX type of experiments, we need to pay close attention to the physical processes behind light propagation through material media and through material free ether. Huygens, contemporary of Newton, was the first one to frame the key postulate behind the propensity of waves to propagate perpetually leveraging an energetic parent tension field. Because the tension field keeps perpetually pushing away the waves, generated through some suitable perturbation of its quiescent energetic state. In his 1690 book [10] Huygens' postulated that this perpetual propagation of a wave is generated via secondary wavelets *emanating out of every point on every wave fron*t. We usually measure the superposition effect of all these arrived secondary wavelets by some frequency resonant detector. Huygens explicitly mentioned that his model of wave propagation *process* require a tension medium (ether) to propagate as its undulation (excitation). Section-2 of this paper has strengthened this viewpoint. Huygens also underscored that the secondary spherical wavelets do not interfere or modify each other's wave properties in the absence of any interacting medium. We have articulated this as Non-Interaction of Waves (NIW) [18] [19]. In 1817, Fresnel gave a simple and elegant mathematical integral representation of Huygens Principle, now known as the Huygens-Fresnel diffraction integral [11], which automatically embeds the NIW property. This is actually one of the two key mathematical foundations behind the continuous and sustained advancement of optical science and engineering, till today. There is a second foundational contribution that describes the physics behind the EM wave generation and propagation. It was given by Maxwell in 1864 [20]. It turns out that the Huygens-Fresnel diffraction integral, a linear summation of spherical waves, is a solution of Maxwell's wave equation, as it is a second order linear differential equation. Maxwell's complete set of equations has also established a Poynting vector, $\boldsymbol{S} = \boldsymbol{E} \times \boldsymbol{B}$. The vector $\boldsymbol{S}$ on a wave front always remains orthogonal to the wave front, even when the wave front suffers tilted propagation due to tilted *refraction* in a new medium with different refractive indices (supporting different velocities).

Light also has another very interesting property. It always prefers to propagate

through a structurally single mode medium of lower tension value (lower velocity with higher refractive index), whenever it has that option. This is why we have been able to invent and implement the fiber optic communication systems and sending the optical signals through glass-fiber-core of higher refractive index, surrounded by a protective glass cladding of lower index. Light remains *entrained* within the core of the glass-fiber for tens of thousands of kilometers with very little loss. Ether has the refractive index of $n_0 = 1$ and air has the refractive index $n_{air} = 1.0003$, or $c_{air} = c_0/1.0003$. Therefore, in the laboratory, the light beams will always be entrained by the stationary air surrounding any MMX interferometer, since air provides a relatively lower tension (higher index) medium for light to propagate. Light propagation will not be entrained by the lower index ether, even though it is permeating through all material media and the entire universe. Hence, the propagation direction of the light beam vector $\boldsymbol{S} = \boldsymbol{E} \times \boldsymbol{B}$ in the MMX interferometer will always remain orthogonal to the pre-aligned mirrors, immersed in the laboratory air. The propagation path cannot be tilted, as was originally sketched by Michelson, shown in **Figure 2(a)** [3].

Figure 2(b) and **Figure 2(c)** show slightly different versions of the same Michelson's interferometer to bring out the common-sense understanding that light beams will travel straight up and down, without getting tilted. **Figure 2(b)** is a monolithic rendition of the Michelson interferometer within a glass cube, with built-in mirrors and a beam splitter. Even if the cube experiences some velocity $\boldsymbol{V}$ in the horizontal direction due to earth's orbital velocity, or in space on a satellite, there will be no fringe shift because the two light paths will remain identical, always entrained by the glass cube. The $\boldsymbol{V}$ vector of the cube-prism cannot tilt the $\boldsymbol{S}$ vector of light away from its vertical path since the $\boldsymbol{S}$ vector is *entrained* by the assembly of the material dipoles of the glass prism of index $n_{gls.} = 1.5$. Within a material medium, $\boldsymbol{S}$ can *no longer be under the control of the stationary or even the dragged ether*. However, there will be a negligibly small Fresnel Drag ([18]-see Ch.11, [21]) of the light beam. Because of its effective miniscule value, we will neglect the Fresnel drag in air here. The intention behind **Figure 2(c)** is to underscore the same point, as we have done for **Figure 2(b)**, except that the interferometer is now residing within the stationary air of the laboratory environment. **Figure 2(c)** is actually equivalent to **Figure 2(a)** with the correction that the light beam propagation vectors remain orthogonal to the two mirrors, without suffering the tilt assumed by Michelson, with longer travel path.

Thus MMX type of experiments should always give null-fringe result. We do not need to assign a new property on to nature that needs to trigger "length contraction" or "time dilation". If we assume that Michelson had believed ether entrained the light ray, and not the "thin" air in the laboratory, then the ether drag would have created an *apparent* tilted path for the arrival of the vertical ray and tilted return again, just as Michelson's drawing in **Figure 2(a)**. However, then the real physical tilt of the light beam would have caused a change in the spatial frequency of the observed fringes, *which was also never reported*.

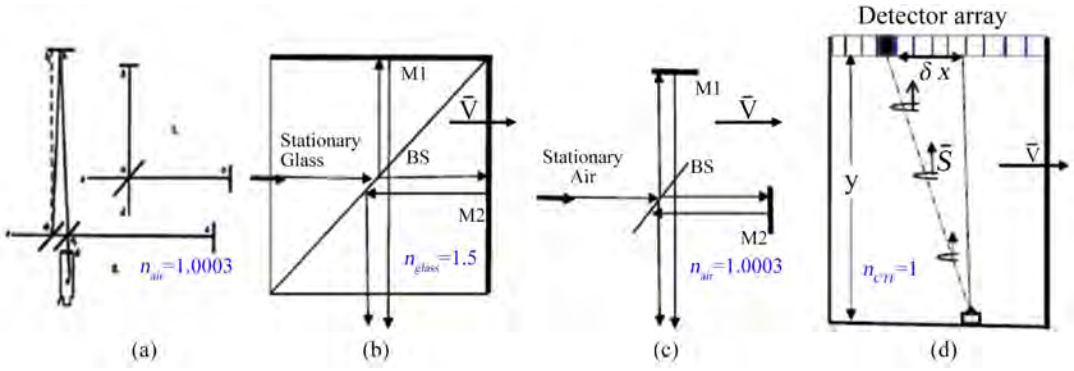

Figure 2. Michelson Interferometer in three versions. (a) Diagram from Michelson's original paper [3]. Notice the triangular longer up-down return path of the light beam compared to the horizontal straight re-tracing path. (b) Michelson interferometer built as a solid monolithic structure out of glass prisms, mirrors and a beam splitter. Zero fringe shift is obvious from equal return paths. (c) Michelson interferometer re-drawn with equal return paths because stationary air of refractive index 1.0003 entrains the light propagation, not the aether. (d) Shift of light pulse in a one-way CTF-entrained propagation, when the apparatus moves transversely in vacuum.

3.2. Can We Validate the Existence of Stationary Ether?

In Section 2 we have established the deep significance for physics that we experimentally validate the cosmic space as a stationary energetic tension field. Experimental validation of Casimir Effect [22] does indicate that the space, in the nanometer domain, is not "empty". However, since the Casimir Effects have been measured only in the nanometer domains, these experiments cannot assure us of the existence of a stationary ether-like energetic tension field as the very foundation of our emergent universe. Therefore, Michelson's brilliant idea, of using the physics of light propagation over a macro distance, has to be properly re-formulated. In this section, we take lessons from the limitations of the MMX experiments and propose a simpler new experiment to determine the existence of ether. Our design should be able to compare and differentiate the measured outcomes of light propagation through some material medium and "completely" material-free ether space.

As mentioned earlier, the generic tendency of light is to choose to travel through the relatively lower tension (higher index and lower velocity) media. Further, the Poynting vector, orthogonal to the collimated optical beam, preserves its spatial direction, while obeying the basic laws of reflection and refraction. This has been pictorially shown in **Figure 2(b)**, where the moving glass-cube-MMX preserves the orthogonal reflection of the return beams, instead of getting reflected at an angle.

We are proposing to test the presence of ether only by comparing the absence or presence of a shift in the arrival location of a *collimated light pulse through one-way travel path*, where the travel path is either filled with air as a medium ($n_{air} = 1.0003$), or is completely empty ($n_{ether} = 1$), inside a super-vacuum chamber, or on a deep space satellite. Let us now assume that the wavelength of light is λ. Then one can argue that if the average number of air molecules within

a volume of λ^3 is statistically less than one, then the E-vector of the light beam would not experience a reduction in the effective tension value of that space. Light will now be guided as an undulation of the pure ether only, with minor amount of scattering of light from encounter with individual molecules.

We can now construct a very simple ether-sensor consisting of a rigid box (see Figure 2(d)). The bottom of the box holds an LED that can send out individual pico second light pulses, on demand, vertically up to the top end. The top of the box, anchored rigidly with the LED base-structure, holds a detector array. It is designed to measure the lateral shift in the arrival position of the light pulse. If the box is full of air, the light pulse would always arrive exactly at the vertical location from the LED, even if we give the box a velocity orthogonal to the optical pulse propagation axis. However, when the box is completely free of air, either inside a super-vacuum chamber, or on a deep space satellite, a velocity of the box to the right and orthogonal to the light-pulse axis, would make the light pulse to arrive left-shifted on the detector array. This is because the Poynting vector orthogonal to the center of the original wave front of the light pulse will always follow its original straight line trajectory inside any homogeneous medium. It is now moving through stationary ether, while the box is moving away to the right.

If the length of the bar is L = 1 m long, then the arrival delay for the light pulse would be 3.33 ns. Note that even though the dashed line of the apparent light path appears to be tilted and longer, the light pulse actually travels the same vertical distance L, while the box moves to the right. Physics of this propagation process is depicted by the vertical Poynting vectors, drawn on the cartoon-pulses, always pointing *vertically up* (Figure 2(d)), while the box moves to the right.

3.2.1. Ether Sensor inside a Super-Vacuum Chamber

Let us assume that we are carrying out the experiment inside a super vacuum chamber leveraging earth's orbital velocity of $\mathrm{v} = 30$ km/sec by aligning the earth's velocity vector orthogonal to the light-path-vector in the ether sensor. This would generate a lateral shift of:

$$\delta x = \mathrm{v}\delta t = \mathrm{v}L/c_{air} \simeq 100\mu \tag{4}$$

Such a lateral displacement can be easily measured by an off-the-shelf linear detector array, or a position sensing quadrant detector. Several countries who are advanced in space technologies can carry out this experiment. They have large vacuum chambers with low pressure capability around 10^{-10} Torr, implying less than about 0.1 air molecule per micron cube at typical room temperature. The visible wavelength being around 0.5 micron, a vacuum of 10^{-10} Torr satisfies the effective free-space condition.

This terrestrial experiment in high vacuum chamber should also be able to establish that air in Michelson's experiment was keeping the light beam entrapped to straight path, instead of the tilted angular path assumed by Michelson, which consistently gave him the null fringe-shift results. One just need to slowly intro-

duce air in the high vacuum chamber and observe that the light beam deflection reduces to zero at a certain pressure when there are a good number of air molecules per λ^3. The determination of this number of air molecules would be a valuable parameter in studying the fundamental physics behind the emergence of refractive index and the need for a certain number of air molecules per λ^3 to generate an "effective continuous medium" for EM waves. *It will also validate that the EM interaction cross section of Angstrom size atoms could be one or two orders of magnate larger than the* λ^2, *especially when the optical frequency is in resonance with quantum level transition of the chosen gas* [23] [24].

If the experiment, when carried out very carefully with the desired free-space equivalent vacuum condition, shows no lateral shift of the light spot, one possible conclusion would be that the ether is being fully dragged around its surface by the massive earth. We doubt this outcome because in our model, ether is universally stationary. EM waves and particles are the excited states of its *various emergent potential gradients*, *not the physical field itself*. EM wave propagation does not make the ether move. Further, the movements of material particles (or bodies) should create only changes in appropriate potential gradients around them.

3.2.2. Ether Sensor on a Deep Space Satellite

Let us assume that the orthogonal velocity of a possible deep space satellite is $\mathrm{v} = 8\ \mathrm{km/sec}$. Then the lateral displacement of the light spot would be:

$$\delta x = \mathrm{v}\delta t = \mathrm{v}L/c_0 = 26.7\mu \tag{5}$$

This is also accurately measurable using an off-the-shelf position sensing quadrant detector. Here also we are assuming that a satellite cannot drag stationary ether.

In both the above experimental environment, one could employ a second identical ether sensor with *the light vector path always aligned parallel to the box-velocity vector*. Then, this second sensor should always show zero lateral shift in the arrival of the light spot. This will provide us with the extra confidence on the results of the experiments.

4. Exploring Direct Unifying Roles of ε_0^{-1} & μ_0 throughout Major Physics Theories

In the introduction, we have presented the argument that $c_0 = \left(1/\varepsilon_0\mu_0\right)^{-1/2} = \left(\varepsilon_0^{-1}/\mu_0\right)^{-1/2}$ is a *secondary* derived parameter. In section 2, we have re-derived Maxwell's wave equation while re-defining the primary *actionable parameters* of the cosmic ether as ε_0^{-1} & μ_0, electric tension and magnetic resistance, respectively. In this section, we show that these two actionable primary parameters are involved in all major theories of physics to validate our key assertion that the cosmic ether has already been functioning as the unifying field of physics.

4.1. Material Media Are Also Energetic Tension Fields, a Modified Versions of the Ether, ε^{-1} & μ

In section 2, after the derivation of Maxwell's wave equation, emulating the energetic mechanical tension field of a stretched string, we have explained how a tension field tries to consistently push away the external perturbation and ends up generating a perpetually moving wave. Material media also perpetually push away EM waves when they are generated inside the media, or wave pulses are sent inside them. In fact, the core properties of the EM wave propagation, including diffraction, are *mathematically very similar* in structure to those for the free space, except the values of the core parameters are modified by the aggregate properties of the material dipoles. The structure of the Poynting vector remains same. The velocity of EM waves becomes:

$$c_{med.}^2 = \varepsilon_{med.}^{-1} \big/ \mu_{med.} \equiv c_0^2 \big/ n_{med.}^2 \tag{6}$$

For most material media, usually, $\mu_{med.} \approx 1$, giving rise to the well-known relation for the refractive index, $n_{med} \approx \varepsilon_{med}^{1/2}$, determined by the collective dipolar properties of the atoms and molecules within the media. One can then surmise that, functionally, the material media also behave as modified electromagnetic tension fields. *We are then guided to postulate that the electrons, protons and neutrons, which build the atoms, and then the material media, should also represent some forms of emergent properties of the same cosmic ether.*

Let us note from Equation (6) that the velocity of light waves are slower inside the material tension fields. Hence the material tension fields are weaker than the material-free Cosmic Ether. This is why material media offer an alternate wave energy sink for the ether. This is why, given the physical proximity, EM waves will always be *pushed* inside the lower tension (higher index) material media. In fact, the atoms and molecules, having quantum mechanical frequency-resonant energy levels, will always "*pull*" in the wave energy, while the EM tension fields will always tend to "*push*" in the wave energy, which is a perturbation to its quiescent state. This is a key point that we have utilized to explain as to why, in Michelson's ether-drag cartoon, **Figure 2(a)**, the vertical light rays could not have been "dragged" by the ether! Light is always entrained by a lower tension air, even though the air molecules are emergent entities of the ether.

4.2. Emergence of Particles, Quantumness, Charge and Superposition Effect without Non-Locality

4.2.1. Particles Are Localized in-Phase Close-Looped (IP-CL) EM Oscillators

Quantum theories are functional field theories [17] [25]. Ether is an energetic tension field. It also accommodates perpetually moving EM waves. We just need the right set of postulates to model the emergence of localized EM oscillators out of the same ether, which will follow Schrodinger's "wave" equation and other quantum field theories.

It is important to appreciate again the emergence of *perpetual velocity of EM*

wave (or any wave) once it has been triggered on its supportive energetic tension field, which is ether for us. This will help us integrate classical mechanics with the quantum mechanics at the very foundation of the emergence of waves and material particles.

The concept is already built into the physical-process driven derivation of the EM wave equation, Equation (3). It *models the real physical processes in nature*, which engenders the perpetual motion (propagation) of a wave once triggered due to some energetic perturbation on the vast electromagnetic complex tension field, ether. Equation (3) is a *linear* first order differential equation allowing for the Superposition Principle (SP). Second, it equates a temporal second derivative ("temporal acceleration") with a spatial second derivative ("spatial acceleration"). This equality, or the built-in balancing condition set by our math implies that we have correctly modeled nature—one of the fundamental tendency of an energetic tension field is to restore its original quiescent energetic state by getting rid of the perturbation energy. If it does not have built-in energy dissipation mechanism, then it will keep pushing away the perturbation perpetually because every pint of a tension field wants to stay in its energetic quiescent state (recall Huygens postulate [10]). This is the cause behind our observations that waves have tendency to move away perpetually. Now, let us look at the Schrodinger's equation, Equation (7) and compare with Equation (3). Unlike EM waves, without the presence of a separate physical

$$i\hbar\frac{\partial\psi(x,t)}{\partial t}=-\frac{\hbar^2}{2m}\frac{\partial^2\psi(x,t)}{\partial x^2}+V(x,t)\psi(x,t) \tag{7}$$

potential gradient $V(x,t)$, Schrodinger's particle does not move spatially. However, like the EM wave equation, it is also a second order linear differential equation and hence accommodates complex amplitude-driven Superposition Principle (SP). Equation (7) does have a "spatial acceleration" term, $\partial^2\psi(x,t)/\partial x^2$; but does not have a balancing "temporal acceleration" term like that for the EM wave, Equation (3). The temporal derivative term, $\partial\psi(x,t)/\partial t$, is first order. Obviously, Schrodinger's particles are not spontaneously moving waves, like the EM waves are. Schrodinger's particles cannot be real physical waves, or guided by "Pilot Waves", even though it works through SP, $\Psi=\sum_n\psi_n$, and the observables are $\Psi^*\Psi$. We have thus created a natural platform for conceptual confusions without properly defining the origin of the Newtonian inertia of elementary particles, while allowing for the initial interaction processes between particles through superposition of their complex amplitudes. This is clearly the foundational limitation of eminently successful QM formalism. It is an incomplete theory, as perceived by Einstein.

We can now justify our postulate of the emergence of elementary particles as localized, self-looped in-phase (IP-CL), EM wave oscillations of the ether. The self-looped EM wave oscillation is perceived by the ether as if it is perpetually pushing it away forever, satisfying the core restoration property of any energetic tension field. Now, this IP-CL wave loop has developed a natural tendency of

inertia of motion, until it is subjected to some physical potential slope (gradient) in its vicinity; even stopping it would require a separate opposing potential gradient. We thus see the natural propensity of particles to obey Newton's two laws of motion. "Locality" of spatially localized particles is inherently undeniable. Further, Newton's third law of real physical action-interaction through energy exchange, guided by some compatible force between the particles, must also be accepted as physical reality, that strengthens the *locality* defined by the physical range of the force. There is really no wave-particle duality, even though the particles are structurally localized IP-CL wave loops. However, particles do have oscillatory complex amplitudes which guide the energy exchange process through the QM superposition principle. Interactions are guided by forces, which we consider as various types of physical potential gradients around them, generated due to the internal complex EM wave motions. Newton's action-reaction is built into these mutually influencing "potential gradients", as they equally try to influence each other.

The quantization of particle energies also emerges naturally from the famous relation, $E = hf_{icl}$, the subscript "icl" is added to underscore the "internal closed-loop" electromagnetic oscillation. The stability, or the life time, of various particles are now determined by the degree of phase matching in the in-phase closed-loop wave propagation. Protons and electrons must have the most precisely phase-matched internal IP-CL oscillations since we do not see them decay.

The phase matching requirements for the closed-looped oscillation also dictates that the energies of the stable particles cannot assume just any values. In fact, Greulich [26] has found an interesting *strongly linear* relation to express the energy of a large number of particles with measurable life times as the multiplication of an integer N with the ratio of the electron energy divided by the fine structure constant α, as in the first part of Equation (8). In the second part of the same

$$E^{prt.} = N\left(E^{el.}/\alpha\right); \quad \Rightarrow \quad f_{icl}^{prt.} = \left(1/\alpha\right) N f_{icl}^{el.} \tag{8}$$

Equation (8), we have re-written it in terms of IP-CL wave frequencies. One can notice some similarity with the closed-cavity longitudinal laser frequency modes with a relation of integral multiples. For particles heavier than electrons, IP-CL frequencies keep increasing linearly as some integral multiple, reduced by the inverse α-factor. This provides some extra corroboration that particles are perpetually propagating *localized* IP-CL EM modes of the ether, somewhat like a circular laser. However, the wave motions have to be very much more complex to be able to generate quantized charge and spin properties.

4.2.2. "Plane Wave" and "Pilot Wave" Are Unnecessary and Add Only Confusions

We should now clarify here that Schrodinger's complex amplitude representation, $\psi \sim a\exp\left[-i2\pi f_{icl}t\right]$, for a free particle should have never been interpreted as a "plane wave". The conservation law tells us that a "plane wave", existing for

all time and spread over all space, cannot exist in this real world. We use the very similar mathematical expression $\exp\left[\pm i2\pi ft\right]$ routinely to analyze the properties of classical pendulum, or of classical AC current oscillators. Further, the oscillatory complex amplitude property, displayed by particles, do not require any separate guidance from de Broglie's "Pilot Waves" because they themselves are IP-Cl harmonic oscillators, containing the necessary complex amplitudes. Originally, the idea was introduced to accommodate the wave-like superposition effects shown by particles. Besides, de Broglie's postulate has a problem of built-in mathematical non-causality (Equation (9)), since the postulated wavelength of the Pilot Wave diverges to infinity as the particle velocity tends to zero:

$$\lambda_k \equiv \frac{h}{p} \Rightarrow \underset{Lt.\mathrm{v}\to 0}{\lambda_k} = \underset{\mathrm{v}\to 0}{Lt.}\frac{h}{m_0\mathrm{v}} \to \infty \tag{9}$$

We have mentioned Planck's advice in the introduction that it is important to identify the primary *action parameter* of natural entities to model their interaction processes. To model particle-particle superposition effects on "external" ("third party") detecting molecules through Superposition Principle, we need to postulate that the particles acquire a different kinetic frequency f_k (different from internal IP-CL frequency f_{icl}). In particle-particle interactions, including kinetic collisions, f_{icl}, or hf_{icl} play key roles while bringing about structural transformations. We now postulate a causal de Broglie kinetic frequency f_k, defined as $(1/2)m\mathrm{v}^2 = hf_k$ which provides us with the necessary harmonic frequency and phase, $a\exp\left[-i2\pi f_k t\right]$, to model particle superposition phenomenon. The causality for the de Broglie frequency is preserved (Equation (10)):

$$f_k \equiv \frac{m}{2h}\mathrm{v}^2 \Rightarrow \underset{Lt.\mathrm{v}\to 0}{f_k} = \underset{\mathrm{v}\to 0}{Lt}\frac{m}{2h}\mathrm{v}^2 \to 0 \tag{10}$$

Recall that frequencies of oscillators are the primary characteristic parameters and are determined by the intrinsic tension property that promotes the physical oscillation.

4.2.3. Role of ε_0^{-1} & μ_0 in the Fine Structure Constant α & Emergence of Charge

We should first recognize that charge is an emergent property out of electromagnetism. While we have found that mathematically the sum of positive and negative charges are always conserved in particle-particle interactions, physically, the charges can completely vanish, as in electron-positron collision: $e^- + e^+ \rightleftharpoons \gamma + \gamma$. It is clear that we can create charge by manipulating electromagnetic gamma waves. Since γ waves are created out of ether, then the charge-property displayed by e^- and e^+ has to emerge out of some form of IP-CL structure of the electromagnetic wave of the ether that allows the formation of electrons and positrons, and hence all other elementary particles also.

Very precisely measured fine structure constant $\alpha = (1/137)$ [27] for elementary particles can be written as:

$$\alpha = \frac{e^2}{2h}\frac{1}{\varepsilon_0 c_0} = \frac{e^2}{2h}\left(\varepsilon_0^{-1}\mu_0\right)^{1/2} \Rightarrow e^2 = 2\alpha h \frac{1}{\left(\varepsilon_0^{-1}\mu_0\right)^{1/2}} \tag{11}$$

In the first part of the above Equation (11), we have re-expressed α in terms of the primary parameters ε_0^{-1} & μ_0 by replacing the secondary derived parameter c_0. Then we have re-expressed the charge in terms of ε_0^{-1} & μ_0, multiplied by the α-constant and Planck's quantization constant *h*, two precisely measured constants of nature. So, we have re-expressed the emergence of charge in terms of ε_0^{-1} & μ_0 (second part in Equation (11)). The square of the quantized charge is inversely proportional to the square root of the product of the electric tension and the magnetic resistance, built into ether as its key functional properties.

Notice that expressing the secondary parameter c_0 in terms of the constituent primary parameters brings back the role of the electric tension and the magnetic resistance in the formation of the elementary particles as IP-CL waves. However, it tells us more. One now needs to visualize the physical processes behind the emergence of quantized charge. Somewhat similar approach is being contemplated by many scientists [28] [29]. We now present some possible approach to develop the IP-CL particle model and the emergence of quantized charge.

Maxwell's wave equation indicates that the wave propagates as a continuously oscillating ±*E*-vector as if it is a localized *emergent oscillating charge*, equivalent to an oscillating current, while triggering the emergence of a resisting orthogonal and oscillating magnetic field. Then, it is not difficult to appreciate that localized Maxwellian IP-CL wave inherently contains oscillating charge and magnetic properties, which the elementary particles do display. Now the challenge is to visualize and mathematically model some localized IP-Cl wave structures that can display static (stationary with the particle) charge-curvatures of opposite slopes around electron and positron models (and eventually to proton models). The "spin" would be a natural consequence of the self-looped waves inside the IP-CL oscillation with its own Poynting vector. *It is now conceptually clear to appreciate the emergence of quantumness in the particle world out of the* 3*D classical ether*. The wave particle-duality is real and it is built-in structurally and permanently, not due to some dependence on the type of experimental set up. We do not need the large number of strange, and non-causal, quantum philosophical interpretations to "understand" quantum mechanics.

4.2.4. Frequencies of IP-CL Particle

The rest energies of the electron and the proton are 0.510 MeV, and 938.272 MeV, respectively. Then, using $E = hf_{icl}$, and $h = 4.135\times10^{-15}\,\text{eV}\cdot\text{s}$, we get the *E*-vector frequencies of the close-looped EM waves for the electron and proton as $f_{icl}^{el} = 1.233\times10^{20}\,\text{s}^{-1}$ and $f_{icl}^{pr} = 2.269\times10^{23}\,\text{s}^{-1}$, respectively. These oscillations for electrons and protons are in the very high energy gamma-wave region, which do not spread out diffractively, unlike much lower frequency EM waves

that diffract. This non-diffractive propensity of extremely high frequency EM waves allow for the formation of stable and localized IP-CL waves. It is well validated that the diffractive spread is inversely proportional to the frequency of the EM waves. It is built into Huygens-Fresnel diffraction integral [11]. However, when the particles collide against a heavy nucleus, or each other, they would break up into a pair of gamma radiations, or other stable and unstable IP-CL particles.

4.2.5. Role of ε_0^{-1} & μ_0 in Determining the Quantized Energy Levels of Hydrogen Atom

Let us note that the quantized energy levels E_n of Hydrogen atoms are also guided by ε_0^{-1} & μ_0 because the inertia (mass) of electrons is due to its IP-CL wave structure (Equation (12)):

$$E_n = \frac{m_e e^4}{8\varepsilon_0^2 h^2}\frac{1}{n^2} = \frac{\left({}_{el}E_0\varepsilon_0\mu_0\right)e^4}{8h^2\varepsilon_0^2}\frac{1}{n^2} = \left(\varepsilon_0^{-1}\mu_0\right){}_{el}\frac{E_0 e^4}{8h^2}\frac{1}{n^2} \tag{12}$$

We should also underscore that the dependence of discrete energy levels on inverse n^2 implies phase dependent propagation behavior of electrons in the atomic orbits, which is mathematically well captured by Schrodinger's wave equation.

4.2.6. Locality of Superposition Effects

We have underscored in section 4.2.1 is that wave-particle duality is a reality of nature because particles are localized IP-CL EM waves. Schrodinger's QM equation represents a logically self-consistent causal relation. There cannot be sudden emergence of non-causal and non-local phenomena only when we carefully set up experiments to measure Superposition Effects (SE). Let us first underscore that the *linear Superposition Principle* (*SP*), $\Psi = \psi_1 + \psi_2$, *is not an observable phenomenon*; Here the operator "+" implies only coexistence, not any interaction. In contrast, SE is an observable phenomenon. We need an appropriate quantum detector that can execute the quantum mechanical square modulus operation on both the superposed signals, $|\Psi|^2 = |\chi\psi_1 + \chi\psi_2|^2$, where χ is the linear dipolar polarizability of the detecting molecules that guides the *interaction process* between the detector and the stimulating signal. SE can becomes observable only after non-linear quadratic operation process *has been executed by a detector through absorption of energy from all the stimulating fields*, ψ_1 *and* ψ_2, *present simultaneously*. We must not defy these mathematical logics that have been working just by repeating the culturally accepted belief that "indivisible single photon interfere". Further, the detecting molecules must be resonant to the incident signal frequency. Just by sending any signals ("photons") do not automatically create observable distribution of the sent signals. Further, the signals sent out, follow their own laws of propagation. EM waves diffractively spread out and particles follow linear trajectory in force-free region. IP-CL particles do not diffract like the Maxwellian waves do. Therefore, the expression for SP below (Equation (13)) is just a causal mathematical expression that we are

sending two streams of signal through two slits on to a distant detector array that can interact with the particles on arrival. The "+" operator in the equation does not represent any particle-particle interaction.

$$p(\tau) = a_1 e^{i2\pi f_k (t+\tau)} + a_2 e^{i2\pi f_k t} \tag{13}$$

It is simply a mathematically correct statement that we are *intending* to send two streams of particles, starting out of, say, through two slits on to a "far-field" detector array. Their arrival from the two spatially separate slits on to any specific off-axis point on the detector array will require traveling by different paths, while taking different travel times, assuming they have been pre-selected for the same velocity $(1/2)mv^2 = hf_k$. See section 4.2.1 for the definition of de Broglie frequency f_k that replaces de Broglie Pilot wavelength λ_k. The detectable (observable) energy distribution would be given by Equation (14):

$$\Psi(\tau) = \left| \chi a_1 e^{i2\pi f_k (t+\tau)} + \chi a_2 e^{i2\pi f_k t} \right|^2 = \chi^2 \left[a_1^2 + a_2^2 + 2a_1 a_2 \cos 2\pi f_k \tau \right] \tag{14}$$

Now the operation "+" within the square modulus sign is executed by the detecting elements via the interaction parameter χ. It is almost impossible for us to send exactly identical number of particles through both the slits with identical release times to make $a_1^2 = a_2^2 = a^2$ and generate pure cosine fringes with unit visibility, which is routinely assumed in making arguments in support of the magical "single particle" SE. The causally correct mathematical logics embedded in Equation (13) representing the detected "fringe intensity" (or particles number) variations defies the interpretation that a single particle can generate SE. The mathematical logic behind the presence of the product $a_1 a_2$ in the interference cross-term implies that the detector accepts energy from both the particle beams (the literal meaning of "superposition"). We rely on the hard causality, built into our mathematics, to advance exploration of physics. Locality of superposition effect is dictated by the interaction process executed by the detectors [30] [31] [32]. Dark fringe locations are due to the resultant *null stimulations* induced on those detecting elements generated by multiple particles due to their mutual phase dependent stimulations. *Dark fringes are not due to non-arrival of particles in those locations*. That is what the literal meaning of the two terms within the sign of square modulus. We should not randomly defy the mathematical logic whenever we are at a loss to explain the *invisible intention processes* that generate the registered data though interactions with detectors. Wave-particle duality (WPD) is real because particles are truly IP-CL wavelets carrying different phases. However, WPD should not be used to justify the non-causal belief that single particle interfere. Stable elementary particles cannot make themselves appear or disappear based simply upon human constructed passive double-slit structure.

4.3. Gravity and Electromagnetism Are Emergent Properties out of ε_0^{-1} & μ_0

We know that all "material" particles and their assembly display gravitational

attractive forces, as has been modeled by Newton as a simple inverse square law and by Einsteinian through more complex formalism as "curvature of space" (General Relativity). We also know that inertial property of a particle with Newtonian inertia (mass) can be expressed in terms of the particle's IP-CL energy and ether properties (Equation (15)):

$$m_0 = E_0/c_0^2 = \left(hf_{cl}\right)\left(\mu_0/\varepsilon_0^{-1}\right) \tag{15}$$

By definition, Newtonian mass display "gravitational curvature" around it as in Equation (16). Below, we have presented the macro mass as a summation of innumerable IP-CL oscillators of quantum frequencies $f_{in}^{(1,n)}$. The issue to notice is that the mutual gravitational force between two massive bodies is *inversely proportional to both the square of the distance and the square of the electric tension of the ether* (Equation (16)).

$$F = G\frac{m_1 m_2}{r^2} = \frac{Gh^2}{r^2}\left(\sum_n f_{cl}^{(1,n)} \cdot \sum_n f_{cl}^{(2,n)}\right)\left(\mu_0/\varepsilon_0^{-1}\right)^2 \tag{16}$$

If the IP-CL wavelet concept for particles is correct, then the correct mathematical closed-looped light propagation model should be able to generate the gravitational force, or create the "curvature of space" (potential gradient) on the ether field. The strength of the "Curvatures of space" increases with the "closed-looped" frequencies (energies) of the particles and is directly sum-able to generate larger and larger gravitational attraction without the need for any phase terms, unlike for interactions between quantum particles or EM waves and particles. We do not need a separate theory of Quantum Gravity that can generate graviton for interaction through "exchange process".

Here, we would like to introduce, without further discussions in the current paper, the postulate that all forces in nature are due to diverse kinds of curvatures in ether generated by the IP-CL EM wavelets, without requiring the concept of exchange particles. We should note that interactions between diverse IP-CL wavelets will naturally go through transient intermediate "photon-like" states as they transition from one stable IP-CL wavelet to assume another stable IP-CL structure, like for example, $e^- + e^+ \rightleftharpoons \gamma + \gamma$. Thus, Feynman's integral technique that utilizes intermediate photons or Bosons, represent more than just a mathematical trick that just works! The method closely represents actual *interaction processes* going on in nature. *That is why Feynman-diagrams are so successful* [33].

There are many publications where the authors have claimed that gravity has electromagnetic origin [34] [35]. We will briefly mention the work of Mallett [36] who has shown that Einstein's formalism does allow for the emergence of "weak gravitational field" due to a *linear* circular laser beam. Mallet has shown that a stationary neutral massive spinning particle at the center of the ring laser will pick up a precession given by Equation (17) (see ref. 36 for detailed definitions); a is the length of one of the arms of a square ring laser, ρ is the linear energy density of the laser beam.

$$\dot{\Omega} = \frac{8\sqrt{2}G\rho}{ac_0^3} = \frac{8\sqrt{2}G\rho}{a\left(\varepsilon_0^{-1}/\mu_0\right)^{3/2}} \tag{17}$$

The induced weak gravitational precession for a macro ring laser is very small, being inversely proportional to $ac_0^3 = a\left(\varepsilon_0^{-1}/\mu_0\right)^{3/2}$. Nonetheless, if a macro linear ring laser can induce inertial frame dragging on a massive particle; it is then inspiring to attempt to model a femto meter size complex IP-CL 3D wavelet model that could generate the actually measured gravitational field strength.

4.4. Cosmology: Energy Conservation, Dark Energy, Dark Matter, Expanding Universe, etc

4.4.1. Hundred Percent of the Energy of the Universe Is Held by the Ether

We have defined cosmic ether very much as a "classical" continuous 3D tension field with core properties being electric tension and magnetic resistance. Everything observable or manifest, consists of *perpetually propagating* EM waves—freely propagating EM waves and localized IP-CL EM waves. This perpetual propagation (velocity) is a classical property of all waves generated on a classical tension medium. It originates because the parent tension field 1) wants to preserve its energetic quiescent state by pushing away perturbations, and because 2) it cannot directly assimilate the energies of the waves-generated perturbation. Then the sum total energy in any interaction between different IP-CL wavelets and between IP-CL and EM waves should always be conserved because the new products are also bound to be some form of waves of the ether. This is the well observed law of conservation of energy in all interactions, an inherent property of the energetic tension field. Therefore, the cosmic ether must be holding 100% of the energy of the observable universe, which includes the energy of all the EM oscillations [4] [18].

Current cosmological theories imply that of the total energy density of the universe, Baryonic matter represent only ~5% , dark matter and dark energy supposed to consist of ~25% and ~70 %, respectively [37]. The energy density of propagating EM wave (photons) energy is negligible, only about ~0.005%. In our model, all the Baryonic (5%) matter consists of IP-CL inertial wavelets. Then ~95% of the energy remains un-manifest in the ether, *providing the stability of the universe*. In other words, for the ether model of the universe, there is no need for Dark energy and Dark Matter [38] [39].

Mannheim's work [39] [40] on Conformal Gravity argues that there is no need for Dark Matter. The postulates of Dark Energy and Dark Matter were proposed to explain cosmological issues related to balancing the total energy density in the universe. Manheim's Conformal Gravity (Equation (18)), as a four-term polynomial, with four but the same fixed set chosen constants, β^*, γ^*, γ_0 and κ, can map the experimental data for the velocity distribution of the stars within a galaxy with their radial distances for about two hundred different galaxies reasonably well. One best case example for the plots of experi-

mental velocity data points (solid dots with the error bars; using Doppler frequency shifts) for the galaxy UGC1230 is shown in Figure 3. The solid curve is the computer plot. Other currently dominant theories of gravity do not have such broad curve fitting capability. [The dashed and dotted curves in Figure 3 correspond to using different terms, or combination of terms, from the Equation (18). They are irrelevant for our discussions here. Readers, who are interested in Conformal Gravity, should consult ref.40 for further details.]

$$\frac{v_{Tot}^2}{R} \to \left[\frac{N^*\beta^* c_0^2}{R^2} + \frac{N^*\gamma^* c_0^2}{2} + \frac{\gamma_0 c_0^2}{2} - \kappa c_0^2 R \right] \tag{18}$$

Let us re-write Equation (18) in terms of the key primary tension parameters of ether, using $c_0^2 = \varepsilon_0^{-1}/\mu_0$, to underscore that the origin of gravitational "curvatures of space" emerges out of electromagnetic ether.

$$\frac{v_{Tot}^2}{R} \to \left[\frac{\varepsilon_0^{-1}}{\mu_0} \right] \left[\frac{N^*\beta^*}{R^2} + \frac{N^*\gamma^*}{2} + \frac{\gamma_0}{2} - \kappa R \right] \tag{19}$$

4.4.2. Cosmological Redshift Is Not a Doppler Effect

Stationary ether model also contradicts Cosmological Redshift [41] [42]. For our universe to evolve causally through diverse interactions between matter-matter and matter-radiation, the values of the tension parameters ε_0^{-1} & μ_0, must remain constant. Any major expansion would appreciably change these parameters and would have shown rapid changes in the values of these primary action parameters, and hence we would have experienced the laws of nature changing and evolving.

Further, the physical processes behind the emergence of Doppler Effect does not corroborate the conditions actually exists. The so called Doppler shifted spectral "Dark Lines" represent the absence of any physical signal. So dark lines

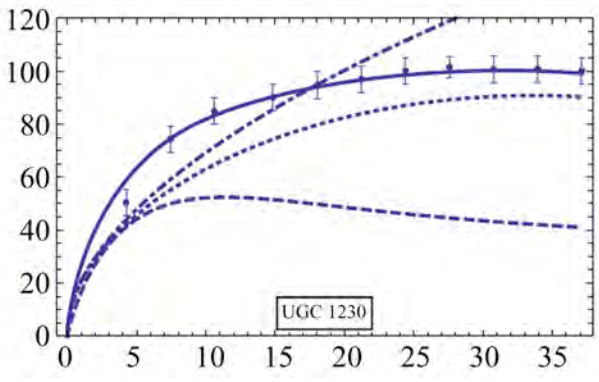

Figure 3. Strength of Conformal Gravity without the need for Dark Energy. Relative velocity distribution of stars with their distance from the center of the galaxy UGC 1230. The solid computer plotted curve fits very well through the experimental data points with their error bars. This is a 3D model of gravity and it does away with the need for Dark Matter [40]. It is better than the 4D model of Einstein's gravity. (The dashed and dotted curves correspond to using different terms, or combination of terms, from the Equation (18); they are not relevant for our discussions in this paper.)

cannot experience Doppler Effect [43]. Let us briefly revisit the origin of Doppler Effect. *Physically real and permanent frequency shift* of light as Doppler Effect happens due to the velocities of the signal emitting individual atoms and molecules relative to the universally stationary ether. This Doppler shifted signal then propagates perpetually through the ether unchanged. However, this same Doppler shifted signal would be perceived by a set of detectors with *further modified and different Doppler shifts*, if they are moving with different velocities relative to the stationary ether. Source velocities and detector velocities both create separate Doppler frequency shifts, the former is real and the latter is apparent [43].

Let us now account for the physical conditions behind the "frequency shifted" dark lines. First, the white light, emanating out from inside the star, must pick up the spectral dark line signatures due to the quantum mechanical *resonance absorptions* by atoms and molecules of the outer layers. Then, the emergent white light with dark lines imprinted on it, propagates through the intervening cosmic space, before reaching us. Therefore, *the frequency shift of the dark line can happen only while the entire white light spectrum undergoes redshift during its travel through the galactic space before reaching us*. The physical processes that create this Cosmological Redshift must be some physical property of the intervening ether whose properties have been modified due to the presence of various gravitational curvatures by the innumerable galaxies, or due to the presence of thin cosmic gases and charges, etc., etc. This is why Hubble Redshift is an energy dissipation dependent phenomenon, not a Doppler Effect. Therefore, *our ether model of the universe is not expanding*.

This also implies that the introduction of the cosmological constant by Einstein in his General Relativity was not necessary, because he assumed the correctness of the expanding-universe interpretation of the observed distance-dependent Cosmological Redshift, as Doppler Effect—as if, all galaxies are receding from each other.

4.5. The Postulates of Special Relativity (SR) Are Automatic Consequence of Ether Model

4.5.1. SR Postulate -1: Velocity of Light Is Same in All Inertial Frames

Einstein's first postulate is essentially built into our model of stationary ether; a separate postulate is not necessary. However, there are some qualifications and limitations. The velocity of all EM waves in all material free regions is automatically the same, $c_0^2 = \varepsilon_0^{-1}/\mu_0$. We also have defined the cosmic ether as the stationary (inertial) reference frame for the entire observable universe. It is the only universal inertial reference frame for us. Planets, on which human-like species can carry out experiments, strictly speaking, are not truly inertial rest frames. They are continuously executing diverse complex motions: axial rotations, elliptical orbital motions and their parental stars' galactic motions (rotations and translation). However, we must note that for material media, sufficiently dense galactic gas clouds, corona of stars, planetary atmosphere, bulk material media on planets, all have different effective and *reduced tension field strength* (higher

refractive index) and also have dispersive frequency-dependent velocities, $c_{med.}^2(\nu) = c_0^2 / n_{med.}^2(\nu)$. In these media, the velocities of EM waves are different. Further, if any of these media are in relative motion with respect to the stationary ether, then the velocity suffers from Fresnel Drag [21] [44].

4.5.2. SR Postulate-2: Laws of Physics Are Same Everywhere in the Universe

We have already underscored that our universe, emergent in the stationary ether, is the only inertial reference frame. The only observables are propagating EM waves and localized IP-CL EM waves. They all are different kinds of excited states of the same cosmic ether. They naturally must follow the same rules on planets in any star, in any galaxy, in the entire observable universe. Therefore, the 2nd postulate is also naturally built into our model for the cosmic ether. We do not need to postulate it separately.

Further, the atoms and the molecules, being assemblies of resonant oscillations of the same cosmic ether (IP-CL modes), they naturally would obey and display the same quantum mechanical behavior in all the stars, in all the galaxies. This is also the obvious reason why the theories, well-validated by experiments on earth, also corroborate the properties of atoms and molecules in distant stars and their planets. We should further note that the empty space between the atoms, and also within the atoms, is the same stationary Cosmic Ether, whether they are in the corona of a star, or in a discharge tube on earth. Clearly, a separate SR theory in Physics is not of critical importance just to appreciate the universality of the laws of physics, as originally articulated by SR, which did not explicitly recognize ether as the stationary energetic tension field.

4.5.3. SR: The Running Time "t" Is Not an Operational, or a Primary Parameter of Any Natural System or Object

Recall that we have underscored in the introduction the importance of "interaction process" and "primary actionable parameter" in modeling natural phenomena, because nature is persistently evolving through diverse interaction processes where the interaction parameters usually define the strength of interactions. The running time, "t" does not fit into either of this characteristic. So, it does not make operational sense to assign running time "t" as the fourth dimension of nature (the universe), having equal footing with the 3D space. The running time "t" is an ingenious invention of human culture. We cannot lead our lives without it.

Let us examine how we measure the running time. We use a standard *physical oscillator* that has a characteristic natural (resonant) frequency, f. Then we invert this frequency into a "period", "dt" = "1/f". Then we keep counting larger and larger number of periods to get a semblance of running time "t". It is not an action guiding parameter of nature. Life times of radio-active elements and unstable particles do represent various physical time intervals as time periods. So, the running time can be expressed as different multiples of their respective "life-times". So, the running time "t" should be kept as a mathematically convenient parame-

ter to keep track of evolution of natural phenomenon, however, without assigning it the status of a primary action parameter of nature. We should note that, frequency being a primary physical parameter of a physical oscillator, it can be "dilated" and "contracted" by applying appropriate changes in its immediate vicinity that can alter the physical parameter that influences the resonance frequency of an oscillator. Therefore, the universe should not be arbitrarily defined as physically four or multidimensional.

5. Conclusions

5.1. Summary

Galileo and Newton ushered in the golden days of physics-thinking by elevating the need to validate the reproducible experimental data after constructing mathematical theories that can explain the operational functions behind the emergence of natural phenomena. After several centuries of outstanding and rapid progress, physics has now become a bit moribund [4] [5] [6] [7], except our steadily accelerating engineering capabilities. This has encouraged us to imagine nature as a profoundly creative system engineer. Accordingly, we have approached to dissect the working theories while searching for the primary operational parameters in them. This approach has also been strongly espoused by Plank [12], as has been mentioned in the introduction. While searching for the appropriate action parameters behind the perpetual velocity of light in the cosmic "vacuum", which is built into Maxwell's wave equation, we are able to identify them as ε_0^{-1} (electric tension) & μ_0 (magnetic resistance). Once we combine this with Einstein's matter-energy inter-convertibility relation, $m_0 = E/c_0^2 = E\left(\mu_0/\varepsilon_0^{-1}\right)$, we have been naturally guided to postulate elementary particles as IP-CL oscillatory modes of the same Cosmic Ether. Then, we have strengthened and justified, using various mathematical expressions out of different working theories, that the Cosmic Ether has always been the unifying platform for our observable universe nurturing diverse kinds of oscillators of it. EM wavelets are freely propagating excited states of the ether. The particles are in-phase closed-looped (IP-CL) modes, which are spatially constrained as localized harmonic oscillators with complete inertia to motion in the absence of any spatially influencing potential gradients (forces) in its vicinity.

5.2. Strengthening Further Our Physics-Thinking

We have already underscored in the introduction that we consider nature as a creative, but logical and causality-driven system engineer. Hence, we need to focus our attention to visualize the invisible interaction processes in nature to understand the realities of nature. This is akin to evolution process congruent thinking ([19]-Ch.12, [45] [46] [47] [48] [49]).

Over the last few decades, many papers and books have been published [4]-[9] raising serious concerns that progress in physics has become stagnant for many decades after the great advances ushered in by the theories of Relativity, and

Quantum Mechanics since the beginning of the last century. We believe this is because we have started to neglect that nature is constantly executing real physical interaction processes to nurture its perpetual evolution, very much like the perpetual velocity, c_0, in its fundamental constituent oscillators. Observable nature is physically real in the sense that the orderly universe has been existing for over a very long period of time, still undetermined; whereas humans have started modeling nature using modern mathematics starting barely some 600 years back. It was Galileo and Newton who successfully demonstrated that mathematics contain deeply logical properties and since then it has turned out to be an invaluable tool to explore nature. However, logics built into mathematics, irrespective of their beauty and harmony, cannot directly define and/or articulate the physical interaction processes hidden behind the causal interaction processes, which nature is executing. That has to be interpreted and articulated by the variable and the subjective, albeit "logical", human minds, and constrained by the mathematical logics and the experimental data. Therefore, the prevailing evidence based science, led by mathematics and validated by experiments, is in-sufficient for our continual progress to keep exploring nature's reality.

Our universe is a constantly recycling system. This is evident from the system engineering marvels of creation and destruction of macro galaxies made out of stars and planets, while recycling the same atoms, built out of the elementary particles. And *all of which are continuously recycling as* "*excited states*" *of the common unchanging platform of the energetic tension field*, *the ether*. Nature is not a speculative philosopher, even though to step out of our beginning ignorance about the laws of nature, we must start by being *philosophic*. Nature is not driven by pure mathematics-type of logics either; even though human invented mathematical logics have been one of the major success tools to help us explore and advance our understandings of nature.

Consider the case of laser modes. Stable fundamental laser modes are mathematically expressed as spatially Gaussian with tails extending to infinity. How can an infinite-tailed laser mode be generated out of spatially-finite laser cavities (gain media)? "Successful" mathematical logics could even lead us to draw wrong conclusions regarding the cause behind an emergent phenomenon while generating correct prediction. *Clearly human invented mathematical logics and cosmic logics are not identical*. The "evidence based science", a combination of our mathematical theories and experimental validations, have been, so far, our major guiding tools towards our advancements. However, the evidence based science is not enough. We should also note that our scientific exploration of the laws of nature has started with essentially complete ignorance. Our conclusion about the experimental data, generated through interaction between different chosen entities, can never be completely conclusive simply because we do not know completely any of the interacting entities within our experimental apparatus. We still do not completely understand what electrons and photons are made of. Therefore, no finite set of experiments can succeeded in finding the complete set of properties of any natural entity as yet. This has been mathematically arti-

culated by Gödel's in his Incompleteness Theorem [50]. We have to continuously keep challenging our best working theories and iteratively re-organize and/or re-structure them as our knowledge keeps advancing incrementally. Our recent progress has been slowed down as our speculative mathematics and philosophically flexible interpretations of the experimental data have started overtaking our excitements without keeping ourselves anchored to visualizing the real engineering processes nature has been utilizing.

Human biological evolution started acceleration with the invention of creating controlled fire on-demand by quick rubbing of dried wood pieces, or by striking a pair of stones. Anthropologists believe that this had happened several hundred thousand years ago, if not even much earlier. The multi-step physical processes behind these innovations involve, first, transferring the biological muscular energy of hands as the kinetic (or thermal) energies on to the molecules and atoms of the wood or the stone pieces. Then *this classical kinetic energy triggers the quantum mechanical processes of ionizing a large number of atoms and molecules*. After that, the second set of quantum processes kicks in. The free electrons from the surrounding air start neutralizing the ionized atoms and molecules, while releasing a wide range of EM radiations - heat, visible and UV. This momentous innovation was achieved by multiple human tribes in different geographic locations through their trial-and-error approach. The pressure for this innovation was triggered by the evolutionary desire to live better compared to the then existing best conditions they had. They did not have any clue about physics or chemistry; they did not have any mathematics, and not even advanced languages. However, the human thinking, driven by the wisdom of trying to emulate the physical processes taking place in nature through trial and error, has set the humans in the right direction to unravel the mysteries of the universe, while enjoying the biological lives and the beauty as a byproduct of nature. *We are here today because of our very ancient forefathers were wise engineers with very innovative minds*.

The field of modern physics has demonstrated a rather remarkable set of advancements, especially, over the last six hundred years. We have now ushered in the Knowledge Age by installing the global Internet System, while mastering the technologies behind light management. However, our dominant thinking has remained frozen to the foundational postulates behind the four distinctly different physics-thinking (epistemologies)—Classical Physics, Relativity *Physics*, *Quantum Physics and Cosmological Physics*. *But*, *we know that the universe is one continuum*. *Therefore*, we need to add the Interaction Process Mapping Epistemology (IPM-E), over and above our currently successful approach of using Measurable Data Modeling Epistemology (MDM-E) [39] [40] to thoroughly understand and visualize the engineering processes nature employs on her energetic tension field, the ether. Our predominant culture has now guiding us to become the consumers of the biosphere, rather than its nurturer, as our ancient forefathers were.

We have to keep on iteratively re-structuring the basic set of postulates behind

all of our separate theories as a single set of coherent and harmonious postulates. This paper is an attempt in this direction. It has logically demonstrated that the old ether is, most likely, the best unifying field for us. We ourselves are just bundles of oscillating, or dancing, excited states of ether!

Conflicts of Interest

The author declares no conflicts of interest regarding the publication of this paper.

References

[1] Amoroso, R.L. and Vigier, J.-P. (2002) Can One Unify Gravity and Electromagnetic Fields? In: Amoroso, R.L., Hunter, G.G. and Vigier, J.-P., Eds., *Gravitation and Cosmology*: *From the Hubble Radius to the Planck Scale*, Kluwer, Dordrecht, 27-38 https://doi.org/10.1007/0-306-48052-2

[2] Sandhu, G.S. (2009) Fundamental Nature of Matter and Fields. iUniverse Books.

[3] Consoli, M. and Pluchino, A. (2018) Michelson-Morley Experiments: An Enigma for Physics and the History of Science. World Scientific Publishing, Singapore. https://doi.org/10.1142/11209

[4] Roychoudhuri, C. (2012) *Journal of Modern Physics*, **3**, 1357-1368. https://doi.org/10.4236/jmp.2012.310173

[5] Smolin, L. (2007) The Trouble with Physics: The Rise of String Theory, the Fall of a Science, and What Comes Next. Houghton Mifflin Co., Boston.

[6] Hossenfelder, S. (2019) Lost in Math: How Beauty Leads Physics Astray. Hachette Book Group, New York.

[7] Rangacharyulu, C. and Polachic, C.J.A. (2019) From Atoms to Higgs Boson: Voyages in Quasi-Spacetime. Pan Stanford, Singapore.

[8] De Koning, W.L. and Van Willigenburg, L.G. (2020) *Physics Essays*, **33**, 299-301.

[9] Romashka, M.Y. (2020) *Gravitation and Cosmology*, **26**, 61-69.

[10] Huygens, C. (1690) Treatise on Light. http://www.gutenberg.org/ebooks/14725

[11] Goodman, J.W. (2017) Introduction to Fourier Optics. W. H. Freeman, New York.

[12] Planck, M. (1914) The Theory of Heat Radiation. Blakiston's Son & Co., Philadelphia.

[13] Elmore, W.C. and Heald, M.A. (1969) Physics of Waves. McGraw-Hill, New York.

[14] Michelson, A.A. and Morley, E.W. (1887) *American Journal of Science*, **34**, 333-345. https://doi.org/10.2475/ajs.s3-34.203.333

[15] Einstein, A. (1905) *Annalen der Physik*, **17**, 891-921, 910-911. https://doi.org/10.1002/andp.19053221004

[16] Einstein, A. (1905) *Annalen der Physik*, **17**, 132. https://doi.org/10.1002/andp.19053220607

[17] Pena, L., Cetto, A.M. and Hernandez, A.V. (2015) The Emerging Quantum: The Physics behind Quantum Mechanics. Springer, Berlin.

[18] Roychoudhuri, C. (2014) Causal Physics: Photon by Non-Interaction of Waves. Taylor and Francis, Abingdon-on-Thames.

[19] Roychoudhuri, C. (2010) *Journal of Nanophotonics*, **4**, Article ID: 043512. https://doi.org/10.1117/1.3467504

[20] Jackson, J.D. (1999) Classical Electrodynamics. Wiley, Hoboken.

[21] Frercks, J. (2005) *Physics in Perspective*, **7**, 35-65. https://doi.org/10.1007/s00016-004-0224-0

[22] Jaffe, R.I. (2005) *Physical Review D*, **72**, 021301(R). https://doi.org/10.1103/PhysRevD.72.021301

[23] Paul, H. (2004) Introduction to Quantum Optics. Cambridge University Press, Cambridge. https://doi.org/10.1017/CBO9780511616754

[24] Roychoudhuri, C. and Prasad, N. (2019) Complex Interaction Processes We Need to Visualize That Successfully Fill the Quantum Cup of a Detector. *Proceedings of SPIE*, Vol. 10926, paper109260T. https://doi.org/10.1117/12.2514835

[25] Schwartz, M. (2014) Quantum Field Theory and the Standard Model. Cambridge University Press, Cambridge.

[26] Greulich, K.O. (2010) *Journal of Modern Physics*, **1**, 300-302. https://doi.org/10.4236/jmp.2010.15042

[27] Peskin, M.E. (2019) Concepts of Elementary Particle Physics. Oxford University Press, Oxford. https://doi.org/10.1093/oso/9780198812180.001.0001

[28] Osmera, P. (2010) *Engineering Letters*, **18**, EL_18_2_02. https://doi.org/10.1063/1.3460240

[29] Alexandrou, C. (2012) *Reviews of Modern Physics*, **84**, 1231. https://doi.org/10.1103/RevModPhys.84.1231

[30] Roychoudhuri, C. (2006) *Physics Essays*, **19**, 333-354. https://doi.org/10.4006/1.3025804

[31] Roychoudhuri, C. (2019) Differentiating the Superposition Principle from the Measurable Superposition Effects in Interferometry. In: *Interferometry—Recent Developments and Contemporary Applications*, IntechOpen, London. https://doi.org/10.5772/intechopen.81432

[32] Roychoudhuri, C. (2019) Experiments to Explore Wave-Particle-Duality Postulate. *Rochester Coherence & Quantum Optics Conference*, *Session I*, Rochester, 4-8 August 2019, Paper # M5A.24. https://doi.org/10.1364/CQO.2019.M5A.24

[33] Mattuck, R.D. (1992) A Guide to Feynman Diagrams in the Many-Body Problem. Dover Publication, Mineola.

[34] Romashka, M.Yu. (2020) *Gravitation and Cosmology*, **26**, 61-69. https://doi.org/10.1134/S0202289320010120

[35] Munhoz-Rojas, P.E. (2019) New Theory of Matter. https://www.researchgate.net/publication/335949958_New_Theory_of_Matter?enrichId=rgreq-ccc60c25d97809beab9ef5a3381d364d-XXX&enrichSource=Y292ZXJQYWdlOzMzNTk0OTk1ODtBUzo4MDUyNjgxNDk1MTQyNDdAMTU2OTAwMjI5NjY5MQ%3D%3D&el=1_x_2&_esc=publicationCoverPdf

[36] Mallett, R. (2000) *Physics Letters A*, **269**, 214-217. https://doi.org/10.1016/S0375-9601(00)00260-7

[37] Antusch, S., *et al.* (2020) *Physics Letters B*, **811**, Article ID: 135888. https://doi.org/10.1016/j.physletb.2020.135888

[38] Rourke, C. (2019) A New Paradigm for the Universe.

[39] Mannheim, P.D. (2006) *Progress in Particle and Nuclear Physics*, **56**, 340-445. https://doi.org/10.1016/j.ppnp.2005.08.001

[40] Mannheim, P.D. (2012) *Foundations of Physics*, **42**, 388-420. https://doi.org/10.1007/s10701-011-9608-6

[41] Gupta, R.P. (2018) *International Journal of Astronomy and Astrophysics*, **8**, 219-229.

[42] Shao, M. (2013) *Physics Essays*, **26**, 183. https://doi.org/10.4006/0836-1398-26.2.183

[43] Roychoudhuri, C. (2013) Tribute to H. John Caulfield: Hijacking of the "Holographic Principle" by Cosmologists. *SPIE Proceedings*, Vol. 8833, 88330E. https://doi.org/10.1117/12.2025349

[44] Panofsky, W.K.H. and Phillips, M. (1962) Classical Electricity and Magnetism. Addition-Wesley, Boston.

[45] Roychoudhuri, C. (2010) The Consilient Epistemology: Structuring Evolution of Logical Thinking. In: *Proceedings* 1*st Interdisciplinary Chess Interactions Conference*, World Scientific, London, 273-295. https://doi.org/10.1142/9789814295895_0016

[46] Roychoudhuri, C. (2015) Replacing Paradigm Shift Model in Physics with Continuous Evolution of Theories by Frequent Iterations. In: *Death and Anti-Death*: *Sixty Years after Albert Einstein* (1879-1955), Vol. 13, Ria University Press, Ann Arbor, Ch. 10.

[47] Roychoudhuri, C. and Tirfessa, N. (2019) Bringing Reality in Physics: System Engineering Approach to Optical Phenomena Following Huygens' Principle. *Proceedings of SPIE*, Vol. 11143, 111433A. https://doi.org/10.1117/12.2523602

[48] Roychoudhuri, C. (2015) Urgency of Evolution Process Congruent Thinking in Physics. *Proceedings of SPIE*, Vol. 9570, paper #7. https://doi.org/10.1117/12.2188498

[49] Wilson, E.O. (1998) Consilience: The Unity of Knowledge, Alfred A. Knopf.

[50] Godel's Incompleteness Theorem. https://en.wikipedia.org/wiki/G%C3%B6del%27s_incompleteness_theorems

Journal of Modern Physics, 2021, 12, 700-729
https://www.scirp.org/journal/jmp
ISSN Online: 2153-120X
ISSN Print: 2153-1196

Decoherence as an Inherent Characteristic of Quantum Mechanics

Riuji Mochizuki

Laboratory of Physics, Tokyo Dental College, Tokyo, Japan
Email: rjmochi@tdc.ac.jp

How to cite this paper: Mochizuki, R. (2021) Decoherence as an Inherent Characteristic of Quantum Mechanics. *Journal of Modern Physics*, **12**, 700-729.
https://doi.org/10.4236/jmp.2021.125045

Received: March 19, 2021
Accepted: April 26, 2021
Published: April 29, 2021

Abstract

In this study, we show that it is possible to explain the quantum measurement process within the framework of quantum mechanics without any additional postulates. We do not delve into a deep discussion regarding what the measurement problem actually is, and only examine the problems that seem to exist between classical and quantum physics. Relations between quantum and classical equations of motion are briefly reviewed to show that the transition from a superposition of quantum states to an eigenstate, namely, decoherence, is necessary to ensure that the expectation values in quantum mechanics obey the classical equations of motion. Several Bell-type inequalities and the Kochen-Specker theorem are also reviewed to clarify the concepts of *nonseparability* and *counterfactual definiteness* in quantum mechanics. The main objective of this study is to show that decoherence is an inherent characteristic of quantum states caused by the quantum uncertainty relation. We conclude that the quantum measurement process can indeed be explained within the framework of pure quantum mechanics. We also show that our conclusion is consistent with the counterfactual indefiniteness of quantum mechanics.

Keywords

Decoherence, Uncertainty Relation, Measurement Problem

1. Introduction

The measurement problem in quantum mechanics is an unresolved problem in modern physics, and a subject of considerable debate [1] [2]. The microscopic world in conventional quantum mechanics is treated differently from the macroscopic world in classical mechanics. However, these two worlds are, in fact, linked to each other. Therefore, it may seem that the present formulation of quantum mechanics is insufficient to describe nature. Nevertheless, for many

decades, it has been unclear how exactly to formulate the measurement problem, which has led to several definitions of this problem.

For a better understanding of the discussion in subsequent sections, we first provide some background on the problems that exist between classical physics and quantum mechanics, and the theories suggested to solve them. In the present work, we examine a Stern-Gerlach-like experiment, where the spin in the z-direction of an electron S is measured, to clarify these problems.

In classical mechanics, the relation between the state of a system under investigation and the physical quantities associated with it is trivial. However, certain assumptions are needed to connect these in quantum mechanics. In its standard formulation, the *eigenstate-eigenvalue link* [3] [4] states that eigenvalues and eigenstates have a one-to-one correspondence except in the case of degeneracy. Thus, in our Stern-Gerlach-like experiment, we assume that

$$\text{eigenvalue} + \hbar/2 \rightleftharpoons \text{eignestate} \left|+\right\rangle, \tag{1}$$

$$\text{eigenvalue} - \hbar/2 \rightleftharpoons \text{eigenstate} \left|-\right\rangle, \tag{2}$$

where $\left|+\right\rangle$ and $\left|-\right\rangle$ represent the eigenstates of S with eigenvalues $+\hbar/2$ and $-\hbar/2$, respectively.

However, some studies have suggested that this condition is unnecessary [5]. Nevertheless, if we do not agree with the eigenstate-eigenvalue link, then it follows that standard quantum mechanics is insufficient to describe nature. To better understand this, we examine the above assumption in more detail. Note that because the assumption eigenstate $\rightarrow$ eigenvalue is a part of Born's rule [6], and discarding this assumption implies discarding Born's rule. Conversely, discarding the assumption eigenvalue $\rightarrow$ eigenstate implies that there may be states other than the eigenstate that correspond to the measured value of the concerned physical quantity. For instance, let a_i be the value obtained after the measurement of a quantity. If the state obtained directly after this measurement is not the eigenstate corresponding to a_i, then it is possible to obtain a measured value that is different from a_i even after the first measurement. Thus, if we discard the assumption eigenvalue $\rightarrow$ eigenstate, then the standard theory of quantum mechanics appears to be insufficient.

We introduce an ideal measurement device M and assume that S and M interact by obeying the Schrödinger equation. Let $\left|n\right\rangle$ be the neutral state of M before measurement, and $\left|p\right\rangle$ and $\left|m\right\rangle$ be the states of M after measurement with measured values $+\hbar/2$ and $-\hbar/2$, respectively. Subsequently, taking into account the eigenstate-eigenvalue link, an ideal measurement process $\hat{U}$ is defined as

$$\left|+\right\rangle\left|n\right\rangle \rightarrow \hat{U}\left|+\right\rangle\left|n\right\rangle = \left|+\right\rangle\left|p\right\rangle, \tag{3}$$

$$\left|-\right\rangle\left|n\right\rangle \rightarrow \hat{U}\left|-\right\rangle\left|n\right\rangle = \left|-\right\rangle\left|m\right\rangle. \tag{4}$$

Let the initial state of S be $\left(1/\sqrt{2}\right)\left(\left|+\right\rangle + \left|-\right\rangle\right)$. Then, the state obtained after the measurement process is given by

$$\hat{U}\frac{1}{\sqrt{2}}\left(|+\rangle+|-\rangle\right)|n\rangle=\frac{1}{\sqrt{2}}\left(|+\rangle|p\rangle+|-\rangle|m\rangle\right). \tag{5}$$

Note that either the measured value $+\hbar/2$ or $-\hbar/2$ is expected as a result of the measurement in Equation (5). However, the measurement process and the eigenstate-eigenvalue link contradict each other because the initial state of S is not the eigenstate corresponding to the eigenvalues $+\hbar/2$ or $-\hbar/2$.

Thus, the above example shows that it is necessary to adopt a modification of standard quantum mechanics. The most traditional approach is to adopt the projection postulate [7]. As will be discussed in Section 2, the transition from a superposition of states to an eigenstate is necessary so that the expectation values in quantum mechanics obey the classical equations of motion. However, this transition cannot be described by the Schrödinger equation because it is not a unitary process. By adopting the projection postulate, the quantum states not only develop unitarily by obeying the Schrödinger equation but also non-unitarily owing to the collapse of the wave packets during the measurement process. For example, a state $|\psi\rangle$ changes to the corresponding eigenstates $|a_i\rangle$ after the measurement with corresponding measured values a_i. Thus, in the Stern-Gerlach-like experiment, a non-unitary change such as

$$\frac{1}{\sqrt{2}}\left(|+\rangle|p\rangle+|-\rangle|m\rangle\right)\rightarrow|+\rangle|p\rangle \text{ or } |-\rangle|m\rangle \tag{6}$$

is permitted in addition to the unitary development represented by Equation (5).

Although the projection postulate is a type of nonlocal requirement, there are several studies that demonstrate its consistency with special relativity [8]. Note that classical information cannot be transferred during the collapse of a wave packet.

In contrast to the above description, the collapse of a wave packet is not assumed in the many-worlds interpretation of quantum mechanics [9] [10]. In this interpretation, even macroscopic states maintain coherent superpositions, and therefore, the assumption that only *one* outcome can be obtained from one appropriate measurement process, which is usually regarded as a matter of course, is discarded.

Decoherence [11] [12] may be regarded as one of the most successful theories to explain the quantum measurement process without any additional postulates. Moreover, it is frequently applied to the many-worlds interpretation [13]. Decoherence was first proposed by Zeh *et al.* [14] [15], which was followed by the important work of Zurek [16]. The efforts of these authors ensured that the decoherence theory was actively studied. In this theory, the observed decay of interference is explained by the interactions between the system and the environmental degrees of freedom. For example, let the state $|Z\rangle$ that represents a unified system consisting of an observed system and a measurement device be described by the superposition of the two states $|a\rangle$ and $|b\rangle$, such that:

$$|Z\rangle=\frac{1}{\sqrt{2}}\left(|a\rangle+|b\rangle\right). \tag{7}$$

Next, we suppose that this state interacts with the state $|E_0\rangle$ representing the environmental degrees of freedom. The interaction dynamics between these states are given by

$$|a\rangle|E_0\rangle \to |a\rangle|E_a\rangle, \tag{8}$$

$$|b\rangle|E_0\rangle \to |b\rangle|E_b\rangle. \tag{9}$$

The density matrix $\hat{\rho}_Z$ of the interacting system is then

$$\hat{\rho}_Z = \frac{1}{2}\left(|a\rangle|E_a\rangle + |b\rangle|E_b\rangle\right)\left(\langle a|\langle E_a| + \langle b|\langle E_b|\right). \tag{10}$$

Note that because the environmental degrees of freedom are very large, the states $|E_a\rangle$ and $|E_b\rangle$ resulting from the interaction are approximately orthogonal if $|a\rangle$ and $|b\rangle$ are distinguishable. Therefore, the reduced density matrix $\hat{\rho}_{reZ}$ of the unified system, which is obtained by tracing out the environmental degrees of freedom, becomes

$$\hat{\rho}_{reZ} = \frac{1}{2}\left(|a\rangle\langle a| + |b\rangle\langle b|\right). \tag{11}$$

Thus, we observe the decay of interference in the system. Moreover, the preferred basis problem has also been studied in this framework by Zurek [17], who also presented a solution for this problem.

However, certain problems remain with the decoherence theory. First, the unitary interaction between the system and the environment does not lead to a complete removal of the interference terms. The reduced density matrix given by Equation (11) does not indicate whether the system is in state $|a\rangle$ or $|b\rangle$ because reduced density matrices represent improper mixtures [18] that only provide a probability distribution. This implies that the coherence has been delocalised into a larger system including the environment [2]. The next problem may be more severe. Note that because the coherent terms disappear *after* in the interaction between the system and the environment, obtaining an outcome for a superposition of states implies direct violation of the eigenstate-eigenvalue link.

Considering the above arguments, it seems necessary to remove certain natural conditions from or add certain new unnatural conditions to standard quantum mechanics to explain the measurement process. In other words, the quantum measurement problem is reduced to the problem of determining these conditions.

Note that in the present study, we do not delve into a discussion regarding what the measurement problem actually is. Instead, we define our problem in the form of the following question: *is it possible to explain the measurement process within the framework of pure quantum mechanics*? In this study, *pure quantum mechanics* refers to the theory of quantum mechanics without any additional postulates, such as the projection postulate. We demonstrate that the answer to this question is, in fact, yes; thus, we can indeed explain the measurement process within the framework of pure quantum mechanics.

The remaining paper is organised as follows.

In Section 2, the relations between the quantum mechanical and classical equations of motion are briefly reviewed. It is shown that the transition from a superposition of states to an eigenstate is necessary to ensure that the expectation values in quantum mechanics obey the classical equations of motion; specifically, decoherence is necessary to connect the classical and quantum worlds.

In Section 3, several Bell-type inequalities are reviewed. The fact that these inequalities do not hold true for quantum mechanics indicates the presence of some sort of nonlocality. Although it is unlikely that the universe is nonlocal, the measurement problem of quantum mechanics is not a problem of explaining the nonlocality itself. The question we should rather ask is whether such theories of quantum mechanics are reasonable enough to explain the measurement process and experiments that demonstrate the reasonableness of its own. The Kochen-Specker theorem is also discussed in Section 3. It is well known that this theorem prohibits *counterfactual definiteness* of quantum mechanics. Nevertheless, it is important to consider the meaning of counterfactual definiteness in relation to the nonlocality.

Section 4 presents the main findings of this study. We show that decoherence is an inherent characteristic of quantum states caused by the quantum uncertainty relation, and it can explain the measurement process within the framework of pure quantum mechanics. It is also shown that there is no inconsistency between decoherence and the counterfactual definiteness discussed in Section 3.

Section 5 concludes the paper.

2. Relation between Quantum Mechanical and Classical Equations of Motion

In this section, we show that the transition from a superposition of states to an eigenstate is necessary to ensure that the quantum mechanical expectation values obey the classical equations of motion.

2.1. Schrödinger Equation, Path Integral Formulation, and Hamilton-Jacobi Equation

The time evolution of physical quantities characterising macroscopic objects is described by the equations of motion in classical mechanics. Conversely, the operators corresponding to the physical quantities characterising microscopic objects do not evolve with time but the states evolve according to Schrödinger equation in the Schrödinger picture of quantum mechanics. Thus, the relation between Schrödinger equation and classical equations of motions is nontrivial. However, it can be visualised easily by adopting the path integral formulation.

2.1.1. Relation between Schrödinger Equation and Hamilton-Jacobi Equation

It has been shown that the phase of a wave function obeys the classical Hamilton-Jacobi equation under certain assumptions [19] [20]. Let $q_i(t)$ be the position at time t of a particle moving in a real field $U(q_i(t),t)$ and $\psi(q_i(t),t)$

be its wave function, where $i=1,\cdots,d$. $\psi\left(q_i(t),t\right)$ obeys the Schrödinger equation such that

$$i\hbar\frac{\partial\psi\left(q_i(t),t\right)}{\partial t}=-\frac{\hbar^2}{2m}\Delta\psi\left(q_i(t),t\right)+U\left(q_i(t),t\right)\psi\left(q_i(t),t\right). \tag{12}$$

If we separate the wave function $\psi\left(q_i(t),t\right)$ into its absolute value $A\left(q_i(t),t\right)$ and phase $S\left(q_i(t),t\right)/\hbar$, such that

$$\psi\left(q_i(t),t\right)=A\left(q_i(t),t\right)\exp\left(\frac{i}{\hbar}S\left(q_i(t),t\right)\right), \tag{13}$$

then Equation (12) can be separated into its real and imaginary parts. The real part is given by

$$-A\frac{\partial S}{\partial t}=-\frac{1}{2m}\left(\hbar^2\Delta A-A\left(\nabla S\right)^2\right)+UA, \tag{14}$$

and the imaginary part is given by

$$\frac{\partial A}{\partial t}=-\frac{1}{2m}\left(2\nabla A\cdot\nabla S+A\Delta S\right). \tag{15}$$

Let us first consider the imaginary part in Equation (15). The right-hand side of Equation (15) multiplied by A yields

$$-\frac{A}{2m}\left(2\nabla A\cdot\nabla S+A\Delta S\right)=-\frac{1}{2m}\nabla\cdot\left(A^2\nabla S\right). \tag{16}$$

Assuming that the momentum p of the particle is $p_i=\nabla_i S$, then Equation (15) multiplied by A results in the continuity equation

$$\frac{\partial\rho}{\partial t}=-\nabla\cdot\left(\rho v\right), \tag{17}$$

where $v=p/m$ is the velocity of the particle and $\rho\equiv A^2$.

Furthermore, ignoring the terms of $O\left(\hbar^2\right)$, Equation (14) becomes

$$\frac{\partial S}{\partial t}+\frac{1}{2m}\left(\nabla S\right)^2+U=0. \tag{18}$$

This is the classical Hamilton-Jacobi equation, assuming that S is the action and ∇S is the momentum of the particle.

Reasonableness of these assumptions based on the similarity between quantum mechanics and optics has been discussed in several textbooks [21] [22].

2.1.2. Path Integral Quantisation

Note that in this section, we omit the subscript i in q_i for simplicity. Adopting the path integral quantisation method [23] makes the discussion in the previous section clearer. In this theory, the wave function $\psi\left(q_F\equiv q(t_F),t_F\right)$ at time t_F can be described as evolving from the wave function $\psi\left(q_I\equiv q(t_I),t_I\right)$ at time t_I, ($t_I<t_F$), such that

$$\psi\left(q_F,t_F\right)=\int\mathcal{D}q\exp\left(\frac{i}{\hbar}\int_{t_I}^{t_F}L\left(q,\dot{q}\right)\mathrm{d}t\right)\psi\left(q_I,t_I\right), \tag{19}$$

where $L\left(q,\dot{q}\right)$ is the Lagrangian and

$$\mathcal{D}q \equiv \lim_{n\to\infty}\prod_{r=0}^{n} \mathrm{d}q_r, \quad q_r \equiv q(t_r), \tag{20}$$

with $q_{n+1} = q_F$, $q_0 = q_I$. Differentiating $\psi(q_F, t_F)$ with respect to t_F, we obtain

$$\frac{\partial \psi(q_F, t_F)}{\partial t_F} = \int \mathcal{D}q \frac{i}{\hbar}\frac{\partial S}{\partial t_F} \exp\left(\frac{i}{\hbar}\int_{t_I}^{t_F} L(q,\dot{q})\mathrm{d}t\right)\psi(q_I, t_I), \tag{21}$$

where

$$S \equiv \int_{t_I}^{t_F} L(q,\dot{q})\mathrm{d}t. \tag{22}$$

On the other hand, applying the Hamiltonian operator $\hat{H}(\hat{q}_F, \hat{p}_F)$, where $\hat{p}_F \equiv -i\hbar(\partial/\partial q_F)$, on the wave function $\psi(q_F, t_F)$ in Equation (19), we obtain

$$\hat{H}(\hat{q}_F, \hat{p}_F)\psi(q_F, t_F) = \int \mathcal{D}q H(q_F, \partial S/\partial q_F) \exp\left(\frac{i}{\hbar}\int_{t_I}^{t_F} L(q,\dot{q})\mathrm{d}t\right)\psi(q_I : t_I), \tag{23}$$

where the terms of $\mathcal{O}(\hbar)$ or higher are ignored. We can see that $H(q_F, \partial S/\partial q_F)$ on the right-hand side of Equation (23) is the classical Hamiltonian function with p_F substituted by $\partial S/\partial q_F$ on comparing Equation (23) with

$$\begin{aligned}\frac{\partial \psi(q_F, t_F)}{\partial t_F} &= \frac{\mathrm{d}\psi(q_F, t_F)}{\mathrm{d}t_F} - \frac{\partial \psi(q_F, t_F)}{\partial q_F}\dot{q}_F \\ &= \frac{i}{\hbar}\int \mathcal{D}q\left(L(q_F, \dot{q}_F) - \frac{\partial S}{\partial q_F}\dot{q}_F\right)\exp\left(\frac{i}{\hbar}\int_{t_I}^{t_F} L(q,\dot{q})\mathrm{d}t\right)\psi(q_I, t_I)\end{aligned} \tag{24}$$

and the Schrödinger equation

$$i\hbar\frac{\partial \psi(q_F, t_F)}{\partial t_F} = \hat{H}(\hat{q}_F, \hat{p}_F)\psi(q_F, t_F). \tag{25}$$

Substituting Equations (21) and (23) into Equation (25), we obtain the Hamilton-Jacobi equation

$$\frac{\partial S}{\partial t_F} + H(q_F, \partial S/\partial q_F) = 0. \tag{26}$$

Then, classical mechanics states that q_F and $p_F = \partial S/\partial q_F$ must satisfy Hamilton's equations of motion:

$$\dot{q}_F - \frac{\partial H}{\partial p_F} = 0, \tag{27}$$

$$\dot{p}_F + \frac{\partial H}{\partial q_F} = 0. \tag{28}$$

As shown above, the classical equations of motion can be derived from the Schrödinger equation in the limit $\hbar \to 0$ without any analogy, if the path integral quantisation method is applied to the wave function. However, it is worth noting that the derived classical equations of motion contain no information about the initial state of the system because the information $\psi(q_I, t_I)$ has been lost in the above formalism; specifically, the discussion here is formal and

hence does not reflect the state of the system. So far, all we have shown with the aid of quantum mechanics is that *classical quantities obey classical equations of motion*. Therefore, we still need to investigate the equations that the corresponding quantities in quantum mechanics (*i.e.* the expectation values of an operator) obey in the classical limit.

2.2. Ehrenfest Theorem

The Ehrenfest theorem [24] demonstrates how quantum mechanical expectation values obey the classical equations of motion. Although Ehrenfest [25] originally proposed the theorem in the Schrödinger picture, in this section we employ the Heisenberg picture. Note that because the operators corresponding to the physical quantities depend explicitly on time in the Heisenberg picture, the relation is rather straightforward. Let $\langle \hat{q} \rangle$ and $\langle \hat{p} \rangle$ be the expectation values of the coordinate $\hat{q}$ and momentum $\hat{p}$, respectively; then, the equations obeyed by $\langle \hat{q} \rangle$ and $\langle \hat{p} \rangle$ in quantum mechanics should be the same as the classical Hamilton's equations of motion under certain conditions.

Let us suppose that a quantum mechanical system is described by coordinates $\hat{q}_i \left(i = 1, \cdots, N \right)$ and their respective conjugate momenta $\hat{p}_i \left(i = 1, \cdots, N \right)$. Operator $\hat{A}$, which does not depend on time in the Schrödinger picture, evolves in the Heisenberg picture obeying

$$\frac{\mathrm{d}\hat{A}}{\mathrm{d}t} = \frac{1}{i\hbar}\left[\hat{A}, \hat{H} \right], \tag{29}$$

where $\hat{H}$ is the Hamiltonian operator and $[\,,\,]$ represents a commutator. Because the commutator between $\hat{q}_i$ and $\hat{p}_j$ is

$$\left[\hat{q}_i, \hat{p}_j \right] = i\hbar\delta_{ij}, \tag{30}$$

therefore, $\hat{H}$ satisfies

$$\left[\hat{q}_i, \hat{H} \right] = i\hbar \frac{\partial \hat{H}}{\partial \hat{p}}, \tag{31}$$

$$\left[\hat{p}_i, \hat{H} \right] = -i\hbar \frac{\partial \hat{H}}{\partial \hat{q}}. \tag{32}$$

Next, substituting $\hat{A}$ with $\hat{q}_i$ and $\hat{p}_i$ in Equation (29) and using Equations (31) and (32), we obtain the evolution equations for the respective expectation values as

$$\frac{\mathrm{d}}{\mathrm{d}t}\langle \hat{q}_i \rangle = \left\langle \frac{\partial \hat{H}}{\partial \hat{p}_i} \right\rangle, \tag{33}$$

$$\frac{\mathrm{d}}{\mathrm{d}t}\langle \hat{p}_i \rangle = -\left\langle \frac{\partial \hat{H}}{\partial \hat{q}_i} \right\rangle. \tag{34}$$

Furthermore, if we assume

$$\left\langle \frac{\partial \hat{H}\left(\hat{q}, \hat{p} \right)}{\partial \hat{q}_i} \right\rangle = \frac{\partial H\left(\langle q \rangle, \langle p \rangle \right)}{\partial \langle q_i \rangle}, \tag{35}$$

$$\left\langle \frac{\partial \hat{H}(\hat{q},\hat{p})}{\partial \hat{p}_i} \right\rangle = \frac{\partial H(\langle q\rangle,\langle p\rangle)}{\partial \langle p_i\rangle}, \tag{36}$$

where H is the classical Hamiltonian, we obtain

$$\frac{\mathrm{d}}{\mathrm{d}t}\langle \hat{q}_i\rangle = \frac{\partial H(\langle q\rangle,\langle p\rangle)}{\partial \langle p_i\rangle}, \tag{37}$$

$$\frac{\mathrm{d}}{\mathrm{d}t}\langle \hat{p}_i\rangle = -\frac{\partial H(\langle q\rangle,\langle p\rangle)}{\partial \langle q_i\rangle}. \tag{38}$$

We note that the above equations are in the form of Hamilton's equations of motion in classical mechanics.

Note that the assumptions in Equations (35) and (36) are justified if $\hat{H}$ is quadratic in $\hat{q}$ and $\hat{p}$ or if the dispersion of the measured $\hat{q}$ and $\hat{p}$ values are small. The dispersion is expected to be small for eigenstates and large for a superposition of states. Therefore, the superposition of states must evolve into eigenstates to ensure that the expectation values of quantum mechanical quantities obey the classical equations of motion.

3. Bell-Type Inequalities and the Kochen-Specker Theorem

In this section, we review Bell-type inequalities and the Kochen-Specker theorem. These theorems indicate that the world described by quantum mechanics is considerably different from the macroscopic world we are familiar with.

It has been experimentally confirmed [26]-[32] that quantum mechanical expectation values violate Bell-type inequalities, strongly suggesting that the quantum mechanical world is nonlocal or *nonseparable*. D'Espagnat [18] defined separability as follows: *If a physical system remains, during a certain time, mechanically* (*including electromagnetically, etc.*) *isolated from other systems, then the evolution of its properties during this whole time interval cannot be influenced by operations carried out on other systems*. Conversely, the Kochen-Specker theorem implies that quantum mechanics is counterfactually indefinite. Nevertheless, the meaning of counterfactual definiteness should be considered in relation to the nonlocality of quantum mechanics; specifically, the Kochen-Specker theorem forbids quantum mechanics to be locally counterfactually definite. In other words, quantum mechanics is not forbidden to be nonlocally counterfactually definite by Bell-type inequalities or the Kochen-Specker theorem. This fact is important to the consisitency of discussion in Subsection 4.2.

3.1. EPR-Bohm Experiment

First, we introduce the Einstein-Podolsky-Rosen (EPR)-Bohm experiment [33] [34], in which the spins of two spin 1/2 particles, labelled as 1 and 2 in **Figure 1**, are measured. The sum of their spins should be zero, and their initial state $|C\rangle$ can be written as

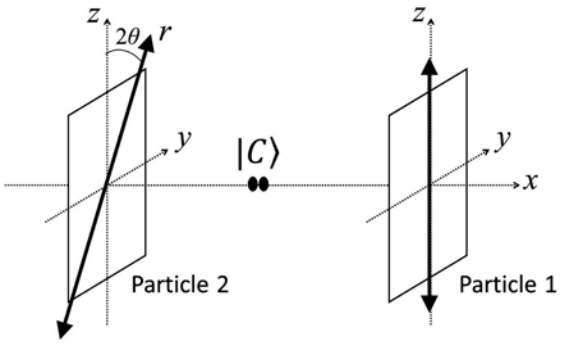

Figure 1. EPR-Bohm experiment.

$$|C\rangle = \frac{1}{\sqrt{2}}\left(|u\rangle_1|d\rangle_2 - |d\rangle_1|u\rangle_2\right), \tag{39}$$

where $|u\rangle_i$ and $|d\rangle_i$ $(i=1,2)$ are the spin eigenstates in the z direction. These satisfy

$$(\hat{\sigma}_z)_i|u\rangle_i = +\frac{\hbar}{2}|u\rangle_i, \tag{40}$$

$$(\hat{\sigma}_z)_i|d\rangle_i = -\frac{\hbar}{2}|d\rangle_i, \tag{41}$$

where $\hat{\sigma}_z$ is the spin operator in the z direction. The spin operator in the r direction, which is perpendicular to the direction of the particles' motion (*i.e.* along x direction) and makes an angle 2θ with the z direction in the yz-plane, is given by

$$\hat{\sigma}_r = \begin{pmatrix} \cos\theta & -\sin\theta \\ \sin\theta & \cos\theta \end{pmatrix} \hat{\sigma}_z \begin{pmatrix} \cos\theta & \sin\theta \\ -\sin\theta & \cos\theta \end{pmatrix}. \tag{42}$$

The eigenstates of $\hat{\sigma}_r$ are $|+\rangle_i$ and $|-\rangle_i$ $(i=1,2)$, given by

$$\begin{aligned} |+\rangle_i &= \cos\theta|u\rangle_i + \sin\theta|d\rangle_i, \\ |-\rangle_i &= -\sin\theta|u\rangle_i + \cos\theta|d\rangle_i, \end{aligned} \tag{43}$$

which satisfy the following equations:

$$(\hat{\sigma}_r)_i|+\rangle_i = +\frac{\hbar}{2}|+\rangle_i, \tag{44}$$

$$(\hat{\sigma}_r)_i|-\rangle_i = -\frac{\hbar}{2}|-\rangle_i. \tag{45}$$

By using Equation (43), $|C\rangle$ can be rewritten as

$$|C\rangle = \frac{1}{\sqrt{2}}\left(|+\rangle_1|-\rangle_2 - |-\rangle_1|+\rangle_2\right). \tag{46}$$

Let us suppose that two observers simultaneously perform measurements on the spins of particles 1 and 2 along the directions z and r, respectively. Rewriting $|C\rangle$ as

$$|C\rangle = \frac{1}{\sqrt{2}}\left[|u\rangle_1\left(\sin\theta|+\rangle_2 + \cos\theta|-\rangle_2\right) - |d\rangle_1\left(\cos\theta|+\rangle_2 - \sin\theta|-\rangle_2\right)\right], \tag{47}$$

we can easily calculate the probabilities of observing the spin combinations $\left(+\frac{\hbar}{2},+\frac{\hbar}{2}\right)$, $\left(+\frac{\hbar}{2},-\frac{\hbar}{2}\right)$, $\left(-\frac{\hbar}{2},+\frac{\hbar}{2}\right)$, and $\left(-\frac{\hbar}{2},-\frac{\hbar}{2}\right)$, which are given by

$$P_{(+,+)} \equiv \langle C|\left(|u\rangle\langle u|\right)_1\left(|+\rangle\langle +|\right)_2|C\rangle = \frac{1}{2}\sin^2\theta, \tag{48}$$

$$P_{(+,-)} \equiv \langle C|\left(|u\rangle\langle u|\right)_1\left(|-\rangle\langle -|\right)_2|C\rangle = \frac{1}{2}\cos^2\theta, \tag{49}$$

$$P_{(-,+)} \equiv \langle C|\left(|d\rangle\langle d|\right)_1\left(|+\rangle\langle +|\right)_2|C\rangle = \frac{1}{2}\cos^2\theta, \tag{50}$$

$$P_{(-,-)} \equiv \langle C|\left(|d\rangle\langle d|\right)_1\left(|-\rangle\langle -|\right)_2|C\rangle = \frac{1}{2}\sin^2\theta, \tag{51}$$

respectively.

It should be noted that these equations hold true for the measurements in which the angle between the spins of the two particles is 2θ.

3.2. Bell's Inequality and CHSH Inequality

3.2.1. Derivation

We examine the EPR-Bohm experiment in which the spin of particle 1 along directions *a* or *a'* and the spin of particle 2 along directions *b* or *b'* are measured. Let *A*, *A'*, *B*, and *B'* be the measured values of the spin divided by $\hbar/2$, respectively. In this section, we assume separability: the measurement of the spin of particle 1 never affects the measurement of the spin of particle 2 and vice versa. We also assume counterfactual definiteness: the spin value is determined separately before the measurement. In other words, each spin is assumed to have a definite value even if the measurement has not actually been performed. Thus, *A*, *A'*, *B*, and *B'* assume a definite value +1 or −1 each.

Based on these assumptions, we define the quantity *M* as

$$M \equiv AB - AB' + A'B + A'B' = A\left(B - B'\right) + A'\left(B + B'\right). \tag{52}$$

Note that because one of the terms on the right-hand side of Equation (52) is always 0 and the other term is always +2 or −2, *M* is always +2 or −2. Therefore, the average value $\bar{M}$ obtained after several measurements of *M* satisfies

$$-2 \le \bar{M} \le +2. \tag{53}$$

This is the CHSH inequality [35].

Next, we examine the case in which *A*, *A'*, *B*, and *B'* are probabilistically determined by hidden local variables [2] [18] [36]. Let us suppose that the measured values depend on a set of hidden local variables represented by λ. Then, *A*, *A'*, *B*, and *B'* depend on λ and assume a value of either +1 or −1 each. Let $P^A_{+(-)}(\lambda)$ be the probability that $A(\lambda)$ has a value $+1(-1)$ for a given λ. The average value $\bar{A}(\lambda)$ of $A(\lambda)$ is then given by

$$\bar{A}(\lambda) = P^A_+(\lambda) - P^A_-(\lambda). \tag{54}$$

Thus, $\bar{A}(\lambda)$ satisfies

$$-1 \le \bar{A}(\lambda) \le +1. \tag{55}$$

Similar inequalities are satisfied by the average values of A', B, and B'. The average value $\overline{AB}$ of AB can be written as

$$\begin{aligned}\overline{AB} &= \int \mathrm{d}\lambda\rho(\lambda)\left[P_+^A(\lambda)P_+^B(\lambda)+P_-^A(\lambda)P_-^B(\lambda)\right.\\ &\quad \left.-P_+^A(\lambda)P_-^B(\lambda)-P_-^A(\lambda)P_+^B(\lambda)\right]\\ &= \int \mathrm{d}\lambda\rho(\lambda)\bar{A}(\lambda)\bar{B}(\lambda),\end{aligned} \tag{56}$$

where $\rho(\lambda)$ is the probability distribution of λ, and $\overline{AB}$ satisfies

$$-1 \le \overline{AB} \le +1. \tag{57}$$

Again, similar inequalities are satisfied by the average values of AB', $A'B$ and $A'B'$.

Next, let us consider $\overline{AB}-\overline{AB'}$:

$$\begin{aligned}\overline{AB}-\overline{AB'} &= \int \mathrm{d}\lambda\rho(\lambda)\left[\bar{A}(\lambda)\bar{B}(\lambda)-\bar{A}(\lambda)\bar{B}'(\lambda)\right]\\ &= \int \mathrm{d}\lambda\rho(\lambda)\left[\bar{A}(\lambda)\bar{B}(\lambda)\pm\bar{A}(\lambda)\bar{B}(\lambda)\bar{A}'(\lambda)\bar{B}'(\lambda)\right.\\ &\quad \left.\mp\bar{A}(\lambda)\bar{B}(\lambda)\bar{A}'(\lambda)\bar{B}'(\lambda)-\bar{A}(\lambda)\bar{B}'(\lambda)\right]\\ &= \int \mathrm{d}\lambda\rho(\lambda)\bar{A}(\lambda)\bar{B}(\lambda)\left[1\pm\bar{A}'(\lambda)\bar{B}'(\lambda)\right]\\ &\quad -\int \mathrm{d}\lambda\rho(\lambda)\bar{A}(\lambda)\bar{B}'(\lambda)\left[1\pm\bar{A}'(\lambda)\bar{B}(\lambda)\right].\end{aligned} \tag{58}$$

From inequality (57), it follows that the absolute value of Equation (58) satisfies

$$\left|\overline{AB}-\overline{AB'}\right| \le \int \mathrm{d}\lambda\rho(\lambda)\left\{\left[1\pm\bar{A}'(\lambda)\bar{B}'(\lambda)\right]+\left[1\pm\bar{A}'(\lambda)\bar{B}(\lambda)\right]\right\}, \tag{59}$$

or

$$\left|\overline{AB}-\overline{AB'}\right| \le 2\pm\left[\overline{A'B'}+\overline{A'B}\right]. \tag{60}$$

Note that the fact that the sum of the spins of particles 1 and 2 is zero when $a=b$ has not been used in the derivation of inequality (60). If we take this into account and put $b'=a'$, then we can substitute $\overline{A'B'}=-1$ into inequality (60) to obtain

$$\left|\overline{AB}-\overline{AB'}\right| \le 1+\overline{A'B}. \tag{61}$$

This was the first inequality proposed by Bell in 1964 [37].

3.2.2. Contradiction between CHSH Inequality and Quantum Mechanics

In this section, we show that quantum-mechanical expectation values violate the CHSH inequality (53).

We calculate the quantum-mechanical expectation value $\langle M\rangle$ of M defined in Equation (52) using Equations (48) to (51). Let $a=z$ and α, β, and γ be the angles that directions a', b, and b' make with the z direction in the yz-plane, respectively. The expectation value of the first term of M then becomes

$$\begin{aligned}\langle AB\rangle &= P_{(+,+)}+P_{(-,-)}-P_{(+,-)}-P_{(-,+)}\\ &= \sin^2(\beta/2)-\cos^2(\beta/2)\\ &= -\cos\beta.\end{aligned} \tag{62}$$

The expectation values of the remaining three terms of M can be similarly calculated. Thus, $\langle M \rangle$ can be written as

$$\langle M \rangle = -\cos\beta + \cos\gamma - \cos(\beta - \alpha) - \cos(\gamma - \alpha). \tag{63}$$

We calculate the maximum and minimum values of $\langle M \rangle$ using Equation (63) to check whether it satisfies the CHSH inequality. $\langle M \rangle$ can be extremised with respect to α, β, and γ, thus yielding three critical conditions. Differentiating equation (63) with respect to α, we obtain

$$0 = \frac{\partial \langle M \rangle}{\partial \alpha} = -\sin(\beta - \alpha) - \sin(\gamma - \alpha), \tag{64}$$

which yields

$$\beta + \gamma = 2\alpha, \tag{65}$$

or

$$\beta - \gamma = \pi. \tag{66}$$

Differentiating with respect to β, we obtain

$$0 = \frac{\partial \langle M \rangle}{\partial \beta} = \sin\beta + \sin(\beta - \alpha), \tag{67}$$

which yields

$$2\beta = \alpha, \tag{68}$$

or

$$\alpha = \pi. \tag{69}$$

Finally, differentiating with respect to γ, we obtain

$$0 = \frac{\partial \langle M \rangle}{\partial \gamma} = -\sin\gamma + \sin(\gamma - \alpha), \tag{70}$$

which yields

$$\alpha = 0, \tag{71}$$

or

$$2\gamma - \alpha = \pi. \tag{72}$$

$\langle M \rangle$, as per Equation (63), has a maximum or minimum value when Equations (65), (68), and (72) are satisfied, such that

$$\langle M \rangle = -2\sqrt{2} \quad \text{when } (\alpha, \beta, \gamma) = (\pi/2, \pi/4, 3\pi/4), \tag{73}$$

$$\langle M \rangle = +2\sqrt{2} \quad \text{when } (\alpha, \beta, \gamma) = (\pi/2, -3\pi/4, -\pi/4). \tag{74}$$

Therefore, we can conclude that quantum-mechanical expectation values violate the CHSH inequality (53).

3.3. Wigner's Inequality and Its Variations

Note that we again assume counterfactual definiteness and nonseparability in the derivation of the inequalities in this section.

3.3.1. Wigner's Inequality

We re-examine the EPR-Bohm type experiment introduced in Section 3.1, where the spin was measured along two of the three directions: a, a' and a''. Let A and B be the definite values of the spin along a divided by $\hbar/2$ of particles 1 and 2, respectively. Similarly, A' and B' are the definite values along a', and A'' and B'' the definite values along a''. Let α be the angle between a and a', β between a' and a'', and γ between a'' and a. Moreover, let $P(A=+1,B'=+1)$ be the probability that $A=+1$ and $B'=+1$, and other probabilities can be defined similarly.

Note that because the sum of the spins of particles 1 and 2 along the same direction is zero, $P(A=+1,B'=+1)$ can be written as

$$\begin{aligned} &P(A=+1,B'=+1)\\ &=p(A=+1,A'=-1,B=-1,B'=+1)\\ &=p(A=+1,A'=-1,A''=+1,B=-1,B'=+1,B''=-1)\\ &\quad+p(A=+1,A'=-1,A''=-1,B=-1,B'=+1,B''=+1), \end{aligned} \tag{75}$$

where $p(A=+1,A'=-1,B=-1,B'=+1)$ is the probability that the definite values are $A=+1$, $A'=-1$, $B=-1$, and $B'=+1$, irrespective of whether they are measurable. Similarly,

$$\begin{aligned} &P(A=+1,B''=+1)\\ &=p(A=+1,A''=-1,B=-1,B''=+1)\\ &=p(A=+1,A'=+1,A''=-1,B=-1,B'=-1,B''=+1)\\ &\quad+p(A=+1,A'=-1,A''=-1,B=-1,B'=+1,B''=+1), \end{aligned} \tag{76}$$

and

$$\begin{aligned} &P(A''=+1,B'=+1)\\ &=p(A'=-1,A''=+1,B'=+1,B''=-1)\\ &=p(A=+1,A'=-1,A''=+1,B=-1,B'=+1,B''=-1)\\ &\quad+p(A=-1,A'=-1,A''=+1,B=+1,B'=+1,B''=-1). \end{aligned} \tag{77}$$

Using these equations, we obtain

$$\begin{aligned} &P(A=+1,B''=+1)+P(A''=+1,B'=+1)\\ &=p(A=+1,A'=+1,A''=-1,B=-1,B'=-1,B''=+1)\\ &\quad+p(A=+1,A'=-1,A''=-1,B=-1,B'=+1,B''=+1)\\ &\quad+p(A=+1,A'=-1,A''=+1,B=-1,B'=+1,B''=-1)\\ &\quad+p(A=-1,A'=-1,A''=+1,B=+1,B'=+1,B''=-1)\\ &=P(A=+1,B'=+1)\\ &\quad+p(A=+1,A'=+1,A''=-1,B=-1,B'=-1,B''=+1)\\ &\quad+p(A=-1,A'=-1,A''=+1,B=+1,B'=+1,B''=-1). \end{aligned} \tag{78}$$

Recalling that probability cannot be less than zero, we obtain Wigner's inequality [38], such that

$$P(A=+1,B''=+1)+P(A''=+1,B'=+1)\geq P(A=+1,B'=+1). \tag{79}$$

Using Equation (48) to confirm that the quantum-mechanical expectation value violates Wigner's inequality (79), we obtain

$$\sin^2\frac{\gamma}{2}+\sin^2\frac{\beta}{2}\geq\sin^2\frac{\alpha}{2}. \tag{80}$$

When $\alpha=2\beta=2\gamma$, inequality (80) becomes

$$2\sin^2\frac{\beta}{2}\geq\sin^2\beta. \tag{81}$$

Moreover, if we use

$$\sin^2\beta=4\sin^2\frac{\beta}{2}\cos^2\frac{\beta}{2}, \tag{82}$$

inequality (81) can be rewritten as

$$\sin^2\frac{\beta}{2}\geq 2\sin^2\frac{\beta}{2}\cos^2\frac{\beta}{2}. \tag{83}$$

The above inequality is violated when

$$-\frac{\pi}{2}<\beta<\frac{\pi}{2}\ \text{ except } \beta=0. \tag{84}$$

3.3.2. Mermin's Inequality

Mermin [39] suggested a variation of Wigner's inequality under the same conditions.

Mermin computed the probability that the spins of particles 1 and 2 measured in different directions have different signs. Let us consider separately the cases where 1) all of them have the same sign, that is, $A=A'=A''=\pm1$ or 2) two of them have the same sign and the other has a different sign. For example, $A=+1,\ A'=A''=-1$.

In case 1), it can be shown trivially that the probability of the spins of the two particles being different is 1. In case 2), the corresponding probability is 1/3. Therefore, the probability that the spins of particles 1 and 2 measured in different directions have different signs exists between 1 and 1/3. This can be expressed as

$$1\geq P(+1,-1)+P(-1,+1)\geq\frac{1}{3}. \tag{85}$$

However, when all the angles between a, a' and a'' are $2\pi/3$, then $P(+1,-1)+P(-1,+1)$ can be calculated using Equations (49) and (50), and becomes

$$P(+1,-1)+P(-1,+1)=\frac{1}{8}+\frac{1}{8}=\frac{1}{4}, \tag{86}$$

which shows that quantum mechanical probabilities violate Mermin's inequality.

3.3.3. Albert's Inequality

Albert [40] [41] also derived an inequality under the same conditions as Wigner's inequality.

Note that the number of combinations of $(A, A', A''; B, B', B'')$ is 8 considering that $A = -B$, $A' = -B'$ and $A'' = -B''$. These are

$$\begin{aligned}
&(+1,+1,+1;-1,-1,-1)\\
&(+1,+1,-1;-1,-1,+1)\\
&(+1,-1,+1;-1,+1,-1)\\
&(-1,+1,+1;+1,-1,-1)\\
&(+1,-1,-1;-1,+1,+1)\\
&(-1,+1,-1;+1,-1,+1)\\
&(-1,-1,+1;+1,+1,-1)\\
&(-1,-1,-1;+1,+1,+1)
\end{aligned} \tag{87}$$

As can be easily checked, each of the above combinations satisfies at least one of the following three conditions: $A = -B', A' = -B''$ and $A'' = -B$. Therefore, the sum of the probabilities that one of these three conditions is satisfied is 1 or more. In other words, we can write

$$\begin{aligned}
1 \le\ & P(A = +1, B' = -1) + P(A' = +1, B'' = -1) + P(A'' = +1, B = -1)\\
& + P(A = -1, B' = +1) + P(A' = -1, B'' = +1) + P(A'' = -1, B = +1),
\end{aligned} \tag{88}$$

where at least one term on the right-hand side must be 1/6 or more. However, when all the angles between a, a' and a'' are $2\pi/3$, every term on the right-hand side of condition (88) is calculated to be 1/8 using Equations (49) and (50). This again shows that quantum mechanical expectation values violate Albert's inequality (88).

3.4. Kochen-Specker Theorem

In the previous section, we derived a series of Bell-type inequalities assuming not only separability but also counterfactual definiteness. Because quantum mechanical expectation values violate these inequalities, it implies that quantum mechanics must be non-separable or counterfactually indefinite or both. Interestingly, the Kochen-Specker theorem [42] solely requires the assumption of counterfactual definiteness.

First, we define the function $f(\hat{A})$ of an operator $\hat{A}$ as follows: $\hat{A}$ is expanded using its eigenvalues a_i and the projection operators $\hat{P}_i^A$ on the respective states corresponding to a_i such that

$$\hat{A} = \sum_i a_i \hat{P}_i^A. \tag{89}$$

Then, $f(\hat{A})$ can be defined as

$$f(\hat{A}) \equiv \sum_i f(a_i) \hat{P}_i^A. \tag{90}$$

Let us suppose that every physical quantity A has a definite value[1] $[A]$ belonging to the spectrum of its corresponding operator $\hat{A}$. In this section, we introduce an assumption that we call "FUNC", which plays an important role in

[1]Note that in this subsection, definite values are denoted with [ ].

the derivation of the Kochen-Specker theorem. According to FUNC, if an operator $\hat{B}$ is defined as $\hat{B} = f\left(\hat{A}\right)$, then the definite values [*A*] and [*B*] satisfy $[B] = f([A])$.

Using FUNC, we derive a sum rule for the commuting operators $\hat{A}$ and $\hat{B}$ in an *N*-dimensional Hilbert space. We also define an operator $\hat{C}$, whose eigenvectors include all the vectors that form an orthonormal basis by simultaneously diagonalising $\hat{A}$ and $\hat{B}$. $\hat{C}$ can be expanded as

$$\hat{C} = \sum_{i=1}^{N} c_i \hat{P}_i^C, \tag{91}$$

where c_i represents the eigenvalues of $\hat{C}$ and $\hat{P}_i^C$ represents the projection operators onto the eigenvectors corresponding to c_i. If functions *f* and *g* satisfy $\hat{A} = f\left(\hat{C}\right)$ and $\hat{B} = g\left(\hat{C}\right)$, then $\hat{A} + \hat{B}$ can be written as

$$\begin{aligned} \hat{A} + \hat{B} &= f\left(\hat{C}\right) + g\left(\hat{C}\right) \\ &= \sum_{i=1}^{N} f(c_i)\hat{P}_i^C + \sum_{i=1}^{N} g(c_i)\hat{P}_i^C \\ &= \sum_{i=1}^{N} h(c_i)\hat{P}_i^C \\ &= h\left(\hat{C}\right), \end{aligned} \tag{92}$$

where

$$h(c_i) \equiv f(c_i) + g(c_i). \tag{93}$$

Therefore, the definite values of the left- and right-hand sides of the above equation also satisfy

$$[A + B] = \left[h(C)\right]. \tag{94}$$

On the other hand, the sum of $[A]$ and $[B]$ becomes

$$\begin{aligned} [A] + [B] &= \left[f(C)\right] + \left[g(C)\right] \\ &= f([C]) + g([C]) \\ &= h([C]) \\ &= \left[h(C)\right]. \end{aligned} \tag{95}$$

Note that the second and fourth steps in Equation (95) are a consequence of FUNC. Thus, combining Equations (94) and (95) we obtain the sum rule

$$[A + B] = [A] + [B]. \tag{96}$$

The Kochen-Specker theorem can be proved using Equation (96). Let $|i\rangle, i = 1, \cdots, M\ (M \le N)$ be the orthonormal eigenstates of a given physical quantity, and

$$\hat{P}_i \equiv |i\rangle\langle i| \tag{97}$$

be the projection operator onto $|i\rangle$, which satsifies

$$I = \sum_{i=1}^{M} P_i, \tag{98}$$

where $\hat{I}$ is the identity operator. By applying the sum rule (given by Equation

(96)) on Equation (98), we obtain

$$[I]=\sum_{i=1}^{M}[P_i]. \tag{99}$$

Note that because all definite values belong to the spectrum of their corresponding operators, $[I]=1$ and $[P_i]=0$ or 1. Thus, one $[P_i]$ must be 1 and the remaining 0 to satisfy Equation (99). In summary, if it is possible to assign every physical quantity a definite value satisfying FUNC, then one of the projection operators onto its eigenstate must be assigned a definite value 1 and the remaining must be assigned a definite value 0. Kochen and Specker [42] proved that it is not possible to assign such definite values to all physical quantities.

We reconsider the assumption FUNC. In FUNC, it is not possible to know which physical quantities are being observed simultaneously. Although it may seem natural that the definite values satisfy FUNC, Bell [43] insisted that *contextual definite values* do not need to satisfy FUNC. This implies that the Kochen-Specker theorem does not deny the existence of contextual definite values. We can say that the spin in each direction has a contextual definite value in the EPR-Bohm experiment introduced in Section 3.1, provided the definite value of the spin in the r direction of particle 2 varies in accordance with the direction of the spin of particle 1, which was measured simultaneously. Furthermore, it is known that quantum mechanics must be nonlocal under such an assumption [44] [45].

3.5. Nonlocality and Weak Values

In view of the discussion in the previous sections, we need to check whether the counterfactual definiteness assumed during the derivations of the Bell-type inequalities is local. We consider the case in which the observed values are determined by local hidden variables, as shown in Equation (54). Note that Equation (58) is necessary for the derivation of CHSH inequality, and the density matrices for AB and AB' must be the same to satisfy Equation (58). Therefore, we can conclude that the counterfactual definiteness assumed in this case is local. Thus, nonlocal counterfactual definiteness (*i.e.* existence of contextual definite values) is not forbidden in the above discussion. Conversely, if quantum mechanics is counterfactually indefinite, then we need to introduce nonlocality to explain the correlation between EPR pairs. Therefore, quantum mechanics must be nonlocal irrespective of whether it is counterfactually definite or indefinite, although it may seem difficult to appreciate this fact.

Weak measurements [46] clearly demonstrate the nonlocality of quantum mechanics. As confirmed by many experiments, the measured values in a weak measurement agree with the corresponding weak values. Nevertheless, the physical meaning of these concepts remained unclear for a long time. However, if we consider the nonlocality of quantum mechanics, then the physical meaning of weak measurements and weak values can be completely understood within the framework of a conventional quantum mechanical approach [47].

4. Decoherence as an Inherent Characteristic of Quantum Mechanics

As stated in the Introduction, most studies in this field have yielded a negative answer to the question regarding whether the measurement process can be explained within the framework of pure quantum mechanics. However, in this section, we demonstrate that the answer is affirmative, that is, we can indeed explain the measurement process within the framework of pure quantum mechanics. We propose a new decoherence theory, in which the uncertainty of microscopic objects gives rise to decoherence as an inherent characteristic of pure quantum mechanics. Note that because this decoherence exists prior to a measurement, the eigenstate-eigenvalue link can be maintained. Moreover, we do not intend to explain the nonlocality or counterfactual indefiniteness of quantum mechanics by means of other concepts, as it is beyond the scope of this work. However, we do attempt to illustrate how the measurement process can be understood within the scope of pure quantum mechanics.

We examine three experiments in this section. First, in Section 4.1, we examine a Stern-Gerlach-like experiment with an electron to illustrate our idea of decoherence. In Section 4.2, we apply our theory to an EPR pair of electrons and show that the correlation between spatially separated particles is not a result of wave packet collapse or similar processes. In Section 4.3, the double-slit experiment with electrons is examined to demonstrate the effectiveness of our theory for cases with continuous eigenvalues. This experiment also illuminates how pure quantum mechanics is able to demonstrate that electrons behave as interfering particles, that is, particles whose detection rate is consistent with interference.

4.1. Stern-Gerlach-Like Experiment

We examine a Stern-Gerlach-like experiment with an electron S whose spin is measured in the z direction, as shown in **Figure 2**. Note that $|+\rangle$ and $|-\rangle$ are the eigenstates of the electron with eigenvalues $+\hbar/2$ and $-\hbar/2$, respectively. S initially travels along the x-axis and enters an inhomogeneous magnetic field along the z-axis, where a magnetic force acts on it. When S exits the magnetic field, its momentum in the z direction is $-p$ if its spin is $+\hbar/2$ and $+p$ if the spin is $-\hbar/2$. We define the momentum eigenstates $|-p\rangle$ and $|+p\rangle$ with eigenvalues $-p$ and $+p$, respectively. Furthermore, $|0\rangle$ is defined as the momentum eigenstate having 0 momentum. Note that because the spin and momentum operators along the same direction commute with each other, the state of S can be described as a simultaneous eigenstate of these two operators. We also define a unitary operator $\hat{U}_S$ that represents the interaction between S and the magnetic field, such that

$$\hat{U}_S|+\rangle|0\rangle = |+\rangle|-p\rangle, \tag{100}$$

$$\hat{U}_S|-\rangle|0\rangle = |-\rangle|+p\rangle. \tag{101}$$

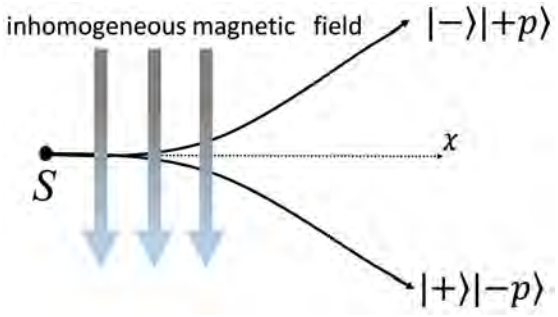

Figure 2. Stern-Gerlach-like experiment.

We define the initial state $|I_S\rangle$ of S to be

$$|I_S\rangle \equiv \frac{1}{\sqrt{2}}(|+\rangle+|-\rangle)|0\rangle. \tag{102}$$

The state $|O_S\rangle$ after the interaction between S and the magnetic field can be written as

$$|O_S\rangle = \hat{U}_S|I_S\rangle = \frac{1}{\sqrt{2}}(|+\rangle|-p\rangle+|-\rangle|+p\rangle). \tag{103}$$

When S reaches one of the detectors, the entire event is recorded. If we ignore the evolution of S's state between the magnetic field and the detector, then $|O_S\rangle$ is the state of S just before detection. The *naïve* density matrix $\hat{\rho}_{S0}$ of S is defined as

$$\hat{\rho}_{S0} = |O_S\rangle\langle O_S|. \tag{104}$$

Note that $\hat{\rho}_{S0}$ and $|O_S\rangle$ differ in physical contents, as explained in the following.

Next, we consider the uncertainty relation. Because we want to measure S's momentum in the z direction, we must allow some uncertainty in its position in the same direction. To account for this uncertainty, we introduce the density matrix $\hat{\rho}_S(\zeta)$ of S translated to a distance ζ in the z direction, which is defined as

$$\hat{\rho}_S(\zeta) \equiv \hat{T}_z(\zeta)\hat{\rho}_{S0}\hat{T}_z^{\dagger}(\zeta), \tag{105}$$

where $\hat{T}_z(\zeta)$ is the translation operator in the z direction. $\hat{T}_z(\zeta)$ satisfies the following equation

$$\langle z+\zeta|\hat{T}_z(\zeta)|O_S\rangle = \langle z|O_S\rangle \tag{106}$$

and is defined by

$$\hat{T}_z(\zeta) \equiv \exp\left(-\frac{i\hat{P}_z\zeta}{\hbar}\right) \tag{107}$$

for the momentum operator $\hat{P}_z$ in the z direction.

Next, we define the average density matrix $\hat{\rho}_{Sav}$ of S as

$$\hat{\rho}_{Sav} \equiv \frac{1}{2\Delta z}\int_{-\Delta z}^{\Delta z} \mathrm{d}\zeta\, \hat{\rho}_S(\zeta), \tag{108}$$

where $2\Delta z$ is the uncertainty in S's position along the z direction and from Equation (105) we can write

$$\begin{aligned}\hat{\rho}_S(\zeta) = \frac{1}{2}\left(\exp\left(\frac{+ip\zeta}{\hbar}\right)|+\rangle|-p\rangle + \exp\left(\frac{-ip\zeta}{\hbar}\right)|-\rangle|+p\rangle\right)\\ \times\left(\langle+p|\langle-|\exp\left(\frac{+ip\zeta}{\hbar}\right) + \langle-p|\langle+|\exp\left(\frac{-ip\zeta}{\hbar}\right)\right).\end{aligned} \tag{109}$$

We want to know what is observed by the macroscopic detector; hence, we set

$$\hbar \ll \Delta p\Delta z = 2p\Delta z, \tag{110}$$

which leads to

$$\frac{1}{2\Delta z}\int_{-\Delta z}^{\Delta z} d\zeta \exp\left(\frac{\pm 2ip\zeta}{\hbar}\right) \simeq 0. \tag{111}$$

Therefore, the average density matrix, which describes the state of S to be detected, loses its interference terms and becomes

$$\hat{\rho}_{Sav} = \frac{1}{2}\left(|+\rangle|-p\rangle\langle-p|\langle+| + |-\rangle|+p\rangle\langle+p|\langle-|\right). \tag{112}$$

The above equation demonstrates the decoherence prior to the measurement process.

Note that $\hat{\rho}_{Sav}$ is not a consequence of the nonunitary (or unitary) time evolution from the state $|O_S\rangle$, but $\hat{\rho}_{Sav}$ is exactly the density matrix corresponding to $|O_S\rangle$ to be detected.

Note also that if condition (110) is weakened, then the interference terms in $\hat{\rho}_{Sav}$ would be retained to a certain extent. Performing the integral Equation in (108), we obtain

$$\begin{aligned}\hat{\rho}_{Sav} = \frac{\hbar}{4p\Delta z}\sin\left(\frac{2p\Delta z}{\hbar}\right)\left(|+\rangle|-p\rangle + |-\rangle|+p\rangle\right)\left(\langle-p|\langle+| + \langle+p|\langle-|\right)\\ + \frac{1}{2}\left(1 - \frac{\hbar}{2p\Delta z}\sin\left(\frac{2p\Delta z}{\hbar}\right)\right)\left(|+\rangle|-p\rangle\langle-p|\langle+| + |-\rangle|+p\rangle\langle+p|\langle-|\right).\end{aligned} \tag{113}$$

Because we do not adopt the projection postulate in this study, we observe in accordance with the eigenstate-eigenvalue link that the first term on the right-hand side of this equation does not contribute to the probability that S will be detected as a *particle* with momentum $-p$ or $+p$ in the z direction. Therefore, there is a $1-(\hbar/2p\Delta z)\sin(2p\Delta z/\hbar)$ probability, which vanishes in the limit $\Delta z \to 0$, that S will be detected as a particle with momentum $-p$ or $+p$ in the z direction if we observe its position with an uncertainty $2\Delta z$.

In studies that propose that the environment causes decoherence, an equation similar to Equation (112) is obtained by taking the partial trace of Equation (104). The state described by Equation (104) is a pure state; hence, the state described by the density matrix after the partial trace is an improper mixed state, which only provides the probability distribution of the outcome. By contrast, Equation (112) represents a proper mixed state and describes the *state* itself to be detected with the macroscopic detector. Therefore, we can conclude that the

state to be detected is not given by Equation (103) but is either $|+\rangle|-p\rangle$ or $|-\rangle|+p\rangle$. In this calculation, we have not used any additional postulates such as the projection postulate. Thus, it is worth noting that this decoherence is not a result of the interaction between S and the detector or other environmental factors, but is rather due to the uncertainty relation.

Note also that the density matrix of S is not always written as shown in Equation (112). If we want to measure another observable of S, then we need to take an average the density matrix over its conjugate observables. Consequently, we can obtain the average density matrix that has a diagonal form in this observable, as illustrated in the remainder of this section.

Let us suppose that an ideal macroscopic measuring device M that measures S's energy is employed instead of the aforementioned detector. Furthermore, S is prepared in its neutral state $|r\rangle$ and is at either of the two energy levels E_+ and E_-, in accordance with its spin, after it exits the magnetic field. $\hat{V}$ is a unitary operator that transforms $|r\rangle$ to $|E_+\rangle$ or $|E_-\rangle$, which are the eigenstates whose eigenvalues are E_+ and E_-, respectively. Thus, we have

$$\hat{V}|+\rangle|r\rangle = |+\rangle|E_+\rangle, \tag{114}$$

$$\hat{V}|-\rangle|r\rangle = |-\rangle|E_-\rangle. \tag{115}$$

The initial state of the unified system is represented by $|J\rangle$, which is defined as

$$|J\rangle \equiv \frac{1}{\sqrt{2}}\left(|+\rangle + |-\rangle\right)|r\rangle. \tag{116}$$

Then, the state of S just prior to detection by M can be written as

$$\hat{V}|J\rangle = \frac{1}{\sqrt{2}}\left(|+\rangle|E_+\rangle + |-\rangle|E_-\rangle\right), \tag{117}$$

and its density matrix $\hat{\rho}_{J0}$ is given by

$$\hat{\rho}_{J0} = \hat{V}|J\rangle\langle J|\hat{V}^\dagger. \tag{118}$$

Note that because we want to measure the energy of S, we require a time interval. Therefore, we define the density matrix $\hat{\rho}_{Jav}$ averaged over the measurement time interval $2\Delta t$ as

$$\hat{\rho}_{Jav} \equiv \frac{1}{2\Delta t}\int_{-\Delta t}^{\Delta t} \mathrm{d}\tau \exp\left(-\frac{i\hat{H}\tau}{\hbar}\right)\hat{\rho}_{J0}\exp\left(+\frac{i\hat{H}\tau}{\hbar}\right), \tag{119}$$

where $\hat{H}$ is the Hamiltonian density of S, which satisfies

$$\hat{H}|E_+\rangle = E_+|E_+\rangle, \tag{120}$$

$$\hat{H}|E_-\rangle = E_-|E_-\rangle. \tag{121}$$

Therefore, we can write

$$\hat{\rho}_{Jav} = \frac{1}{2\Delta t}\int_{-\Delta t}^{\Delta t} \mathrm{d}\tau \hat{\rho}_J(\tau) \tag{122}$$

with

$$\hat{\rho}_J(\tau)=\frac{1}{2}\left(\exp\left(\frac{-iE_+\tau}{\hbar}\right)|+\rangle|E_+\rangle+\exp\left(\frac{-iE_-\tau}{\hbar}\right)|-\rangle|E_-\rangle\right)\times\left(\langle E_-|\langle-|\exp\left(\frac{iE_-\tau}{\hbar}\right)+\langle E_+|\langle+|\exp\left(\frac{iE_+\tau}{\hbar}\right)\right). \tag{123}$$

To obtain a macroscopic result, we set

$$(E_+-E_-)\Delta t\gg\hbar, \tag{124}$$

which leads to

$$\frac{1}{2\Delta t}\int_{-\Delta t}^{\Delta t}\mathrm{d}\tau\exp\left(\frac{\pm i(E_+-E_-)\tau}{\hbar}\right)\simeq 0. \tag{125}$$

Therefore, the average density matrix in this case becomes

$$\hat{\rho}_{Jav}=\frac{1}{2}\left(|+\rangle|E_+\rangle\langle E_+|\langle+|+|-\rangle|E_-\rangle\langle E_-|\langle-|\right). \tag{126}$$

Thus, we observe that equation (126) is diagonal in $\mathcal{S}$'s energy.

4.2. EPR-Bohm Experiment

In this section, we re-examine the EPR-Bohm experiment, which was briefly reviewed in Section 3.1. We adopt the same setup as in the previous section, where particles 1 and 2 enter inhomogeneous magnetic fields along the z and r directions, respectively. When the particles exit the magnetic fields, each particle gains a momentum in its respective direction of the magnetic field. Initially, neither particle has a momentum in the z or r direction. If we define the zero momentum state of the particles as $|0\rangle_i$, then the state $|I_C\rangle$ before entering the magnetic field can be written as

$$|I_C\rangle=|C\rangle|0\rangle_1|0\rangle_2, \tag{127}$$

where $|C\rangle$ is defined in Equation (39). The state $|O_C\rangle$ after interaction between the electrons and magnetic fields becomes

$$\begin{aligned}|O_C\rangle&=\hat{U}_C|I_C\rangle\\&=\frac{1}{\sqrt{2}}\Big[|u\rangle_1|-p\rangle_1\left(\sin\theta|+\rangle_2|-q\rangle_2+\cos\theta|-\rangle_2|+q\rangle_2\right)\\&\quad-|d\rangle_1|+p\rangle_1\left(\cos\theta|+\rangle_2|-q\rangle_2-\sin\theta|-\rangle_2|+q\rangle_2\right)\Big],\end{aligned} \tag{128}$$

where the unitary operator $\hat{U}_C$ represents the interaction, and p and q are the momenta in the z and r directions, respectively. As discussed in the previous section, we must allow some uncertainty in the position of the particles along the corresponding directions. Therefore, the density matrix $\hat{\rho}_{Cav}$ that describes the state to be measured is defined as

$$\hat{\rho}_{Cav}\equiv\frac{1}{4\Delta z\Delta r}\int_{-\Delta z}^{\Delta z}\mathrm{d}\zeta\int_{-\Delta r}^{\Delta r}\mathrm{d}\xi\hat{\rho}_C(\zeta,\xi), \tag{129}$$

where $\hat{\rho}_C(\zeta,\xi)$ is the density matrix of particle 1 translated to a distance ζ in the z direction and particle 2 translated to a distance ξ in the r direction. By using

$$\hat{T}_{1z}(\zeta) \equiv \exp\left(-\frac{i\hat{P}_{1z}\zeta}{\hbar}\right), \tag{130}$$

$$\hat{T}_{2r}(\xi) \equiv \exp\left(-\frac{i\hat{P}_{2r}\xi}{\hbar}\right), \tag{131}$$

where $\hat{P}_{1z}$ and $\hat{P}_{2r}$ are the momentum operators of particle 1 in the z direction and particle 2 in the r direction, respectively, and $\hat{\rho}_C(\zeta,\xi)$ can be written as

$$\hat{\rho}_C(\zeta,\xi) \equiv \hat{T}_{1z}(\zeta)\hat{T}_{2r}(\xi)|O_C\rangle\langle O_C|\hat{T}_{2r}^{\dagger}(\xi)\hat{T}_{1z}^{\dagger}(\zeta). \tag{132}$$

Similar to the previous section, because we want to know what is observed by the macroscopic detectors, we set

$$\hbar \ll p\Delta z, \ \ \hbar \ll q\Delta r, \tag{133}$$

which leads to

$$\frac{1}{2\Delta z}\int_{-\Delta z}^{\Delta z} \mathrm{d}\zeta \exp\left(\frac{\pm 2ip\zeta}{\hbar}\right) \simeq 0, \tag{134}$$

$$\frac{1}{2\Delta r}\int_{-\Delta r}^{\Delta r} \mathrm{d}\xi \exp\left(\frac{\pm 2iq\xi}{\hbar}\right) \simeq 0. \tag{135}$$

Therefore, the interference terms disappear and the average density matrix takes a form similar to that in Equation (112):

$$\begin{aligned}\hat{\rho}_{Cav} = \frac{1}{2}\Big[&\sin^2\theta\left(|u\rangle|-p\rangle\langle -p|\langle u|\right)_1\left(|+\rangle|-q\rangle\langle -q|\langle +|\right)_2 \\ &+\cos^2\theta\left(|u\rangle|-p\rangle\langle -p|\langle u|\right)_1\left(|-\rangle|+q\rangle\langle +q|\langle -|\right)_2 \\ &+\cos^2\theta\left(|d\rangle|+p\rangle\langle +p|\langle d|\right)_1\left(|+\rangle|-q\rangle\langle -q|\langle +|\right)_2 \\ &+\sin^2\theta\left(|d\rangle|+p\rangle\langle +p|\langle d|\right)_1\left(|-\rangle|+q\rangle\langle +q|\langle -|\right)_2\Big].\end{aligned} \tag{136}$$

Because Equation (136) describes a proper mixed state, the state to be detected is not a superposition but rather *one* of the following states: $\left(|u\rangle|-p\rangle\right)_1\left(|+\rangle|-q\rangle\right)_2$, $\left(|u\rangle|-p\rangle\right)_1\left(|-\rangle|+q\rangle\right)_2$, $\left(|d\rangle|+p\rangle\right)_1\left(|+\rangle|-q\rangle\right)_2$, and $\left(|d\rangle|+p\rangle\right)_1\left(|-\rangle|+q\rangle\right)_2$. It is worth noting that the correlation between the spins of the two particles should not be a result of the measurement process, as it is with a wave packet collapse, because Equation (136) represents the density matrix of the electrons *prior* to the measurement process. Therefore, we should not regard the EPR experiment as evidence for instantaneous propagation during a wave packet collapse.

Conversely, we need to consider the relation between the discussions in this and the previous section. Note that because we can obtain only one average density matrix for an observed pair of electrons, as discussed earlier, we do not need to assume that the state prior to the measurement possesses a definite value of the spin in each direction. In other words, the probable counterfactual definiteness is not local but contextual. As discussed in the previous section, contextual counterfactual definiteness is not forbidden by Bell-type inequalities or the Kochen-Specker theorem. The spin in either direction is not fixed in the initial state

given by Equation (39), whereas the spin of each electron in the respective directions is fixed in state described by Equation (136). The transformation between Equations (39) and (136) is owing to the uncertainty relation. However, as stated in Section 1, we do not intend to explain the nonlocality of quantum mechanics by means of other concepts. We only attempt to illustrate how measurement processes can be understood within the scope of pure quantum mechanics in this study.

4.3. Double-Slit Experiment

In this section, we examine the double-slit experiment, where electrons are emitted from a source at certain time intervals (see Figure 3). The electrons travel along the *x*-axis through a double slit in the $x=0$ plane and eventually arrive somewhere on the screen in the $x=L$ plane. The slits are separated in the *z* direction such that the two slits are positioned at $z=z_1$ and $z=z_2$. We define the eigenstate $|z\rangle$ of the *z* coordinate operator $\hat{z}$ as

$$\hat{z}|z\rangle = z|z\rangle. \tag{137}$$

Moreover, we define $|\psi\rangle$ as the state of the electron at $x=X\ (0\le X<L)$, and $|\psi_1\rangle$ and $|\psi_2\rangle$ as the states obtained after the electron passes through slits 1 and 2, respectively. Thus,

$$|\psi\rangle = |\psi_1\rangle + |\psi_2\rangle \tag{138}$$

The wave function $\psi(z)$ is defined as

$$|\psi\rangle = \int_{-\infty}^{\infty} \mathrm{d}z\, \psi(z)|z\rangle, \tag{139}$$

with the normalisation

$$\int_{-\infty}^{\infty} \mathrm{d}z |\psi(z)|^2 = 1. \tag{140}$$

The probability density that the electron is observed at $x=X$, $z=z_0$ is given by

$$\begin{aligned}\langle z_0\rangle &= \langle\psi|z_0\rangle\langle z_0|\psi\rangle \\ &= \int \mathrm{d}z \int \mathrm{d}z'\, \psi^*(z')\psi(z)\langle z'|z_0\rangle\langle z_0|z\rangle \\ &= |\psi(z_0)|^2.\end{aligned} \tag{141}$$

$\psi_1(z)$ and $\psi_2(z)$ can be defined in the same way as in Equation (139), which gives

$$|\psi_1\rangle = \int_{-\infty}^{\infty} \mathrm{d}z\, \psi_1(z)|z\rangle, \tag{142}$$

$$|\psi_2\rangle = \int_{-\infty}^{\infty} \mathrm{d}z\, \psi_2(z)|z\rangle. \tag{143}$$

Then, we have

$$\psi(z) = \psi_1(z) + \psi_2(z), \tag{144}$$

and the probability density $|\psi(z_0)|^2$ is written as

$$|\psi(z_0)|^2 = |\psi_1(z_0)|^2 + |\psi_2(z_0)|^2 + 2\Re\left(\psi_1(z_0)\psi_2^*(z_0)\right). \tag{145}$$

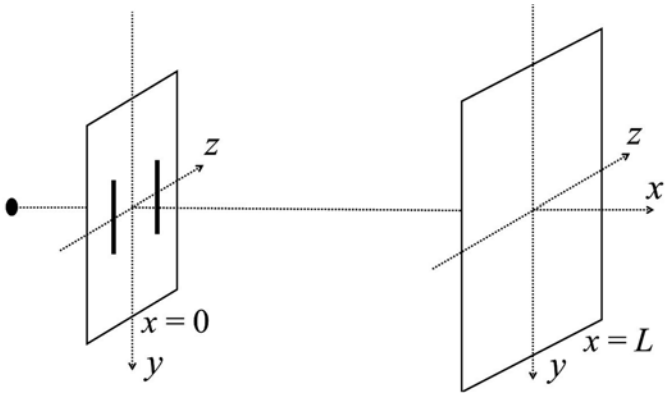

Figure 3. Double-slit experiment.

4.3.1. Decoherence on the Screen

In this section, the electrons are not assumed to be observed just after passing through the slits. Although the interference terms are included in the probability density $|\psi(z)|^2$, each electron behaves as a particle on the screen. Therefore, we illustrate here that the density matrix of the electrons to be observed on the screen is not given by $|\psi\rangle\langle\psi|$ but is rather proportional to

$$\int \mathrm{d}z |\psi(z)|^2 |z\rangle\langle z|. \tag{146}$$

In contrast to the discussion in the previous sections, we need to allow some uncertainty in the momentum in the z direction because we want to know the position in this direction. Therefore, we define the average density matrix $\hat{\rho}_{\psi av}$ that describes the state of the electron to be observed on the screen as

$$\hat{\rho}_{\psi av} \equiv \frac{1}{2h\Delta p}\int_{-\Delta p}^{\Delta p} \mathrm{d}\pi \hat{\rho}_{\psi}(\pi), \tag{147}$$

where $\hat{\rho}_{\psi}(\pi)$ is defined as

$$\hat{\rho}_{\psi}(\pi) \equiv \hat{\mathcal{T}}(\pi)|\psi\rangle\langle\psi|\hat{\mathcal{T}}^{\dagger}(\pi), \tag{148}$$

with

$$\hat{\mathcal{T}}(\pi) = \exp\left(\frac{i\hat{z}\pi}{\hbar}\right). \tag{149}$$

$\hat{\mathcal{T}}(\pi)$ is the operator that transforms the momentum and satisfies

$$\langle p+\pi|\hat{\mathcal{T}}(\pi)|\psi\rangle = \langle p|\psi\rangle, \tag{150}$$

where $|p\rangle$ is the eigenstate of the momentum in the z direction. Thus, we can write

$$\hat{\rho}_{\psi av} = \int_{-\Delta p}^{\Delta p} \frac{\mathrm{d}\pi}{2h\Delta p}\int \mathrm{d}z \int \mathrm{d}z' \psi^*(z')\psi(z)\exp\left(\frac{i(z-z')\pi}{\hbar}\right)|z\rangle\langle z'|. \tag{151}$$

In this experiment, we want to know where the electron impinges on the screen, therefore we set

$$\hbar \ll (z-z')\Delta p, \tag{152}$$

which leads to

$$\int_{\Delta p}^{\infty} \mathrm{d}\pi \exp\left(\frac{i(z-z')\pi}{\hbar}\right) = 0. \tag{153}$$

Using the above equation, we can introduce a delta-function in Equation (151) as follows:

$$\frac{1}{2\Delta p}\int_{-\Delta p}^{\Delta p} \mathrm{d}\pi \exp\left(\frac{i(z-z')\pi}{\hbar}\right) \sim \frac{1}{\delta(0)}\int_{-\infty}^{\infty} \mathrm{d}\pi \exp\left(\frac{i(z-z')\pi}{\hbar}\right) = \frac{h}{\delta(0)}\delta(z-z'), \tag{154}$$

such that Equation (151) becomes

$$\hat{\rho}_{\psi av} = \frac{1}{\delta(0)}\int \mathrm{d}z \int \mathrm{d}z' \psi^*(z')\psi(z)\delta(z-z')|z\rangle\langle z'| = \frac{1}{\delta(0)}\int \mathrm{d}z |\psi(z)|^2 |z\rangle\langle z|. \tag{155}$$

Note that Equation (155) is the desired form of the density matrix. The state that Equation (155) describes is a proper mixture, and hence, we can predict that each electron will behave as a particle. However, because $|\psi(z)|^2$ is a probability density that includes the interference terms, the electrons form a striped interference pattern when they impinge on the screen.

4.3.2. Decoherence Near the Slits

Next, we examine the case in which the electrons are assumed to be observed near either of the slits, namely, at $x = X \simeq 0$. In this case,

$$\psi_1(z)\psi_2^*(z) = 0, \tag{156}$$

which follows from the definitions of $\psi_1(z)$ and $\psi_2(z)$. Therefore, equation (155) becomes

$$\hat{\rho}_{\psi av} = \frac{1}{\delta(0)}\int \mathrm{d}z \left(|\psi_1(z)|^2 + |\psi_2(z)|^2\right)|z\rangle\langle z|, \tag{157}$$

which shows that the interference terms have disappeared. If we now observe the electron on the screen again, its probability density is no longer given by $|\psi(z)|^2$ but rather by $|\psi_1(z)|^2 + |\psi_2(z)|^2$.

4.4. Summary

We examined three fundamental experiments in this work. We studied the Stern-Gerlach-like experiment to explain how the uncertainty relation between the position and momentum of a particle introduces decoherence prior to a measurement. The EPR-Bohm experiment was considered to conclude that the correlation of the EPR pair is not a consequence of the instantaneous propagation during a wave function collapse. We also discussed its relation to the contextual counterfactual definiteness of quantum mechanics. Finally, we showed that our theory can be applied to experiments with continuous eigenvalues, such as the double-slit experiment with electrons. Thus, we demonstrated how pure quantum mechanics describes the fact that electrons behave as interfering particles, namely, particles whose detection rate is consistent with interference.

5. Conclusions

In this study, we demonstrated that decoherence is one of the inherent characteristics of pure quantum mechanics. Quantum states describe both the wave as well as particle behaviour of microscopic objects, specifically, the microscopic objects propagate as waves and are observed as particles. In this context, it is worth paying careful attention to the meaning of the phrase *observing the wave nature of a state*. It is equivalent to saying *identifying the state propagating as a wave by observing many particles*. As shown in Section 4.3, there is essentially no difference between observing the electrons on the screen and near the slit. Irrespective of where the electrons are observed, they are observed as particles, which helps us determine the amplitude of the corresponding state.

Therefore, we conclude that the quantum measurement process can be explained within the framework of pure quantum mechanics. Moreover, we believe that our study can be applied to a more general discussion about the quantum-to-classical transition in nature.

Conflicts of Interest

The author declares no conflicts of interest regarding the publication of this paper.

References

[1] Schlosshauer, M., Kofler, J. and Zeilinger, A. (2013) *Studies in History and Philosophy of Science Part B*, **44**, 222-230. https://doi.org/10.1016/j.shpsb.2013.04.004

[2] Laloë, F. (2013) Do We Really Understand Quantum Mechanics? Cambridge UP, Cambridge.

[3] Gilton, M.J.R. (2016) *Studies in History and Philosophy of Science Part B: Studies in History and Philosophy of Modern Physics*, **55**, 92-100. https://doi.org/10.1016/j.shpsb.2016.08.005

[4] Schlosshauer, M. (2004) *Reviews of Modern Physics*, **76**, 1267-1305. https://doi.org/10.1103/RevModPhys.76.1267

[5] Zurek, W.H. (2005) *Physical Review A*, **71**, Article ID: 052105. https://doi.org/10.1103/PhysRevA.71.052105

[6] Born, M. (1926) *Zeitschrift für Physik*, **37**, 863-867. https://doi.org/10.1007/BF01397477

[7] von Neumann, J. (1932) Mathematische Grundlagen der Quantenmechanik. Springer-Verlag, Berlin.

[8] Peres, A. and Terno, D.R. (2004) *Reviews of Modern Physics*, **76**, 93. https://doi.org/10.1103/RevModPhys.76.93

[9] Everett, H. (1957) *Reviews of Modern Physics*, **29**, 454. https://doi.org/10.1103/RevModPhys.29.454

[10] DeWitt, B.S. and Graham, N. (2016) The Many-Worlds Interpretation of Quantum Mechanics. Princeton UP, New Jersey.

[11] Joos, E., Zeh, H.D., Kiefer, C., Giulini, D., Kupsch, J. and Stamatescu, I.-O. (2003) Decoherence and the Appearance of a Classical World in Quantum Theory. 2nd Edition, Springer-Verlag, Berlin. https://doi.org/10.1007/978-3-662-05328-7

[12] Schlosshauer, M. (2007) Decoherence and the Quantum-to-Classical Transition. Springer-Verlag, Berlin.

[13] Saunders, S., Barrett, J., Kent, A. and Wallace, D. (2010) Many Worlds? Everett Quantum Theory and Reality. Oxford UP, Oxford. https://doi.org/10.1093/acprof:oso/9780199560561.001.0001

[14] Zeh, H.D. (1970) *Foundations of Physics*, **1**, 69-76. https://doi.org/10.1007/BF00708656

[15] Kübler, O. and Zeh, H.D. (1973) *Annals of Physics*, **76**, 405-418. https://doi.org/10.1016/0003-4916(73)90040-7

[16] Zurek, W.H. (1981) *Physical Review D*, **24**, 1516-1525. https://doi.org/10.1103/PhysRevD.24.1516

[17] Zurek, W.H. (1982) *Physical Review D*, **26**, 1862-1880. https://doi.org/10.1103/PhysRevD.26.1862

[18] d'Espagnat, B. (1976) Conceptual Foundations of Quantum Mechanics. 2nd Edition, W. A. Benjamin, San Francisco.

[19] Dirac, P.A.M. (1958) The Principles of Quantum Mechanics. 4th Edition, Oxford UP, London.

[20] Landau, L.D. and Lifshitz, E.M. (1977) Quantum Mechanics (Non-Relativistic Theory). 3rd Edition, Pergamon Press, Oxford.

[21] Messiah, A. (1961) Quantum Mechanics. Wiley, New York.

[22] Blokhintsev, D.I. (1964) Quantum Mechanics. Springer, Berlin. https://doi.org/10.1007/978-94-010-9711-6

[23] Feynman, R.P. and Hibbs, A.R. (1965) Quantum Mechanics and Path Integrals. McGraw-Hill, New York.

[24] Schiff, L.I. (1968) Quantum Mechanics. 3rd Edition, McGraw-Hill, New York.

[25] Ehrenfest, P. (1927) *Zeitschrift für Physik*, **45**, 455. https://doi.org/10.1007/BF01329203

[26] Freedman, S.J. and Clauser, J.F. (1972) *Physical Review Letters*, **28**, 938-941. https://doi.org/10.1103/PhysRevLett.28.938

[27] Aspect, A., Grangier, P. and Roger, G. (1981) *Physical Review Letters*, **47**, 460-463. https://doi.org/10.1103/PhysRevLett.47.460

[28] Aspect, A., Grangier, P. and Roger, G. (1982) *Physical Review Letters*, **49**, 91-94. https://doi.org/10.1103/PhysRevLett.49.91

[29] Aspect, A., Dalibard, J. and Roger, G. (1982) *Physical Review Letters*, **49**, 1804-1807. https://doi.org/10.1103/PhysRevLett.49.1804

[30] Ghosh, R. and Mandel, L. (1987) *Physical Review Letters*, **59**, 1903-1905. https://doi.org/10.1103/PhysRevLett.59.1903

[31] Michler, M., Weinfurter, H. and Zukowski, M. (2000) *Physical Review Letters*, **84**, 5457-5460. https://doi.org/10.1103/PhysRevLett.84.5457

[32] Hasegawa, Y., Loidl, R., Badurek, G., Baron, M. and Rauch, H. (2003) *Nature*, **425**, 45-48. https://doi.org/10.1038/nature01881

[33] Einstein, A., Podolsky, B. and Rosen, N. (1935) *Physical Review*, **47**, 777-780. https://doi.org/10.1103/PhysRev.47.777

[34] Bohm, D. (1951) Quantum Theory. Prentice-Hall, Englewood Cliffs.

[35] Clauser, J.F., Horne, M.A., Shimony, A. and Holt, R.A. (1969) *Physical Review Letters*, **23**, 880-884. https://doi.org/10.1103/PhysRevLett.23.880

[36] Clauser, J.F. and Horne, M.A. (1974) *Physical Review D*, **10**, 526-535. https://doi.org/10.1103/PhysRevD.10.526

[37] Bell, J.S. (1964) *Physics*, **1**, 195-200. https://doi.org/10.1103/PhysicsPhysiqueFizika.1.195

[38] Wigner, E.P. (1970) *American Journal of Physics*, **38**, 1005. https://doi.org/10.1119/1.1976526

[39] Mermin, N.D. (1981) *American Journal of Physics*, **49**, 940. https://doi.org/10.1119/1.12594

[40] Alberrt, D.Z. (1992) Quantum Mechanics and Experience. Harvard UP, Cambridge.

[41] Maccone, L. (2013) *American Journal of Physics*, **81**, 854. https://doi.org/10.1119/1.4823600

[42] Kochen, S. and Specker, E. (1967) *Journal of Mathematics and Mechanics*, **17**, 59. https://doi.org/10.1512/iumj.1968.17.17004

[43] Bell, J.S. (1966) *Reviews of Modern Physics*, **38**, 447. https://doi.org/10.1103/RevModPhys.38.447

[44] Redhead, M. (1987) Incompleteness, Nonlocality, and Realism. Oxford UP, Oxford.

[45] Brown, H.R. and Svetlichny, G. (1990) *Foundations of Physics*, **20**, 1379-1387. https://doi.org/10.1007/BF01883492

[46] Aharonov, Y., Albert, D.Z. and Vaidman, L. (1988) *Physical Review Letters*, **60**, 1351. https://doi.org/10.1103/PhysRevLett.60.1351

[47] Mochizuki, R. (2018) *International Journal of Theoretical Physics*, **57**, 1338. https://doi.org/10.1007/s10773-018-3662-1

Call for Papers

Journal of Modern Physics

ISSN: 2153-1196 (Print) ISSN: 2153-120X (Online)
https://www.scirp.org/journal/jmp

Journal of Modern Physics **(JMP)** is an international journal dedicated to the latest advancement of modern physics. The goal of this journal is to provide a platform for scientists and academicians all over the world to promote, share, and discuss various new issues and developments in different areas of modern physics.

Editor-in-Chief

Subject Coverage

Journal of Modern Physics publishes original papers including but not limited to the following fields:

Biophysics and Medical Physics
Complex Systems Physics
Computational Physics
Condensed Matter Physics
Cosmology and Early Universe
Earth and Planetary Sciences
General Relativity
High Energy Astrophysics
High Energy/Accelerator Physics
Instrumentation and Measurement
Interdisciplinary Physics
Materials Sciences and Technology
Mathematical Physics
Mechanical Response of Solids and Structures
New Materials: Micro and Nano-Mechanics and Homogeneization
Non-Equilibrium Thermodynamics and Statistical Mechanics
Nuclear Science and Engineering
Optics
Physics of Nanostructures
Plasma Physics
Quantum Mechanical Developments
Quantum Theory
Relativistic Astrophysics
String Theory
Superconducting Physics
Theoretical High Energy Physics
Thermology

We are also interested in: 1) Short Reports—2-5 page papers where an author can either present an idea with theoretical background but has not yet completed the research needed for a complete paper or preliminary data; 2) Book Reviews—Comments and critiques.

Notes for Intending Authors

Submitted papers should not have been previously published nor be currently under consideration for publication elsewhere. Paper submission will be handled electronically through the website. All papers are refereed through a peer review process. For more details about the submissions, please access the website.

Website and E-Mail

https://www.scirp.org/journal/jmp **E-mail: jmp@scirp.org**

What is SCIRP?

Scientific Research Publishing (SCIRP) is one of the largest Open Access journal publishers. It is currently publishing more than 200 open access, online, peer-reviewed journals covering a wide range of academic disciplines. SCIRP serves the worldwide academic communities and contributes to the progress and application of science with its publication.

What is Open Access?

All original research papers published by SCIRP are made freely and permanently accessible online immediately upon publication. To be able to provide open access journals, SCIRP defrays operation costs from authors and subscription charges only for its printed version. Open access publishing allows an immediate, worldwide, barrier-free, open access to the full text of research papers, which is in the best interests of the scientific community.

- High visibility for maximum global exposure with open access publishing model
- Rigorous peer review of research papers
- Prompt faster publication with less cost
- Guaranteed targeted, multidisciplinary audience

Scientific Research Publishing

Website: https://www.scirp.org

Subscription: sub@scirp.org

Advertisement: service@scirp.org